Evolution of Cretaceous sediments in the Mamfe Basin, SW Cameroon: Depositional environments, Palynostratigraphy, and Paleogeography

Dissertation zur Erlangung des Doktorgrades

an der Fakultät für Mathematik, Informatik und Naturwissenschaften

Fachbereich Geowissenschaften

der Universität Hamburg

vorgelegt von

Humphrey Njeatih Ajonina

Aus

Ajei Ngie, Kamerun

Hamburg

2016

Tag der Disputation: 11.05.2016

(Date of oral defense)

Folgende Gutachter empfehlen die Annahme der Dissertation:

(The following evaluators recommend the admission of the dissertation):

Professor Dr. Christian Betzler

Professor Dr. Gerhard Schmiedl

Eidesstattliche Erklärung

Hiermit erkläre ich an Eides statt, dass ich die vorliegende Dissertationsschrift selbst verfasst und keine anderen als die angegebenen Quellen und Hilfsmittel benutzt habe.

Declaration on oath

I hereby declare, on oath, that I have written the present dissertation by my own and have not used other than the acknowledged resources and aids.

Ort/Datum	Unterschrift
(Place/date)	*(Signature)*

Summary

The Mamfe Basin is a WNW-ESE trending half-graben in southeastern Nigeria that extends into southwestern Cameroon. This basin is the southernmost part of the West and Central African rift system that resulted from the breakup and subsequent separation of South America from Africa during the early Cretaceous. It is located about 150 km to the northeast of the meeting point of the early Cretaceous Benue Trough-Equatorial Atlantic-South Atlantic rift system triple junction.

The sedimentary infill of the Mamfe Basin is over 4500 m thick and formerly referred to as the Mamfe Formation. Until date, the Mamfe Formation lacks any direct or clearly defined age determination in geological and paleontological literature. The formation has over the years been correlated with Albian-Cenomanian sediments in the adjoining southern Benue Trough on the basis of presumed lithological similarities, and is mapped as the basal unit of the Asu River Group.

This research was undertaken to characterize the depositional environments and age of the sedimentary infill of the Mamfe Basin within the context of the early Cretaceous paleogeography of the eastern Gulf of Guinea region from southern Benue Trough to northern Gabon. Sedimentological, palynofacies, organic geochemical, palynological, and foraminiferal analyses were carried out on outcrop samples that were collected from the Cameroonian sector of the Mamfe Basin.

Results of this research indicates that the sedimentary infill of the Mamfe Basin includes siliciclastics, carbonates, evaporites, and volcaniclastics. Twenty macrofacies were identified and grouped into nine facies associations: proximal alluvial fan, floodplain, palustrine marshes, fluvio-lacustrine, moderate to deep (sublittoral-profundal) lake, littoral-shoreline marshes, deltaic swamps, medial alluvial fan, and fluvial channel/overbank. Based on the vertical and lateral relationship of the facies associations, a revised lithostratigraphic framework consisting of five formations is proposed for the Mamfe Basin. These formations from bottom to top are Etuko, Nfaitok, Manyu, Okoyong, and Ikom-Munaya. These formations are partitioned by unconformities into three depositional sequences.

The basal (pre-rift) depositional sequence overlies the Pan-African basement, and consists of non-fossiliferous proximal alluvial fan debris flow deposit that outcrop in the northeastern margin of the basin in and around Etuko. This unit is dated as pre-middle Barremian based on the palynological age of the overlying depositional sequence.

The middle (syn-rift) depositional sequence is underlain by an erosional unconformity and is named the Mamfe Group. This group consists of three formations, which from bottom to top are Nfaitok (fluvio-palustrine), Manyu (lacustrine), and Okoyong (fan-delta). Micropaleontological analysis of samples from the Mamfe Group yielded 128 pollen and spores taxa with many new previously undescribed species, very rare foraminifera and no dinoflagellates. Angiosperm pollen grains are rare, and *Dicheiropollis etruscus* and elater-bearing pollen are absent. Age-diagnostic palynomorphs within the microflora assemblage suggests that the Mamfe Group is younger than early Barremian and older than middle Albian. The palynoflora assemblage correspond to the West Africa regional palynostratigraphic reference section and zones CV to CIX of SNEA (P) in Gabon, and palynozones P-190 to P-280 in South America (Brazil) that have been assigned a middle Barremian-early Albian age. The Aptian age of the lacustrine facies of the Manyu Formation suggests that the Mamfe Basin was part of the Barremian-middle Albian Medio-African and NE-Brazilian Great Lakes. A late Aptian-early Albian marine ingression into the Mamfe Basin from the Douala Basin is represented by halite dominated evaporites and rare *Praebulimina* sp. and *Hedbergella* sp. The evaporites deposit in the Mamfe Group represent the northernmost fringes of the South Atlantic salt province.

The upper (post-rift) depositional sequence is underlain by a regional angular unconformity that coincides with the opening of the Equatorial Atlantic and Benue Trough. It consists of non-fossiliferous fluvial deposits in the western part of the basin that have been named Ikom-Munaya Formation.

Lithofacies, palynofacies, microflora, and clay mineral composition of the studied sedimentary succession of the Mamfe Basin indicates a progressively shift from a warm and dry arid to semi-arid climate in the fluvio-palustrine and lacustrine units towards a more humid and wet climate in the fan-delta and fluvial successions at the top. The age of the sediments in the Mamfe Basin indicates that the basin is not a rift-splay segment of the Benue Trough as earlier suggested. Vitrinite reflectance, thermal alteration index, and illite crystallinity paleothermal data all suggest burial depths of between 1200 and 4000 m. The westward younging of sediments in the Mamfe basin is due to uplift and erosion in the eastern part of the basin rather than the previously reported westward migration of depocenter.

Zusammenfassung

Das Mamfe-Becken ist ein West-Nordwest/Ost-Südost streichender Halbgraben in Südost-Nigeria, der sich bis in das südwestliche Kamerun erstreckt.

Dieses Becken bildet den südlichsten Teil des West- und Zentralafrikanischen Rift-Systems, das aus dem Auseinanderbrechen und der darauf folgenden Trennung Südamerikas von Afrika während der frühen Kreidezeit resultierte.

Es liegt ca. 150 km nordöstlich von dem Tripelpunkt, an dem der unterkretazische Benue-Graben mit dem äquatorial-atlantischen und dem südatlantischen Rift-System zusammentrifft.

Die sedimentäre Füllung des Mamfe-Beckens ist mehr als 4500 Meter mächtig und wurde vormals als Mamfe-Formation bezeichnet. Bis heute fehlt für die Mamfe-Formation eine klar definierte Altersbestimmung in der geologischen und paläontologischen Literatur. Die Formation wurde aufgrund mutmaßlicher Gesteinsähnlichkeiten jahrelang mit den Alb- bis Cenomanen Sedimenten des benachbarten südlichen Benue-Grabens in einen engen Zusammenhang gestellt, , und als basale Einheit der Asu River Group kartografisch erfasst.

Die hier vorliegende Untersuchung wurde vorgenommen, um Ablagerungsmilieu und Alter der sedimentären Füllung des Mamfe-Beckens zu beschreiben und sie in einen Zusammenhang mit der unterkretazischen Paläogeographie der Region des östlichen Golfs von Guinea zu stellen, die vom südlichen Benue-Graben bis zum nördlichen Gabun reicht. Dazu wurden sedimentologische, palynofazielle, biogeochemische, palynologische und Foraminiferen-Analysen an Aufschluss-Proben durchgeführt, die im Kameruner Sektor des Mamfe-Beckens gesammelt wurden.

Die Ergebnisse dieser Untersuchungen zeigen, dass die sedimentäre Füllung des Mamfe-Beckens Siliziklastika, Carbonate, Evaporite und Vulkanoklastite enthält. Zwanzig Makro-Fazies-Typen wurden identifiziert und in neun Fazies-Assoziationen eingruppiert: naher Schwemmfächer, Überschwemmungsgebiet, Sumpf, fluvio-lakustrisch, mäßiger bis tiefer See, küstennahe Ufer-Sumpf, Delta-Moor, mittlerer Schwemmfächer und fluviales Überschwemmungsgebiet.

Basierend auf der vertikalen und lateralen Beziehung der Fazies-Assoziationen wird für das Mamfe-Becken ein revidiertes lithostratigraphisches Modell mit fünf Formationen vorgeschlagen. Diese Formationen sind von unten nach oben: Etuko, Nfaitok, Manyu, Okoyong und Ikom-Munaya. Diese Formationen werden anhand von Diskordanzen in drei Ablagerungssequenzen unterteilt.

Die basale Ablagerungssequenz überlagert das Panafrikanische Grundgebirge und besteht aus fossilleerem Schuttstrom des nahen Schwemmfächers, das im nordöstlichen Randbereich des Beckens und im Gebiet von Etuko ansteht. Diese Einheit konnte anhand des palynologischen Alters der darüber liegenden Schicht auf ein vor- bis mittelbarremisches Alter eingestuft werden.

Die mittlere Ablagerungssequenz ist unterlagert von einer Erosionsdiskordanz und wird Mamfe-Gruppe genannt. Diese Gruppe besteht aus drei Formationen. Diese sind von unten nach oben: Nfaitok (Fluss-Sumpf), Manyu (lakustrisch) und Okoyong (Fächer-Delta).

Mikropaläontologische Analysen von Proben aus der Mamfe-Gruppe erbrachten 128 Pollen- und Sporengruppen mit vielen neuen, bislang unbeschriebenen Gattungen, sehr seltenen Foraminiferen und ohne Dinoflagellaten. Pollenkorn von Angiospermen ist selten und Dicheiropollis etruscus sowie Elaterit-Pollen fehlen. Eine palynomorphe Altersdiagnose innerhalb der Mikroflora-Gemeinschaft deutet darauf hin, dass die Mamfe-Gruppe jünger ist als das frühe Barremium und älter als mittlere Albium. Die Palynoflora-Gemeinschaft entspricht dem ostafrikanischen regionalen palynostratigraphischen Referenzprofil und hier den Zonen CV bis CIX von SNEA (P) in Gabun, sowie den Palynozonen P-190 bis P-280 in Südamerika (Brasilien), die dem mittleren Barremium bis frühen Albium zugeordnet werden. Die Einstufung der lakustrischen Fazies der Manyu-Formation in das Aptium deutet darauf hin, dass das Mamfe-Becken Teil der mittelafrikanischen und nordost-brasilianischen Großen Seen war, die ein Alter vom Barremium bis zum mittleren Albium aufweisen. Eine marine Ingression in das Mamfe-Becken vom Doula-Becken in der Zeit vom späten Aptium bis frühen Albium wird belegt durch das Vorkommen von riesigen Halit-dominierten Evaporiten sowie das seltene Vorkommen von Praebulimina sp. und Hedbergella sp. Die Evaporit-Ablagerungen in der Mamfe-Gruppe implizieren, dass die südatlantische Salzprovinz sich weiter nach Norden ausdehnte als das Douala-Becken.

Die obere Ablagerungssequenz wird unterlagert durch eine regionale angulare Diskordanz, die mit der Öffnung des äquatorialen Atlantiks und des Benue-Grabens in der Zeit vom frühen bis zum mittleren Albium übereinstimmt. Sie besteht aus fossilleeren, fluvialen Ablagerungen im westlichen Teil des Beckens und wird Ikom-Munaya-Formation genannt.

Mikrofauna, Lithofazies, Palynofazies und Tonmineralzusammensetzung der Sedimente der mittleren und oberen Ablagerungssequenzen weisen hin auf einen fortschreitenden Wechsel von einem trocken-ariden zu einem semi-ariden Klima in den Nfaitok- und Manyu- Formationen und weiter zu einem stärker humiden und feuchten Klima in den Okoyong uund Ikom-Munaya-Formationen. Das Alter der Sedimente im Mamfe-Becken belegt, dass das Becken kein Rift-Splay-Segment des Benue-Grabens ist, wie zuvor angenommen. Die westwärts fortschreitende Verjüngung der Sedimente im Mamfe-Becken entstand stärker durch die Anhebung von 1200 bis 4000 Metern des östlichen Beckenbereichs als durch die früher beschriebene westwärts orientierte Wanderung des Sedimentationszentrums.

Acknowledgement

This dissertation is a summary of a research on the geology of the Mamfe Basin that started in 1996 at the University of Ibadan, Ibadan Nigeria under the supervision of Dr. Clement E. Bassey. Over the years in the course of this research, I have received material, technical, intellectual, and moral support from so many people who I cannot acknowledge by name because of space limitation. I feel obliged to mention just a representative few who will share my sincere gratitude with the rest who nevertheless, remain in the living memory of this research work.

I will begin by expressing my very profound gratitude to Prof. Christian Betzler for accepting to supervise this research, and generously giving to me the time that it has taken to put all this work together. Prof, I will never be able to thank you enough and will forever be grateful for your extra ordinary patience and kindness to me. God bless you.

I am also grateful to Prof. Isaac Njilah for his continuous encouragement, the Institute for Geological and Mining Research (IRGM) Yaounde and Godlove N. Eghombi for providing additional samples used in this study. I am grateful to Prof. S.W. Petters and Dr. Christian Heine for providing proprietary geophysical data on sediment thickness variation in the Mamfe Basin.

I am grateful to Mr Iku Z.N. and his family for their hospitality during the course of many field studies in Mamfe. I am grateful to Prof. Andreas Dahmke, Dr. Emmanuel Eseme, and Prof. Wolfgang Kuhnt for their assistance with geochemical and foraminiferal analyses. I will also like to express my appreciation to Mr Peter Stutz for his assistance with thin sections preparations, Joachim Ludwig for XRD analysis, and Dr. Yvonne Milker for SEM analysis.

I am particularly very grateful to Dr. Wolfgang Volkheimer for initiating the palynological analysis of samples from the Mamfe Basin. I benefitted immensely from the three months research work under his supervision at the Unidad de Paleopalinología, Instituto Argentino de Nivología, Glaciología y Ciencias Ambientales (IANIGLA), Mendoza Argentina. Many thanks to Dr. Ricardo Villalba, Dr. Mercedes Prámparo and their colleagues at IANIGLA and especially Jose Angelo, and Leticia Escodero for making my stay in Mendoza colourful and memorable.

Palynological analysis was also undertaken at the Center for Tropical Paleoecology and Archaeology (CTPA), Smithsonian Tropical Research Institute (STRI) Panama under the supervision of Dr. Carlos Jaramillo. Many thanks to him and to Paula Mejia and Francy Carvajah for their help in pollen and spores identification. Fluorescence Confocal Laser Scanning Microscopy (CLSM) of selected pollen and spores was done at STRI Laboratory of Electron and Confocal Microscopy by Mr Jorge Ceballos. I am thankful to STRI for funding my three months research visit at CTPA-STRI Panama.

I would like to acknowledge the International Association of Sedimentologists, Palaeontological Association London, and University of Hamburg for offering me student travel grants to present part of the results of this research at the following conferences: 4th International Limnogeology Congress in Barcelona (2007), 12th International Palynological Congress and the 8th International Organisation of Palaeobotany Conference in Bonn (2008), and the 8th European Palaeobotany - Palynology Conference in Budapest (2010). I also benefitted from the Merit Scholarship program of the University of Hamburg for which I am very grateful.

My appreciation to friends and former colleagues of the Basin Research Group Institute for Geology (IfGeo) - UHH Dr. Mustafa Abdullah, Dr. Sebastian Cäsar, Dr. Sebastian Lindhorst, Annemarie Gerhard, Glarius N. Nyongbela, and Mamat for useful discussions and encouragement. Not forgotten are my colleagues at the IRGM Yaounde Dr. J.V. Hell, Dr. G. Tanyileke, Dr. J.T. Eyong, Eseme Victor, G.N. Eghombi and others for their encouragement.

I will like to acknowledge specifically the assistance received from Hartmut and Ursula Nielsen, Babara Sonntag, Dr. and Mrs. Onuma, Glen Ganz, for their moral and material sacrifices that helped in the completion of this work. God richly bless you.

My deep appreciation to the national coordinator of the Redeemed Christian Church of God (RCCG) Germany Pst. Samuel Jegede and all the RCCG pastors and brethren in Germany and Belgium. Special thanks to all members of RCCG Peace Chapel Hamburg for their prayers and moral support. I also extend my gratitude to bro. Thomas Chika, Pst. Ossai Okeke, Pst. Felix Ojeugo, and Pst. Sunny Ndukwe all of Christ Ambassadors Ministries International (CAMI)

As always, I am eternally indebted to my family for standing by and with me while this work lasted. Very special thanks to the wonderboy Abohrobot Ufonajei, Rita Boateng, Marlies Pagel, and the families of Dr. Gordon. N. Ajonina, Dr. Samuel. Ajonina, and Dr. & Dr. (Mrs.) Buzie for their unflinching support.

To God be all the glory and honour for making this work a reality.

Table of Contents

1

INTRODUCTION

The Mamfe Basin is also known as Mamfe embayment, Ikom-Mamfe embayment, Mamfe gulf, or Mamfe rift (Wilson, 1928; Reyment, 1965; Dumort, 1968; Whiteman, 1982; Adediran et al., 1987, 1991; Petters et al., 1987; Petters, 1991; Edet and Okereke, 2014; Oden et al., 2015). It is an intracratonic rift in eastern West Africa, and is found within the region bounded by latitude 5º 30´ and 6º 10´ north of the equator and longitude 8º 30´ and 9º 35´ east of the Greenwich meridian. This basin is about 150 km northeast of the Niger Delta, the centre of the Cretaceous South Atlantic rift system triple junction, and about 200 km from the Atlantic coast of the Gulf of Guinea (**Fig. 1.1**). It is a southeasterly trending branch of the Benue Trough in southeast Nigeria that is sandwiched between the Oban and Bamenda (Obudu) Massifs, and extends into the southwestern part of the Republic of Cameroon. The basin is about 130 km long and its width decreases eastward from about 60 km at its confluence with the Abakaliki Basin in southeast Nigeria to less than 10 km at its eastern end near Etuko in southwest Cameroon. It has a total surface area of about 4248 km^2, half of this lies within Cameroon.

The Mamfe Basin is part of a suite of inland sedimentary basins in Nigeria and Cameroon that are believed to have resulted from the breakup and subsequent separation of South America from Africa in the Early Cretaceous (**Fig. 1.2**). Some of these basins are believed to have been part of the pre-Aptian Medio-African and NE-Brazilian Cretaceous Great Lakes (Popoff, 1988). The basins are classified as either coastal or inland (interior). The coastal basins are located along the Atlantic coast, and are filled with both continental and marine sediments ranging in age from Early Cretaceous to Recent. The inland basins are a suite of genetically related intracontinental rifts that Fairhead (1988) referred to as the West and Central Africa rift systems (WCARS). They contain mostly continental siliciclastic and volcaniclastic sediments of mostly Cretaceous age that were deposited in fluvial, marine, lacustrine, and deltaic settings. Most of the geological researches in sedimentary basins in Cameroon and Nigeria were focused on the coastal basins because of their higher petroleum resources compared to the inland basins. However, there is now an increase in research interest in the inland basins because of dwindling discoveries and reserves in the coastal basins, and the discovery of commercial quantities of petroleum in inland basins in the Republic of Chad and Sudan.

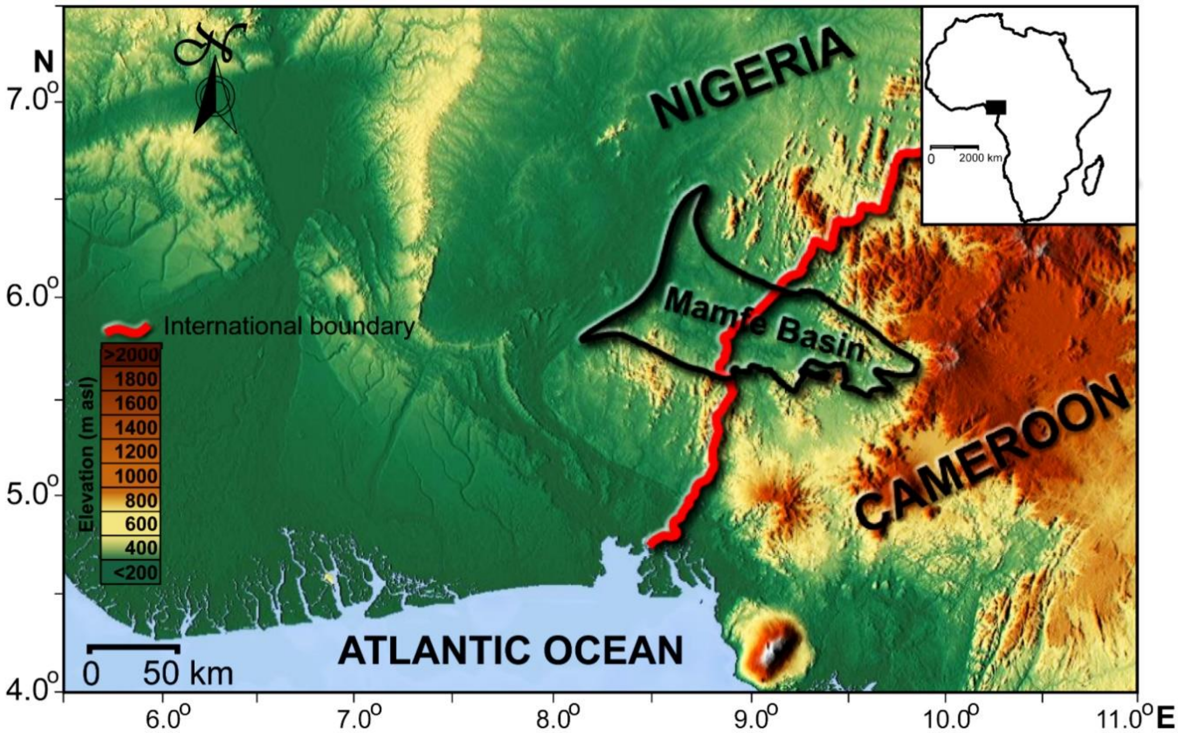

Figure 1.1. Relief map of eastern Gulf of Guinea showing outline of the Mamfe Basin (modified from Google maps-for-free Relief Map). Inset is sketch map of Africa showing location of relief map.

The Mamfe Basin is the southernmost basin within the West and Central Africa rift system. It is thought to be a rift splay segment of the southern Benue Trough (Ajonina, 1997; Ajonina et al., 2001, Bassey et al., 2013), and is regarded as one of the three sub basins that constitute the southern (lower) Benue Trough (SBT), the other sub basins are the Abakaliki and Anambra Basins (Reyment, 1965; Whiteman, 1982; Petters et al., 1987; Petters, 1991).

The Benue Trough is the main component of WCARS, and has attracted a lot of geological researches because it was one of the arms of the Early Cretaceous South Atlantic triple junction. Most of the researches in the southern Benue Trough have been in the Anambra and Abakaliki Basins with the Mamfe Basin receiving very little attention in comparison to other sub basins within SBT. The comparatively little research in the Mamfe Basin accounts for the scarcity of published literature on its geology, and the reason why it is generally considered as the least studied of all the West and Central African rift system (Petters et al., 1987; Genik, 1993). The lack of interest in the geology of the Mamfe Basin might be attributed to the non-discovery of commercial quantities of industrial minerals during the preliminary reconnaissance studies in the basin (Wilson, 1928; Le Fur, 1965), and the thin sediment thickness (700 m) and presumed Albian age that was assigned to the sedimentary infill by Reyment (1965).

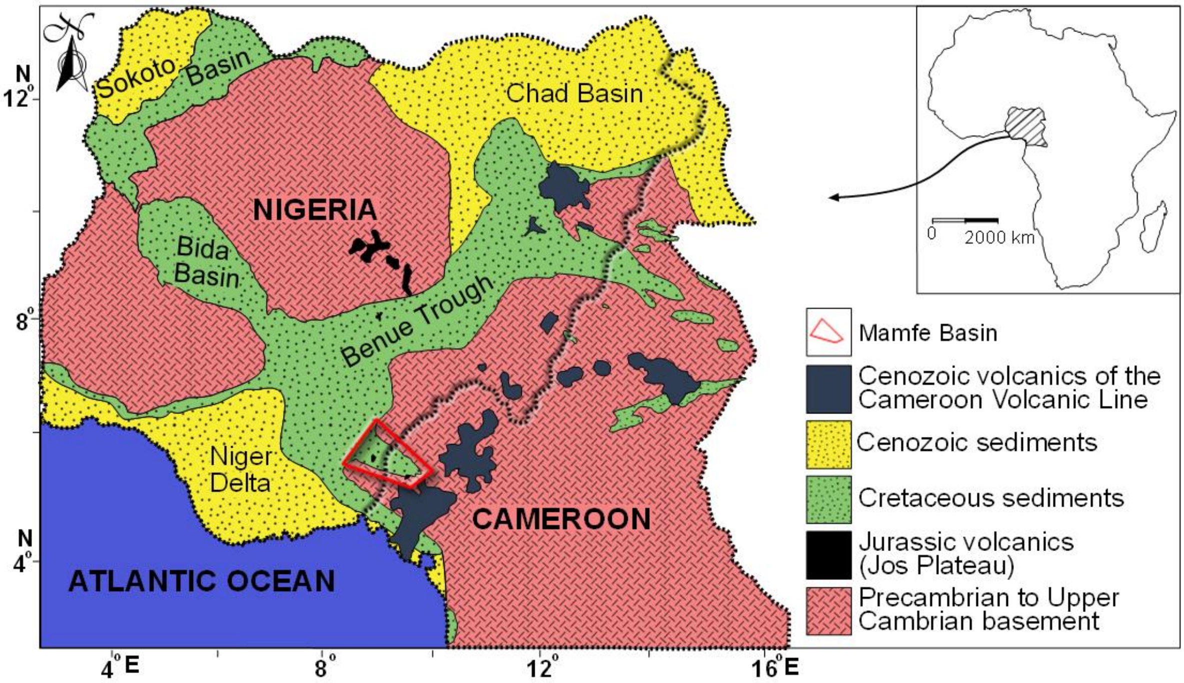

Figure 1.2. Simplified geological map of Cameroon and Nigeria showing the main sedimentary basins and location of the Mamfe Basin (modified from Avbovbo, 1980; Whiteman, 1982, and Toteu et al., 2001).

However, recent geophysical studies in the basin have indicated that the sedimentary infill in most parts of the basin is over 2000 m thick and exceeds 4000 m in the central part (Petters et al., 1987; Hell et al., 2000; Heine, 2007, pers. Comm.). This sediment thickness data suggests that this basin was one of the major depocenters in the southern Benue Trough sub region in the Early Cretaceous. The lithic infill of the basin consists of conglomerate, sandstone, green to black shale, siltstone, and evaporites. Recent publications on research in the Mamfe Basin include those of Fairhead et al., (1991); Ajonina and Bassey (1997); Ajonina et al. (2001; 2006; 2008, 2010); Hell et al. (2000); Eseme et al. (2002, 2006a & b); Eyong (2003); Ndougsa et al. (2007); Abolo (2008); Bassey et al., (2013); and Eyong et al., (2013); Oden et al., (2015).

1.1 Research problem

Although recent studies have resulted in an improvement in our understanding of the geology of the Mamfe Basin, researchers still differ in opinions regarding the age and environment of deposition of its lithic infill. The origin of halite dominated evaporites in the basin is still an open question. Also, it is not certain whether the volcaniclastic sediments in the basin and uplift are related to Cretaceous tectonism or post Cretaceous tectonic activities associated with the neighbouring Cameroon Volcanic Line (CVL). The environment of deposition of the lithic infill has been reported to be fluvial, deltaic, lacustrine, and marine (Wilson, 1928; Le Fur, 1965; Reyment, 1965; Dumort, 1968; Petters, 1978a, 1995; Petters et al., 1987; Wright et al, 1985, Tanyileke et al., 1996; Tijani et al., 1996; Ajonina, 1997; Ajonina and Bassey, 1997; Ajonina et al, 1998; 2001, 2006; Tijani, 2004; Eyong 2003; Eseme et al., 2006; Abolo, 2008; Bassey et al., 2013; Eyong et al., 2013). The diverse views on the environment of deposition are largely due to rarity of good exposures, non- to poorly-fossiliferous nature of the outcropping sediments, lack of subsurface samples (no wells have thus far been drilled in the basin) as well as insufficient geophysical data.

At present, the sediments in the Mamfe Basin lack any direct and clearly defined age determinations in geologic or paleontologic literature. The lithic infill is assumed to range in age from Albian to Cenomanian (Reyment, 1965; Reyment and Tait, 1972; Adeleye, 1975; Hoque, 1977, 1984; Ojoh, 1990; Bassey and Ajonina, 2002; Abolo, 2008). The sediments have been correlated with the Albian to early Cenomanian Asu River Group in the Abakaliki region of the southern Benue Trough, an attribution based only on lithologic similarity (e.g. Reyment, 1965; Murat, 1972; Dessauvagie, 1974; Petters and Ekweozor, 1982a; Whiteman, 1982). It is not certain if the Mamfe Basin was part of the early Cretaceous Medio-African and NE-Brazilian Cretaceous Great Lakes because no biostratigraphically diagnostic fossils have thus far been reported from its sedimentary infill. Whether the evaporites in this basin are related to the early Cretaceous South Atlantic salt province is still a matter of speculation.

Because of the lack of paleontologic or radiometrically based ages, and good exposures of laterally extensive beds in the Mamfe Basin, it is possible that the correlations of its lithic infill with sediments in the southern Benue Trough and paleogeographic reconstructions for the sub region may be erroneous and misleading (Murat, 1972; Dessauvagie, 1974; Hoque, 1977; Adeleye and Fayose, 1978; Benkhelil, 1989; Ojoh, 1990; Ajonina et al. 2001; Bassey and Ajonina, 2002; Bassey et al., 2013)

1.2 Research aim and objectives

This research is aimed at determining the evolution in space and time of the sediments in the Cameroonian sector of the Mamfe Basin within the framework of the Early Cretaceous paleogeography of the eastern Gulf of Guinea region. This aim will be realised through the following objectives:

1. Multiscale and multidisciplinary facies analysis to establish the environments of deposition and a comprehensive stratigraphic framework for outcrops of Cretaceous sediments in the basin.
2. Determine the provenance of the sediments and their paleothermal evolution.
3. Micropaleontological analysis to determine the age of the sediments and their correlation with coeval sedimentary successions in West Africa and NE Brazil.
4. Provide a conceptual model of the role of climate and tectonics on the evolution in time and space of the sedimentary succession in the Mamfe Basin within the framework of the Cretaceous paleogeography of the eastern Gulf of Guinea region from southern Benue Trough to northern Gabon.

1.3 Location and accessibility of the study area

This study is confined to the Cameroonian sector of the Mamfe Basin (**Fig. 1.3**). The area is bounded by latitudes 5° 31´ and 5° 56´ north of the equator and longitudes

8° 50´ and 9° 35´ east of the Greenwich meridian. It has a network of both principal (trunk A) and secondary roads. The principal roads link major towns and the neighbouring country Nigeria while the secondary roads link the local communities to the principal roads (**Fig. 1.3**). Most of the roads are seasonal, and several of them are impassable in the heart of the rainy season (August-September).

The Manyu/Cross River that traverses the entire basin is navigable from Mamfe beach to Agborkem (Nigeria) throughout the year. Fieldwork in the Mamfe Basin is preferably done in the dry season when the roads are dry and most of the rivers with exposures along their banks are low or dry.

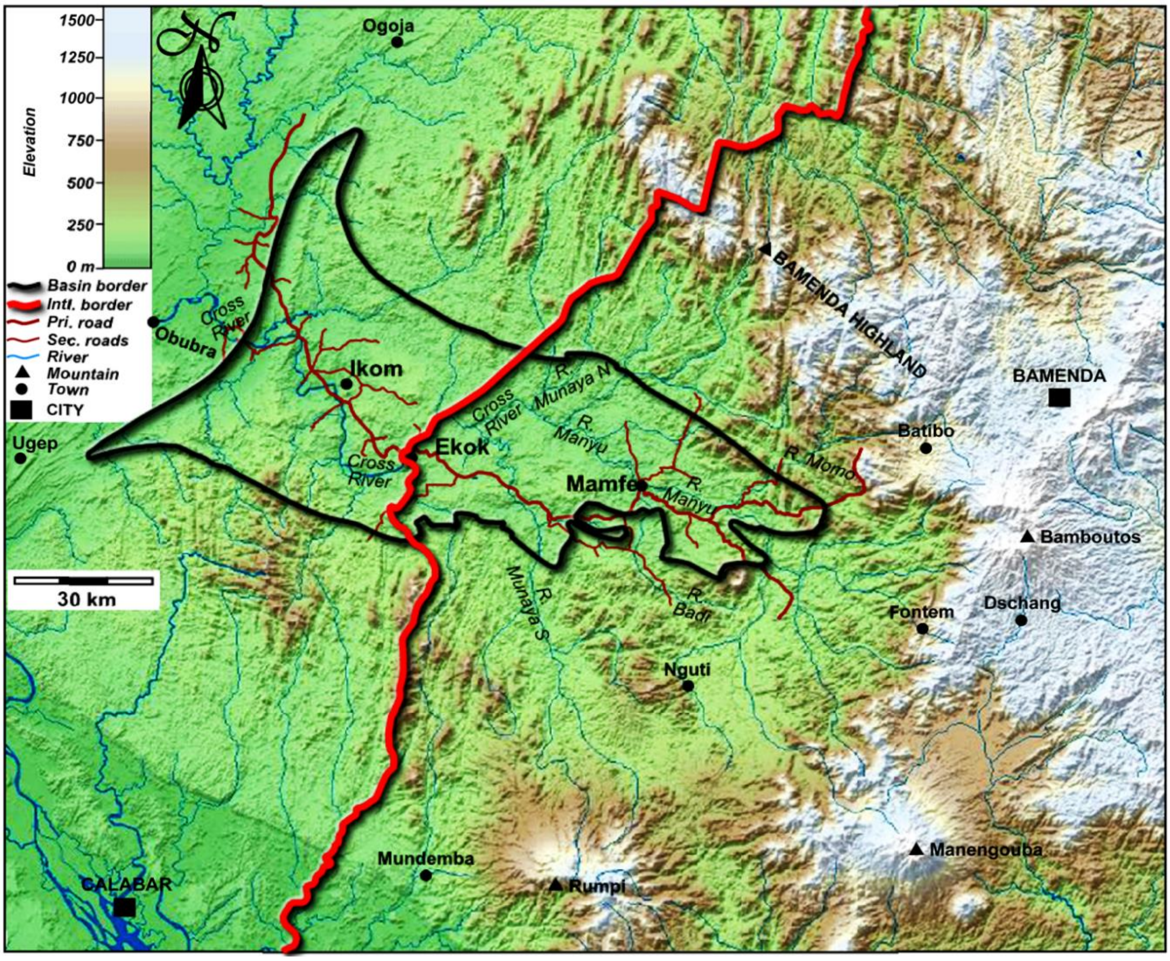

Figure 1.3. Terrain map of SE Nigeria and SW Cameroon showing drainage and road network within the Mamfe Basin (modified from Google Terrain Map).

1.4 Physiography of the Mamfe Basin

1.4.1 Relief and drainage

The present day Mamfe Basin is an intermontane basin. The basin has a low relief, and is characterised by gentle undulating terrain that ranges in height from 90 to 300 m above sea level. There are no outstanding hills or ridges. The low lying area is almost encircled by mountains except to the west where the basin extends into Cross River State in southeast Nigeria (**Fig. 1.3**).

The Mamfe Basin is also known as the Manyu River Basin, and receives numerous fast flowing 3rd to 4th order streams and rivers from the surrounding highlands. The drainage pattern is dendritic, with mostly transverse rivers draining into a 5th order axial trunk river (River Manyu) that flows from east to west and is called Cross River in its lower course. The main rivers of the basin include River Momo, Mone, Ebinisi, and Munaya north that drain the Obudu Massif/Bamenda highland (Sankwala mountains/Oshie ridge (1624 m)) to the north. River Badi and R. Manyu and its tributaries drain Mt. Bamboutus (2740 m) and Mt. Manengouba (2250 m) to the east and southeast respectively. River Munaya South and its tributaries drain Mt. Rumpi (1768 m) in the south.

1.4.2 Vegetation and climate

The study area is located within the tropical rainforest and has climate and vegetation that is characteristic of this equatorial region (**Fig. 1.4**). The forest in the northern part of the basin in Nigeria is conserved and known as the Cross River National Park, while the forest in the southern part of the basin constitutes the Cross River National Forest (Nigeria) and Korup National Park (Cameroon). Where the forest is not conserved, it has been subjected to extensive human interference (e.g. settlement, farming and lumbering) resulting to the development of secondary forest and derived savannah (characterized by the presence of tropical rainforest tree species in association with grassland species typical of the Savannah).

The area has an equatorial climate that is hot and humid, and consists of a wet (rainy) and a dry season that are modified by the deviation of the monsoon wind and the relief of Mount Cameroon (Neba, 1987). The rainy season begins in April and lasts until October, with the heaviest rainfall in September. All the months of the year receive some rainfall, and the mean annual rainfall varies between 2018 mm and

3370 mm (Ngwa, 1985; Neba, 1987; Edet and Okereke, 2014). The dry season begins in November and ends in April. Temperatures during the dry season are generally high. The Temperature ranges between 23º C and 30º C, with a mean annual temperature is 24º C. Humidity is high throughout the year. This equatorial climate and vegetation promotes rapid weathering of outcrops as shown in **Figure 1.5**.

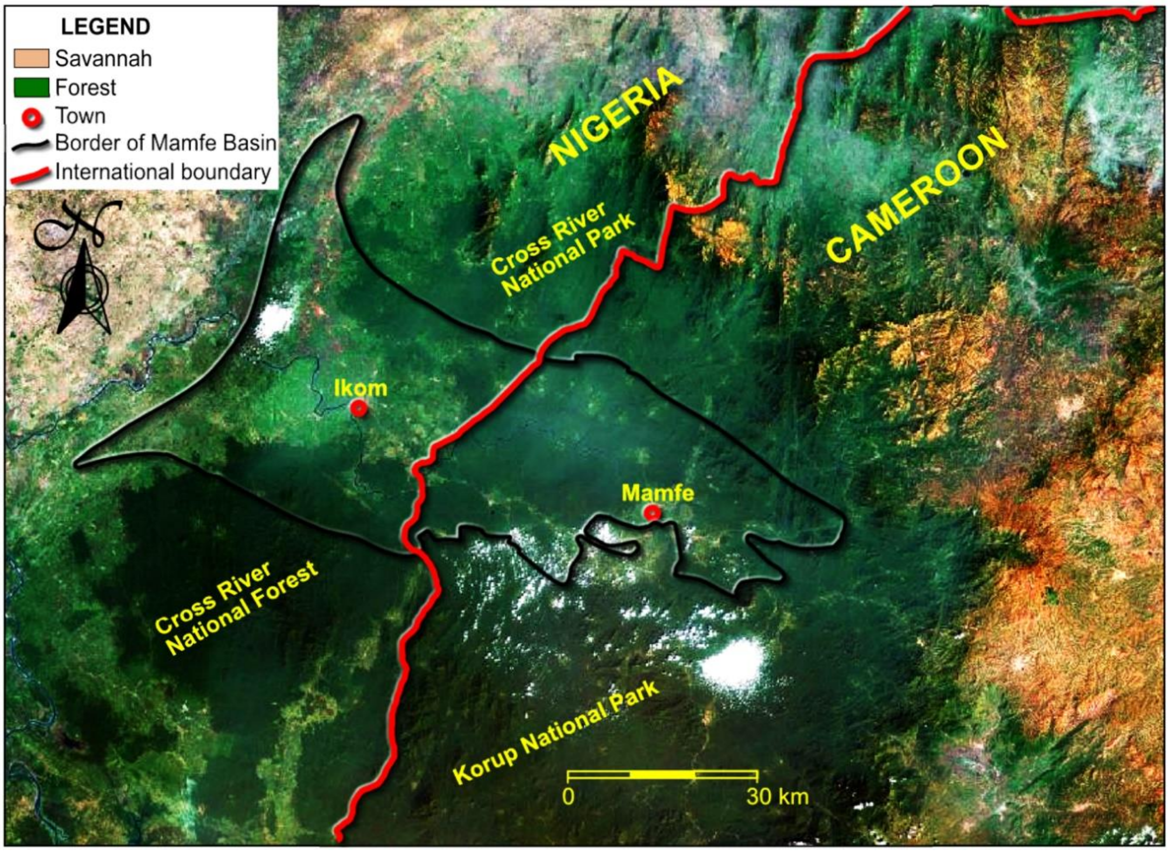

Figure 1.4. Satellite image of SE Nigeria and SW Cameroon showing vegetation in the Mamfe Basin and adjacent areas (modified from Google Earth).

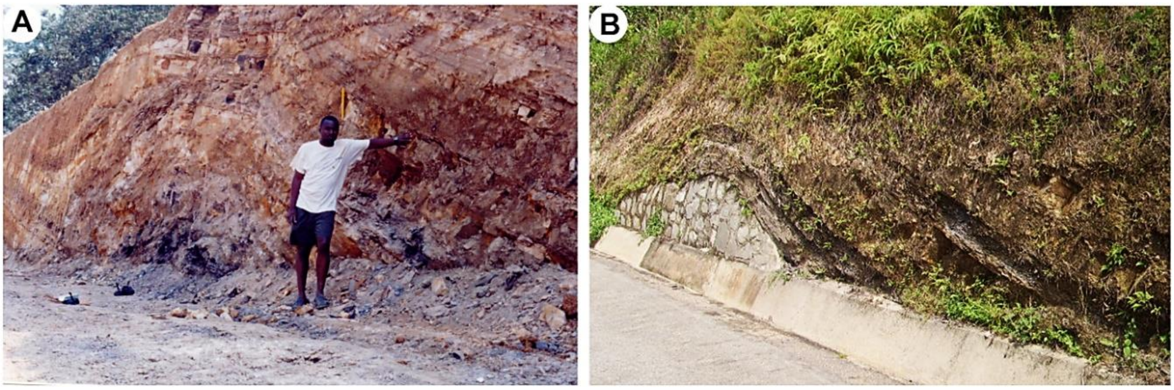

Figure 1.5. Effect of climate on the rate of weathering on an outcrop in the Mamfe Basin: A = 2001, and B same outcrop in 2006. The outcrop is located near Okoyong at latitude 05^{o} 44' N, and longitude 09^{o} 21' E.

1.5 Outline of thesis

This thesis comprises of six chapters that deal with the various aspects of its title and objectives of the research.

Chapter One is an introduction to the location and geography of the Mamfe Basin. It also highlights the main research problems and the resulting aims and objectives of the research. The various objectives are addressed in subsequent chapters of the thesis.

Chapter Two is a review of the regional geological setting of the Mamfe Basin within the context of the tectonic evolution and paleogeography of intracratonic rifts in West and Central Africa and Northeastern Brazil that resulted from the break-up and subsequent separation of South America from Africa in the Cretaceous.

Chapter Three deals with outcrop to microscope scale facies analysis and multi-proxies characterisation of the paleoenvironments in which the Cretaceous sediments in the Mamfe Basin were deposited as well as their provenance. A revised and comprehensive stratigraphic framework based on the spatial and temporal distribution of the sediments in the basin is proposed.

Chapter Four uses palynological analysis to determine the age of the sediments in the Mamfe Basin. Palynostratigraphic data is used to establish correlation with other sedimentary basins in West Africa and northeastern South America (NE Brazil).

Chapter Five integrates the data on sedimentology, palynofacies analysis, paleothermometry, and biostratigraphy presented in previous chapters into a conceptual model of the paleogeography and sedimentary evolution of the Mamfe Basin.

Chapter Six summarizes the major results relating to depositional environments, age, petroleum potentials, paleogeography and sedimentary evolution of the Mamfe Basin. It also offers some recommendations for further research.

2

REVIEW OF TECTONIC SETTING AND REGIONAL GEOLOGY

2.1 Introduction

The Mamfe Basin is a side rift on the eastern flank of the southern Benue Trough (SBT) region in southeastern Nigeria. It is sandwiched between the Bamenda and Oban Massifs and extends into the southwestern part of the Republic Cameroon. This N.110^{o} E trending rift-splay segment is about 130 km long and its width decreases steadily eastward from a maximum of 60 km at its confluence with the Benue Trough (Abakaliki basin) to less than 10 km at its eastern extremities (Etuko) in Cameroon.

It is located at the northeastern-most part of the Gulf of Guinea, about 200 km from the continental margin of the Atlantic coast, 150 km northeast of the Niger Delta, and midway along the Cameroon Volcanic Line chain of volcanoes. This basin is generally regarded as one of the three sub basins that make up the southern Benue Trough. These sub basins from east to west are Mamfe, Abakaliki, and Anambra Basins.

The Mamfe Basin is the smallest and southernmost of the NW-SE trending inland rifts that are physically linked to the Benue Trough, the others being the Bida Basin on the NW margin of the Anambra Basin and the Yola Basin in the northern Benue Trough that extends into northern Cameroon where it is referred to as the Garoua Basin. The coastal SE trending branch of the trough on the southeast flank of the Oban Massif is called the Calabar Flank. Although this branch is physically linked to the Benue Trough, it is not considered to be a part of the southern Benue Trough.

The Mamfe Basin is bordered to the north by the Bamenda Massif, to the east by uplift of the Cenozoic Cameroon Volcanic Line (CVL) and to the south by the Oban Massif. The structural features of the Mamfe Basin (e.g. fold axis parallel to basin axis, magmatic intrusions) are similar to those of the Benue Trough which suggests that both basins have a closely related tectonic framework and geodynamic evolution (Ajonina et al., 2001). On the basis of its structural features and shape, Ajonina (1997) proposed that the Mamfe Basin is a rift-splay segment of the southern Benue Trough that is separated from the contiguous Abakaliki Basin by a NE-SW trending basement horst which he named “Ikom ridge”. A similar basement structural feature (Okitipupa ridge) in the Benin Flank of the southern Benue Trough separates the Niger Delta from the Benin (Dahomey or Lagos) Basin.

2.2 Regional tectonic setting

2.2.1 Origin of the Benue Trough and associated rift basins

The Benue Trough is an aborted extensional (pull-apart) intracratonic rift basin located within the Central African mobile belt. This mobile belt is bordered to the west by the West African craton and to the east by the Congo craton. The trough is about 1000 km long and 50-150 km wide and extends obliquely (SW-NE) from the northern limit of the Niger Delta to Lake Chad. The trough is the principal component of a set of physically and genetically linked intracontinental Mesozoic “passive” pull-apart basins that extend inland from the Atlantic coast of the Gulf of Guinea in southeastern Nigeria northwards into Niger and Libya and eastwards through southern Chad into Sudan and Kenya (**Fig. 2.1**).

These passive (inactive) intracontinental rifts are collectively referred to as the West and Central African rift systems (WCARS; Fairhead, 1988, 1992) or the Mid-African Rift System (Kampunzu and Popoff, 1991). WCARS comprises of West African rift system (WARS) and the Central African rift system (CARS). Browne and Fairhead (1983) were of the opinion that the Garoua (WARS) and Doba (CARS) Basins were continuous and became separated in the Tertiary as a result of the development of the Adamawa uplift in Central Cameroon. The difference between the two systems is that WARS is filled by Cretaceous–Tertiary sediments of marine and non-marine origin while CARS is filled mostly by Cretaceous non-marine sediments.

WCARS probably extended into South America as the southwest-northeast trending Araripe-Potiguar Depression in northeastern Brazil (Mabesoone et al., 2000). This depression has been referred to as the Northeast Brazilian rift system (NBRS; Matos, 1992).

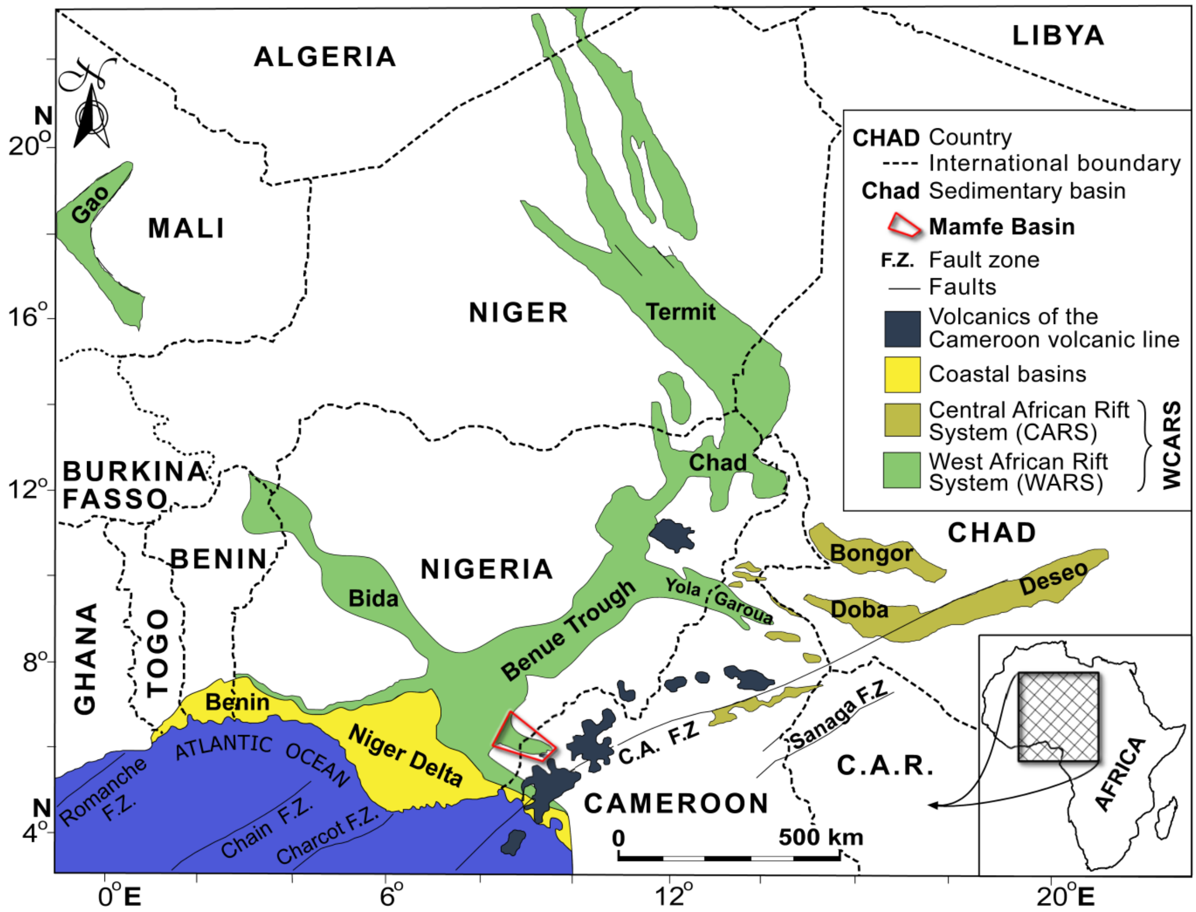

Figure 2.1. Map of the West and Central African rift systems (WCARS) in western Central Africa (modified from Genik, 1993).

Both WCARS and NBRS are thought to have resulted from the breakup of Gondwana and subsequent separation of South America from Africa in the late Jurassic-early Cretaceous (Nwachukwu, 1972; Olade, 1975; Petters, 1978a; Ofoegbu, 1985; Benkhelil, 1989; Guiraud et al., 1992; Guiraud and Maurin, 1992; Matos, 1992; Maluski et al., 1995; Basile et al., 2005; Bumby and Guiraud, 2005).

The breakup of the two continents was along the South Atlantic rift system (hereafter referred to as SARS) that was made up of three rift branches of different orientations (**Fig. 2.2**, Equatorial Atlantic, Benue/WCARS, and Southern Atlantic branches respectively) that intersected in a triple junction between the Niger Delta and Kribi (**Fig. 2.3**; Grant, 1971; Burke et al., 1972; Olade, 1975; Matos, 1992).

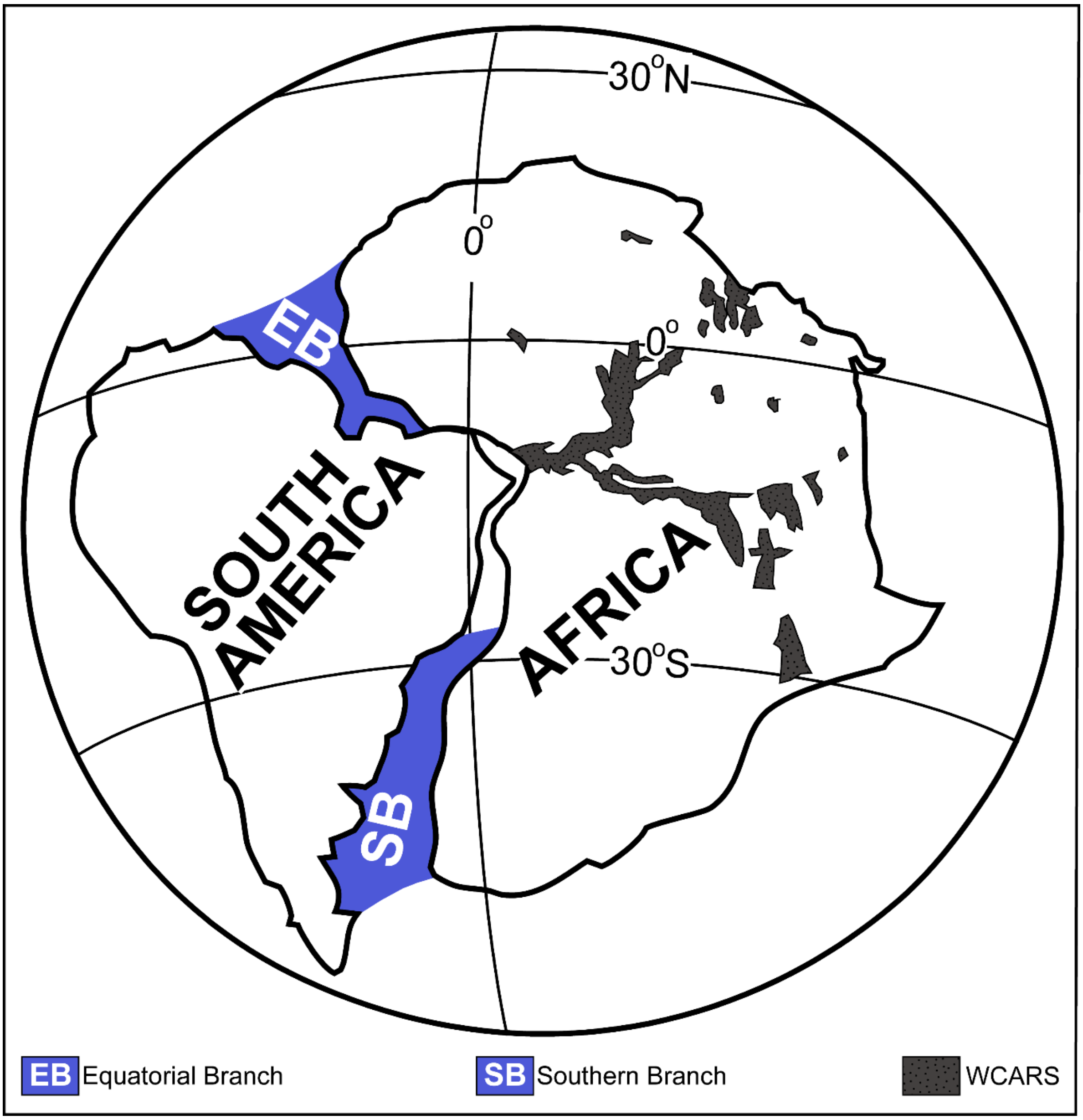

Figure 2.2. Hauterivian-Barremian (ca. 130 Ma) paleomap of Africa and South America showing the South Atlantic Ocean tripple junction rift system (modified from Binks and Fairhead, 1992).

The equatorial and southern branches of the triple junction developed into what are now the continental margins of the Southern and Equatorial Atlantic Ocean while the third branch developed into the Benue Trough and associated intracratonic rift basins that make up WCARS. Binks and Fairhead (1992) defined the Equatorial Atlantic as the region in West Africa and northern South America that lies between the Bahamas fracture zone and the Ascension fracture zone. This region is also referred to as the Gulf of Guinea or the Equatorial Segment of the South Atlantic Ocean (Moulin et al., 2010; Chaboureau et al., 2012, 2013). Its northwestern and southeastern limits are near Freetown (Sierra Leon) and Kribi (Cameroon) respectively (**Fig. 2.4**).

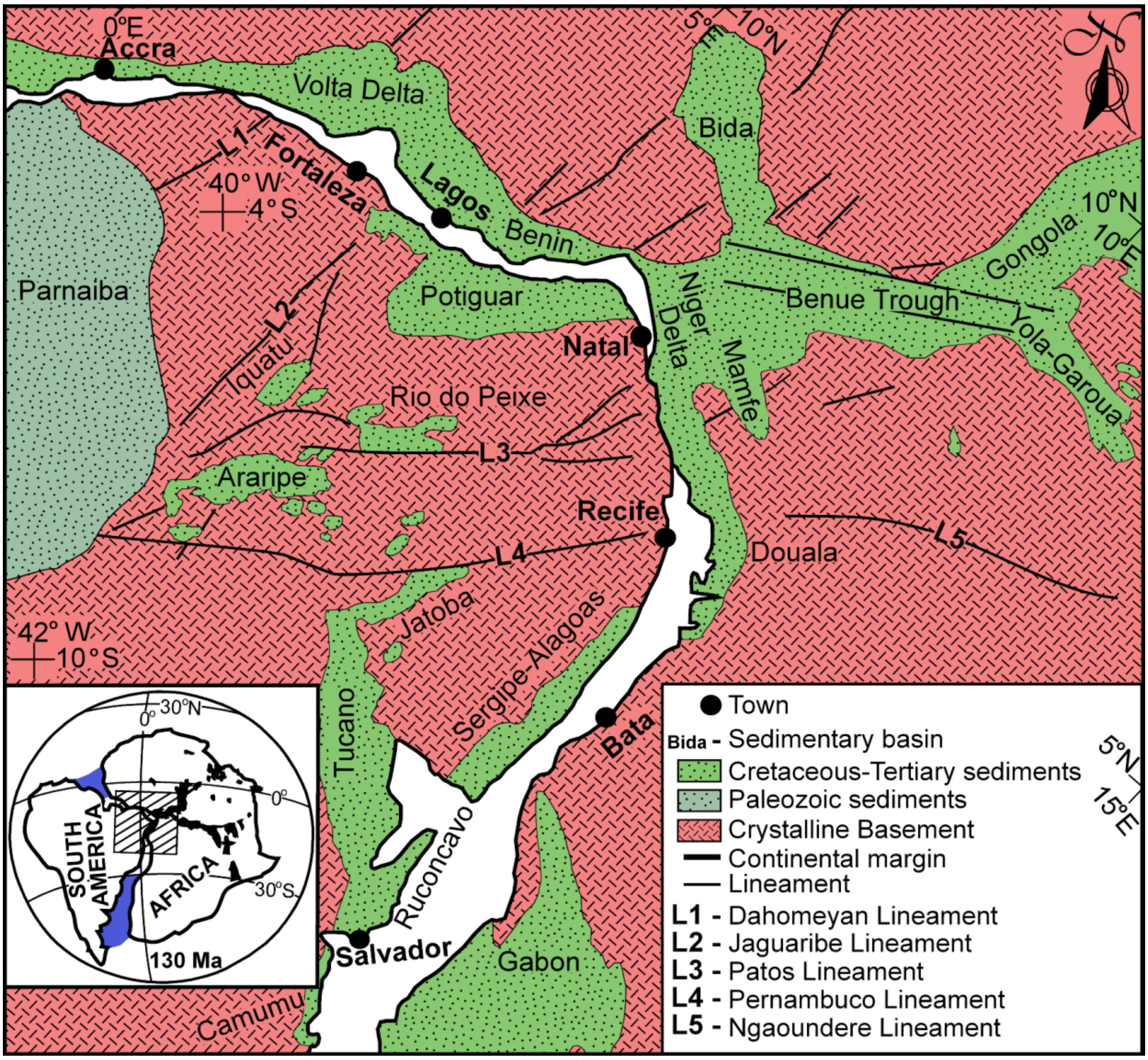

Figure 2.3. Early Cretaceous pre-drift geological sketch of part of the Equatorial and Central Segments of the South Atlantic Ocean showing distribution of sedimentary basins in northeastern Brazil and eastern West Africa (modified from Sibuet et al., 1984; Matos, 1992; Valença et al., 2003; Garcia et al., 2005; and Moulin et al., 2010). Inset is the Hauterivian-Barremian paleomap of Africa and South America showing the location of the geological sketch.

The Southern Atlantic (the Central and Austral Segments of Moulin et al., 2010) comprises the region between southwestern Africa and eastern South America. Although the Benue Trough is often cited as one of the best example of a failed arm of a triple junction, its origin and evolution is still controversial. The controversies coupled with its rich economic mineral deposits have been an attraction for many geological studies. Most of the early researches on the trough were focused on understanding the nature of continental rifting and seafloor spreading in the equatorial Atlantic region. The trough has been interpreted as an aborted branch of a rift-rift-rift(r-r-r) triple junction (Wright, 1968, 1976; Olade, 1975; Fairhead and Okereke, 1988) or a faulted arm of a rift-rift-fault (r-r-f) rift system (Grant, 1971; Popoff, 1988; Benkhelil, 1989).

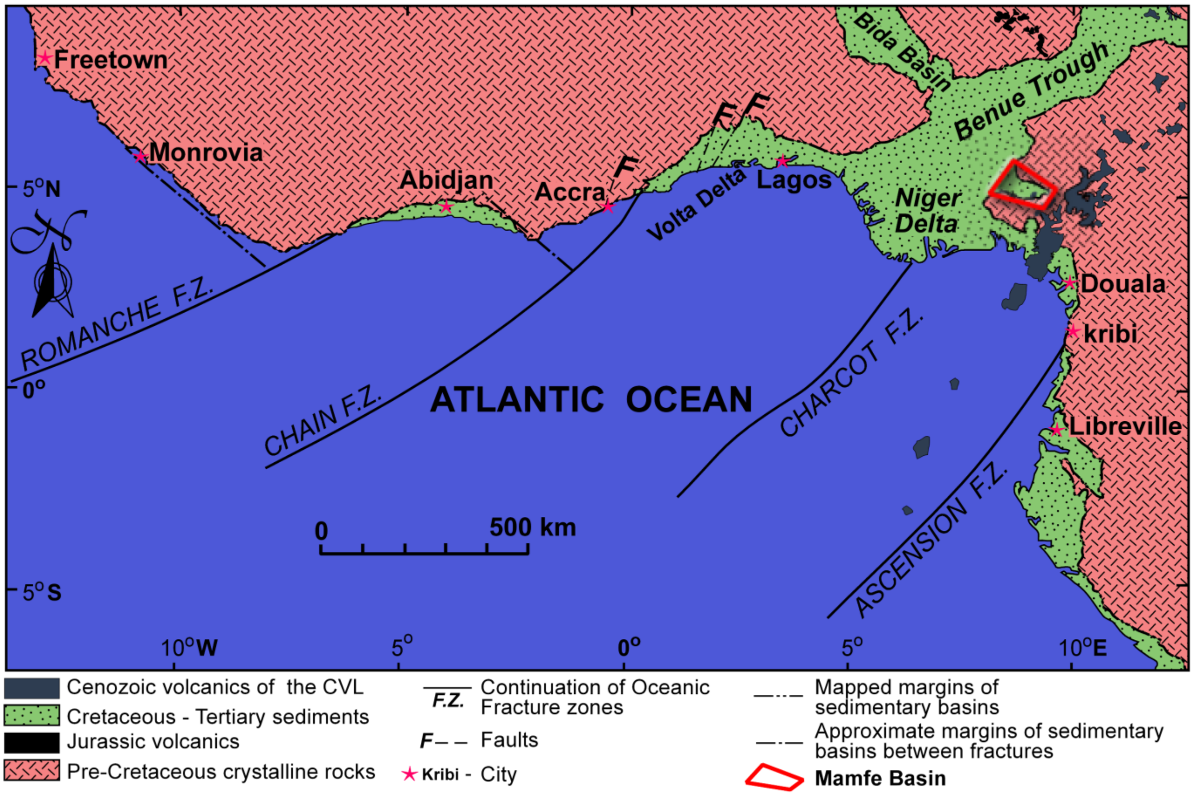

Figure 2.4. Geological sketch showing the connection of the West African rift system with Cretaceous rift basins along the continental margin of the Equatorial Atlantic (Gulf of Guinea), and projection of fracture zones (modified from Burke et al., 1972).

The timing of the final separation of South America from Africa and when definitive open ocean connection between the Equatorial and South Atlantic oceans has not been completely resolved and remains controversial (Torsvik et al., 2009; Aslanian and Moulin, 2010; Moulin et al., 2010). The latest Aptian-early Albian marine fauna exchange between these oceans was once considered to mark the onset of open ocean connections in the two oceans. However, recent geophysical studies suggest that the continental breakup was in the Campanian and not Albian, and that the last land bridge between Africa and Brazil was around the Romanche Fracture zone (**Fig. 2.4**) and not in the Pernambuco-Niger Delta area (Fairhead, 1988; Binks and Fairhead, 1992; Davison et al., 2005). The late Aptian-early Albian fauna exchange between the Equatorial and South Atlantic oceans is thus believed to have resulted from temporal intracontinental sea ways associated with the late Aptian-early Albian eustatic sea level high stand (Arai, 2000).

The intracratonic rift basins that make up WCARS and the coeval counterparts in Northeast Brazil were formed as a result of the reactivations of pre-existing Braziliano-Pan-African lineaments by tensional or trans-tensional regime (Rand and Mabesoone, 1982; Benkhelil, 1989; Fairhead and Green, 1989, Guiraud et al., 1992;

Bellieni et al., 1992; Matos, 1992; Cainelli and Mohriak, 1999; Pedreira and Bahia, 2000; Valença et al., 2003; Arthaud et al., 2008).

The trend, spatial distribution and geometry of these rifts depended on the location and orientation of inherent Braziliano - Pan-African structural zones of weakness in the basements. Estimating the exact timing of these reactivations event has not been possible largely because of lack of age diagnostic fossils in the basal sedimentary infill of the basins that is comprised mostly of coarse-grained fluviatile siliciclastics. The location and orientation of the basin-bounding fault was apparently controlled by the trend, strike and dip of planar structures (e.g. gneissosity, schistosity, shear zones) within the basement.

The rifts are generally perpendicular to the extensional direction, and developed at the restraining bends of transcurrent faults or in the overlapping zone of echelon faults (Benkhelil, 1989). Many of these rifts are half grabens that have reached the mature stage of rifting and contain very thick sediments on the faulted margin (Benkhelil, 1989; Binks and Fairhead, 1992).

The Mamfe Basin is the southernmost of these intracontinental rifts that formed at the southeastern end of a NW trending Pan-African lineament that extends to the Gao Basin in eastern Mali (**Fig. 2.1**). All the basins in NE Brazil and WCARS having mainly pre-Aptian sedimentary infill are believed to have been formed synchronously with the progressive northward propagation of the Southern Branch of the Atlantic rift (**Fig. 2.2**) from Neocomian to Barremian. NW-SE trending rifts in WCARS containing mostly post-Barremian sediments are thought to have been formed by NE-SW tensional regime that is believed to have been associated with the west to east opening of the Equatorial Atlantic in the Aptian-Albian (Rand and Mabesoone, 1982; Asmus and Baisch, 1983; Guiraud et al., 1992, Matos, 1992; Valença et al., 2003).

Contemporaneous magmatic activities in the Benue Trough region (e.g. Jos) and Potiguar Basin in northeast Brazil during the late Jurassic-early Cretaceous is believed to be the forerunner of the opening southern segment of the South Atlantic Ocean while Aptian-Albian magmatic activity in the region (e.g. Abakaliki) is believed to be associated with the opening of the equatorial segment of the Atlantic Ocean (Benkhelil, 1989; Ojoh, 1990; Guiraud and Maurin, 1992; Guiraud et al., 1992; Genik, 1993). Unlike in NBRS, sediments older than Jurassic have not been recorded in WCARS. The oldest dated sediments in the WCARS thus far are Hauterivian in age and found in the Hama-Koussou Basin in northern Cameroon (Dejax and Brunet, 1996).

The sedimentary infill of the WCARS range in age from Neocomian to Recent, and consists mostly of siliciclastic and volcaniclastics sediments of predominantly Cretaceous age that were deposited in fluvial, lacustrine, marine, and deltaic settings. The Cretaceous sediments infill of many of the basins is commonly 4 to 7 km thick and rarely exceeds 10 km (Genik, 1993). Post rift Cenozoic sediments when present, could be up to 4 km thick (Avbovbo et al., 1986, Genik, 1993).

2.2.2 Cretaceous tectono-sedimentary evolution

The early Cretaceous tectonic and sedimentary evolution of WCARS and coeval intracratonic basins in northeast Brazil (**Fig. 2.3**) was characterized by polyphase rifting resulting to a multi-stage tectono-sedimentary evolutionary history. Sedimentation pattern within these rift basins appear to have been influenced principally by rifting tectonics. On the basis of structural style and facies association, four major tectono-sedimentary evolutionary stages (pre-rift, syn-rift, erosion, and post-rift) have been recorded in rift basins in the Afro-Brazilian Depression (Murat, 1972; Benkhelil, 1989; Matos, 1992; Genik, 1993). These tectonic sequences record different stages of extensional and compressional deformation during the breakup of Gondwana and subsequent separation of South America from Africa from late Jurassic to Maastrichtian (Olade, 1975; Matsumoto, 1980; Rand and Mabesoone, 1982; Hoque and Nwajide, 1984; Reyment and Dingle, 1987; Popoff, 1988; Benkhelil, 1989; Adediran et al., 1991; Matos, 1992; Genik, 1993; Cainelli and Mohriak, 1999; Mabesoone, 2000; Basile et al., 2005; Garcia et al., 2005; Guiraud et al., 2005; Arthaud et al., 2008; Mohriak et al., 2012).

2.2.2.1 Pre-rift stage (Paleozoic-early Berriasian)

This stage corresponds to a period of basin initiation, regional subsidence and formation of the Afro-Brazilian Depression (ABD) and the beginning of reactivation of pre-existing Precambrian lineaments in the basement rocks. ABD was a large and shallow sag basin developed during the initial breakup of Gondwana, before the separation of South America from Africa (Da Rosa and Garcia, 2000; Garcia et al., 2005). There are no evidences of definitive rifting during this stage which marked the onset of lithospheric extension, small asthenospheric uplift and thinning of the upper mantle and continental crust of a stable mostly emergent platform. This was accompanied by minor incipient faulting and creation of local shallow depocenters in which alluvial and fluvial siliciclastics were deposited. The Sedimentary succession deposited during this stage lie unconformably on the crystalline Precambrian basement rocks and could be up to 300 m thick (Guiraud and Maurin, 1992; Genik, 1993). It comprises a wedge of polymictic matrix supported conglomerates and immature coarse and conglomeratic sandstones that accumulated in proximal and medial alluvial fans along fault lines. These basal sediments pass basin-ward into finer distal alluvial, braided and meandering streams facies. Tectonic activity slowed down considerably towards the end of this stage but subsidence and sedimentation continued. These sediments are commonly separated from the overlying rift succession by an erosional unconformity or a transitional contact (Petters, 1991; Mateer et al., 1992; Genik, 1993; Scotese et al., 1999; Catuneanu et al., 2005, Guiraud et al., 2005; Mohriak et al., 2012).

2.2.2.2 Syn-rift stage (Neocomian-Maastrichtian)

This was the main period of intracontinental rifting associated with increased and vigorous lithospheric extension and asthenospheric uplift. The geodynamic forces responsible for the breakup of Gondwana and separation of South America from Africa did not generate enough energy to rift the main body of the two continents beyond the aulacogen stage resulting to the formation of intracontinental rift basins (Fairhead and Binks, 1991; Binks and Fairhead, 1992; Genik, 1992, 1993; Guiraud et al., 2005).

Rifting was contemporaneous with subsidence and sedimentation. Two rifting episodes have been recognized in WCARS and NBRS and divided into 3 phases: syn-rift phase I, II and III (Matos, 1992; Genik, 1993; Cainelli and Mohriak, 1999; Valença et al., 2003; Guiraud et al., 2005).

Syn-rift phase I was from Neocomian to Albian, and resulted in 200-5000 m of subsidence (Genik, 1993). It ended in the Albian with a regional unconformity. Deposits of this phase are characterized by alluvial-fluvial deposits which passes upward into fluvio-lacustrine from the Barremian to end of Albian.

Syn-rift phase II was from late Albian to Campanian. It began with a short-lived period of rifting in early Cenomanian that was followed by a long period of thermo-tectonic subsidence of up to 6000 m (Genik, 1993). Regional subsidence during this phase resulted to marine transgression from the South Atlantic through the Benue Trough, and from the Tethys through Algeria and Mali (Reyment, 1972, 1980; Petters;

1978a,b; Reyment and Dingle, 1987; Petters and Ekweozor, 1982a,b; Benkhelil, 1989). This marine transgression coincides with Haq et al. (1987) late Cretaceous eustatic sea level high stand. The highest extend of the transgression was in Santonian. Regression began in the Santonian due to epeirogenic uplift. Rift phase II was ended by a regional unconformity.

Syn-rift phase III from Maastrichtian to Early Oligocene resulted in up to 3000 m thermo-tectonic subsidence in WARS (Genik, 1993). This rifting phase was terminated by regional unconformity in the Eocene. This Eocene regional unconformity was followed by the Post-rift phase from Miocene to Recent (Guiraud et al., 1992; Genik, 1993).

The West and Central African rift systems differs from the East African rift system (EARS, Chorowicz, 2005) in that the former is associated with relatively minor magmatic activity of which the volcanics of the Benue Trough are the best known examples (Fitton, 1980).

2.2.3 Magmatism

The Jos, Benue, and Cameroon Volcanic Line magmatic provinces represent three landmarks in the plate tectonic evolution of Nigeria and Cameroon. The transitional alkaline and theolitic magmatic province of the Benue Trough constitutes a spatial link between the alkaline to peralkaline plutonic province of the Jos Plateau to the north, and the alkaline Cameroon Volcanic Line to the south (Maluski et al., 1995).

2.2.3.1 Benue Trough

The Benue Trough has been tectonically active since early Cretaceous but post Cretaceous activity was shifted to the Cameroon Volcanic Line (Fitton, 1980). Three episodes of magmatic activity have been recognised from within the Benue Trough region which corresponds to different rifting episodes (Fitton, 1980; Benkhelil, 1989; Maluski et al., 1995).

A late Jurassic to Albian (147 to 106 Ma) phase was marked by widespread magmatic activity throughout the trough. Volcanic products of this phase are common in the northern Benue Trough where they are represented by alkaline and theolitic transitional basalts.

The Cenomanian to Santonian (97 to 81 Ma) phase has been recognized only in the southern Benue (e.g. Obubra) and is represented by diverse alkaline rocks such as basalts, dolerites, phonolites, trachytes, rhyolites, lamprophyres, and tephrites (Fairhead et al., 1991).

A late Maastrichtian to Eocene (68 to 49 Ma) phase was also restricted to the Southern Benue and characterized by alkaline or theolitic hypabyssal intrusions. Although the Benue Trough region has been tectonically active since early Cretaceous to Paleogene, post Mesozoic activity was shifted to the Cameroon Volcanic Line.

2.2.3.2 Cameroon Volcanic Line (CVL)

The Cameroon Volcanic Line (CVL) is a 1600 km long SW-NE trending Y-shaped chain of genetically related Cenozoic transitional to strongly alkaline intraplate volcanoes that extends from the Atlantic island of Annobon (formerly known as Pagalu), across the Gulf of Guinea towards the centre of the African continent (Fitton, 1980; Fitton and Dunlop, 1985; Njilah 1991; Marzoli et al., 2000, Rankenburg et al., 2005; Elsheikh et al., 2014; Nkono et al., 2014). It is one of the few volcanic chains in the world that are characterized by both oceanic and continental volcanism (Njilah et al., 2004). The continental sector of this chain comprises from south to north of the following mountains: Etindi, Cameroon, Manengouba, Bamboutus, Oku, Ngaoundere, and Biu plateau at its northern end (**Fig. 2.5a**). Mount Cameroon that is located about 154 km east of the Mamfe Basin is the only volcano in the continental sector that has been active in the last centuries, with the most recent activity occurring in 2001 (Njilah et al., 2004).

Earliest magmatism along the line is represented by syenite and granitic ring complexes ranging in age from 65 to 35 Ma. The oldest extrusive rocks are 65 Ma on the continental sector, and 35 Ma on the oceanic sector (Fairhead, 1988). Cenozoic volcanic cones are found in virtually all parts of the line and in the Mamfe Basin. Products of volcanism in the CVL have evolved from olivine basalt and trachy-andesites in the late Cretaceous/Paleocene through phonolites and trachytes in the Miocene, to basalt from Quaternary to present day (Maluski et al., 1995; Ngako et al., 2006). Radiometric dating of basalt samples from eastern Abakaliki Basin (Obubra) and western Mamfe Basin (Ikom) gave ages of 82.0 ± 4 Ma for Obubra and 10.5± 1.2 Ma for Ikom (Fairhead et al., 1991). No age determination has been carried out on volcanic rocks in the eastern part of the basin in and around Mamfe.

Volcanism along the continental sector of the CVL shows a NE to SW migration of magmatic activity with time. This southwest migration is believed to be due to a NE movement of the African plate above a deep-seated thermal anomaly (Fitton and Dunlop, 1985; Marzoli et al., 2000; Ngako et al., 2006). Volcanism on the continental sector tends to be associated with the Ngaoundere fracture zone, and has been accompanied by regional uplift of about 1 km but without any apparent evidence of rift faulting (Fitton, 1980; Browne and Fairhead, 1983).

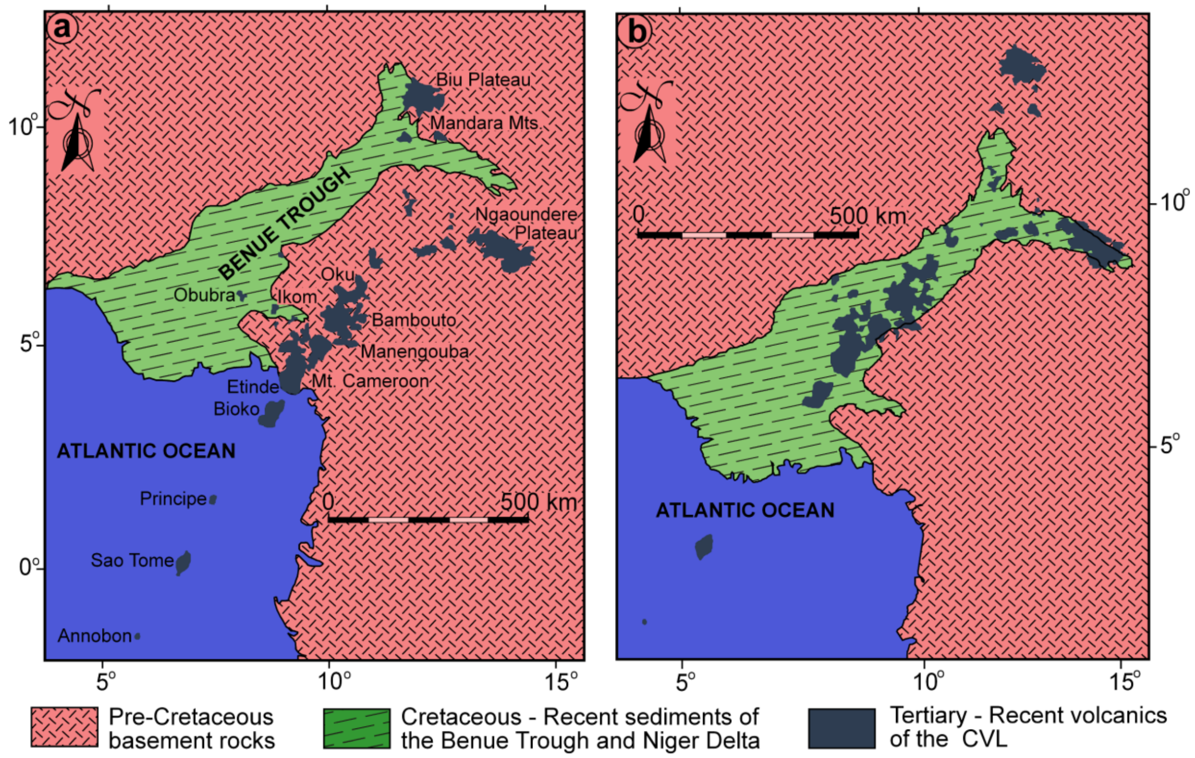

Figure 2.5. (**a**).Geological sketch-map of part of the eastern West Africa showing similarity in the trend of the Benue Trough and volcanoes of the CVL. (**b**)**.** The CVL superimposed on the Benue Trough by rotating the former clockwise relative to the latter by 7° about a pole at 12.2° N, 30.2° E (redrawn from Fitton, 1980).

2.2.3.3 Relation between the Benue Trough and the CVL

The remarkable similarity in the shape, magmatic activity, and size of the Benue Trough and the CVL such that they can perfectly be superimposed (**Fig. 2.5b**) by a 7° rotation of one relative to the other about a pole in Sudan suggests a genetic relation between these two geologic features (Fitton, 1980). The geometrical coincidence is thought to be as a result of the displacement of the African plate such that the “Y”-shaped hotspot in the asthenosphere which was supposed to have been positioned beneath the Benue Trough now lies beneath Cameroon. The evolution of both features must thus have been controlled by the same forces (Wright, 1968). The

Benue Trough and the CVL are thus regarded as complimentary features and magmas that are destined for the Benue rift reach the surface as the CVL instead. This interpretation is supported by the general NE-SW decrease in the age and the similarity in the geochemical and isotopic composition of the alkali basalts of the Benue Trough and those of the CVL (Halliday et al., 1988, Maluski et al., 1995).

According to a model by Fitton (1980), the displacement of magmatic activity from the Benue Trough to the CVL occurred between 80-65 Ma. The West African rift system according to this model is a classic example of a rift system interrupted in the cause of its development. However, despite the long history of rift valley-type magmatism and associated uplift, the CVL is practically devoid of sediments and has never developed a graben structure that is comparable to that of the East African rift. The CVL could be under tension and thus be regarded as a truly “active” rift valley (in comparison with “passive”) rift system (Fitton, 1980). Uplift by more than 1000 m along the southern flank of the Benue Trough is thought to be a direct consequence of its genetic relation with the CVL.

2.3 Regional Geology

2.3.1 Overview of the geology of Cameroon and Nigeria

The geology of Cameroon and Nigeria is characterised by a diverse suite of rocks that ranges in age from Precambrian to Recent (**Fig. 2.6** and **2.7**). These rocks can broadly be classified into three categories: pre-Ordovician crystalline Basement Complex, Jurassic to Recent volcanic rocks and Cretaceous to Recent sediments.

2.3.1.1 Crystalline Basement Complex

The crystalline Basement Complex lies within the Pan-African mobile belt, and underlies most of the territory of Cameroon and Nigeria. It is exposed in more than 50% of Nigeria and more than 80% Cameroon (**Fig. 2.6** and **2.7**). These rocks range in age from Neoproterozoic to Upper Cambrian. They are made up mostly of quartzo-feldspathic migmatites and gneisses with numerous Older Granites intrusions and occasional quartzites, marbles and amphibolites (Oyawoye, 1972; Avbovbo, 1980; Ofoegbu, 1985; Toteu et al., 2004).

The Basement is in some parts of the countries covered by thick Mesozoic to Recent sediments or volcanics. The volcanic rocks are divisible into three magmatic provinces that show a general north-to-south migration in time and space. The oldest (Jurassic) volcanic rocks are restricted to the Jos Plateau while Cretaceous to Recent magmatism occurs in the Benue Trough and Cameroon volcanic line (**Fig. 2.7**; Maluski et al. 1995). A brief account of Mesozoic-Cenozoic volcanism in the region has already been provided in section 2.2.3.

2.3.1.2 Sedimentary basins

Sedimentary rocks occur in 27 sedimentary basins that are found within the Basement Complex of Cameroon and Nigeria. These sedimentary basins occur as either isolated paleodepressions or are a part of a larger continuous paleodepression that is separated into subbasins by basement high, volcanics, or political boundaries (Hourcq, 1956; Avbovbo, 1980). The sizes of these basins vary from a few square kilometres to thousands of square kilometres (Hourcq, 1956).

Most of the basins have half-graben geometry and their origin and evolution are related to the West and Central African rift system (WCARS). These basins have been broadly classified into two groups: coastal basins and inland (interior) basins (**Fig. 2.7**). The sedimentary infill of these basins unconformably overlies the crystalline Basement Complex, and comprises mainly of siliciclastics that range in age from Neocomian to Recent (**Fig. 2.8**). As of date, sediments older than Neocomian have not been reported from either Cameroon or Nigeria but are nevertheless suspected to occur at depth in the centre of some of the basins. The sedimentary infill of the basins varies in thickness from a few tens of metres to as much as 6000 m (Reyment, 1965; Petters and Ekweozor, 1982a; Petters, 1991; Petters et al., 1995; Benkhelil, 1989; Okeke et al., 1987; Guiraud, 1990; Maurin and Guiraud, 1990; Ojoh, 1990; Dejax and Brunet, 1996; Reijers and Petters, 1997; Hell et al., 2000; Obaje et al., 2004; Akande et al., 2005; Oboh-Ikuenobe et al., 2005; Ntamak-Nida et al., 2008).

The coastal basins are situated along the continental margins of the Atlantic coast and are sometimes referred to as the coastal basins of the Gulf of Guinea (Adediran et al., 1991). These coastal basins occupy the location of the intersection of the South Atlantic rift system triple junction (**Fig. 2.2** and **2.3**). Their sedimentary infilling are mostly marine and range in age from Neocomian to Recent (Reyment, 1965; Murat, 1972; Petters et al., 1995; Jan du Chêne, 2000; Ntamak-Nida et al., 2008).

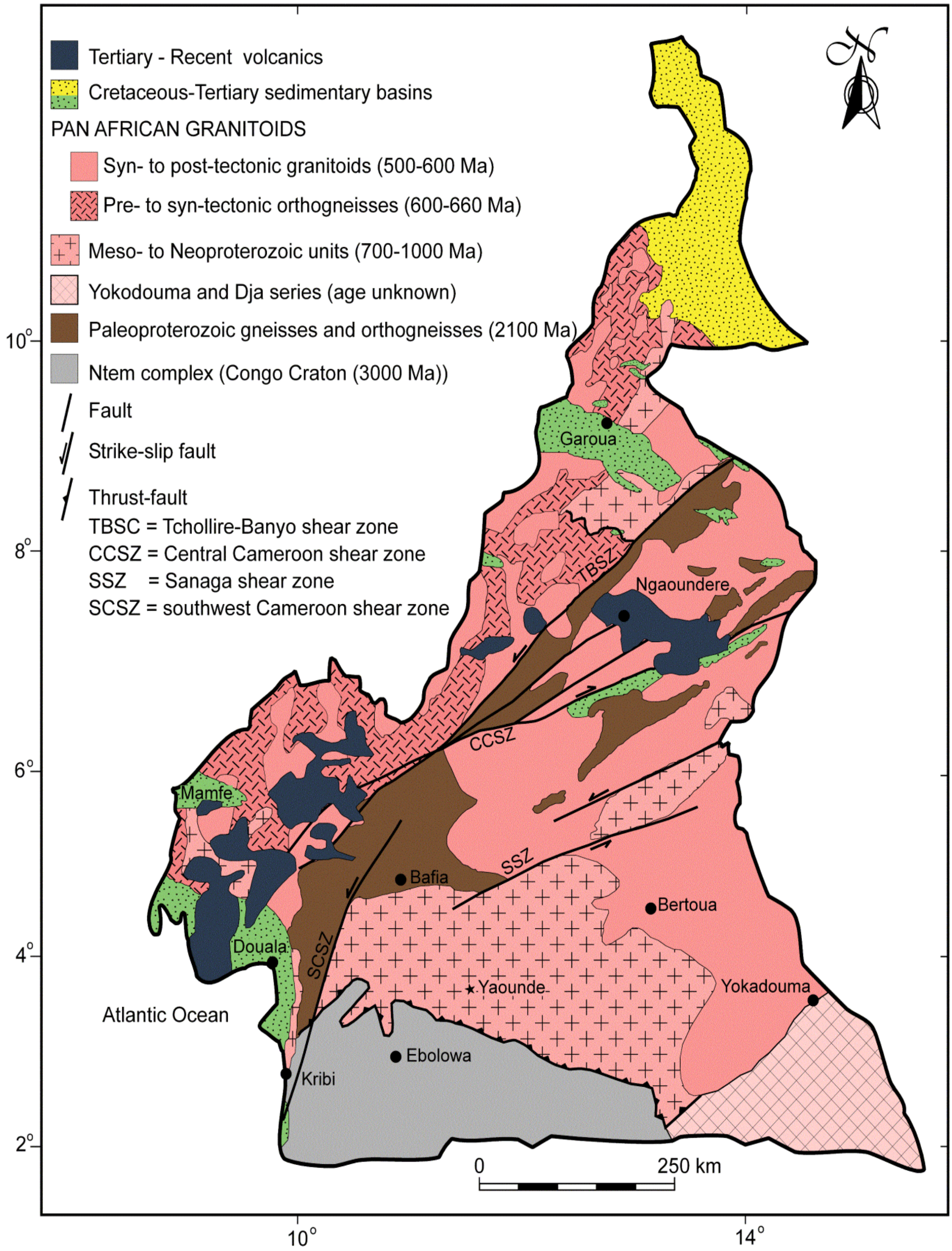

Figure 2.6. Simplified geological map of Cameroon (modified from Toteu et al., 2001).

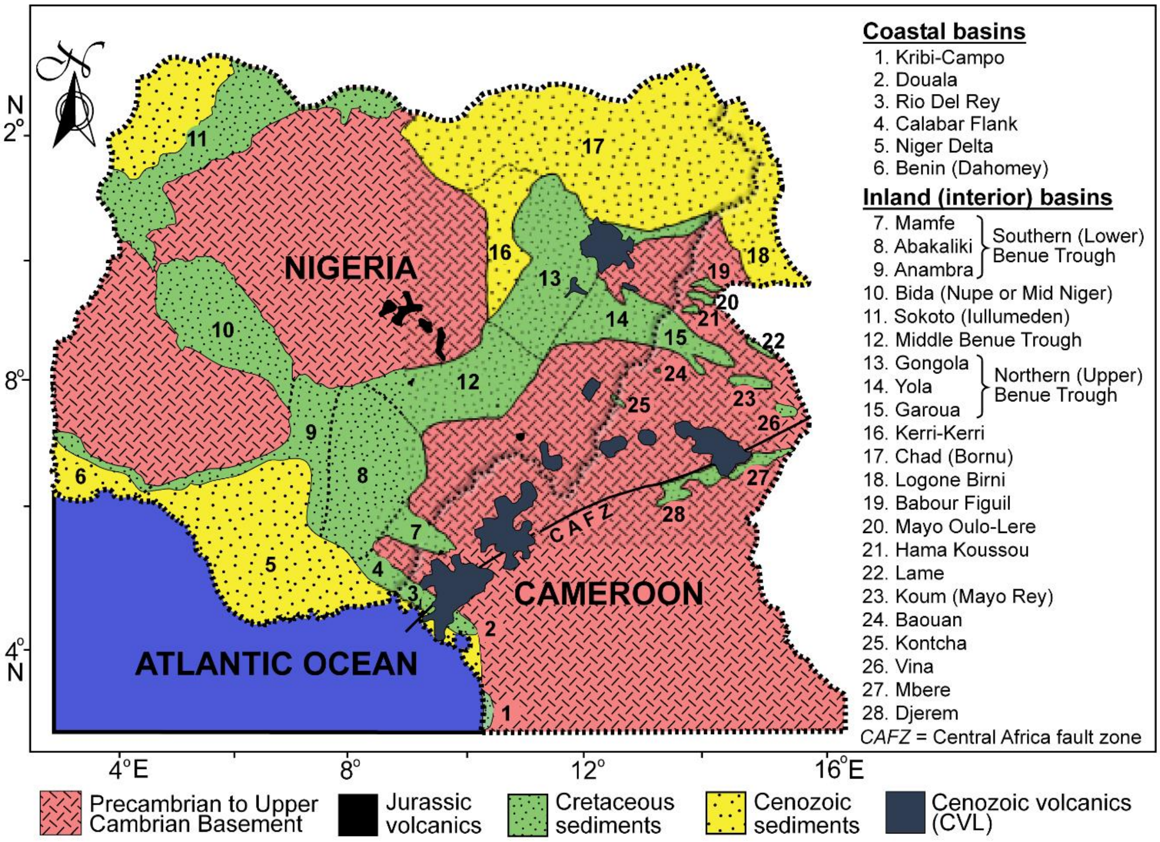

Figure 2.7. Geological sketch-map of Cameroon and Nigeria showing the distribution of sedimentary basins, and the Cameroon Volcanic Line (modified from Avbovbo, 1980; Maurin and Guiraud, 1990; Toteu et al., 2001).

The inland (interior) basins are a suite of intracontinental rifts that belong to the WCARS, the failed arm of the South Atlantic rift system. Those that contain pre-Aptian sediments are believed to have resulted from the northward propagation of the Southern Atlantic rift, while those lacking Aptian sediments were formed in connection to the opening of the Equatorial rift and Benue Trough. Basins belonging to CARS occur in north and northeastern Cameroon and are filled with mainly continental sediments.

The Benue Trough is the main interior basin. Its sedimentary succession is 5000-6000 m thick and ranges in age from Aptian to Maastrichtian (Allix et al., 1981; Benkhelil, 1989; Benkhelil et al., 1998; Ojoh, 1990; Obaje et al., 1994; Abubakar et al., 2006). The other interior basins are considered to be satellite basins that served as forerunners to the formation of the trough (Dejax and Brunet, 1996). The trough is bounded in the NE and SW by Tertiary to Recent sediments of the Chad Basin and Niger Delta.

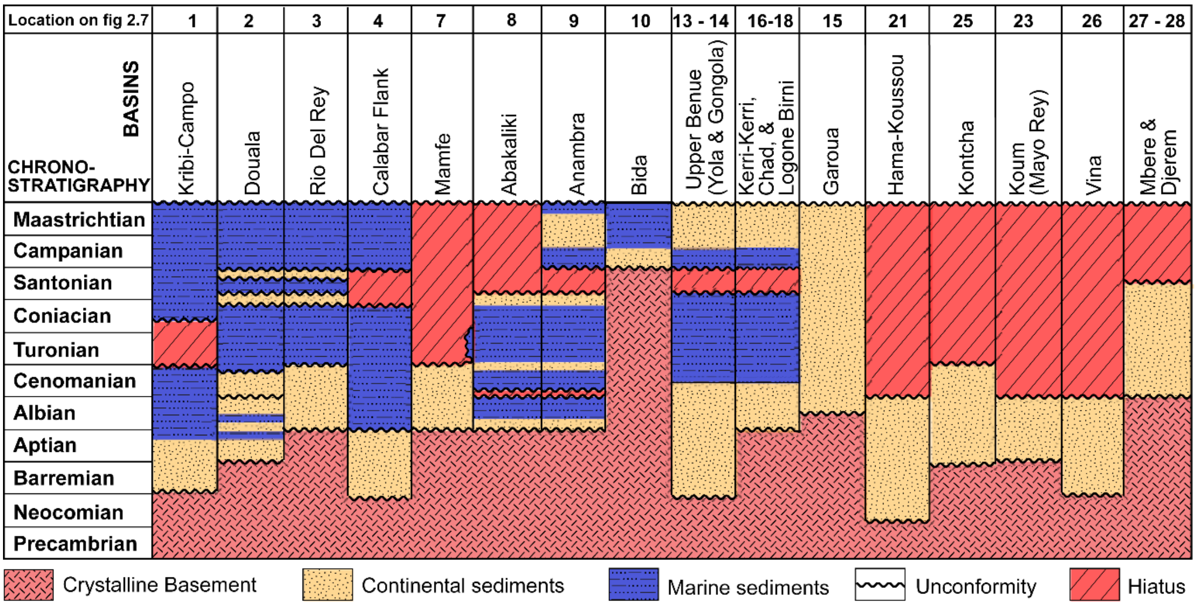

Figure 2.8. Cretaceous sedimentary successions in selected sedimentary basins in Cameroon and Nigeria (compiled from Reyment, 1965; Benkhelil, 1989; Guiraud, 1990; Maurin and Guiraud, 1990; Ojoh, 1990; Petters, 1991, 1995; Mateer et al., 1992; Dejax and Brunet, 1996; Ala and Selley, 1997; Reijers and Petters, 1997; Akande et al., 2005, 2012; Obaje et al., 2004; Brownfield and Charpentier, 2006; Ntamak-Nida et al., 2008, 2010)

The Benue Trough is made up of several subbasins and is broadly divisible based on geography, stratigraphy and structural features into three main domains: the southern (lower), middle, and northern (upper) Benue Trough respectively. The southern and middle Benue Trough are characterized by flat to gently undulating topography, while the northern part is marked by a rugged terrain arising from many Tertiary volcanic plugs (Benkhelil, 1989).

The southern Benue Trough (SBT, **Fig. 2.7**) is made up of three subbasins which from east to west are: Mamfe, Abakaliki, and Anambra Basins respectively (Odigi and Amajor, 2008). It extends from the northern limit of the Niger Delta to Gboko and Makurdi area where it is separated from the middle Benue Trough by the “Gboko-Line” (Whiteman, 1982; Obaje et al., 2004). The middle Benue Trough comprises of two subbasins: Keana and Bashar-Muri Basins in the south and north respectively. The northern (upper) Benue Trough has four subbasins: Lamurde-Lau; Kerri-Kerri, Gongola, and Yola/Garoua Basins respectively (**Fig. 2.7**).

2.3.2 Geology of SE Nigeria and SW Cameroon

The area in southeastern Nigerian and southwestern Cameroon that lies within latitude 4º to 7º 20’ N and longitude 7º 10’ to 9º 35’ E (**Fig. 2.9**) is located within the equatorial domain of the eastern Gulf of Guinea, and is referred to in this study as the eastern Gulf of Guinea sub region. It is comprised of the southern Benue Trough (Mamfe, Abakaliki, and Anambra Basins), eastern Niger Delta, Calabar Flank to northern Douala Basin, Oban and Bamenda Massifs.

2.3.2.1 Crystalline Basement Complex

The southern Benue Trough is underlain and bordered by crystalline basement rocks that crop out as massifs. The Bamenda (or Obudu) and Oban Massifs bordering the Mamfe Basin to the north and south respectively, are the southern part of the Adamawa uplift. These massifs according Iliya and Bassey (1993) were continuous in the pre-Cretaceous time. The Adamawa uplift is part of the Central African Fold Belt (CAFB) that extends from eastern Nigeria to the northern border of the Congo craton (Penaye et al., 1993).

The Basement complex is made up predominantly of migmatitic metasediments. These metasediments were derived from rocks believed to have been eroded from Paleoproterozoic and Neoarchean basement rocks and deposited in a passive margin environment at the northern edge of the Congo craton (Ekwueme and Kröner, 2006; Njanko et al., 2006). The metasediments are made up of migmatites, gneisses, and schists that resulted from a regional granulite-facies metamorphism during the Pan-African thermotectonic event (600 ± 150 Ma; Ekwueme and Onyeagocha, 1986; Ekwueme et al., 1991, 2000; Toteu et al., 2001; Ferré et al., 2002).

The Neoproterozoic unit (700-1000 Ma) comprises of volcano-sedimentary migmatitic schists and gneisses that are intruded by pre-to syn-tectonic orthogneisses (600-660 Ma), granites and granodiorites (**Fig. 2.6**). The granitoids have high calc-alkaline affinities (Njanko et al., 2006). The late- to post-tectonic granitoids (500-600 Ma) comprise of dolerites and pegmatites dykes and veins that were emplaced during the waning phase of the Pan-African events (Ekwueme et al., 1991; Toteu et al., 2001).

The schists are of four types: fine-grained quartz-mica schist, medium-grained garnet-mica schist, and migmatitic coarse-grained garnet-sillimanite and kyanite-sillimanite schists. The gneisses are quartzo-feldspathic and mostly coarse-grained and consist of four varieties: banded gneiss, granite gneiss, migmatitic gneiss, kyanite gneiss and biotite-hornblende gneiss.

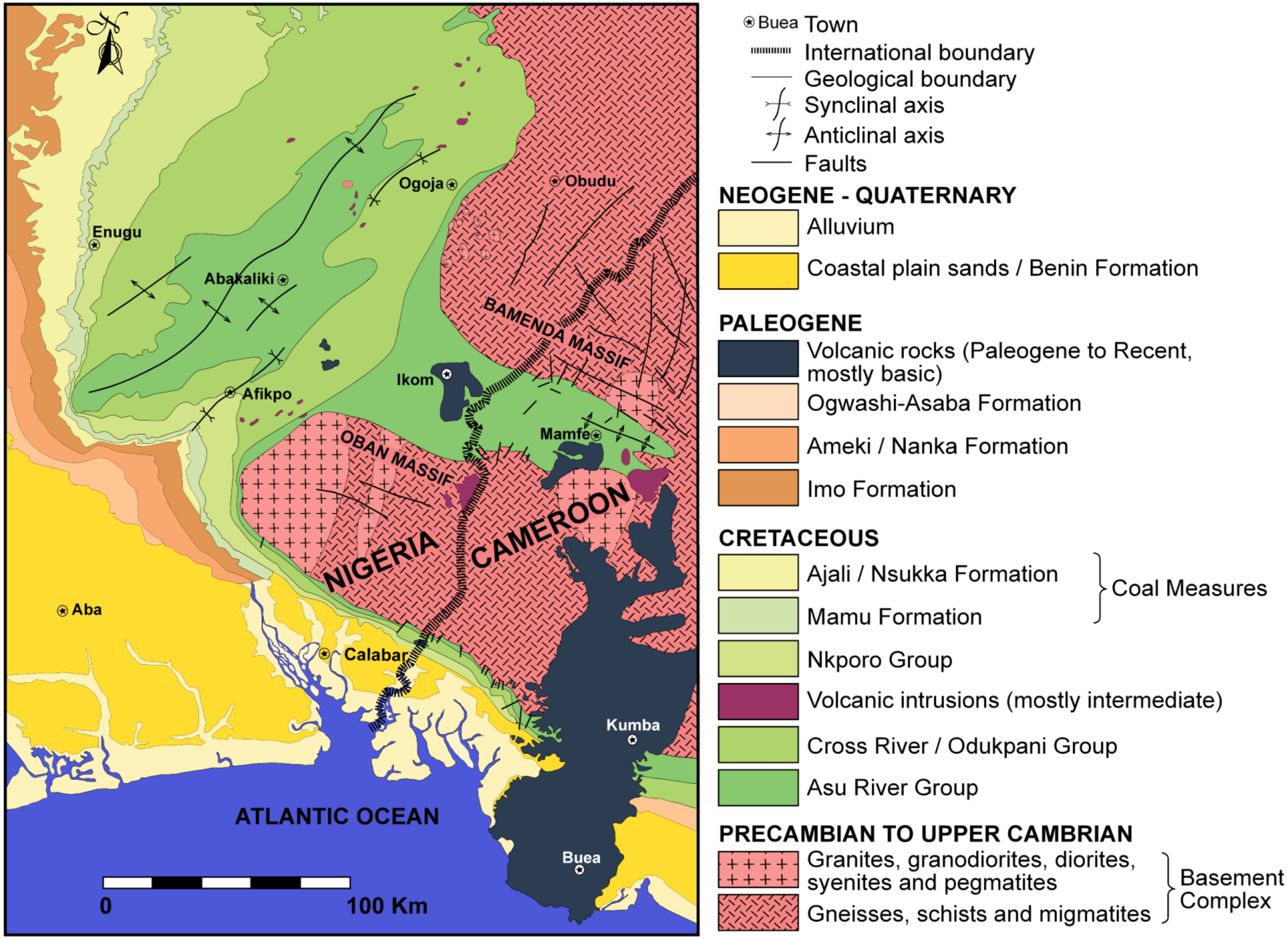

Figure 2.9. Geological map of southeastern Nigeria and part of southwestern Cameroon (modified from Dumort, 1968; Gerbeth et al., 1976; and Toteu et al., 2001).

Other minor rock types that are found within the migmatitic schist-gneiss complex make up the Younger Granites and include anatectic granites, biotite-muscovite granites, coarse-grained hornblende-pyroxene gneisses (charnockites) that are probably of andesite volcanic suite parentage, diorites, amphibolites, quartzite and leptynites. As a whole, the basement rocks within this region have a predominantly N-S to NE-SW foliation trend (Toteu et al. 2004; Ekwueme and Kröner, 2006; Arthaud et al., 2008; Dada, 2008).

2.3.2.2 Cretaceous sedimentary evolution and stratigraphy

There are four coastal basins (Douala, Rio Del Rey, Calabar Flank, Niger Delta), and three inland basins (Mamfe, Abakaliki and the Anambra) in the eastern Gulf of Guinea region (**Fig. 2.6** and **2.9**). All the inland basins are physically and stratigraphically related and their sedimentary infill varies in thickness from a few meters to over 6000 m (**Fig. 2.10** and **2.11;** Offodile, 1976; Petters et al., 1987; Ojoh,

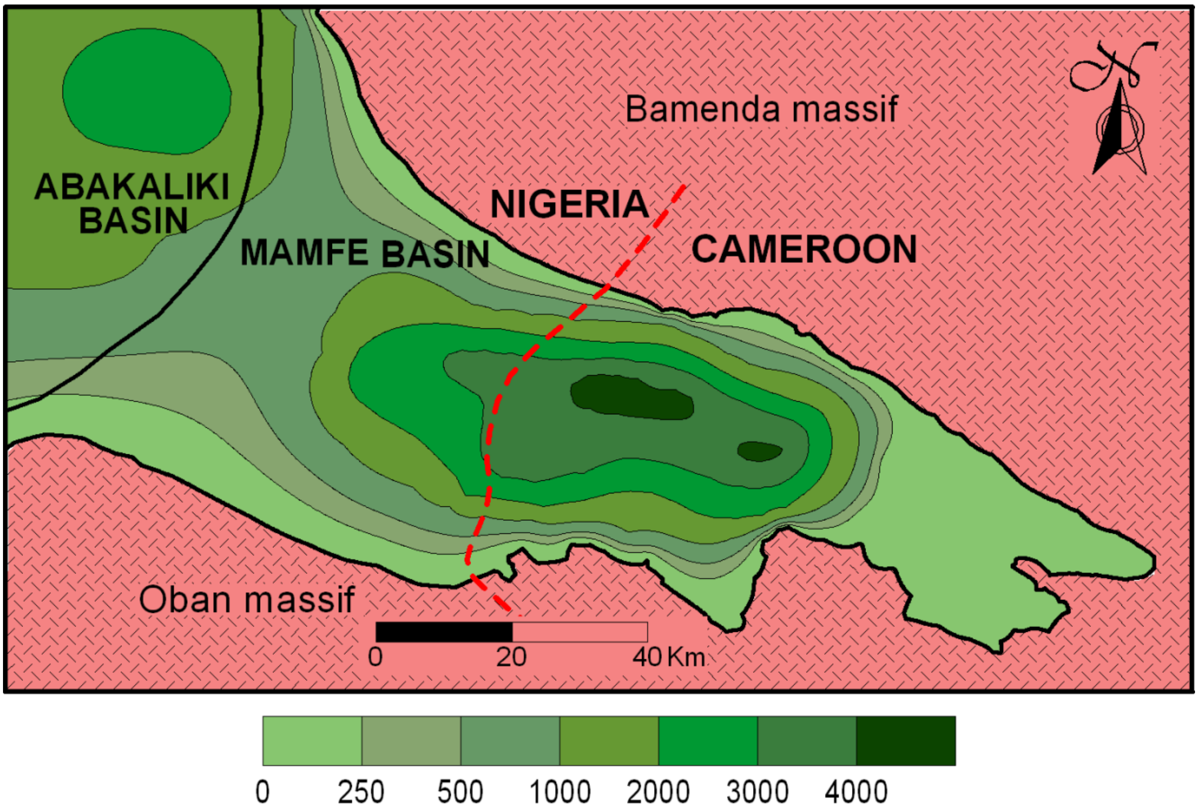

Figure 2.10. Isopach map of eastern Abakaliki Basin and the Mamfe Basin based on gravity data (modified from Petters et al., 1987; Heine, 2007).

1990; Obaje et al. 2004; Heine, 2007).

The sub region is generally poor in good natural outcrops because of its near flat topography, thick vegetation and alluvial cover, and equatorial climate. Most of the outcrops are highly weathered and limited in thickness and areal extend. Stratigraphic units are mostly composite sections that are named after a type locality or type area where best exposures of the unit are found. Type sections are rare because of incomplete exposure of units in any of the outcrops.

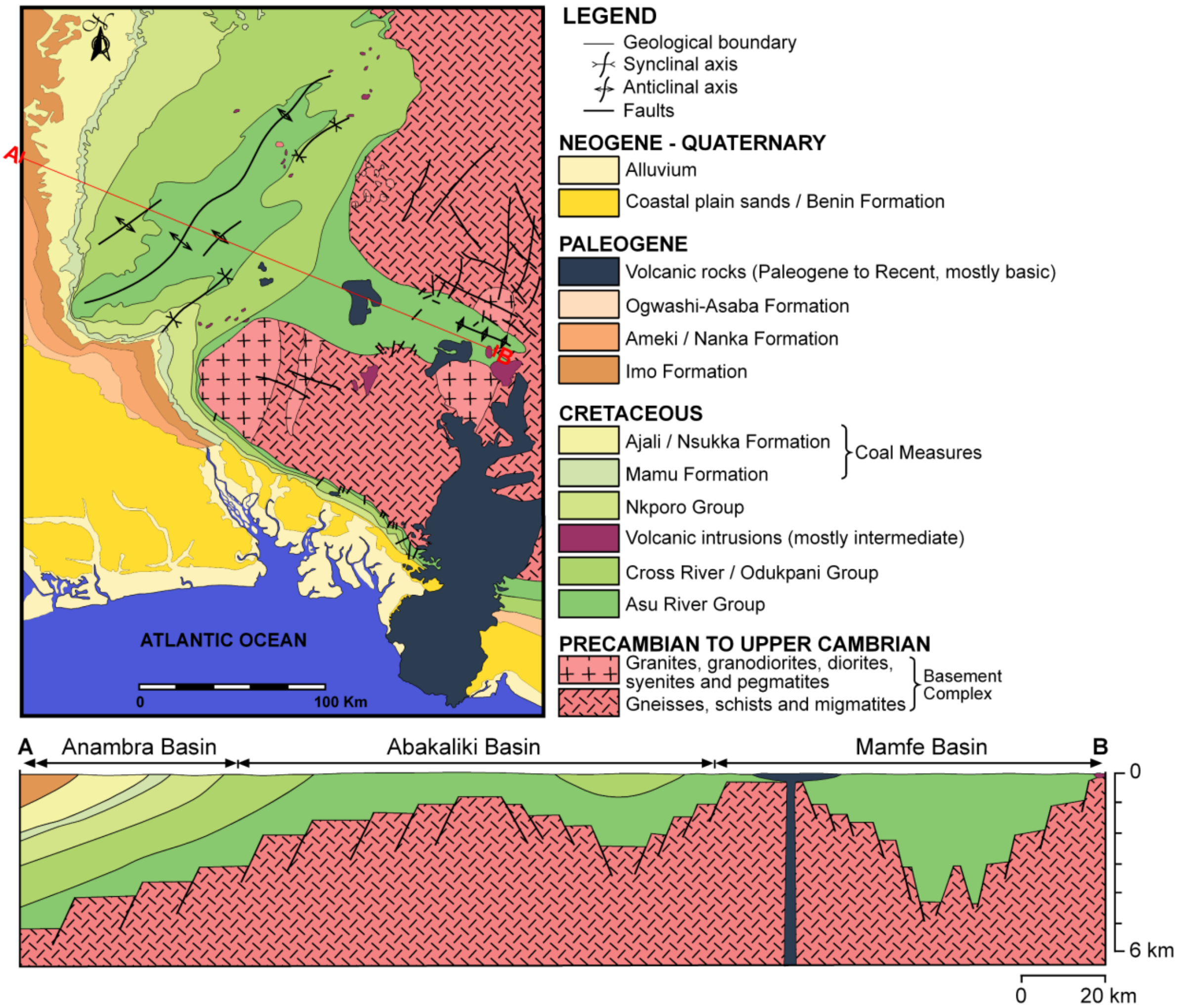

Figure 2.11. NW-SE schematic cross-section across the southern Benue Trough from Anambra Basin to Mamfe Basin. (sediment thickness based on Petters et al., 1987; and Heine, 2007).

Stratigraphic subdivision of the poorly exposed basin infill has been based on either lithologic similarity or age, which has led to much confusion in the definition, ranking, and nomenclature of stratigraphic units (Petters and Ekweozor, 1982a; Agumanu, 1989). Some researchers refer to a unit as a formation while others refer to the same unit as a group. The same stratigraphic unit might be assigned a different name in a different area, or could be subdivided into different stratigraphic units based on its age. As a consequence of scarcity of good exposures, inadequate stratigraphic and petrologic description, many stratigraphic subdivisions and nomenclature (both in name and hierarchy of unit) have been proposed by different researchers for the Cretaceous sediments in the southern Benue Trough (e.g. Reyment, 1965; Le Fur, 1965; Dessauvagie, 1974; Petters and Ekweozor, 1982b; Whiteman, 1982; Agumanu, 1989; Ojoh, 1990; Petters et al., 1995; Reijers, 1996, 1998; Reijers and Petters, 1997; Ajonina et al., 2001; Eyong, 2003; Abolo, 2008).

Despite the diversity in the stratigraphic nomenclature, there is a consensus that the Cretaceous sedimentary succession of the southern Benue Trough can be differentiated into three mappable sedimentary cycles that are separated by late Albian-early Cenomanian, and mid-late Santonian unconformities. These sedimentary cycles are third order depositional sequences that represent different episodes of marine transgression and regression in the trough (Murat, 1972; Reyment, 1980; Petters and Ekweozor, 1982a). These depositional sequences comprise from bottom to top of Asu River Group, Cross River Group, and the post Santonian coal measures.

This study has adopted the lithostratigraphic and chronostratigraphic subdivisions and nomenclature proposed by Petters and Ekweozor (1982a), Petters (1983, 1991, 1995); Benkhelil (1989); Akande and Viczian (1995); Reijers (1998) and Obaje (2009). The adapted lithostratigraphy successions in the Calabar Flank and southern Benue Trough (Anambra, Abakaliki, and Mamfe Basins) is shown in **Figure 2.12**.

The Abakaliki Anticlinorium is the main structural unit of the southern Benue Trough. It is composed of tightly folded Albian to Santonian sediments that are intruded by magmatic rocks. The anticlinorium is bounded to the NW by relatively undeformed Late Cretaceous sediments of the Anambra Basin, in the east by Early Cretaceous sediments of the Mamfe Basin, and in the south by the complimentary Afikpo syncline, the Calabar Flank and the Niger Delta. The Niger Delta is filled mainly by post Cretaceous sediments and is thus not considered in this review.

The Calabar Flank is located between the northeastern extremities of the Niger Delta and the southwestern border of the Oban Massif. It is a southeast trending segment of the SE flank of the southern Benue Trough along the Atlantic coast. It extends into the Republic of Cameroon where it is referred to as the Rio Del Rey and Douala Basins (2-4 of **Fig**. **2.7**). This coastal basin is generally not considered to be part of the southern Benue Trough even though it is physically, stratigraphically and structurally linked to it (Reijers, 1998). The sedimentary succession in the Calabar

Flank range in age from Neocomian to Recent, and has a total thickness of over 3500 m (Nyong and Ramanathan, 1985; Oti and Koch, 1990; Reijers and Petters, 1997).

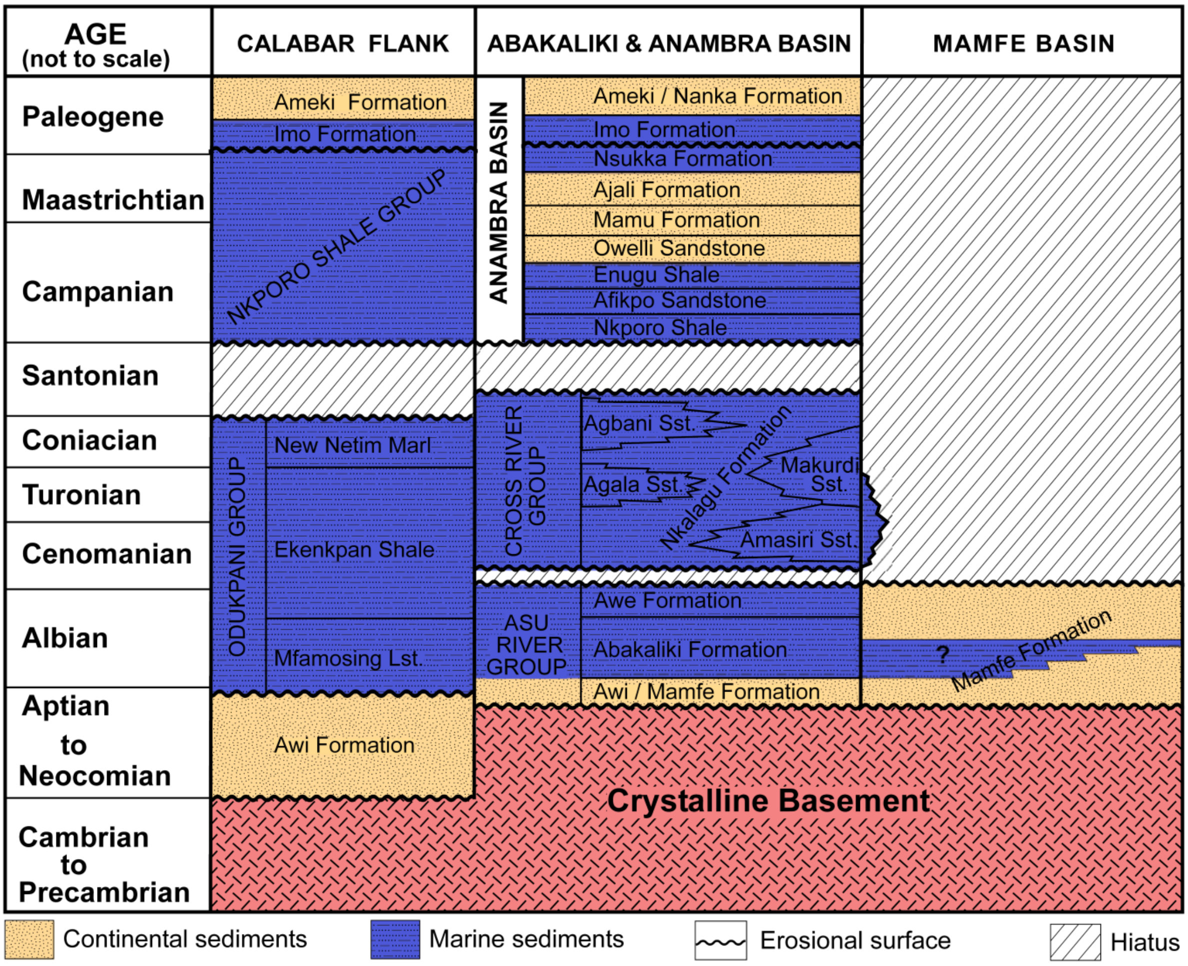

Figure 2.12. Cretaceous-Paleogene stratigraphic succession in the Calabar Flank, Abakaliki, Anambra and Mamfe Basins (modified from Petters and Ekweozor, 1982a; Petters, 1983, 1991; Benkhelil, 1989; Akande and Viczian, 1995; Reijers, 1998; and Obaje, 2009)

2.3.2.1 Asu River Group

Sediments that make up the Asu River Group are the initial clastic infill of the southern and middle Benue Trough, and represent the first depositional sequence that is enclosed by the basement and early Cenomanian unconformities. The type section is Asu River near Abakaliki (Reyment, 1965). Its sediments vary in thickness from 1500 m in the southern Benue Trough to 3100 m in the middle Benue Trough (Offodile, 1976; Adighije, 1981; Ofoegbu, 1985; Benkhelil, 1989; Akande and Viczian, 1995; Obaje et al., 2004). The group consists of sandstones, shales, siltstones and limestones of Albian age that are intruded by Cenomanian and Santonian magmatic rocks (Benkhelil, 1989). The group is subdivided into three formations which from bottom to top are Mamfe/Awi, Abakaliki, and Awe Formations.

2.3.2.1.1 Mamfe Formation

The sedimentary infill of the Mamfe Basin is collectively and formally referred to as the Mamfe Formation. The type locality of this formation is at the banks of River Manyu in Mamfe (Wilson, 1928; Reyment, 1954, 1965). This formation constitutes the basal unit of the Asu River Group, and is considered to be either diachronous or contemporaneous with the Awi Formation that outcrops in the Calabar Flank (Dessauvagie, 1974; Adeleye and Fayose, 1978; Petters and Ekweozor, 1982a; Whiteman, 1982). The Mamfe Formation exhibits cyclic sedimentation. It consists mostly of non-to-poorly fossiliferous shales that vary in colour from green to black, medium to coarse-grained, poorly sorted and sometimes cross stratified arkosic sandstones; conglomerates; siltstones; volcaniclastics as well as evaporites (Wilson, 1928; Reyment, 1954, 1965; Le Fur, 1965; Dumort, 1968; Ajonina and Bassey, 1997; Ajonina et al., 2001, 2006; Bassey and Ajonina, 2002; Eseme et al., 2002; Eyong, 2003; Abolo, 2008). This formation has variously and informally been subdivided into five series (Le Fur, 1965); a lower and upper member (Ajonina and Bassey, 1997; Bassey and Ajonina, 2002; Bassey et al., 2013), three members (Abolo, 2008), and four formations (Eyong, 2003).

The environment of deposition of sediments belonging to this formation is very controversial and has been described as marine, transitional, fluvio-deltaic and lacustrine (Wilson, 1928; Reyment, 1965; Petters, 1978a & b, 1991, 1995; Wright et al, 1985; Ajonina et al., 2001). A maximum thickness of over 4500 m has been established for this formation at the centre of the Mamfe Embayment (Petters et al., 1987; Hell et al., 2000; Heine, 2007). The sediments have been faulted and moderately to strongly folded (maximum dip of 50°) and have an approximately east – west fold axis (Reyment, 1965; Ajonina, 1997). The age of this formation is believed to range from Albian to Turonian (Reyment, 1954, 1965; Adeleye, 1975; Uzuakpunwa, 1974, 1980; Whiteman, 1982; Hoque, 1984; Ojoh, 1990; Petters, 1991; Abolo, 2008). The shales near the confluence of the Mamfe Basin with the Benue Trough are marginal marine deposits and considered to be Cenomanian-Turonian in age (Petters, 1991).

2.3.2.1.2 Awi Formation

It is the basal facies of the Asu River Group in the Calabar Flank where it outcrops and lies unconformably on the Oban Massif. The type section of this formation is located about 9 km south of Awi village along the Calabar-Odukpani–Awi road (Adeleye and Fayose, 1978). The Awi Formation is about 50 m thick, and lithologically and structurally similar to the Mamfe Formation. It is cyclothermic and made up mostly of brownish to grey, angular, poorly sorted, very coarse to very fine-grained fining upward arkosic sandstones; conglomerates; siltstones; black poorly fossiliferous shales and occasionally lignitized mudstones. Its environment of deposition is fluvio-deltaic (Adeleye and Fayose, 1978; Nton, 1990). It is believed to range in age from late Neocomian to late Aptian (Murat, 1972; Adeleye and Fayose, 1978; Reijers, 1998). The Awi Formation is overlain by late Aptian-middle Albian shallow marine karstified platform carbonates (Mfamosing Limestone Formation) that represents the earliest marine sediments in the eastern Gulf of Guinea (Petters, 1982, 1983, 1991, Reijers, 1998).

2.3.2.1.3 Abakaliki Formation

The Abakaliki Formation is comprised of alternating succession thick shales, thin karstic limestone and siltstones with subordinate sandstones. This formation is believed to have been deposited during the first marine transgression from the southern Atlantic Ocean into the southern and middle Benue Trough between middle and late Albian. During this time, the Abakaliki Basin was the site of deep basin deposition while carbonates and sandstones were deposited on the basin margins and the Anambra Basin platform, and deltaic deposition in the middle Benue Trough (Murat, 1972; Petters, 1978b; Benkhelil, 1989; Ojoh, 1990). Subsidence in the Abakaliki is believed to have lasted until Santonian at which time compressional movements folded and uplifted the basin and forced its depocenter to migrate to the Anambra basin which began to subside from then onward. The Abakaliki Formation is dated as middle Albian on the basis of ammonite fauna and microflora (Reyment, 1965; Reyment and Tait, 1972; Offodile, 1976; Doyle et al., 1982).

2.3.2.1.4 Awe Formation

The Awe Formation is a wedge-shape regressive deposit that is over 1000 m thick. It comprises of medium to coarse-grained sandstones alternating with carbonaceous shales and sandy limestones (Offodile, 1976). This formation is dated as late Albian-early Cenomanian on the basis of gastropod fauna (Offodile, 1976).

The regressive phase of the first marine transgression started at the end of Albian and lasted until middle Cenomanian (Murat, 1972). During this time, Keana Sandstone and Bima Sandstones were deposited in the middle and northern Benue Trough respectively. The upper boundary of Awe Formation is an erosional unconformity that marks the top of the Asu River Group and is the upper boundary of the first depositional sequence in the trough.

2.3.2.2 Cross River Group / Odukpani Group

The Cross River Group represents deposits of the second marine transgression into the Benue Trough from late Cenomanian to early Santonian. This second depositional sequence is about 2000 m thick and bonded at the bottom and top by early Cenomanian and mid Santonian unconformities. The deposits in the Abakaliki and Anambra Basins consist of an alternation of shales and limestones (Nkalagu Formation) interfingering with sandstones. They are mapped as the Odukpani Group in the Calabar Flank (**Fig. 2.12**).

The type area of the Cross River Group is the Cross River plain in SE Nigeria (Petters and Ekweozor, 1982a). The Group includes lithologically similar units that had previously been mapped chronostratigraphically by Dessauvagie (1974) as the Odukpani Formation (Cenomanian), Ezeaku Formation (earliest Turonian) and Awgu Formation (late Turonian-early Santonian).

The Nkalagu Formation consists of thick massive to laminated, hard dark grey to black calcareous shale that are sometimes interbedded with siltstones with thin shaly/sandy thin limestone bands and calcareous sandstone. The limestone is thin to thick, grey to dark grey, and sometimes shaly and marly. Nkalagu Formation was deposited under anaerobic bottom conditions. The Nkalagu Formation passes laterally towards the basin margin into regressive coarse-grained cross-bedded sandstones (Amasiri Sandstone, Makurdi Sandstone, Agala Sandstone and Agbani Sandstone). The transgression maxima in the southern Benue Trough occurred at the end of Turonian, during which time the Gulf of Guinea is believed to have been connected with the Neo-Tethys Ocean across the Sahara platform through the Niger Basin and Lake Chad (Reyment and Dingle, 1987; Benkhelil, 1989; LeFranc and Guiraud, 1990; Petters, 1991). Deposits of this transgression maxima are represented by the Awgu shale in the Abakaliki Basin, and carbonates in the Anambra Platform (Benkhelil, 1989; Ojoh, 1990). Regression began in the Coniacian and ended in the Santonian.

The Albian-Coniacian deposits in the Calabar Flank are referred to as the Odukpani Group and have been subdivided into Mfamosing Limestone, Ekenkpan Shale and New Netim Marl (Reijers, 1998; Ehinola et al., 2008). The Mfamosing Limestone consists of shallow-marine, karstified platform carbonates. The Ekenkpan and New Netim Formations are transgressive marine shales and marls that were deposited during relative rise in sea level (Reijers and Petters, 1997).

Deposition of the Cross River and Odukpani Group was terminated by a forced regression in mid-late Santonian. The regression was due to epeirogenic uplift that was accompanied by a sharp basin modifying tectonic pulse that is often referred to as the "Santonian squeeze". The epeirogenic uplift is believed to be related to the reorganization of the Equatorial and South Atlantic plates (Fairhead and Binks, 1991). This tectonic event led to a 15º anticlockwise rotation of the axis of some basins (e.g. Yola, Bongor, Doba) in WCARS; Genik, (1993), and folding in the Benue Trough (Avbovbo et al., 1986; Benkhelil, 1989). Folding in the Benue Trough led to a westward displacement of its depositional axis. It is estimated that about 2000 m thick sediments were eroded from the Abakaliki Basin due to the Santonian folding and uplift (Burke et al., 1972).

2.3.2.3 Post Santonian units

After the complete emergence of the Abakaliki area, sediments were eroded from the uplifted Abakaliki Basin and deposited in the subsiding Anambra platform. The Campanian deposits (Nkporo Shale, Afikpo Sandstone and Enugu Shale) were deposited in shallow marine and paralic environments (**Fig. 2.9** and **2.12**). Maastrichtian deposits (coal measures) comprising Owelli Sandstone, Mamu Formation, Ajali Sandstone, and Nsukka Formation were deposited in fluvio-deltaic and shallow marine setting at the margins of the Anambra Basin (Akande and Mücke, 1989; Benkhelil, 1989; Nwajide and Reijers, 1996; Obaje, 2009).

2.3.3 Review of previous geological studies in the Mamfe Basin

The Mamfe Basin is also known as the Ikom-Mamfe Basin, Ikom-Mamfe Embayment, Mamfe Embayment, or Mamfe Gulf. Field and preliminary gravimetric and magnetometric surveys have revealed that this basin is a half graben with a segmented NW-SE trending border fault on its northern margin (**Fig. 2.13** and **2.14**; Petters et al., 1987, Fairhead et al., 1991; Ajonina, 1997; Hell et al., 2000; Eyong, 2003; Ndougsa-Mbarga et al., 2007; Heine, 2007; Oden et al., 2012, 2015).

The earliest geological investigations in the Mamfe Basin were carried out during the German colonial administration in Cameroon (Guillemain, 1908; Guillemain and Harbort, 1909; Jaekel, 1909). The results of these investigators were re-evaluated by Wilson (1928) in the course of a reconnaissance survey for coal in the region. Wilson's notes on the geology of the Mamfe Basin have served as the basis of published geological maps of the basin.

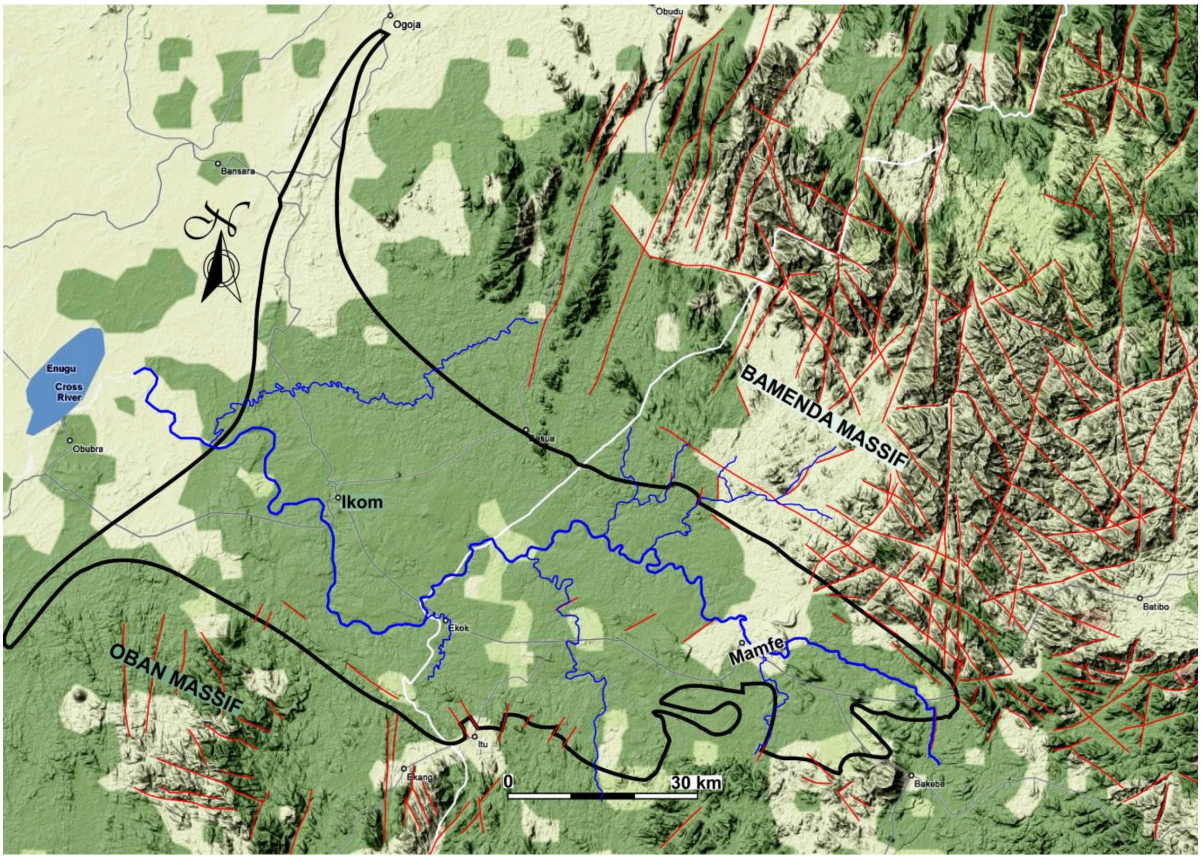

Figure 2.13. Terrain map of southeastern Nigeria and southwestern Cameroon showing lineaments in the Bamenda and Oban Massifs and outline of the Mamfe Basin (modified from Google 2010 Tele Atlas).

The basin was also under investigation by Reyment (Reyment, 1954, 1965) who estimated a sediment thickness of 700 m for the outcropping sedimentary motif which he named the Mamfe Formation with a type locality at the banks of Cross River in Mamfe. He correlated the formation with Cretaceous sediments in southeastern Nigeria. Subsequent studies by Le Fur (1965) led to the identification of five lithologic series (CG1 to CG5) in the Cameroonian sector of the basin. The lithostratigigraphic description of Mamfe Formation has been reviewed by Belmonte (1966); Petters et al. (1987), Petters (1995), Ajonina and Bassey (1997), Eyong (2003), and Abolo (2008), Bassey et al. (2013); and Eyong et al. (2013).

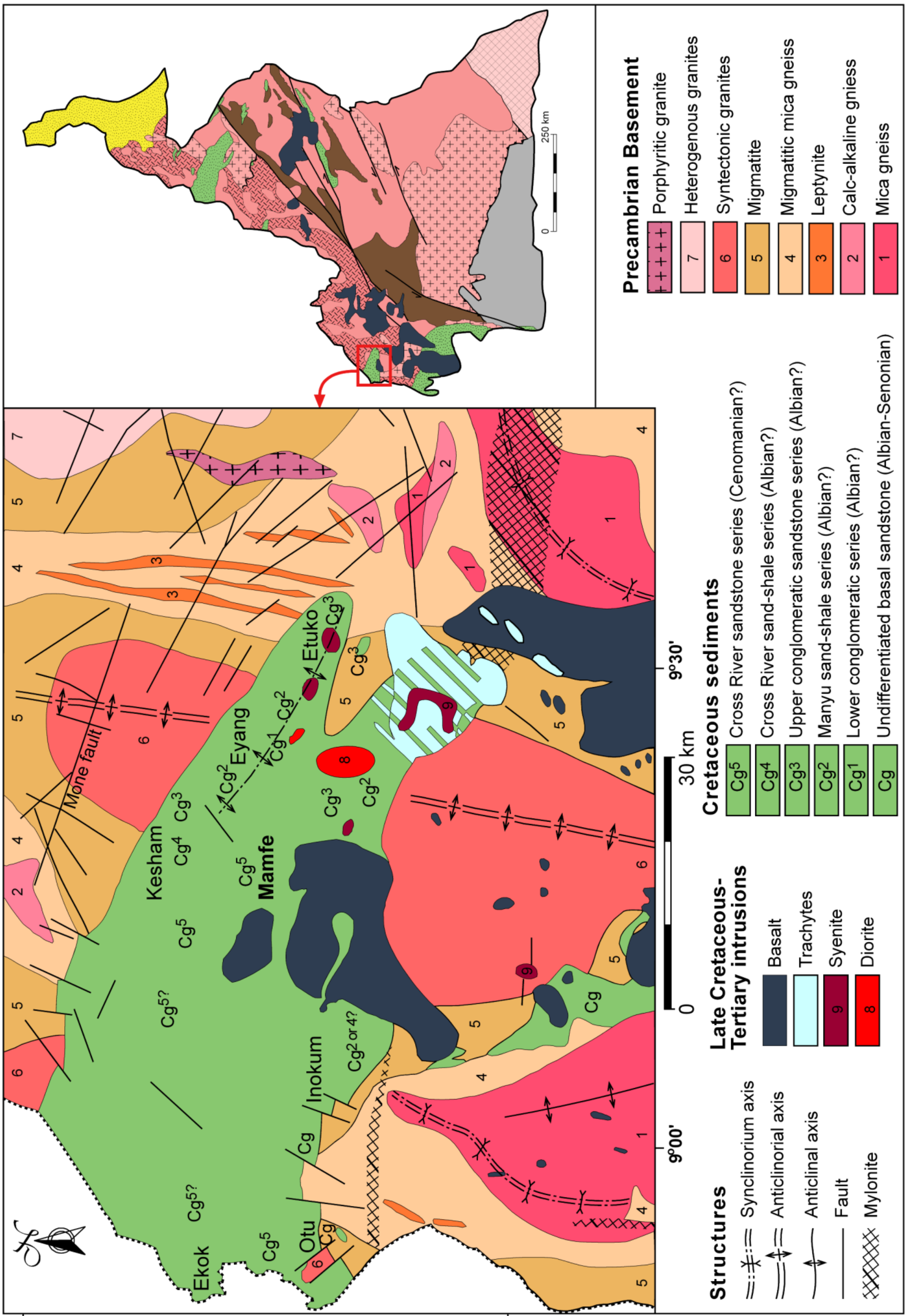

Figure 2.14. Geological map of the Mamfe region (redrawn from Dumort, 1968).

Geologic studies of Cretaceous sedimentary rocks in other sedimentary basins in the coastal basins of Cameroon and southeastern Nigeria by Nwachukwu (1972), Dessauvagie (1974), Hoque (1977), Adeleye and Fayose (1978), Petters and Ekweozor (1982a), Ojoh (1990) have led to a lithostratigraphic correlation of the rocks with those in the Mamfe Basin.

No regional biostratigraphic correlations have thus far been attempted because of the non-to poorly non-fossiliferous nature of the outcropping sediments in the Mamfe Basin. Fossils that have thus far been identified in sediments of the Mamfe Basin include impressions of Lower Cretaceous ichthyodectiform fish *Proportheus kameruni jaekel* (Mann, 1913 in Wilson, 1928), ostracods, gastropods, ichnofossils, conchostracan of the genus *Estheriina* (Eyong, 2003), and abundant microflora (Ajonina et al., 2008, 2010b). The reported fauna have no biostratigraphic significance because of their uncertain age, low diversity, and cosmopolitan distribution during the early Cretaceous (Maisey, 2000; Lana and Carvalho, 2002; Eyong, 2003).

The aspect of the depositional environments and petroleum geology of the Mamfe Basin has been reported by Wright et al. (1985); Ajonina (1997); Ajonina and Bassey (1997); Ajonina et al. (2001, 2006, 2007); Bassey and Ajonina (2002); Eyong (2003), Eseme et al. (2006); Bassey et al. (2013); Eyong et al. (2013) while the paleogeography of the adjacent areas in the Benue Trough have been outlined by Murat (1972), Adeleye (1975), Whiteman (1982), and Ojoh (1990). Reports on the geochemistry of the brines emanating from the Mamfe sediments includes those of Tanyileke et al. (1996); and Eseme et al. (2001, 2006). Geophysical and structural studies in the basin and adjoining areas include that of Petters et al. (1987); Fairhead et al. (1991); Iliya and Bassey (1993); Hell et al. (2000); Ndougsa-Mbarga et al. (2007); Heine (2007); Kamguia et al. (2008), Oden et al. (2012); Edet and Okereke (2014); Oden et al. (2015).

3

DEPOSITIONAL ENVIRONMENTS AND STRATIGRAPHY OF THE MAMFE BASIN

ABSTRACT

Multiscale facies analyses using sedimentological, palynological and geochemical techniques were used to characterize the environments of deposition of the Cretaceous sedimentary infill of the Mamfe Basin in Cameroon.

Twenty sedimentary facies were identified and grouped into 9 facies associations. On the basis of vertical and lateral relationship of the facies associations, a revised lithostratigraphic framework is proposed for the sedimentary infill of this basin which until date is formerly known as the Mamfe Formation.

The sedimentary succession in the Mamfe Basin consists of mixed siliciclastics, carbonate, evaporites, organics and volcaniclastic. Results of the analyses indicate that the basin has a tripartite depositional history and stratigraphic framework which corresponds to three unconformity bonded depositional sequences. The basal sequence is made up of pre-rift alluvial fan deposits that are named Etuko Formation. The middle sequence consists of syn-rift fluvio-lacustrine and deltaic deposits that are named Mamfe Group. The group consists of three formations which from bottom to top are: Nfaitok, Manyu, and Okoyong Formation. The upper sequence consists of post-rift piedmont alluvial and fluvial deposits that are named Ikom-Munaya Formation.

The westward younging of sediments in the Mamfe basin is attributable to exhumation in the eastern part of the basin due to activity of the Cameroon Volcanic Line (CVL) rather than the previously reported westward migration of depocenter.

3.1 Introduction

The Mamfe Basin is located on the eastern flank of the southern Benue Trough in Nigeria, where it occurs as a southeasterly trending bifurcation that extends into SW Cameroon (**Fig. 3.1**). It is about 150 km due NE of the Niger Delta and 200 km north of the present day equatorial margin of the eastern Gulf of Guinea. The basin is about 130 km long and its width ranges from 10 to 60 km at its eastern and western ends respectively. The Cameroonian sector of this basin (**Fig. 3.2a**; hereafter referred to as the study area, or "Eastern Mamfe Basin", or "EMB") has a surface area of over 2100 km^2. The sedimentary infill of the Mamfe Basin is over 4500 m thick (Petters et al., 1987; Hell et al., 2000; Heine, 2007), and unconformably overlies the Pan-African crystalline Basement Complex.

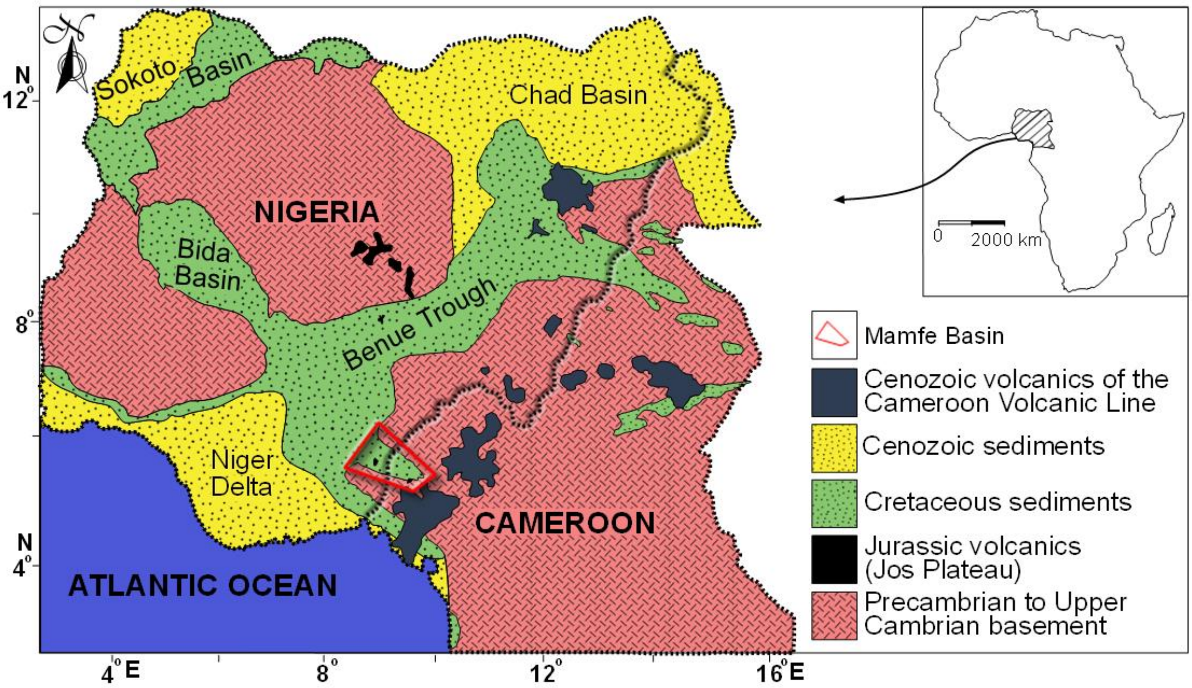

Figure 3.1. Simplified geological map of Nigeria and Cameroon showing the location of the Mamfe Basin and the main sedimentary basins (modified from Avbovbo, 1980; Whiteman, 1982, and Toteu et al., 2001). Inset is the map of Africa showing the location of Nigeria and Cameroon.

Although geological research in the Mamfe Basin started during the German colonial administration in Cameroon more than a century ago (Jaekel, 1909), the basin is still a frontier basin with rare published literature on its geology. Up to now, no well has been drilled in the Mamfe Basin, and the basin is generally regarded as a neglected and least studied of all the Early Cretaceous rift basins in West and

Central Africa (Petters et al., 1987; Genik, 1993).

The sedimentary infill of the Mamfe Basin consists of thick folded and faulted heterolithic suite of friable to indurated siliciclastics that has been defined as the Mamfe Formation (Reyment, 1954). It consists of a cyclic succession of mostly massive arkosic sandstones and greenish grey to black calcareous shales and mudstones, with intercalations of siltstones and conglomerates. There is yet no consensus among researchers on the age and environments of deposition of the sediments in this basin.

The discrepancies in opinion on the age and depositional environments of the lithic infill of the Mamfe Basin are largely because age and paleoenvironmental interpretations to date are based mainly on lithological description of poorly exposed, commonly weathered, and mostly poorly- to non-fossiliferous outcrops as well as lack of subsurface samples. These paleoenvironmental inferences that are based on lithological descriptions of outcrop data without any paleontological and geochemical control are questionable, and can be likened to attempting to solve a jigsaw puzzle that have many missing pieces, and the pieces that are left are faded, and have partly lost their interlocking connections. Also, paleoenvironmental interpretations and correlation in the Mamfe Basin have not taken into consideration issues such as the different depositional gradients that are associated with its half graben geometry, interaction between basin-floor axial river and basin-margin transverse tributaries on sedimentation pattern (e.g. Leeder et al., 1996; Kim et al., 2011), as well as uplift in the eastern part of the basin.

The environment of deposition of the sediments in the Mamfe Basin have been reported to be fluvial, deltaic, lacustrine, marine, and estuarine (Wilson, 1928; Reyment, 1954, 1965; Le Fur, 1965; Petters, 1978a, 1991, 1995; Petters et al., 1987; Wright et al, 1985; Tanyileke et al., 1996; Tijani et al., 1996; Ajonina and Bassey, 1997; Ajonina et al, 1998, 2001; Eyong 2003; Eseme et al., 2006). The sediments are assumed to range in age from Neocomian to Turonian (Jaekel, 1909; Reyment, 1954, 1965; Le Fur, 1965; Hoque, 1977, Ajonina, 1997; Ajonina and Bassey, 1997; Ajonina et al., 2008, 2010, 2012; Bassey and Ajonina, 2002; Eseme et al., 2002; Abolo, 2008; Bassey et al., 2013). Correlations within the basin have been hampered by poor and scattered exposures, rapid facies change and lack of stratigraphic markers. The lithic infill of the Mamfe Basin on the basis of lithological features is thought to be coeval with the basal sediments in the Calabar Flank and southern Benue Trough, and has thus been correlated with the Asu River Group in SE Nigeria (Reyment, 1965;

Reyment and Tait, 1972; Murat, 1972; Dessauvagie, 1974*;* Adeleye and Fayose, 1978; Petters and Ekweozor, 1982a; Whiteman, 1982; Petters, 1991; Ajibola, 1997; Ajonina, 1997; Obaje, 2009).

Rapid facies change in the scattered outcrops, lack of conventional stratigraphic markers and the poor to non-fossiliferous nature of the sediments in the basin necessitated the use of multidisciplinary techniques in the characterization of the depositional environments and age of its lithic infill.

An integrated sedimentological, palynofacies, and organic geochemical analyses were utilized in this study to provide an improved petrologic description and more concise paleoenvironmental interpretations and age determination for the outcropping Cretaceous sediment in Cameroonian sector of the basin. It is uncertain whether the Mamfe paleolake was a shallow playa or deep and chemically stratified. Knowledge of the age of the sediments and whether the parent brine of the associated evaporites evolved in a shallow playa or deep and chemically stratified marine or non-marine setting is important for modelling the early Cretaceous paleogeography of the eastern Gulf of Guinea from southern Benue Trough/Niger Delta to northern Gabon.

Palynofacies in the sense of Combaz (1964, 1980) is the organic matter that is recovered from a rock by standard palynological processing technique. This distinctive association of acid-resistant organic components of sediment are viewed as sedimentary particles that accumulated under certain conditions and reflect a particular source area and depositional environments or processes. Their composition, preservation, and distribution are sensitive recorder of the changes in the depositional system such as hydrodynamics, basin redox, and relative distance from terrestrial source areas (Tyson, 1995; O’Brien, 1996; Buckley and Tyson, 2003; Schieber, 2003a; Petersen et al., 2004). This acid resistant organic matter is thus routinely used to support paleoenvironmental interpretation and correlation, and is very helpful in areas or within successions in which conventional biostratigraphic markers are scares or lacking (Batten and Stead, 2005).

The term palynofacies is used in this study in the sense of Tyson (1995) to mean a body of sediment containing a distinctive assemblage of palynological organic matter that is thought to reflect a specific set of environmental conditions or be associated with a characteristic range of hydrocarbon potentials. The total palynological organic matter residue recovered from a sample is referred to as kerogen. The words “kerogen category” as used in this study is synonymous with kerogen type (organic geochemistry) and maceral group (organic petrography).

Total organic carbon (TOC) measurement is the first screening parameter for petroleum source rock evaluation (Bordenave, 1993; Bordenave et al., 1993; Peters and Cassa, 1994), and is also a very useful parameter for assessing depositional environments when combined with palynofacies and certain bulk geochemical parameters and biological markers (biomarkers) of saturated hydrocarbons (Tyson, 1995; Batten, 1996; Rull, 2002; Peters et al., 2005b; Carvalho et al., 2006; Martinez et al., 2008; Shalaby et al., 2012). The utilization of palynofacies and geochemical analytical techniques in this study to characterize the paleoenvironments of deposition in the Mamfe Basin is thus relevant and necessary.

The interpretation of the sedimentary infill of the Mamfe Basin in terms of facies and facies associations has led to the establishment of a sedimentological model, and the reconstruction of conceptual depositional gradient on which the depositional elements are positioned. Knowledge of the depositional environments and their vertical and lateral relationships was used to revise the lithostratigraphic subdivision of the Mamfe Basin (e.g. Reyment, 1965; Ajonina et al., 2001, 2006; Eyong, 2003; Abolo, 2008). To avoid duplicity and confusion in the name and rank of stratigraphic units in the study area with formerly defined stratigraphic units in neighbouring basins in SE Nigeria, some of the names used by Eyong (2003) and Abolo (2008) have adopted with revision or redefinition for the proposed stratigraphy of the Mamfe Basin that is presented in this study.

3.2 Materials and Methods

3.2.1 Field studies

Extensive geological field studies were carried out on the Cameroon sector of the Mamfe Basin over a period of three years. Samples were collected from the locations shown in **figure 3.2**. Field studies involved sample acquisition and systematic vertical and lateral description of the arrangement of lithologies and their variability in terms of strata thickness, orientation, texture, composition, sedimentary structures, fossil content and discontinuity surfaces. Because of thick vegetation and alluvial cover, and poor accessibility, fair to good exposures of Cretaceous sediments are limited and were found mostly along river banks and road cuts. In a few cases, samples were collected from building excavation sites and hand-dug wells. Directional features were measured with a Silva compass clinometer (model 15T) and features of geologic interest photographed. The geographic coordinates of each sample location was recorded with a Garmin GPS (model 76TM). The GPS coordinates where later transferred onto a Minna geodetic datum georeferenced base map of the Mamfe Basin using MapInfo (version 8.0) GIS platform.

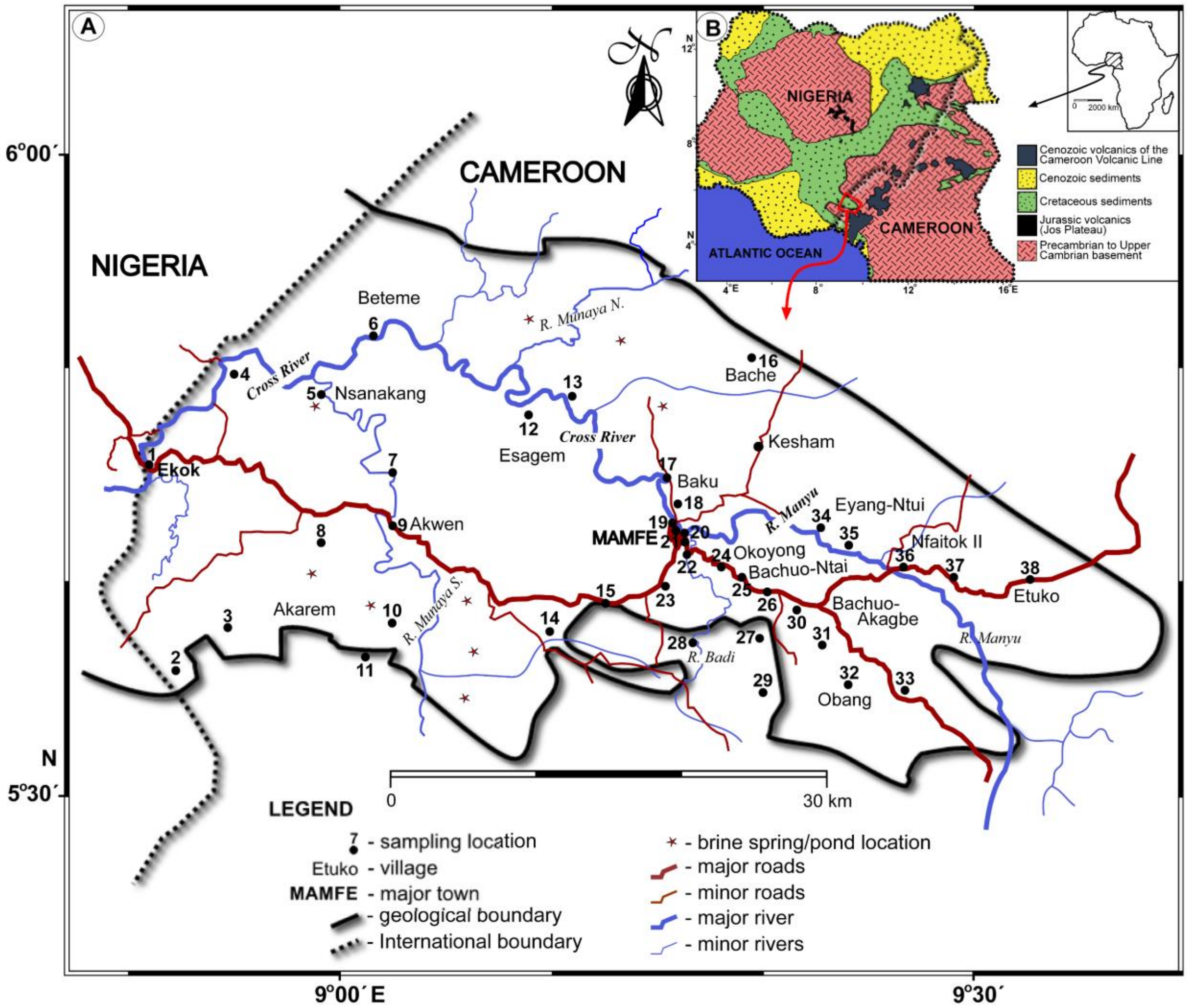

Figure 3.2. (**A**) Map of the Eastern Mamfe Basin (study area) showing sampling locations. (**B**) map of Cameroon and Nigeria showing the geographic location of the map area.

3.2.2 Sedimentological analysis

Analysis of sedimentary texture, structures and mineralogy were carried out on polished and thin sections of selected representative samples. The polished and thin sections were analysed with polarizing optical microscope (Olympus BH-II) and scanning electron microscope (Zeiss LEO 1455 VP). Petrographic and clay mineral analysis were carried out within the context of stratigraphic framework so as to be able to quantify and compare petrographic features (e.g. grain size, sorting, detrital mineralogy, cement, porosity and diagenetic modifications) within and between different lithologic units.

Some shale and mudstone samples were pulverized and analysed for their clay content with a Philips X'pert diffractometer PW 1830/00 X-ray generator. X-ray diffraction (XRD) measurements were at a scanning rate (step size) of 0.02 degrees 2 theta ($^o2\theta$) per second. Four different XRD measurements were made for each sample: non-oriented powder mount (measured over an angular range between 3 and 70 $^o2\theta$), air-dried oriented mount, glycol-solvated oriented mount (glycolated), and glycolated sample heated to a temperature of 550° C. XRD measurements on the air-dried oriented mount, glycolated, and heated sample was over the angular range of 3-30 $^o2\theta$. Clay mineral identification was carried out visually based on their peak position and relative intensities on the resulting diffractograms and with the incorporated Philips X'pert XRD Data processing software.

The full width at half maximum intensity (FWHM) of the first (001) illite diffraction (10-Ǻ) on air-dried oriented powder mounts, which is known as illite crystallinity (IC) or Kübler index (KI) (Kübler, 1968; Kübler and Jaboyedoff, 2000; Guggenheim et al., 2002) was measured. The resulting data (expressed in $\Delta^o2\theta$) was used to evaluate the thermal maturation (burial metamorphism) conditions of the studied Cretaceous succession. Measured KI values were calibrated to the Crystallinity Index Standard (CIS) scale using the procedure and standards of Warr and Rice (1994). The equation that was used to convert measured illite crystallinity values to the standardized scale (CIS), was: $KI_{(CIS)} = 1.2517\ KI_{(uncalibrated)} + 0.0829$ ($r^2 = 0.96$).

Lithofacies were defined on the basis of sedimentary texture, structures, composition and geometry. The description and classification of the various lithofacies identified in this study uses the scheme of Miall (1996, 2010) with minor modifications and addition. Also adopted for this study is the stratification thickness classification of Ingram (1954), grain-size terminology of Blair and McPherson (2009), and paleo-oxygenation terminology of Tyson and Pearson (1991). The name mudrock is used as a group name for siliciclastic sediments composed mainly of silt and clay-sized particles (Stow and Piper, 1984; Stow, 2005). The names shale and mudstone are used in the restricted sense of Potter (2003) to mean laminated and massive mudrocks respectively.

3.2.3 Palynofacies analysis

Palynofacies analysis uses transmitted light and fluorescence light microscopy to evaluate the total microscopic particulate organic-matter assemblage within a sedimentary rock following the chemical breakdown and removal of any carbonate and siliciclastic mineral constituents. The remaining acid resistant insoluble particulate organic matter provides invaluable information on the sedimentary facies, paleoenvironments (depositional energy, basin redox conditions, and relative distance from terrestrial source areas), source rock potentials, and sequence stratigraphy (Tyson, 1995; Tyson and Follows, 2000; Buckley and Tyson, 2003; Batten and Stead, 2005; Oboh-Ikuenobe et al., 2005).

Representative mudstone, shale, and siltstone samples were subjected to standard non-oxidative palynological processing techniques (Tyson, 1995; Wood et al., 1996; Traverse, 2007) at the Unidad de Paleopalinología, Instituto Argentino de Nivología, Glaciología y Ciencias Ambientales (IANIGLA), Mendoza Argentina, and the Center for Tropical Paleoecology and Archaeology (CTPA), Smithsonian Tropical Research Institute (STRI) Panama. The resulting organic residues were sieved through a 10 µm mesh prior to mounting on glass slides using glycerine jelly. The content of the slides was evaluated using transmitted light microscopes (Zeiss Axio imager A1, and Nikon Eclipse 80*i*) and an Olympus BX61W fluorescence confocal laser scanning microscope (CLSM,) that was equipped with a diode laser source with variable filter excitation and detection wavelength. The emitted fluorescence light was detected at wavelengths of 483 nm or more.

Palynofacies (kerogen) analysis involved identification and counting of 300 particulate organic matter on each slide. Because there is no standardized classification for particulate organic matter and many published classification schemes (e.g. Combaz, 1964; Batten, 1996; Tissot and Welte, 1984; Hart, 1986, 1996; Tyson, 1995, Oboh-Ikuenobe et al., 2005, Ercegovac and Kostić, 2006), the classification scheme used in this study was adapted to the types of organic components and palynomorph groups that were present in the kerogen residue. The scheme used in this study is derived and simplified from Tyson (1995), Oboh-Ikuenobe et al., (2005), and Ercegovac and Kostić, (2006).

To assess the pattern of distribution of the kerogen, the percent relative numeric frequency (% RNF) of the kerogen components were subjected to cluster analysis using StatSoft STATISTICA (v.8) software. Unweighted pair group average linkage (UPGMA) cluster analysis (in Q-mode) was used for grouping samples into palynofacies assemblages.

A semi-quantitative estimation of thermal maturity was done by visual comparison of palynomorph colour to the thermal alteration index colour chart of Pearson (1984, in Traverse, 2007). The colour of palynomorphs was matched with corresponding colour on Pearson's chart and the TAI value noted. TAI values were calculated following the method of Firth (1993). The mean thermal maturation level of each sample was based on estimates from 2 to 5 palynomorphs taxa (or structured and amorphous macerals in samples lacking palynomorphs) instead of a single taxon because of the low abundance and diversity in palynomorphs in most samples. Waples (1980) TAI-R_o interconversion table was used to convert mean TAI values to maximum vitrinite reflectance values in oil (i.e. estimated R_o %). The depth/reflectance/geothermal gradient relations diagram of Suggate (1998) were used to estimate maximum temperatures and depths of burial assuming an average regional geothermal gradient of 38°C/km (Akande and Erdtmann, 1998; Akande et al., 2012).

3.2.4 Organic geochemical analyses: Total Organic Carbon (TOC), and Gas Chromatography (GC)

The TOC of selected shale and mudstone samples was measured by dry combustion in a Coulomat 702 (Ströhlein Instruments, Kaarst, Germany) at the Institute of Geosciences, University of Kiel. Samples with TOC content above 2.5 wt.% were subjected to solvent extraction and afterward gas chromatography at the School of Geology and Geophysics, University of Oklahoma, USA.

Powdered samples weighing between 11-18 g were solvent-extracted for 48 hours by means of a Sohxlet apparatus using with a mixture (50:50 vol./vol.) of dichloromethane (DCM) and methanol (MeoH). The extracts were concentrated in a rotating vapour evaporator at 97 rpm. They were dissolved in DCM and an excess of 40-fold *n*-pentane added, stored in a refrigerator for 8 hours and then centrifuged at 1250 rpm for 30 minutes in order to separate maltenes from asphaltenes. The maltenes were fractionated into saturates, aromatics and polar fractions using glass column chromatography on activated silica gel. The saturate fraction was eluted using *n*-hexane followed by the aromatic fraction using *n*-hexane/DCM (70:30 vol./vol.) and the polar fraction using DCM/MeoH (95:5 vol./vol.).

The saturate fractions were analysed by gas chromatography using an Agilent

6890 Gas chromatograph (DB-Petro column, 100 m x 0.25 mm ID x 0.5 um) by injection of 10 mg/mL in the split (20:1) mode. The GC oven was held isothermally at 35 ºC for 1.5 minutes and heated to 60 ºC at 2 ºC/minute. The GC was held isothermally at 60 ºC for 1 minute and then raised to 300 ºC at 3 ºC/minute and held isothermally for 20 minutes. Normal and branched alkanes in the saturate fractions were identified based on GC retention times. Various peaks in the chromatogram were integrated and used to calculate some of the bulk and molecular geochemical parameters that are used in paleoenvironmental interpretations and source-rock characterization.

3.2.5 Sediment thickness

Geophysical data on sediment thickness in the Mamfe Basin (Fairhead et al., 1991; Hell et al., 2000; Heine, 2007, personal communication) was analysed with Golden Software (Surfer v. 8.09) to generate isopach map of the Mamfe Basin

3.3 Results and Interpretation

Integration of the results of sedimentological, palynological and organic geochemical analyses of the samples that were collected from the locations shown in **figure 3.2** led to the identification of twenty sedimentary facies. The description and inferred depositional processes of these facies are summarized in **table 3.1.** Facies were distinguished on purely descriptive basis, and are considered to be products of specific depositional process or processes (Benvenuti, 2003; Boggs, 2009; Dalrymple, 2010a). The capital letter in the facies code indicates the dominant grain size: G = gravel, S = sand and F = very fine sand to clay. The lower-case letters serve as mnemonic for the characteristic structure or texture or both of the facies (e.g. m = massive, h = horizontal stratification, t = trough cross-stratification, g = graded, etc.).

Table 3.1. Faceis description and interpretation of depositional processes.

Facies code	**Facies**	**Description**	**Inferred depositional processes**
Gcm	Massive, clast-supported conglomerates	Consists of sub- angular to well-rounded, very poor to poorly sorted clasts that are 10 to 800 mm in diameter, and a matrix of coarse sand. Most are massive, and some are crudely stratified and show reverse grading in their basal part and crude imbricate towards the top. They commonly have lenticular or wedge-shape geometry and local low relief erosional bases.	Rockfall; debris flow; hyperconcentrated flows, sheetflood or channelized flows (Blair and McPherson, 1994, 1999, 2008, 2009; Miall, 1996, 2010; Benvenuti, 2003; Boggs, 2009; Leeder, 2011).
Gmm	Massive, matrix-supported conglomerates	Clasts are of poorly sorted, sub-angular to sub-rounded, 5 to 600 mm in diameter, and supported by a matrix of poorly sorted coarse sand. They show weak reverse gradation at the basal part and imbrications towards the top, and commonly have wedge shape geometry.	Debris flows (Blair and McPherson, 2009; Boggs, 2009; Miall, 2010; Leeder, 2011) or mass deposition of traction load by frictional freezing (Benvenuti, 2003).
Gp	Planar cross-bedded clast-supported conglomerates	The clasts range in diameter from 20 to 110 mm. The matrix consists of poorly sorted coarse to pebbly sand. They have erosive bases and lenticular geometry.	Fluvial transverse bars building into areas of flow expansion or deeper water (Miall, 1996; Blair and McPherson, 1994).
Ghg	Horizontally bedded clast-supported conglomerates	Consists of sub-rounded to well-rounded clasts that are 20 to 350 mm in diameter, and a coarse sand matrix. They show crude surface-parallel to sub-parallel planar stratification, weakly normal or reverse graded, imbrication of large clasts, and have non erosive bases.	Bulking of sediments in stream flood, longitudinal bar, bedload traction carpet within active channel (Blair and McPherson, 1994; Smith, 2000; Benvenuti, 2003).

Gvb	Clast-supported volcaniclastic breccia	Consists mostly of angular to sub-angular mafic clasts and a calcareous matrix, and chaotic peperite texture. Mudrock clasts are rare. Clasts are 20 to 400 mm in diameter, poorly sorted, and commonly coated with reddish clayey rims.	Quench fragmentation of basaltic lava extruded into water or saturated sediments (Lajoie, 1984; Gomes and Fernandes, 1995; Ricci-Lucchi and Amorosi, 2003; Rakovan, 2005; Stow, 2005; Boggs, 2009; Gill, 2010).
Sm	Massive sandstone	Medium- to very coarse-grained and pebbly, poorly sorted, angular to subrounded grains. Bioturbation and loadcasts are rare. Their bases are sharp or erosive or both.	Rapid deposition from high density turbulent suspension, sediment gravity flow (Miall, 1996).
St	Trough cross-bedded sandstone	Coarse to pebbly, poorly sorted, crudely reverse-graded. Bases are either sharp or erosional.	Upper part of a lower flow regime (Miall, 1996)
Sp	Planar cross-bedded sandstone	Fine- to medium or coarse-grained and poor to moderately sorted. Mostly solitary cross set with minor low relief erosional bases. Bioturbations are rare.	Lower and upper flow regime transverse and linquoid bedforms, lateral accretion (Eberth and Miall, 1991).
Sh	Horizontally bedded graded sandstone	Very fine or fine- to medium or very coarse-grained, poor to moderately sorted, angular to subrounded grains. Show normal or reverse gradation. Units are surface-parallel planar bedded and may contain mudstone clasts. Those that are very fine- to medium-grained are micaceous, and contain carbonaceous streaks (charcoal).	Deposition from a waning turbulent current during lower or upper flow regime, (Miall, 1996; Ricci-Lucchi and Amorosi, 2003; Fielding et al., 2009).
Src	Current ripple-laminated sandstone	Very fine- to medium or coarse-grained, poor to moderately sorted, angular to subrounded grains. They are micaceous, graded and rarely contain ferric nodules and bioturbation. Their bases are sharp.	Lower flow regime (Reineck and Singh, 1980; Leeder, 1982, 2011; Miall, 1996).
Srw	wave ripple-laminated silty sandstone	Very fine- to fine-grained moderately sorted silty sandstone with interbedded mud streaks. Symmetrical ripples commonly associated with lenticular and flaser bedding.	Suspension fall-out from shallow water with bottom oscillating lower flow regime (Talbot and Allen, 1996; Flemming, 2003; Leeder, 2011).

Fl	Heterolithic siltstone and very fine or fine sandstone	Interbedding of very fine or fine-grained sandstone and siltstone. Whitish to dark grey and thin to thickly planar laminated. Some have small current ripples, desiccation marks, bioturbation and ferric nodules. Some of the dark grey variety contain microflora.	Suspension fall-out from waning flood water on floodplain or abandoned channel (Leeder, 1982; Miall, 1996; Aslan, 2003).
Fsm	Massive siltstone	Grey to brownish in colour with indistinct lamination. Bioturbation is common and sedimentary rock fragments are rare. They often have lenticular geometry and sharp bases.	Rapid deposition of suspension load from waning high energy hyperconcentrated flash flood in a flood plain (Miall, 1996; Alexander and Fielding, 2006; Pizzuto et al., 2008).
Fsl	Thin to thickly laminated siltstone	Colour varies from whitish, greenish to grey. Most are micaceous and some are calcareous, contain carbonaceous streaks (charcoal), or ripple cross lamination.	Suspension fall-out in low energy water ponded on a floodplain (Nanson and Croke, 1992; Pizzuto et al., 2008).
P	Dark brown to brick-red sandstone and variegated mudrocks	Consists of non-calcareous mudrocks, and fine to pebbly sandstones. Some are bioturbated, have erosive tops, ferric nodules and root traces.	Subaerial weathering and fossilization of alluvial deposits on poor- to well-drained oxic, neutral to acidic overbank floodbasin and deltaic plain (Miall, 1996; Kraus, 1999, 2002; Retallack, 2001; Thomas et al., 2002; Bridge, 2003; Sheldon, 2005; Sáez et al., 2007; Sheldon et al., 2009).

Fm	Greenish to dark grey mudstone	Colours highly variable from green, mottle green, grey to dark grey. Some of the grey and dark grey variety are weakly calcareous and contain slump, convolute and flame structures, bioturbation, and carbonaceous streaks. Lack macrofossils and some are rich in well preserved microflora. Their palynological organic matter (kerogen) is dominated by black debris or phytoclasts (30-90%), with some lacking amorphous organic matter (AOM). Their TOC ranges from 0.29 to 0.92 wt.%.	Suspension fall-out in moderately agitated shallow water with oxic bottom water or muddy slurries (O'Brien and Slatt, 1990; Tyson, 1995; Potter, 2003; Schieber, 2003b; Pizzuto et al., 2008; Bond and Wignal, 2010).
Fmla	Greenish grey to dark grey micaceous shale	Shale with thin to mostly thick and sometimes indistinct parallel lamination. Some are calcareous and with desiccation marks. Rhythmically interstratified with siltstones and very fine- to fine-grained sandstone. Their bases are either sharp or gradational. Rarely bioturbated and poor in microflora. Kerogen contains moderate quantity of AOM (44-52%) and black debris is often more than 25%. TOC ranges from 0.55 to 0.86 wt.%.	Rapid deposition from a storm generated cloud of suspended sediments in relatively quiet dysoxic-oxic water (Tyson, 1995; O'Brien and Slatt, 1990; Lamb and Mohrig, 2009).

Fmlb	Dark grey shale /marlstone	Thin- to thickly laminated calcareous or carbonaceous shale/marlstone. Laminae are planar/wavy, and parallel or discontinuous, lenticular, sub-parallel. Indistinct or wispy lamination is characterized by preferred orientation of platy particles. Some contain thin to thick laminae of clay & organics/siltstone or dolomite/siltstone couplets, sedimentary rock fragments, phosphatic peloids, calcareous/ pyrite nodules, rhizocretions, and mica. Bioturbation is weak to moderate, and desiccation marks are rare. The contact with siltstone is commonly sharp and locally scoured. The siltstone is moderately sorted, and either laminated, graded, rippled, lenticular or rarely massive. Most are non-fossiliferous and some contain ostracods and microflora. They contain high quantity of AOM (60-74%), and their TOC ranges from 0.54-2.52 wt.%.	Suspension fall-out from periodic or quasi-continuous low energy and low density hyperpycnal interflows or underflows in quiet, shallow to moderately deep water with dysoxic-suboxic bottom condition (Reineck and Singh, 1980; O'brien and Slatt, 1990; O'Brien, 1996; Schieber, 1998, 2003a, 2007; Wignall et al., 2005; White and Arthur, 2006; Bhattacharya and MacEachern, 2009; Lamb and Mohrig, 2009; Bond and Wignall, 2010).
Fmlc	Black shale/ marlstone	Characterized by thin to thick laminations that are continuous, planar and parallel. Laminae consist of doublets or triplets alternation of siltstone and organic-rich layer or micritic carbonate layer or both. Pyrite, carbonate, and phosphatic peloids/nodules are common. Micro-slumped structures, fossils, synaeresis cracks and burrows are rare. Microflora when present is poorly preserved and infested by pyrite. Their kerogen is dominated by AOM (75-92%), and TOC ranges from 2.15 to 7.46 wt.%.	Gradual fall-out from suspension in distally quiet deep water with no bottom flowing currents and anoxic to suboxic bottom water conditions (Hallam, 1967; Javor and Mountjoy, 1976; Tyson, 1995; O'Brien, 1996; Bohac et al., 2000, 2013; Potter, 2003; Bond and Wignall, 2010).

C	Coal	Massive, thin seam within pebbly sandstone. Kerogen dominated by black debris (99%) and rare resin particles.	Highly degraded and altered sapropelic coal in an abandoned waterlogged fluvial channel with high groundwater table (Roberts et al., 1994; Miall, 1996; Davis-vollum et al., 2008).
V	Igneous intrusions and extrusions	Medium- to fine-grained magmatic rocks within Cretaceous sediments. Occur mostly as dykes and sills, and rarely as extrusives. They range in composition from diorite, dolerite, basalt, trachyte to rhyolite.	Plutonic, hypabyssal, and volcanic igneous rocks (Le Maître and IUGS, 2002; Philpotts and Ague, 2009; Gill, 2010).

Samples from nearby locations were correlated and the locations grouped into a locality that is represented by a composite lithologic profile. Typical composite sections from selected localities in the study area are shown in **figure 3.3** to **3.5**. The sample number code (e.g. 38-10) represents the sampling location and bed number. Symbols for lithology, sedimentary structures and fossils used in this chapter are shown in **figure 3.6**

The kerogen in majority of the analysed samples consists mostly of nine types of particulate organic matter (kerogen components). These components are described in **table 3.2** and illustrated in **figure 3.7** to **3.9**. The abundance of the distinguished kerogen components in relation to total kerogen is based on percent relative numeric frequency (%RNF) and not volume (Buckley and Tyson, 2003), and is categorized as follows: very high (>75%), high (50-74.9%), moderate (30-49.9%), low (10-29.9%), and very low (< 10%).

Q-mode cluster analysis of palynofacies data revealed four superclusters labelled A to D, and consisting of seven clusters (**Fig. 3.10**). The superclusters are termed palynofacies assemblages. A visual representation of the main components of the different palynofacies assemblage is shown as histograms in **figure 3.11**. A summary of the relative abundance (%RNF) of the components is also provided. The paleoenvironmental significances of these palynofacies assemblages is inferred from their plot on the Tyson (1995) AOM–Phytoclast–Palynomorph ternary diagram which is shown if **figure 3.12**.

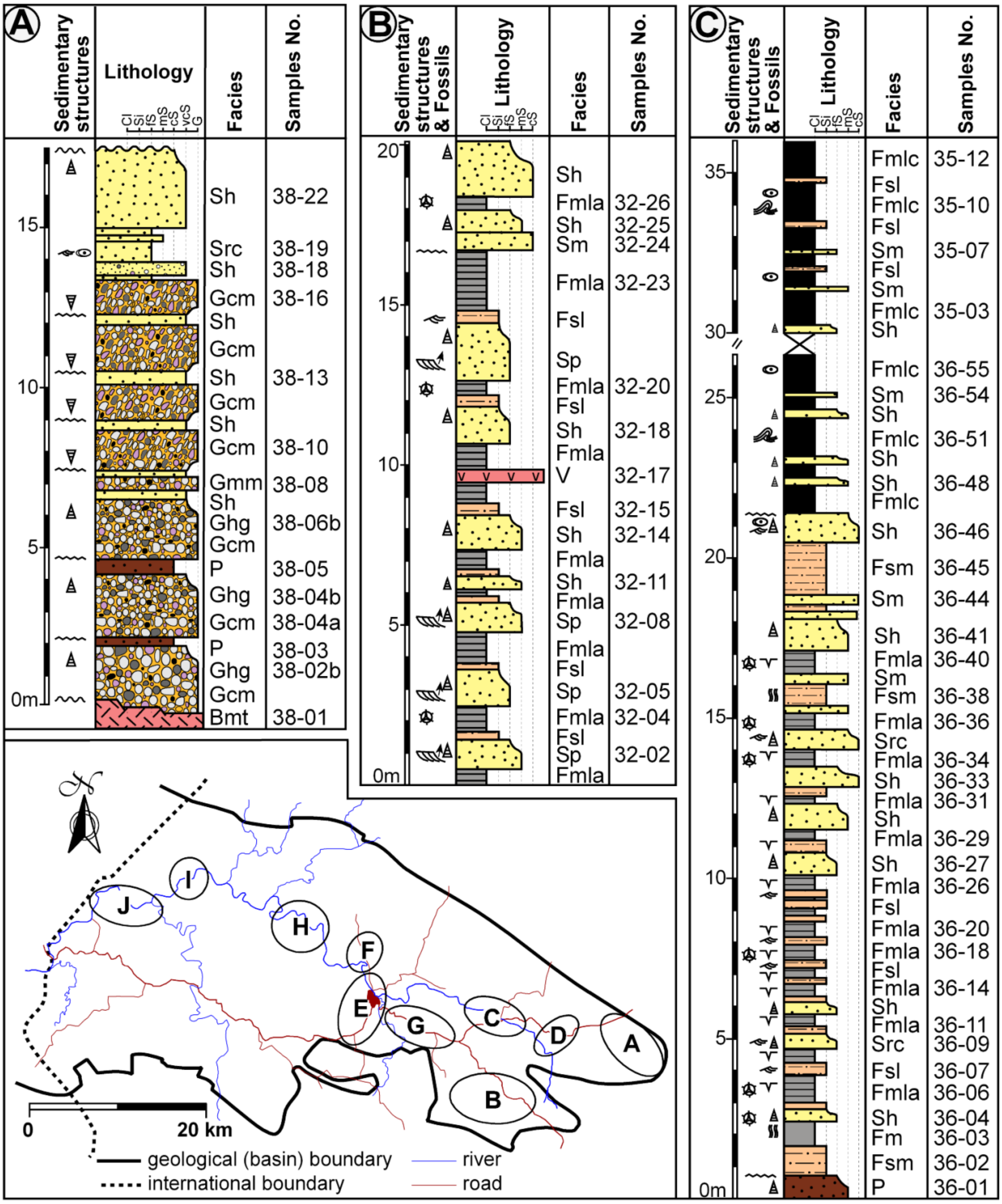

Figure 3.3. Composite lithologic profiles for locality (**A**) Etuko, location 38; (**B**) Obang and Mbinjong, location 32 & 33; and (**C**) Ngeme and Nfaitok II, locations 34–36. The locality of each composite section is shown as a ring on the inset map and the locations are shown in figure 3.2.

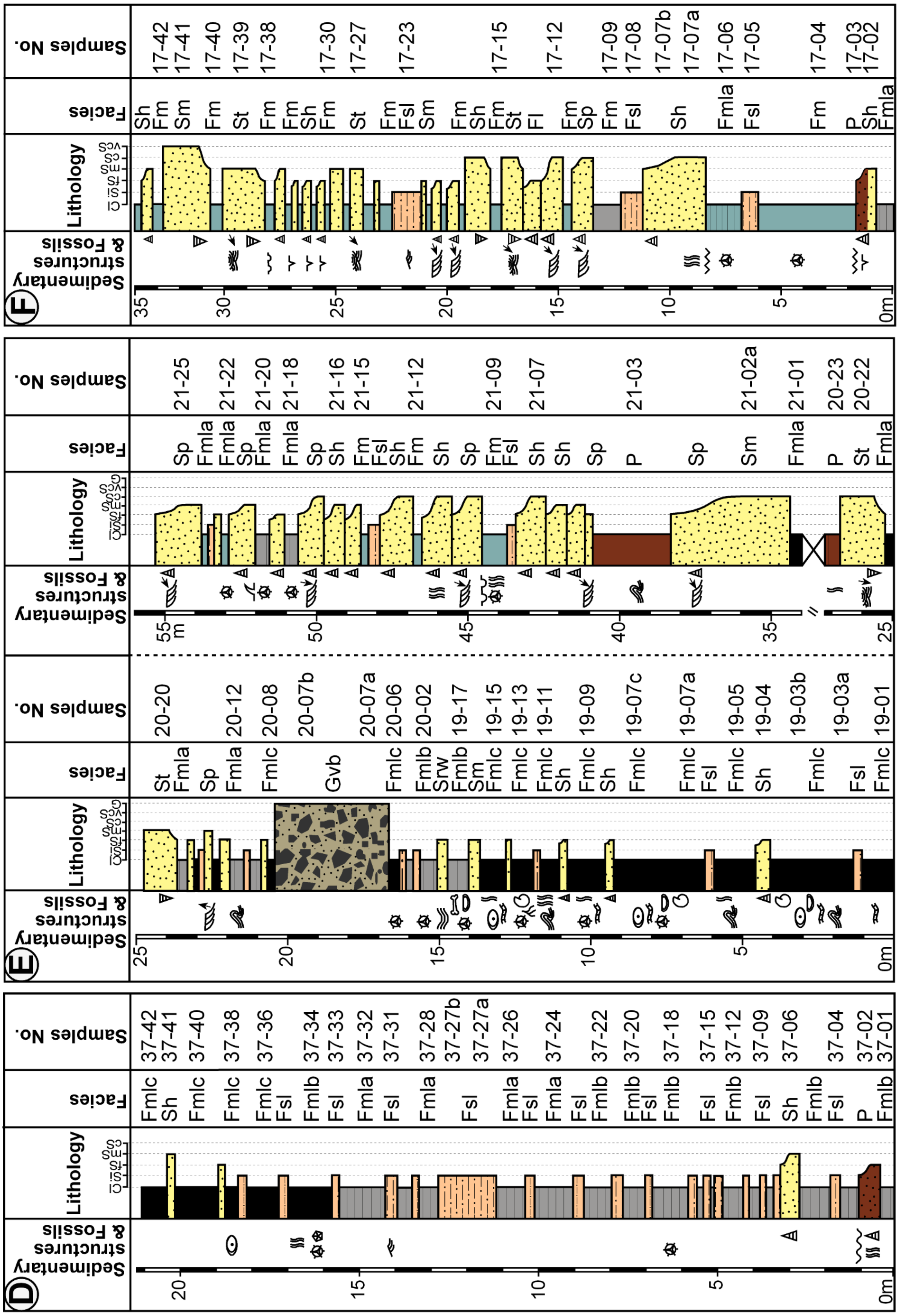

Figure 3.4. Composite lithologic profiles for locality (D) Nchemba, location 37; (E) Mamfe and Besongabang, location 18–23; (F) Baku, location 16. The location of section D, E and F are shown in the inset map of figure 3.3.

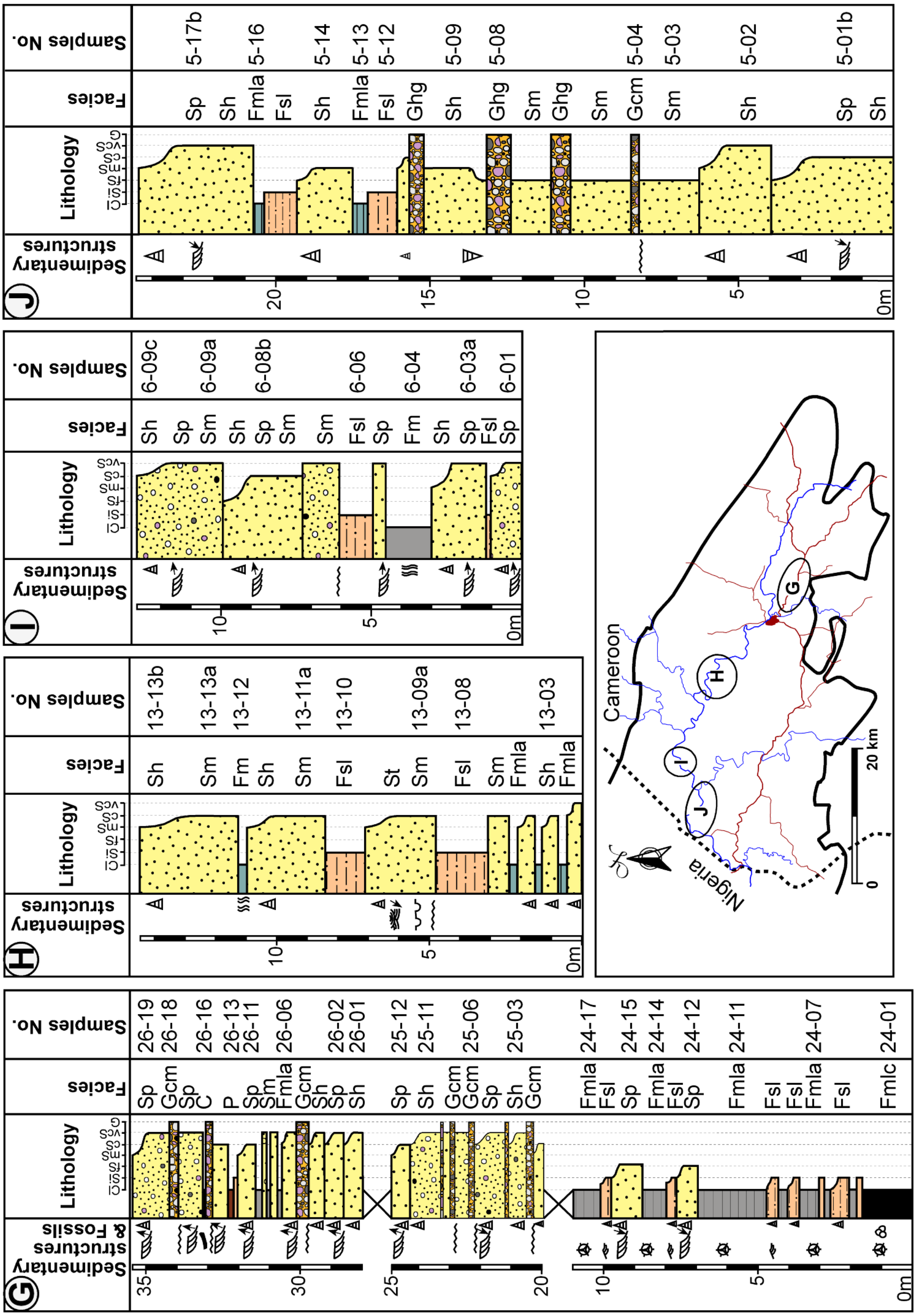

Figure 3.5. Composite lithologic profiles for locality **(G)** Okoyong and Bachuo-Ntai, location 24–26, & 30; **(H)** Esagem and Adolf Kamp, location 12 & 13; **(I)** Beteme, location 6; and **(J)** Nsanakang, location 4 & 5.

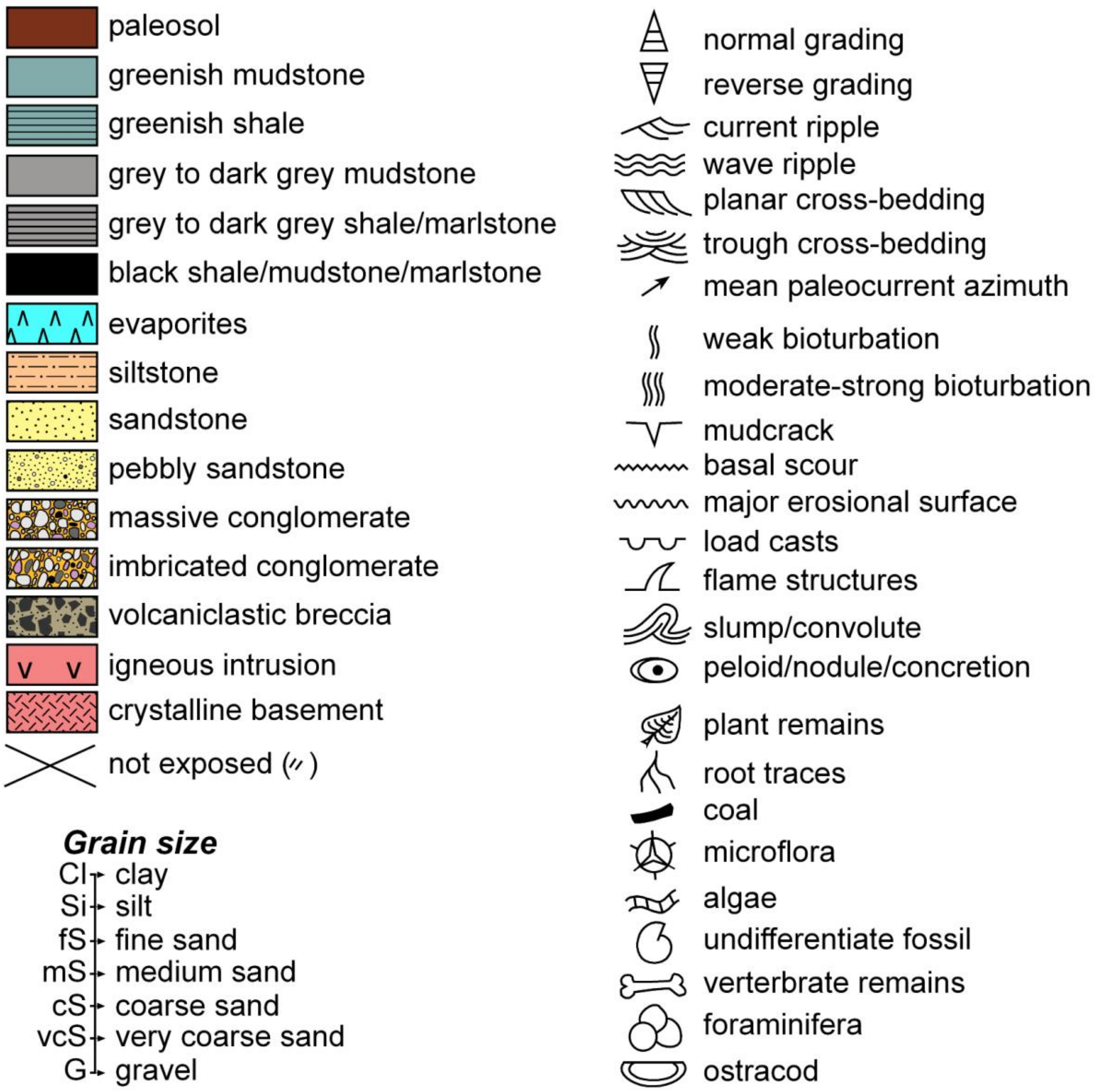

Figure 3.6. Generalized legend of symbols for lithology, sedimentary structures and fossils used in this dissertation.

Table 3.2. Description of kerogen components identified in this study.

Kerogen components	Description
Amorphous organic matter (AOM)	Unstructured, irregularly-shaped particles that vary in texture from granular to spongy (**figure** 3.7A–E), or membranous to finely divided (**figure** 3.7F), or have specks (**figure** 3.7G). They are generally non-fluorescent, and vary in colour from yellow through greyish to brown and dark-brown (**figure** 3.7H). They range in size from 5 to 310 µm.
Resin (amber)	Yellow to reddish, globular or lath-shaped angular amorphous particles that are 53-175 µm in size (**figure** 3.7I & J).

Fungal fragments	Grey to brownish fungal remains such as fruiting body, spores, hyphae and mycelia, and range in size from 10 to 150 µm (**figure** 3.7K & L).
Palynomorphs	Consists of pteridophytes and bryophytes spores (**figure** 3.7A-C), gymnosperm (**figure** 3.8D-G) and rarely angiosperm pollen grains (**figure** 3.8H). Some occur as tetrad or agglomerate of more than 4 sporomorphs (**figure** 3.8I), some are carbonized (**figure** 3.7J) or infested with pyrite crystals (**figure** 3.8K). Their sizes range from 21 to 80 µm.
Freshwater Algae	Aquatic yellowish brown to dark-brown algal remains that are sub-angular to rounded in outline, and range in size from 30 to 135 µm (**figure** 3.8L).
Woody fragments	Are non-fluorescent phytoclast fragments with lath or rectangular or equant shape and sharp angular edges. They are light-brown, yellow-brown or dark-brown, and range in size from 10 to 450 µm. They consist mostly of gymnosperms tracheid fragments showing valve-like perforations (pits). The pits are either surrounded by a thickened concentric darker rim (bordered pit, **figure** 3.9A) or lack a thickened rim (simple pit, **figure** 3.9B), and are arranged in a uniseriate (**figure** 3.9C) or biseriate (**figure** 3.9D) or triseriate (**figure** 3.9A) pattern. Some tracheid fragments show pits having ladder-like (scalariform) shape (**figure** 3.9E).
Cuticle and cortex fragments	Light brown to orange-brown relatively equant or rectangular shape phytoclast fragments showing regular polygonal or rectangular cells (**figure** 3.9F-H). They are generally non-fluorescent and range in size from 10 to 250 µm.
Dark brown-Black fragments	Dark brown to nearly black phytoclast fragments that range in size from 10 to 200 µm (**figure** 3.9I). Some are without discernible biostructures.
Black debris	Opaque, structured to unstructured phytoclasts, sometimes with dark-brown thin edges. They range in size from 10 to 450 µm, are rectangular (bladed or lath-shaped) to equant (equidimensional) in shape, and have angular to subrounded outline (**figure** 3.9J). Some have finely preserved microstructure (**figure** 3.9K & L).

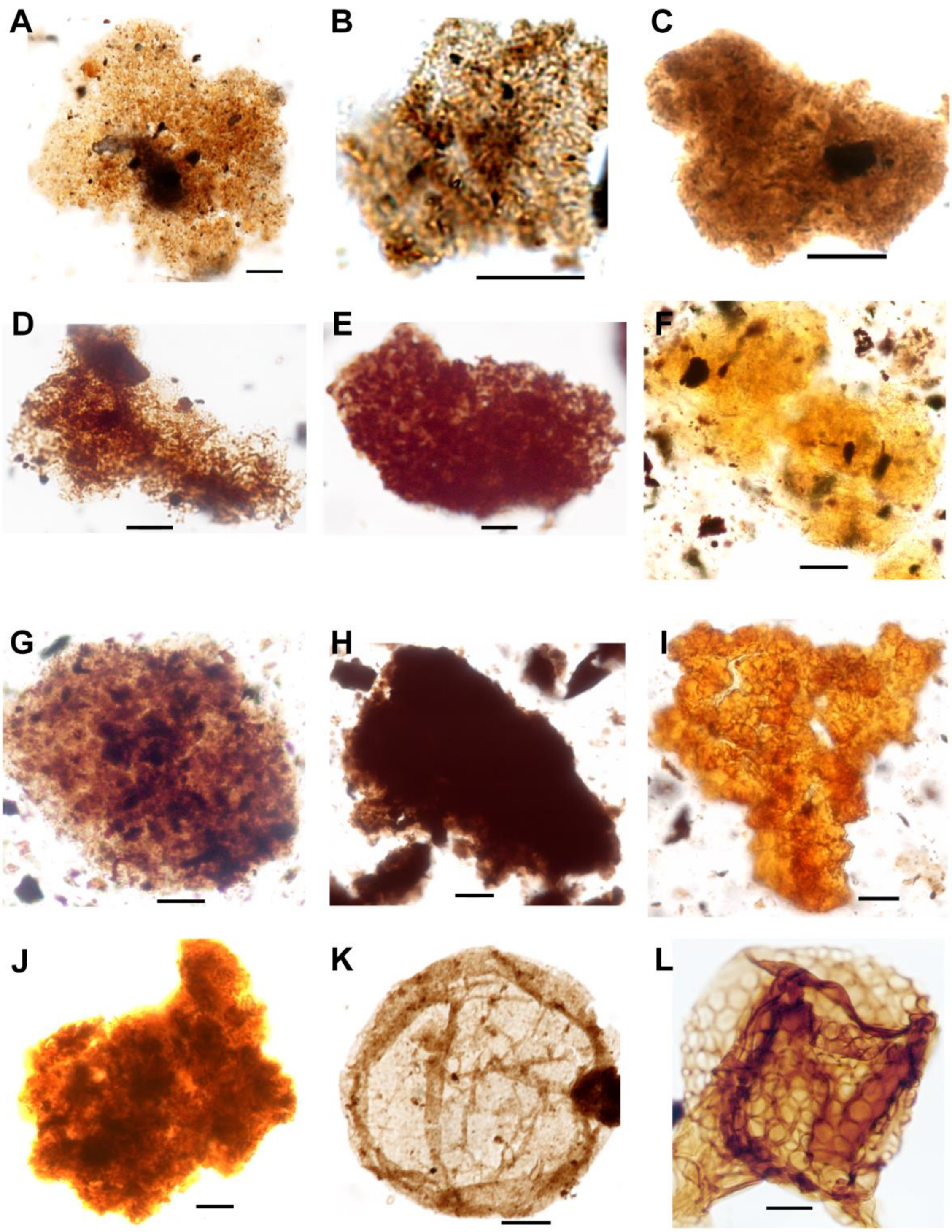

Figure 3.7. Photomicrographs of typical amorphous organic matter (AOM), resin, and fungal remains used for palynofacies analysis. Unless stated (e.g. SB = 20 µm), the scale bar in each illustration is 10 µm. Codes after sample number in illustrations K and M are the slide number and the England Finder coordinates. (**A**) diffuse edged spongy AOM, sample 24-14; (**B**) granular AOM, sample 36-36; (**C**) spongy AOM, sample 36-36; (**D**) diffuse edged granular AOM (SB = 20 µm), sample 24-01; (**E**) granular AOM, sample 36-51; (**F**) membranous AOM (SB = 50 µm), sample 19-09; (**G**) AOM with specks (SB = 20 µm), sample 19-13; (**H**) brown-black fragment (SB = 30 µm), sample 20-06; (**I**) resin fragment (SB = 20 µm), sample 19-13; (**J**) resin (SB = 50 µm), sample 36-51; (**K**) fungal spore, sample 37-34, p4328, H41/0; (**L**) fungal fruiting body (SB = 30 µm), sample 17-04, p4331, M18/4.

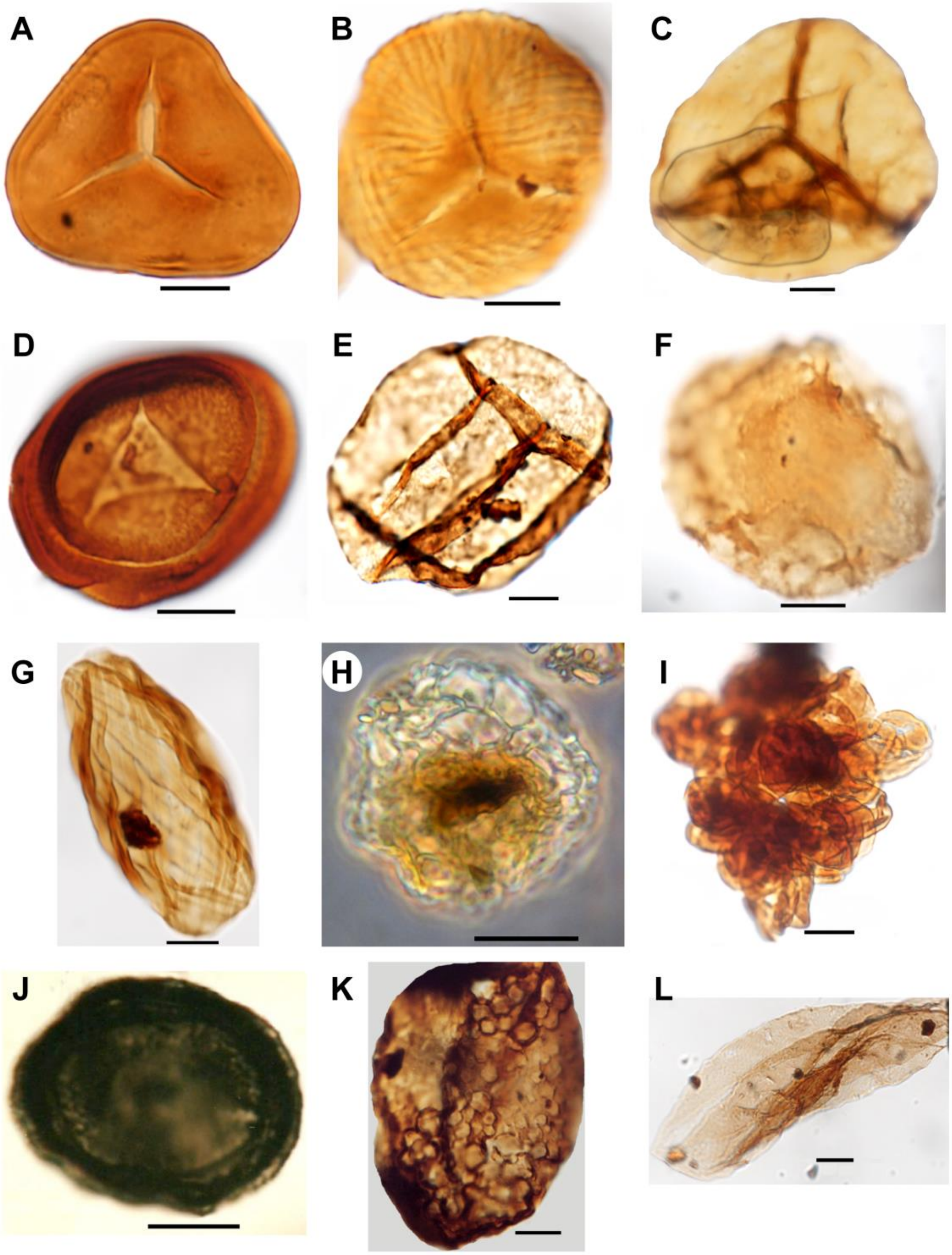

Figure 3.8. Photomicrographs of representative palynomorphs and algal remains used for palynofacies analysis. Unless stated, the scale bar (SB) in each illustration is 10 µm. Codes after sample number are the slide number and the England Finder coordinates (e.g. C46/4) or Leitz Orthoplan coordinates (e.g. 40.4/101.9). (**A**) *Cyathidites minor*, sample 21-09, p4329, C46/4; (**B**) *Cicatricosisporites hallei*, sample 24-01, 9601e, K39/0; (**C**) *Biretisporites* sp., sample 24-01, 9601g, X36/0; (**D**) *Classopollis simplex*, sample 17-06, 9298h, J39/2; (**E**) *Araucariacites australis*, sample 24-14, 9304b, Q21/4; (**F**) *Callialasporites dampieri*, sample 24-01, 9601i, V23/2; (**G**) *Gnetaceaepollenites* sp., sample 17-06, 9298g, R24/0; (**H**) *Afropollis jardinus*, sample 24-01, 9601g, 40.5/106.5; (**I**) agglomerate of *Todisporites* sp., (SB = 20 µm), sample 21-18, 9305g, H35/4; (**J**) carbonized *Classopollis* sp., sample 20-06, 9532b, 40.4/101.9; (**K**) pyritized palynomorph, sample 19-13, 9531b, 30.1/97.0; (**L**) *Ovoidites* sp., (SB = 20 µm), sample 17-06, 9298i, Z21/1.

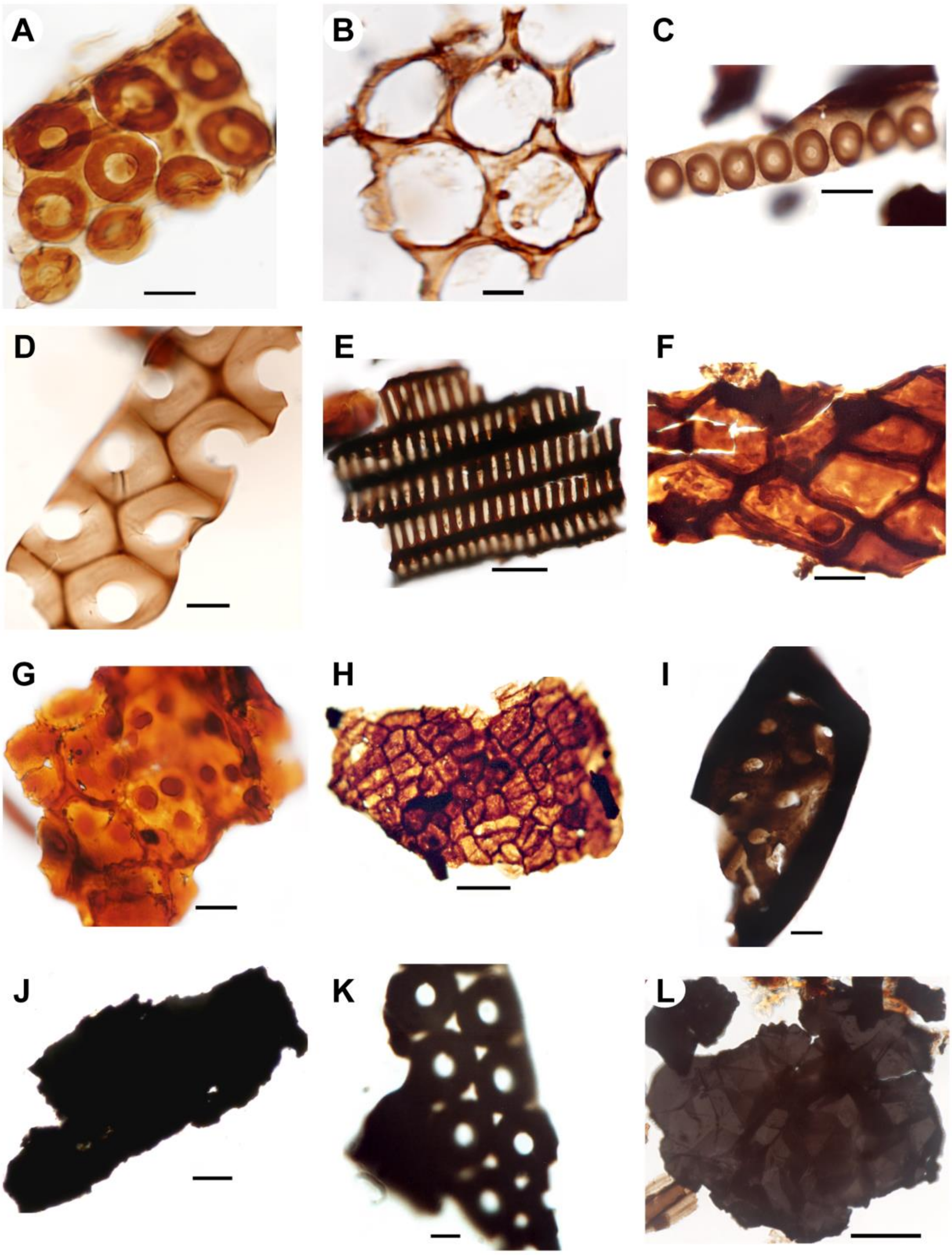

Figure 3.9. Photomicrographs of typical phytoclasts used for palynofacies analysis. Unless stated, the scale bar (SB) in each illustration is 10 µm. (**A**) rectangular shape wood tracheid fragment with triseriate bordered pits, sample 17-06; (**B**) wood tracheid with simple pits, sample 17-06; (**C**) lath-shaped wood tracheid with uniseriate bordered pits (SB = 20 µm), sample 24-01; (**D**) lath-shaped wood tracheid fragment with biseriate bordered pits (SB = 20µm), sample 21-18; (**E**) relatively equant shape dark brown tracheid fragment with scalariform pitting (SB = 20 µm), sample 21-18; (**F**) cuticle fragment with rectangular-polygonal cell outlines, sample 17-06; (**G**) cuticle fragment with polygonal cell outlines (SB = 20 µm), sample 21-18; (**H**) cuticle fragment with epidermal cellular structure, sample 24-14; (**I**) brown-black (partially carbonized) tracheid fragment, sample 20-06; (**J**) lath-shaped opaque phytoclast (SB = 50 µm), sample 19-13; (**K**) opaque wood tracheid showing well preserved pits, sample 21-22; (**L**) charcoalified phytoclast fragment (SB = 30 µm), sample 17-06.

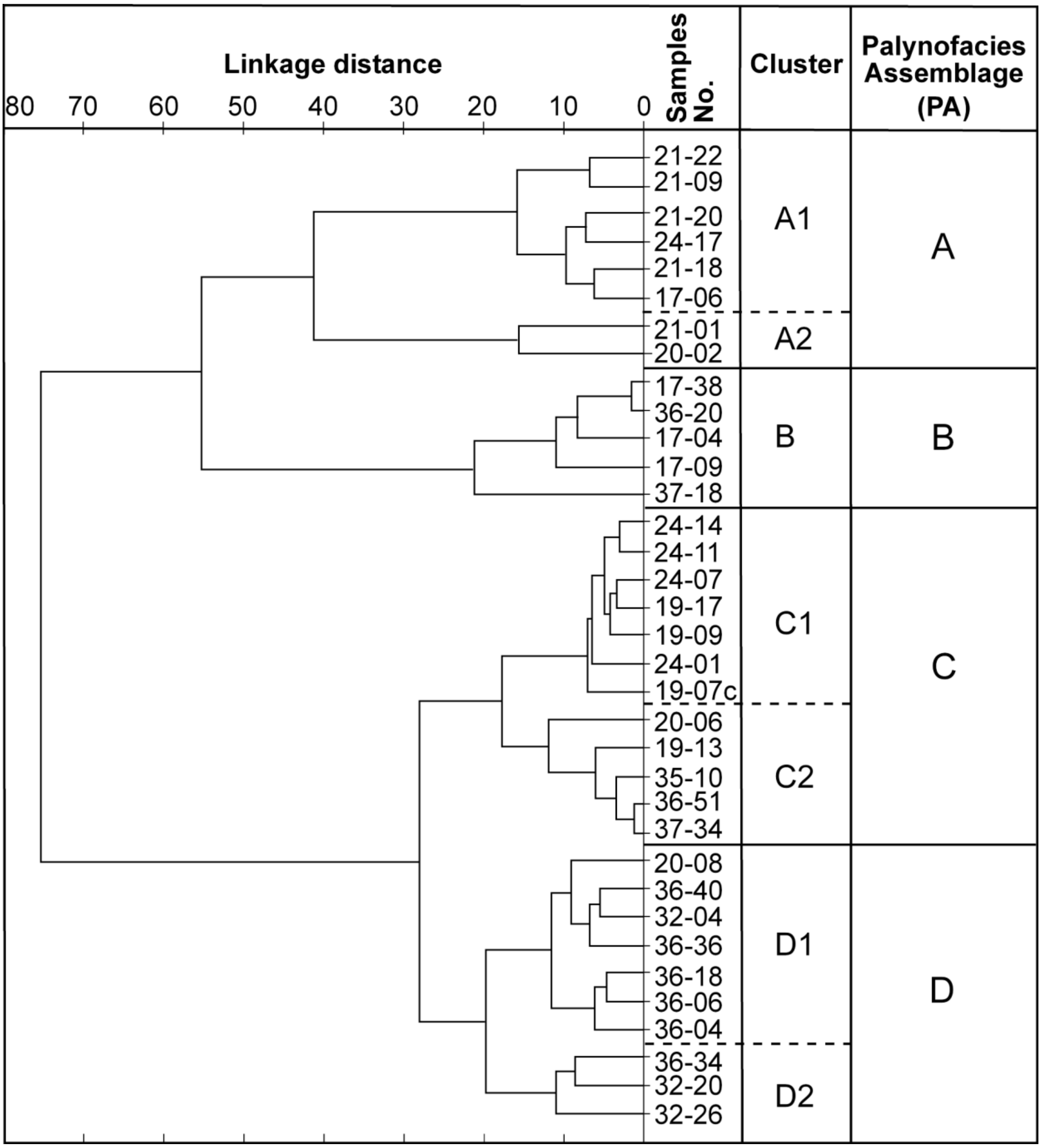

Figure 3.10. Dendrogram of average linkage cluster analysis of dispersed organic matter showing the grouping of samples into four palynofacies assemblages (A-D).

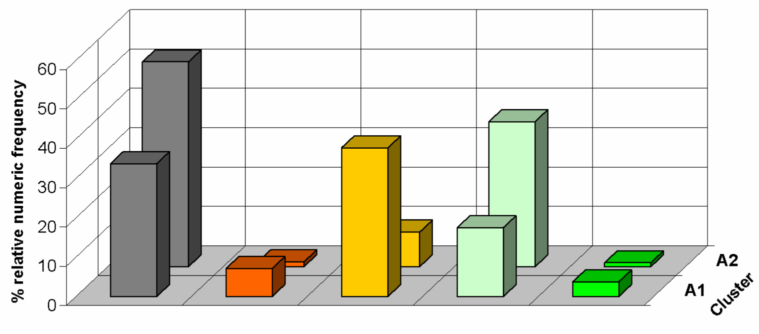

Palynofacies assemblage A

Kerogen components	Range (%RNF)	Mean
1. Black debris	30.0 – 58.9	38.41
2. Str. phyto	6.6 – 43.3	30.57
3. AOM	8.3 – 40.0	22.35
4. Unstr. phyto	0.7 – 9.3	5.63
5. Palynomor.	0.0 – 4.7	3.04

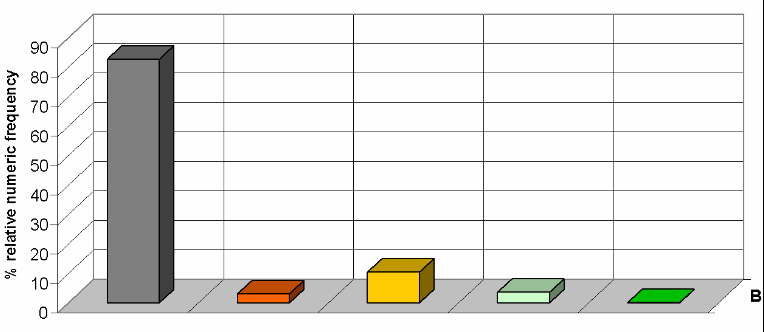

Palynofacies assemblage B

Kerogen components	Range (%RNF)	Mean
1. Black debris	68.4 – 90.0	82.71
2. Str. phyto	6.8 – 14.6	10.45
3. AOM	0.0 – 10.2	3.63
4. Unstr. phyto	1.4 – 6.5	3.07
5. Palynomor.	0.0 – 0.4	0.14

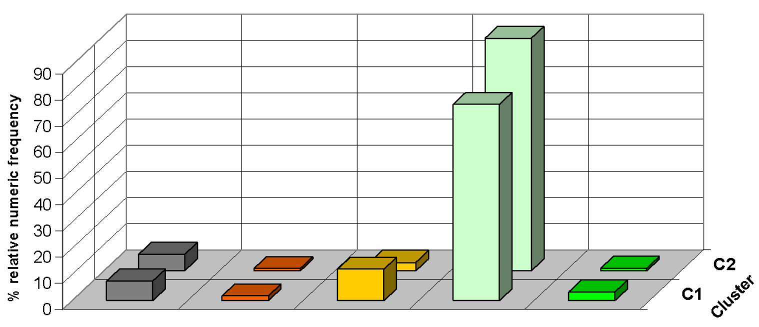

Palynofacies assemblage C

Kerogen components	Range (%RNF)	Mean
1. AOM	70.7 – 92.0	80.78
2. Str. phyto	2.0 – 13.7	8.39
3. Black debris	4.0 – 12.7	7.03
4. Palynomor.	0.0 – 5.7	2.36
5. Unstr. phyto	0.0 – 2.7	1.42

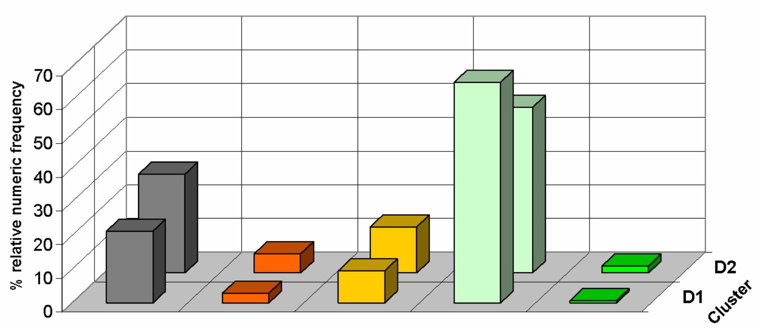

Palynofacies assemblage D

Kerogen components	Range (%RNF)	Mean
1. AOM	44.7 – 74.0	60.60
2. Black debris	18.0 – 31.3	23.73
3. Str. phyto	6.7 – 17.3	10.78
4. Unstr. phyto	0.3 – 9.0	3.77
5. Palynomor.	0.0 – 3.3	1.13

Legend

- Black debris (Opaque)
- Unstructured phytoclasts
- Structured phytoclasts
- Amorphous organic matter (AOM)
- Palynomorphs

Figure 3.11. Representative bar charts of the main kerogen components for the four palynofacies assemblages.

Closely related or similar sedimentary facies were grouped into assemblages of genetically related facies, referred to as facies association (FA, **table 3.3**). The proportion (percent relative thickness to total thickness) of each facies within a facies associated was calculated from the sum of its thickness in measured sections, and classified as either dominant (≥ 20%) or subordinate (< 20%) facies (**table 3.3**).

The proportion of each facies in the facies associations are shown graphically in **figure 3.13.** The facies proportions diagram does not represent facies succession or substitution trend. Interpretations of depositional environments are based on facies association and not individual facies because most depositional processes attributed to individual facies are not unique to one environmental setting (Dalrymple, 2010). Limitations imposed by small size of outcrops and lack of 3-D control hindered the interpretation of most of the facies associations in terms of architectural elements (Miall, 1985; 1996; 2010)

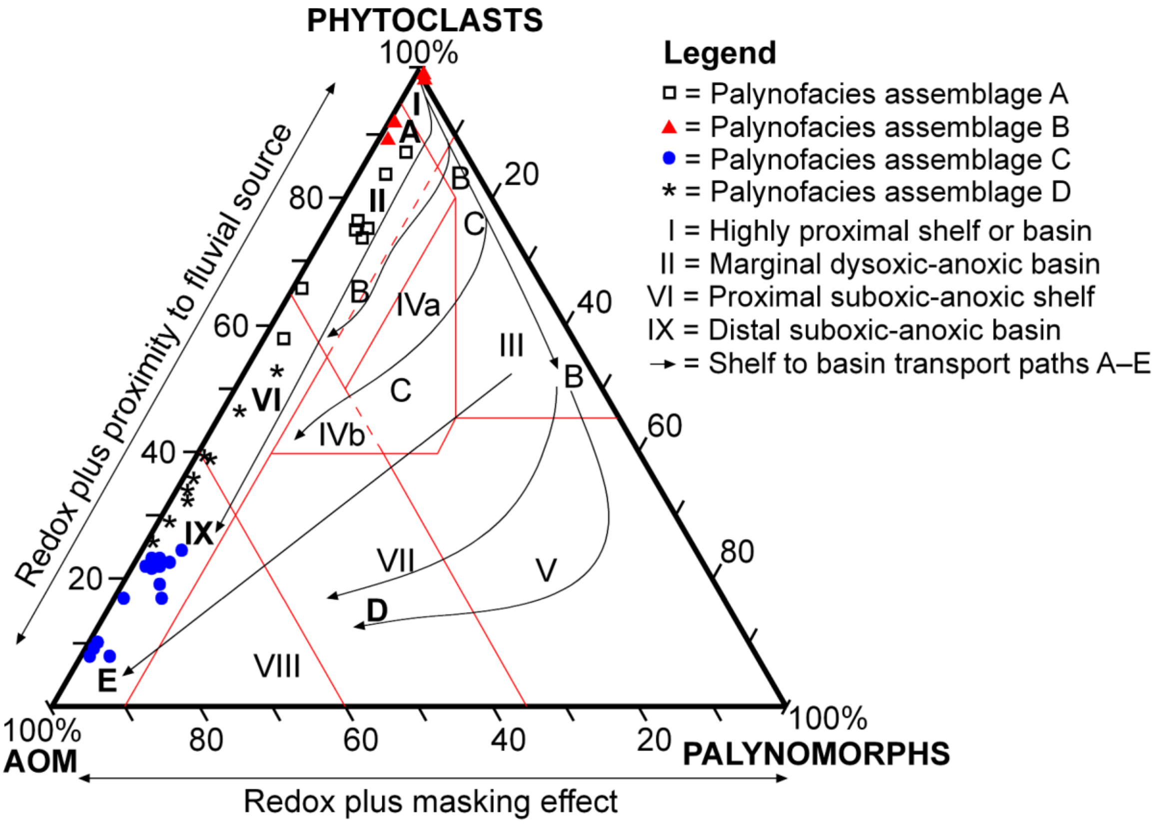

Figure 3.12. Ternary AOM-Phytoclast-Palynomorph (APP) kerogen plot of the studied samples.

The facies associations are described in the following sub-sections according to their temporal and spatial distribution on the inferred depositional gradient from mountain front piedmont through fluvio-deltaic plain to profundal lake (**Fig. 3.14** and

3.15).

Table 3.3. Facies associations and interpretation.

Facies Association	Dominant lithofacies	Subordinate lithofacies	Palynofacies Assemblage	Paleoenvironmental Interpretation
FA1	Gcm, Sh	Ghg, Gmm, P, Src	/	Proximal alluvial fan
FA2	Fmla, Sh, Sp	Fsl, Sm,	D1, D2	Floodplain
FA3	Fmla, Fsl, Fmlb	Sh, P, Fsm, Fm, Src	B, C2	Palustrine
FA4	Sh, Fsm	Fmla, Sm, Src, Fsl	D1, D2	Fluvio-lacustrine
FA5	Fmlc	Gvb, Sh, Fmlb, Fsl, Sm, Srw	C2, C1, D1	Sublittoral-profundal
FA6	Fm, Fmla	Fmlc, Fsl, Sm, Fmlb, P, Sh, Sp	A2, B, C1	Littoral-shoreline
FA7	Sh	Fm, Fmla, St, Sm, Sp, Fsl, P, Fl	A1, B, C1	Fluvio-deltaic
FA8	Sp, Sh	Gcm, Sm, Fmla, P, Gmm, Fsl, C	/	Medial alluvial fan
FA9	Sh, Sm	Sp, Fsl, Ghg, Fm, Fmla, St, Gcm	/	Fluvial channel-overbank

A lake basin can be regarded as an enclosed, small-scale, tideless ocean basin, with potentially many of the same controlling factors affecting deposition (Keighley, 2008). Their subenvironmental zonation is thus similar to that of marine basins (Tucker and Wright, 1990; Ferber and Wells, 1995; Bohacs et al., 2000; Keighley, 2008; Plint, 2010; Renaut and Gierlowski-Kordesch, 2010).

The utilization of lithological, paleontological and geochemical data in the interpretation and reconstruction of the depositional setting of a sedimentary unit relies on the observation that every hydrodynamic, biological and chemical process produces a specific record of its action in the enclosing sediment (Reineck and Singh, 1980; Reading, 2003; Dalrymple, 2010a). A given environment of deposition is characterized by certain processes that produce specific features. The observable features in the sediment (e.g. texture, structure, organic content, and type of fossils) are used to infer processes, and an assemblage of processes is used to infer environment of deposition. Facies are thus the building block for the reconstruction of depositional environments.

Table 3. 4. Terminology for the description of bottom water oxygenation (from Tyson and Pearson, 1991).

Oxygen concentration (ml/l)	Environment	Biofacies
2.0-8.0	Oxic	Aerobic
0.2-2.0	Dysoxic	Dysaerobic
0.0-0.2	Suboxic	Quasi-anaerobic
0.0 (H_2S)	Anoxic	Anaerobic

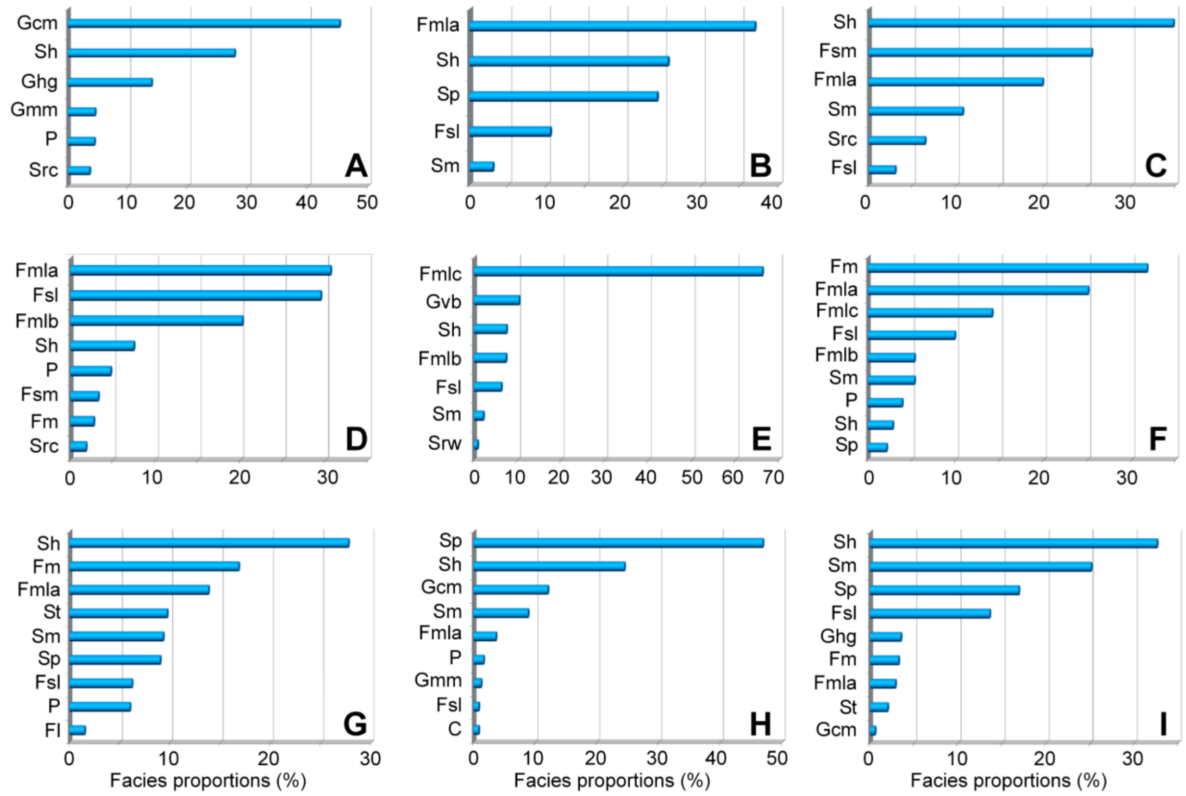

Figure 3.13. Summary of facies proportions within the facies associations. (**A**) FA1, proximal alluvial fan; (**B**) FA2, floodplain; (**C**) FA4, fluvio-lacustrine; (**D**) FA3, palustrine; (**E**) FA5, sublittoral to profundal; (**F**) FA6, littoral-shoreline marshes; (**G**) FA7, fluvio-deltaic swamps; (**H**) FA8, medial alluvial fan; (**I**) FA9, fluvial channel-overbank.

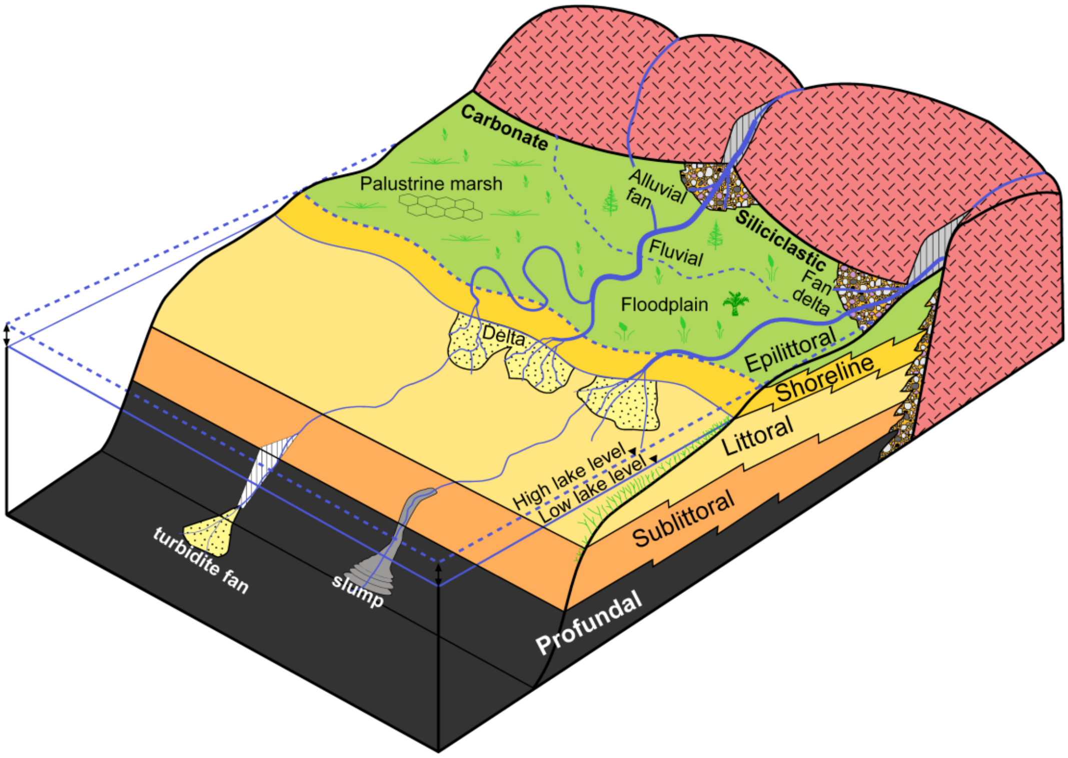

Figure 3.14. A conceptual model of the arrangement and evolution of depositional zones in and adjacent to Mamfe paleolake (Adapted from Tucker and Wright, 1990; Gierlowski-Kordesch, 2010).

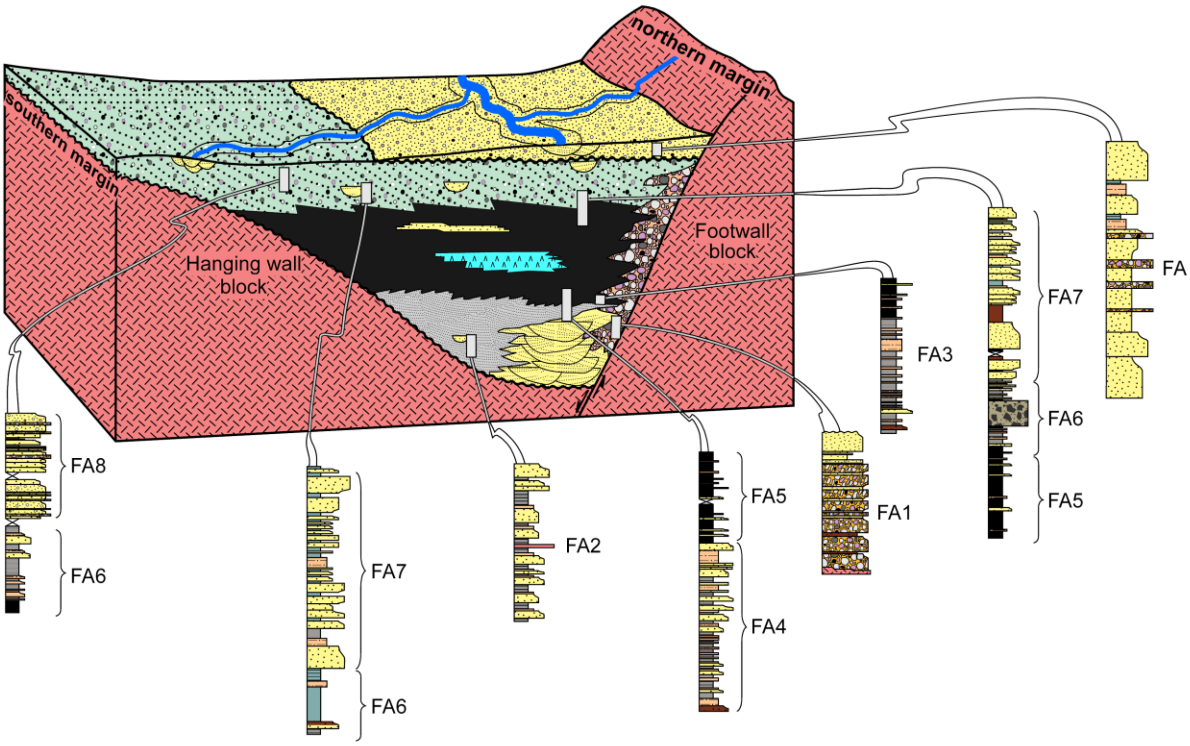

Figure 3.15. A conceptual transverse section of the Mamfe half-graben showing inferred location of representative lithologic sections and facies associations.

3.3.1 FA (Facies association) 1: Proximal alluvial fan

3.3.1.1 Description

FA1 is about 18.3 m thick, and consists of couplets of cobble- to boulder-rich conglomerate and pebbly sandstone or paleosol. It outcrops mainly along the basin master fault at the northeastern margin of the Mamfe Basin in Cameroon. It is generally brownish, and made up of interbedding of 6 lithofacies (**table 3.3**). Lithofacies succession and substitution trend in this facies association is shown in **figure 3.3A**, and their relative proportions in **figure 3.13A**. Facies Gcm, Sh and Ghg account for 87% of its total thickness in outcrops.

Gcm facies (massive, clast-supported conglomerates) consists of 10-800 mm diameter (medium pebbles to medium boulders) extraformational clasts that are sub-angular to subrounded and poorly sorted. Units are crudely stratified and range in thickness from 40-170 cm, are underlain by low relief erosional surfaces, have lenticular geometry, and show a thinning upward trend. Some of the units show crude coarsening upward in their basal part and imbrication towards the top. Gcm is often succeeded by crude horizontally bedded conglomerates (facies Ghg). The boundary between Gcm and Ghg is commonly diffused.

Ghg ranges in thickness from 20-50 cm, and is comprised predominantly of poorly sorted subrounded clasts that are 20-350 mm in diameter. Ghg show normal grading in the uppermost part and is overlain by either dark brown to brick-red paleosols (facies P) or horizontal planar bedded sandstone (facies Sh).

Facies P consists of medium to coarse-grained, poorly sorted ferruginized sandstone. Units are 30-80 cm thick and show a thickening upward trend. The uppermost unit is overlain by an indurated massive hematite-rich ferricrete (iron hardpan).

Facies Sh is comprised predominantly of poorly sorted, fine to very coarse-grained and pebbly arkosic sandstone. Units are 15-255 cm thick, commonly show fining upward in their upper part, and have a thickening upward trend. It is rarely interbedded with ripple laminated fine-grained sandstone (facies Src). Src is 65 cm thick and contain abundant ferric nodules.

The Gmm facies is a clast-rich massive matrix-supported conglomerate. The clasts are subangular to subrounded, 20-600 mm in diameter, poorly sorted and float in a matrix of coarse-grained sand. Units are 13-28 cm thick and commonly underlain and overlain by facies Sh.

3.3.1.2 Interpretation

The sedimentological characteristics of FA1 (abundant coble to medium boulder-size clasts, poor sorting, clast-supported fabric, lack of mudrocks etc.) and its spatial distribution along the footwall of the master fault at the northeastern margin of the basin suggests that it is a debris flow (Blair and McPherson, 1994, 2008, 2009) or hyperconcentrated flow (Miall, 1996, 2010; Benvenuti, 2003; Boggs, 2009; Leeder, 2011; Talling et al., 2012) dominated proximal alluvial deposit. No direct morphological features suggesting fan geometry were observed in the small and scattered outcrops of this FA, so it could preferably be referred to as alluvial slope deposit (sensu Blair and McPherson, 1994; Smith, 2000).

The texture (medium pebble to medium boulder sized clasts, poor sorting, subangular to subrounded clasts) suggests rapid deposition and short transport distance from source areas by high competence and high capacity sediment-gravity flow processes. Sediment availability and delivery could have been promoted by high relief and weathering associated with tectonic uplift and fracturing in the Bamenda Massif (e.g. Blair, 1999a & b; Iverson, 1997, 2003, 2014; Blair and McPherson, 2009; Dalrymple, 2010b). The boulder size clasts are believed to have been transported to the fan site as rockfall.

Clast size distribution within FA1 suggests that the deposit evolved from subaerial debris flow or hyperconcentrated flow dominated processes in the lower part to a mixture of debris flow and braided stream dominated processes in its middle and upper part (e.g. Smith, 2000; Volker et al., 2007). The FA is considered to be non-cohesive debris flow (sensu Blair and McPherson, 1994) and braided stream deposits of transverse tributaries rivers draining the Bamenda highland and mt. Bamboutos (**Fig. 1.3, 2.13**; e.g. Kim et al., 2011). No sloping margins suggestive of channelized flows were observed in outcrops.

The Gcm facies is interpreted as representing the outside margin of the debris flow levee while the rare Gmm facies represent the inner margin of debris flow levee or clast-rich debris flow lobe (Blair and McPherson, 1994, 2009). The poor sorting and mostly massive nature of this FA suggests a competence and capacity driven deposition as a result of decrease in flow velocity and flow depth at the foot of the Bamenda highland (Massif).

FA1 is a multistorey stack that represents at least 7 depositional episodes. The stacking pattern suggests that flows repeatedly reoccupy the same sites and that periods of rapid deposition alternated with intervals of low or non-deposition, weathering, pedogenesis, and erosion. It is divisible into a lower (FA1a), middle (FA1b) and upper (FA1c) sections respectively.

FA1a is underlain by crystalline basement rocks and is about 7.4 m thick. It represents at least 3 episodes of subaerial debris flow deposition. Each depositional episode consists of a finning upward succession of facies Gcm, Ghg, and P, and is overlain by a low relief erosional surface (basal scour). The basal scour is thought to have been produced by reworking (fine fraction winnowing) of older alluvial surface by overland flows (rills) prior to the following depositional episode.

Decrease in maximum clast size upwards from medium boulders in facies Gcm through fine boulders in facies Ghg to pebbly sandstone in facies P is believed to be an indication of a decrease in sediment supply as a result of one or more of these factors: decline in flow competence and flow velocity (waning flow); retrogradation and subsidence (e.g. Benvenuti, 2003; Nanson and Gibling, 2003); gradual abandonment of fan segment due to avulsion (e.g. Smith, 2003; Blair and McPherson, 1994, 2009); decrease in tectonic activity; drier climate; or selective depletion in the coarser clasts due to their preferential movement during flow to the front of the debris flow (e.g. Blair and McPherson, 2008).

The ferruginized sandstone (paleosol) bed that marks the upper part of each depositional episode is evidence of secondary processes related to subaerial exposure during intervals of low or non-deposition. These secondary processes include: oxidation and hydrolysis of clasts containing feldspars and iron-bearing minerals into clays and hematite; winnowing of fine fraction from the surface of the previous primary deposit; pedogenesis in inactive lobes with stable surfaces (e.g. Bridge, 2003), and erosion. Ferruginization is believed to have been enhanced by low water table in topographically higher and well drained part of the fan (e.g. Beauvais and Colin, 1993; Sheldon, 2005; Hillier et al., 2011) during warm and dry climate (e.g. Tardy et al., 1991; Mack et al., 1993; Retallack, 2001; Kraus and Riggins, 2007; Bheemalingeswara et al, 2013).

The middle section (FA1b) is 6 m thick, and is a coarsening upward succession that is thought to represent at least 4 episodes of progradational debris flow deposition. It is made up of interbedding of facies Gcm and Sh. Facies Gcm are crudely imbricated and show reverse gradation in their basal part. Facies Sh is very coarse and pebbly sandstone that is interpreted to be waning flow deposits. Lack of the subaerial weathering and pedogenic features observed in FA1a in the middle section suggests that intervals of low- to non-deposition between debris or hyperconcentrated flow episodes were comparatively of shorter duration, and a higher water table due perhaps to a wetter climate. The middle unit is thus inferred to have resulted from basin-ward advancement of the fan due to increase in sediment supply to the fan site. Increase in sediment yield may be attributed to renewed tectonic activity (uplift), denudation, and wetter climate (e.g. Blair and McPherson, 1994; Iverson, 1997).

The upper section (FA1c) is a 4.9 m thick fining upward succession that is made up mostly of very coarse to pebbly sandstone (facies Sh) with interbeds of ripple-laminated fine- to medium-grained sandstone (facies Src) with ferric nodules. The ferric nodules suggest a neutral to alkaline water-logged soils (Retallack, 1988). FA1c is interpreted to be a braided stream deposit. The top of FA1c is marked by 80 cm thick highly weathered and ferruginized, strongly indurated, massive, medium-grained sandstone (ferricrete or iron-hardpan). The iron-hardpan has been designated as the top of FA1, and is interpreted to have formed during periods of little or no tectonic activity and prolong subaerial exposure in a contrasted hot and dry climate (e.g. McFarlane, 1991; Tardy et al., 1991; Miall, 1996; Retallack, 2001; Velde and Meunier, 2008; Sheldon and Tabor, 2009).

FA1 is nonfossiliferous and underlain by crystalline basement rocks, and is inferred to be the basal sedimentary succession of the Mamfe Basin. This inference is supported by palynological and illite crystallinity data of the overlying FA2. FA1 correspond to the type 1 (incipient) fan of Blair and McPherson (1994), and is believed to be a pre-rift deposit that is associated with regional tectonic uplift in the Late Jurassic to Early Cretaceous (e.g. Brunet et al., 1988; Benkhelil, 1989; Petters, 1991; Guiraud et al., 1992; Wilson and Guiraud, 1992; Basile et al., 2005; Bumby and Guiraud, 2005). It is thought to be coeval with early Cretaceous pre-rift basal alluvial fan and braided stream deposits that have been reported from other basins within the Afro-Brazilian Depression (e.g. Popoff, 1988; Petters, 1991; Matos, 1992; Maluski et al., 1995; Da Rosa and Garcia, 2000).

Although FA1 does not show fan morphology on outcrops, it is believed to be an alluvial fan and will be referred to from now on as basal proximal debris flow alluvial fan (DAF).

3.3.2 FA 2: Floodplain Deposits

3.3.2.1 Description

This facies association consists of alternation of dark grey shale (Fmla), and horizontally bedded sandstone (Sh), planar cross-bedded sandstone (Sp) with intercalations of siltstone (Fsl) and massive sandstone (Sm). It outcrops in the southeastern margin of the Mamfe Basin in and around Mbinjong and Obang. Measured composite section from these locations is about 20.3 m thick. Lithofacies succession and substitution trend in this facies association is shown in **figure 3.3B**, and their relative proportion in **figure 3.13B.**

The dark grey shale account for about 37% of the total thickness of this FA. Beds of this facies range in thickness from 25 to-195 cm. They are thickly laminated, some are bioturbated, or contain microflora. The have TOC ranging from 0.86-2.52 wt.%, and their kerogen is dominated by amorphous organic matter with subordinate black debris and structured phytoclasts. They belong to palynofacies assemblage D (**Fig 3.10-3.12**)

Facies Sh is fine to medium and rarely coarse-grained arkosic sandstone. They are poorly sorted and graded, and range in thickness from 40-180 cm. They are massive at the base and graded towards the top where they pass gradationally into thickly laminated siltstone (facies Fsl). The boundary between the sandstone and the overlying siltstone is often sharp. Bed thickness of the siltstone range from 20 to 40 cm.

Facies Sp are medium to coarse-grained cross-bedded arkosic sandstone ranging in thickness from 95-185 cm. They are poorly sorted, massive at the base and graded towards the top into grey thinly laminated siltstone (facies Fsl).

3.3.2.2 Interpretation.

The sedimentary textures and structures, and palynofacies attributes of the dominant lithofacies of this FA suggests deposition in a predominantly low energy environment. Lithofacies substitution trend and inferred depositional processes attributed to each of the facies (**table 3.1**) favour a floodplain setting. Abundant amorphous organic matter and high TOC suggest relatively quiet dysoxic-suboxic conditions during deposition. FA2 is interpreted to be axial river floodplain deposits on the hanging-wall of the Mamfe half graben (**Fig. 3.15**).

3.3.3 FA 3: Palustrine

3.3.3.1 Description

This facies association is 27.6 m thick and outcrops mainly around Nfaitok and Nchemba and Etuko area. The association is characterized by tabular geometry. It consists of an alternating succession of grey calcareous shale (Fmla), dark grey marlstone (Fmlb) and micaceous siltstone (Fsl) with interbeds of very fine-grained sandstones (Sh) and massive siltstone (Fsm). Typical lithofacies succession and substitution trend within this FA are represented in the lower part of **figure 3.3C & figure 3.4D,** and facies proportion in **figure 3.13D.**

Calcareous shale and marlstone make up 51 % of this FA. Their beds range in thickness from 10 to 130 cm. They are thin to thickly laminated, rarely-fossiliferous, and have TOC ranging from 0.31 to 2.61 wt.%. Their AOM content ranges from 0-90.7%, structured phytoclast from 5-21.1%, and black debris from 4-90%. Their clay fraction is made up mostly of kaolinite with subordinate illite. Desiccation marks are common and burrows are rare.

The micaceous siltstone vary in thickness from 20 to 168 cm. The siltstones are micaceous, thickly laminated and occasionally graded and cross rippled.

The horizontally bedded sandstones (Sh) are very fine- to fine-grained, moderately sorted, and range in thickness from 40 to 70 cm. Some of the sandstone units show ripple or cross lamination.

3.3.3.2 Interpretation

Predominance of fine-grained deposits in this FA suggests deposition in a low energy environment. Samples from this FA belong to palynofacies assemblage (PA) B and C which from the AOM–Phytoclast–Palynomorph (APP) ternary diagram (**Fig. 3.12**) were deposited in a proximal to marginal dysoxic to anoxic basin. The high TOC content of the samples corroborate this inference. Occasional abundance of black debris and fungal remains recorded in some samples indicate shallowing and subaerial exposure leading to diffusion of oxygen to the surface of the sediments (e.g. Hart, 1996). Desiccation marks and occasional paleosol units within this FA indicates intervals of subaerial exposure during deposition. The FA is thus interpreted as a palustrine deposit.

3.3.4 FA4: Fluvial-lacustrine

3.3.4.1 Description

Lithofacies that make up this facies association outcrop in Nfaitok. It consists of a 10 m thick alternating succession of horizontally bedded sandstone (Sh), massive siltstone (Fsm), and grey shale (Fmla) with interbeds of massive sandstone(Sm) and current ripple-laminated sandstone. Lithofacies succession and substitution trend within this FA is represented by the middle part of the lithologic profile of **figure 3.4C**, their relative proportions in **figure 3.13D** and representative outcrop is shown in **figure 3.16.**

Horizontally bedded sandstone range in thickness from 70-100 cm and make up 35% of this FA. They are arkosic, fine to coarse-grained, poorly sorted, and show a coarsening upward trend.

Facies Fmla range in thickness from 20-77 cm account for 25% of this FA. They contain microflora, TOC ranging from 0.68-1.17 wt.%. Their kerogen consists of 52-70% AOM, 13.3-15.35 structured phytoclasts, and 15.7-31.35 back debris.

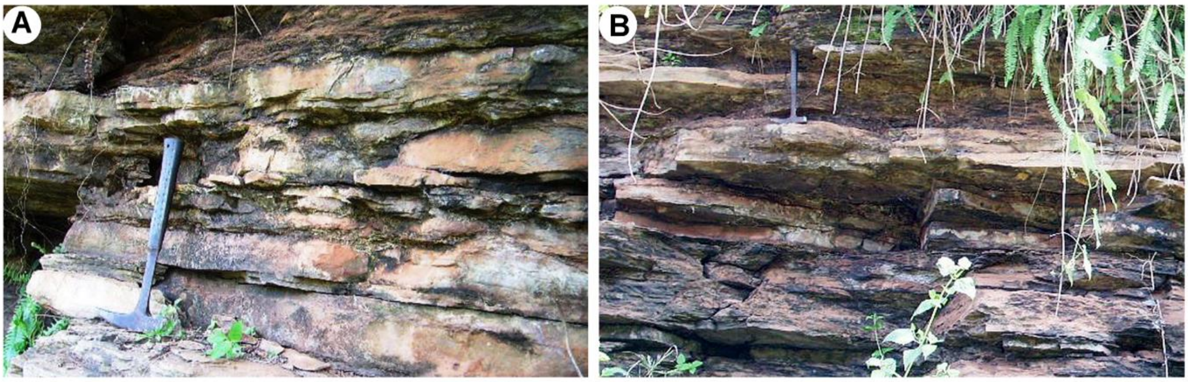

Figure 3.16. Field photos of fluvio-lacustrine sediments at Nfaitok.

3.3.4.2 Interpretation

It is reasonable to infer alternating fluvial and lacustrine depositional setting from the hydrodynamic conditions associated with lithofacies substitution trend within this FA. Samples from this FA belong to the palynofacies assemblage D which from the APP plot (**Fig. 3.12**) and their TOC content indicate that the shales were deposition in a relatively quiet dysoxic-oxic water body.

3.3.5 FA5: Sublittoral-profundal

3.3.5.1 Description

This FA is 37.4 m thick, and outcrops in Ngeme, Nfaitok (upper part and lower **Fig. 3.3C**), Nchemba (upper part of **Fig. 3.4D**), Mamfe (lower part of **Fig. 3.4E**) and Besongabang area. It is made up predominantly (66%) of dark grey to black calcareous shale and marlstone (Fmlc) that are intercalated with sandstones (Sm) and siltstones (Fsl), and volcaniclastics (Gvb). Typical outcrop and microfacies of this FA is shown are shown in **figure 3.16C-E, figure 3.17, & 3.18**.

Fmlc account for 66% of this FA. Beds range in thickness from 40-310 cm. Bed thickness increases upward as a result of decrease in the frequency of interbedding with sandstones and siltstones. They are very thin to very thickly laminated. The laminations are continuous, planar and parallel. The laminae consist of doublets or triplets alternation of siltstone and organic-rich layer or micritic layer or both. Pyrite, carbonate and phosphatic peloids/nodules are common. Micro-slumped structures, macrofossils, synaeresis cracks and burrows are rare. Microflora when present is poorly preserved and infested by pyrite. They are rich in organic carbon with TOC ranging from 2.65-7.46 wt.%. Their clay mineral fraction is dominated by illite. Their kerogen is dominated by AOM (75-92%) with an exception in the carbonaceous shale where black debris constitutes between 91-94%.

The sandstones are very fine- to fine-grained, poor to moderately sorted and vary in thickness from 10-50 cm. They are commonly planar laminated (Sh) and rarely wave ripple-laminated (Srw) or massive (sm). The siltstone (Fsl) are 15-30 cm thick.

Towards the top of this FA, the black shale/marlstone beds progressively become thinner and pass upward into a 60 cm thick sandstone and a succession of whitish wave ripple-laminated micaceous siltstones and marlstones, covered by a succession of grey shales, sandstones and carbonaceous shale (**Fig. 3.18C**) that are conformably overlain by a 385-800 cm thick volcaniclastics deposit. The volcaniclastic unit is made up of poorly sorted and angular to subrounded clasts of basalt and grey shale in a calcareous matrix. The clasts are 2-40 cm in diameter and surrounded by dark brown rims.

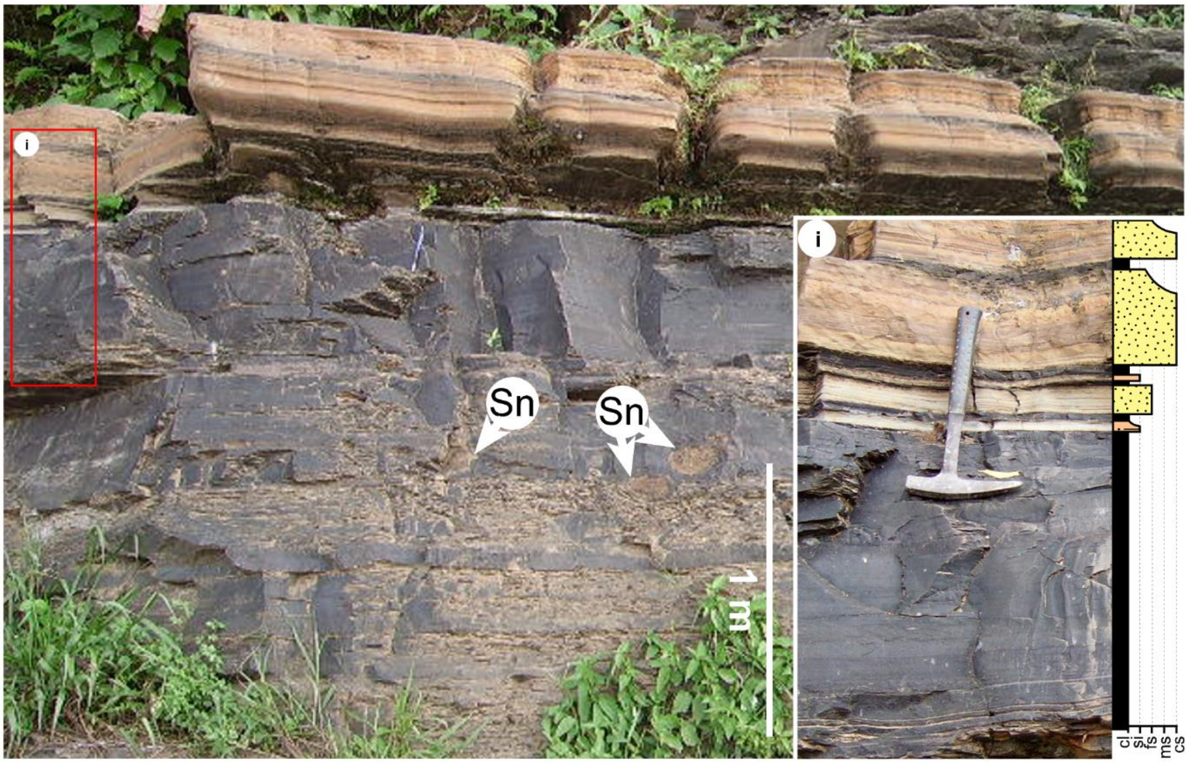

Figure 3.17. Field photos of profundal sediments at Satum, Mamfe. Sn = siderite nodule.

3.3.5.2 Interpretation

The main features recorded in this facies association indicate deposition from suspension in a low energy environment that was thermally or chemically stratified. Lack of current structures points to deposition below wave base. The thickening upward of the shale units with corresponding decrease in the frequency of intercalation with siltstone and sandstone indicates a deepening upward that was caused by increase in the base level with a consequent increase in distance from the shoreline. It is therefore a transgressive sequence. The intercalated sharp base sandstone units in the shale are interpreted to be turbidites that originated from periodic river flood discharge into the lake.

The colour of the shale, high TOC and AOM content, rare bioturbation and abundant pyrite are indicative of a reducing environment (e.g. Kelt, 1988; Tyson, 1995; Tyson and Buckley, 2003). Results of geochemical analysis indicate that the organic matter of these shales have low terrigenous/aquatic ratios (0.09-0.23) and are composed mainly of low molecular weight *n*-alkanes that are dominated by n-C_{17} and n-C_{18} (**Fig. 3.19**). The amorphous material is therefore aquatic in origin with little contribution from terrestrial higher plants. The high TOC and biological marker signatures are suggestive of favourable conditions of preservation of organic matter produced by a flourishing algal community on the surface of the lake. The shales have a low oxygen and gammacerine index (Eseme et al., 2006), suggestive of a low oxygen and high salinity environment. The usually high black debris in the carbonaceous shale is attributed to contact metamorphism by the overlying volcaniclastics deposit. The chaotic and peperite texture of the volcaniclastic bed (**Fig. 3.18A-B**) suggest that it is a hydroclastic deposit (hyaloclastite). The brown spheroidal coatings on the basaltic clasts are weathered quenched glassy rims.

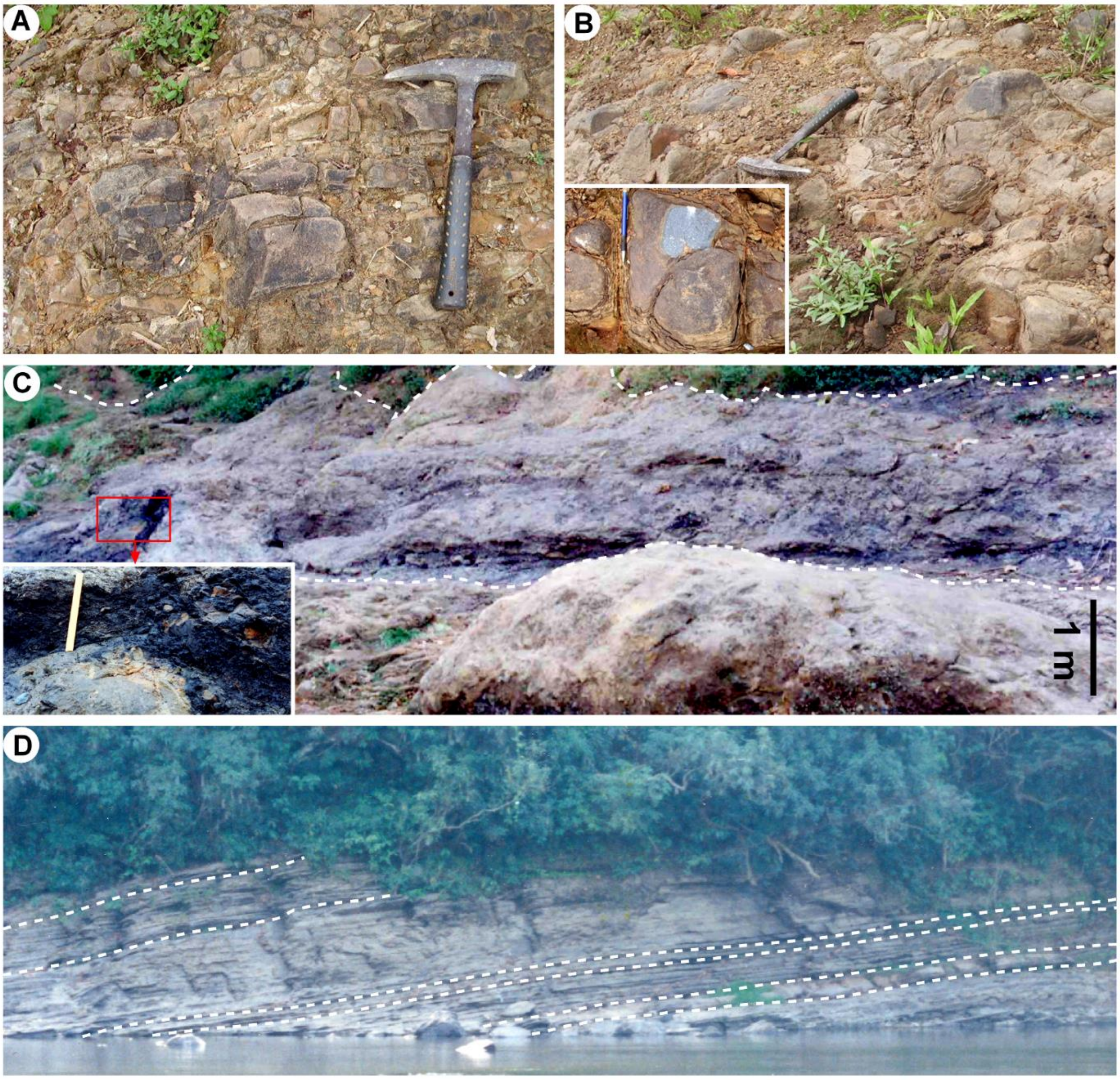

Figure 3.18. Field photos of FA5 along Cross River in Mamfe. (**A-B**) volcaniclastic (Gvb), (**C**) carbonaceous shale.

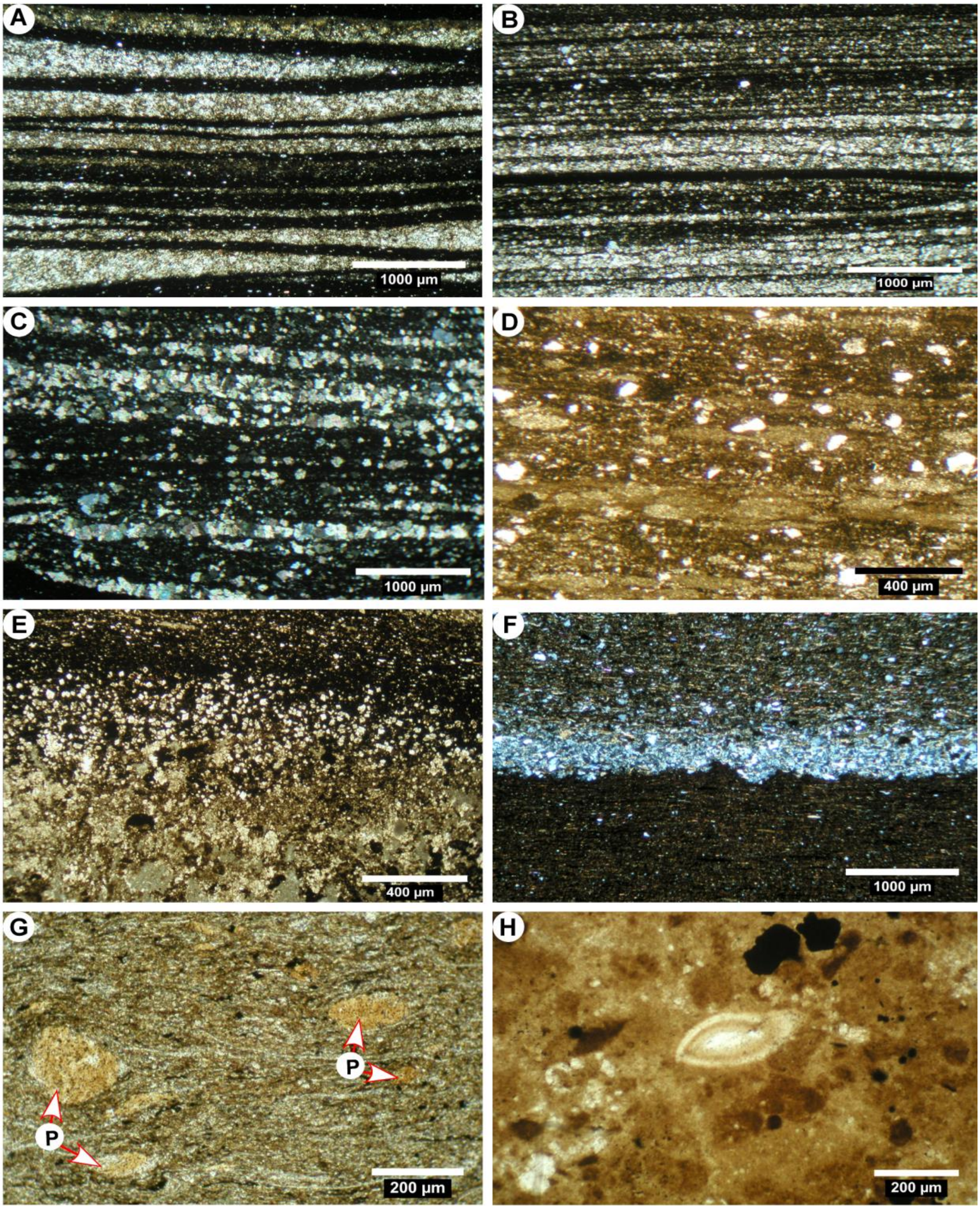

Figure 3.19. Thin section photomicrographs of calcareous shale and marlstone of FA5. (**A**) Alternation of organic-rich clay lamimae with lenticular siltstone/carbonate laminae. Laminae are planar and continous and some are discontinous. (**B**) Alternation of very thin (20-200 µm thick) parallel to sub-parallel and continous laminae of silt and organic-rich laminae. Laminae have sharp contacts and thin upward. (**C**) Very thinly laminated dolomitic laminae with low amplitude ripple marks interlaminating with organic-rich laminae. (**D**) Lenticular silt with fine-grained sand clasts. (**E**) Euhedral crystals of dolomite floating in black organic-rich clay with diffuse contact. (**F**) Massive mudstone laminae with loadcast and flame structures light layers are quartz-rich. (**G**) Phosphatic nodules- P in microbial-rich marlstone. (**H**) Ostracod.

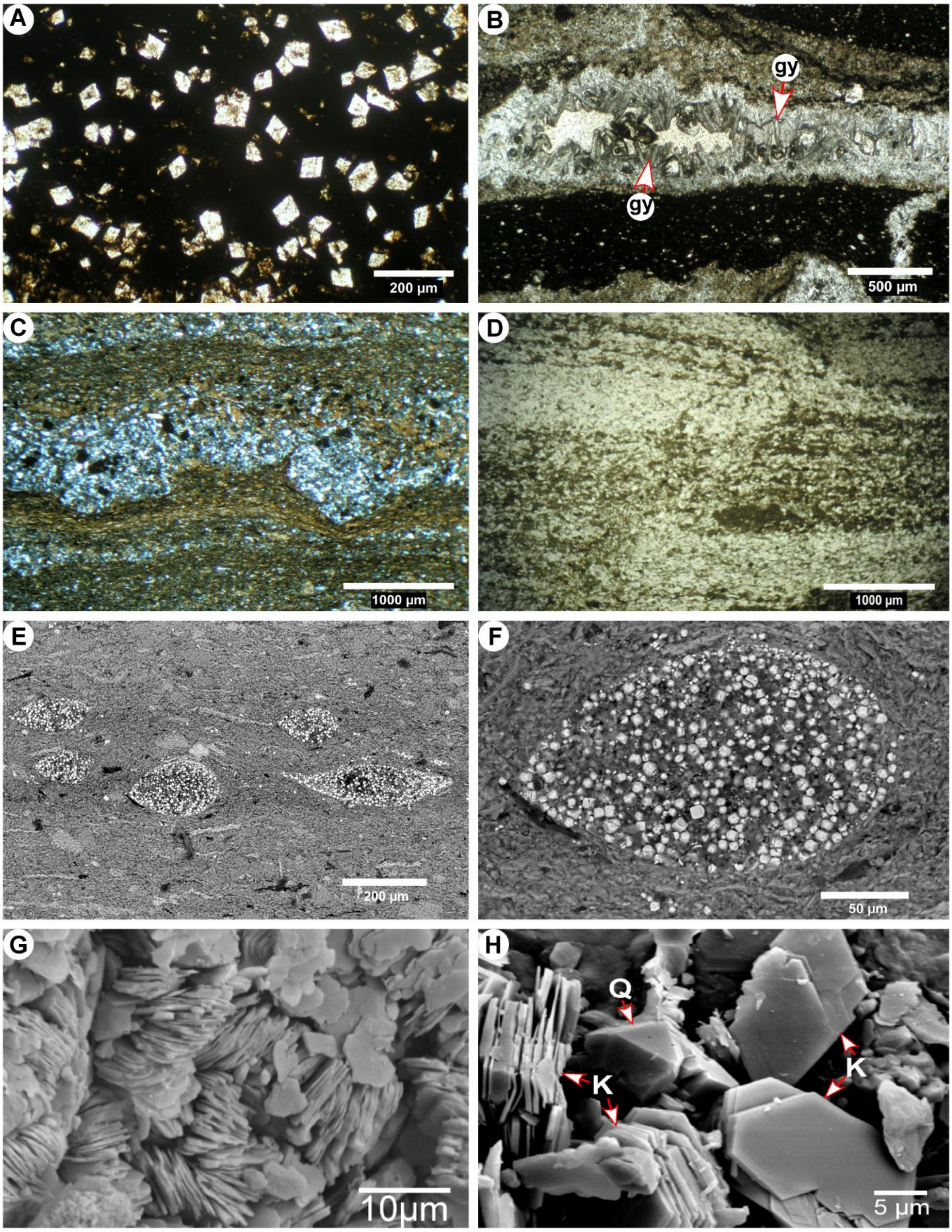

Figure 3.20. Thin section and BSE photomicrographs showing: (**A**) euhedral crystals of dolomite in black organic-rich clay. (**B**) laths of cavity-filling gypsum- gy in dolomitic marlstone. (**C**) convolute lamination. (**D**) micro-slump, (**E** & **F**) Pyrite infested microflora, (**G** & **H**) authigenic quartz– Q, and kaolinite- K in calcareous shale.

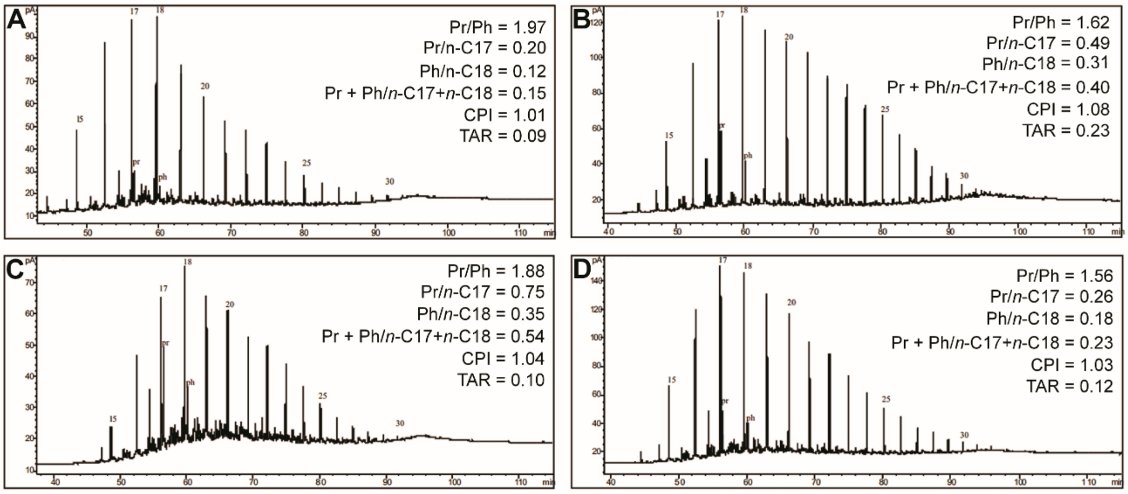

Figure 3.21. Representative gas chromatograms of saturate fraction with summary of molecular geochemical parameters for (**A**) sample 37-34, **(B**) sample 19-13, (**C**) sample 36-51, (**D**) sample 35-03. Pr = pristane, Ph = phytane.

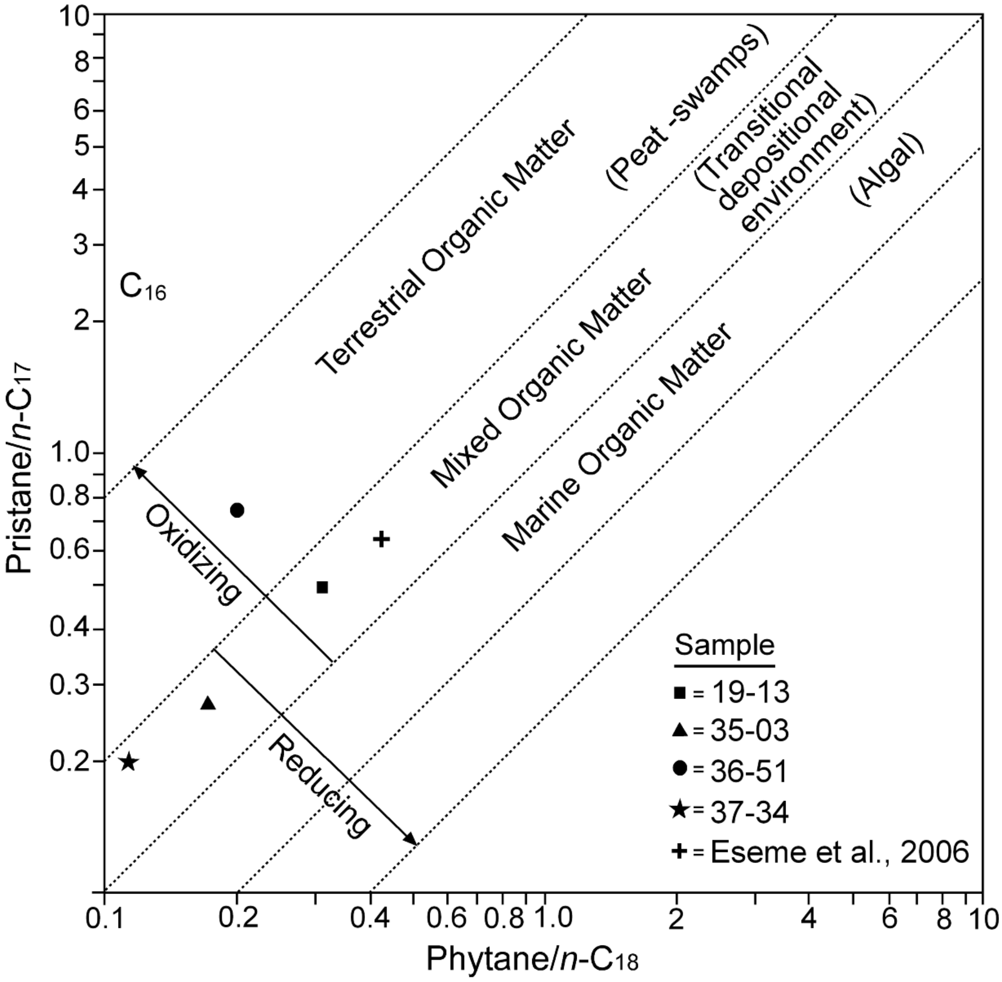

Figure 3.22. Isoprenoid plot of pristane/*n*-C_{17} *versus* phytane/*n*-C_{18}, showing redox conditions and depositional environments for some samples from FA5.

The gas chromatograms of saturate fractions of lacustrine samples are shown in **figure 3.19**. The chromatograms display a full suite of saturate hydrocarbons between C_{13} and C_{32} *n*-alkanes and isoprenoids hydrocarbons. The chromatograms also shows that the samples are very similar although they are from different locations within the basin.

The *n*-alkane distribution shows a unimodal distribution with a predominance of low molecular weight compounds (*n*-C_{16} to *n*-C_{21}) with a peak between *n*-C_{17} and *n*-C_{19} which suggests a relatively low terrestrial organic-matter contribution and predominance of aquatic organic-matter.

The Pristane/Phytane (Pr/Ph) ratio is one of the most commonly used geochemical indicator of redox conditions in the depositional environment (Lijmbach, 1975; Hunt, 1995; Peters et al., 2005; Romero and Philip, 2012; Rodriguez and Philip, 2015). The Pr/Ph ratio of the samples analysed in this study range from 1.56 to 1.97 (**Fig. 3.21**) suggesting deposition in suboxic conditions (Sarmiento and Rangel, 2004; Basent et al., 2005). The Pr/*n*-C_{17} and Ph/*n*-C_{18} ratios as shown in **figure 3.22** reflects the same interpretation.

The low TAR ratio (0.09-0.23) for all the studied lacustrine samples indicates a predominantly aquatic organic matter input in source deposited under anoxic to dysoxic environment. The cross plot of Pr/nC_{17} vs Ph/nC_{18} shows the organic source input deposition in a reducing environment

The fibrous gypsum infilling (**Fig. 3.20B**) is interpreted as the final residual by-product of the fractional dissolution and recrystallization of the halite in a way that is similar to the Bambata Formation in Angola (Gindre-Chanu et al., 2015).

The occurrence of pyrite in all samples may be related to the activity of sulphate-reducing bacteria during saline water intrusion (e.g. Brown and Cohen, 1995).

3.3.6 FA6: Littoral-shoreline

3.3.6.1 Description

This FA is 14.2 m thick and outcrops in Baku, Satum and Okoyong. It is made up predominantly of greenish to dark grey calcareous mudrocks (82%) with intercalations of siltstone (10%) coarse-grained sandstones (8%). The facies proportion for the lithofacies that make up this FA is shown in **figure 3.13F**.

The mudstone (Fm) is 450 cm thick and rich in microflora, and TOC range from 0.28-0.34 wt.%. Kerogen contain abundant structured phytoclasts and black debris and low AOM. The micaceous shale varies in thickness from 15-165 cm, and have TOC ranging from 0.34-0.38 wt.%. They contain moderate quantity of AOM. Dark grey to black shale (Fmlb-c) vary in thickness from 30-170m, have TOC ranging from 0.65-3.16 wt.%. Some are very rich in microflora. Their kerogen is dominated by AOM. Phytoclasts and black debris content is generally low.

The sandstone facies of this FA vary in thickness from 20-40 cm. They are generally coarse-grained, poor to moderately sorted, and may be laminated (Sh) or massive (Sm). The siltstones (Fsl) are 20-80 cm thick, thin-thickly laminated and micaceous.

3.3.6.2 Interpretation

The predominance of fine-grained lithofacies in this FA suggests deposition in a low energy environment. Samples from this FA grouped into palynofacies assemblage A to D which according to APP plot (**Fig. 3.12**) were deposited in a proximal to marginal basin setting with mostly dysoxic to suboxic conditions. This inference is supported by the wide variation in the TOC content of the sediments. The sum of the depositional processes attributed to each lithofacies (**table 3.1**) and their organic matter content suggests that FA5 are littoral-shoreline deposits.

3.3.7 FA7: Fluvio-deltaic

3.3.7.1 Description

This FA is 52.3m thick and made up predominantly of sandstones that are interbedded with greenish shales and mudstone. Outcrops are found in Mamfe, Baku, and Okoyong (**Fig. 3.23**). Lithofacies succession and substitution trend in outcrops are shown in **figure 3.4E, 3.4F, and 3.5G**, and their relative proportion in the FA in **figure 3.13G**. FA7 has been differentiated into a basal unit comprised of a coarsening and thickening upward sandstones that are interbedded with grey to dark grey shale and an upper unit made of a succession of fining-upward sandstone, siltstone and shale.

In the coarsening and thickening upward succession, the sandstone beds are 200-400 cm thick and exhibit a thickening upward trend. Their grain size varies from medium to coarse and sometimes pebbly. They are mostly poorly sorted, angular to sub angular and subarkosic in composition. They may be massive (Sm), planar (Sp) to current-rippled laminated or trough cross-bedded (St). The boundaries between the sandstones and shales are sharp. The shale beds range in thickness from 25 to 60 cm. They are massive (Fm) or thin to thickly laminated (Fmla), and their TOC vary from 0.29-1.71 wt.%. The top of the thickening upward succession is marked by a 180-320 cm thick dark brown shale.

The fining-upward succession comprises an alternation of sandstones, siltstones and shales. The sandstones are fine to coarse grained, poorly sorted and vary in thickness from 25 to 340 cm. Stacked units are 600 cm thick. Planar lamination, planar cross lamination (Sh) and cross bedding (St) are common and burrows are locally present. They pass upward gradationally into laminated micaceous siltstones that are 5-77 cm thick. The shale units are 10-250 cm thick, and vary in colour from black in the lower part of the section, passing upward to dark grey, grey, green and mottled green at the top. They are often laminated (Fmla) or massive (Fm). Soft sediment deformation is locally present (**Fig. 3.23E**). Some of the shales and mudstone contain charcoal fragments. Most are rich in well preserved microflora. The kerogen residue is dominated by black debris (20-50%), wood fragments and plant cuticles (30-50%), and relatively low amorphous organic material (15-25%).

3.3.7.2 Interpretation

The coarsening upward gradation and the thickening upward of sandstone units as well as the vertical gradation from planar lamination, planar cross bedding and trough cross bedding represent a shallowing upward which is evidence of mouth bar progradation. The dark brown shale indicates subaerial exposure and weathering. The fining-upward succession are upper deltaic plain deposits. The amalgamated medium to coarse-grained facies are distributary channel deposits and the intercalated conglomeratic units represent basal lag accumulated on scoured surfaces. The medium to fine-grained, planar cross-laminated sandstones and micaceous siltstone units represent natural levees.

The colour, organic carbon concentration and presence of agglomerate of *Todisporites* sp. (**Fig. 3.8I**) in dark grey to black shales suggest deposition in a reducing environment (e.g. ponds) on a poorly drained deltaic plain. The algae *ovoidites* sp. (**Fig. 3.8L**) is diagnostic of freshwater marshes (Rich et al., 1982) and its presence in the microflora of this FA indicates freshwater marshes on the upper deltaic plain. The comparatively low concentration of amorphous organic material and high wood and cuticle fragments in the kerogen residue of shales are consistent with that for deltaic environments (e.g. Tyson, 1993). An average TAI of 2.0 indicates that the shales are thermally mature. Illite crystallinity values are within the diagenetic grade of metamorphic transformation (Kübler and Jaboyedoff, 2000; Lee and Lee, 2001).

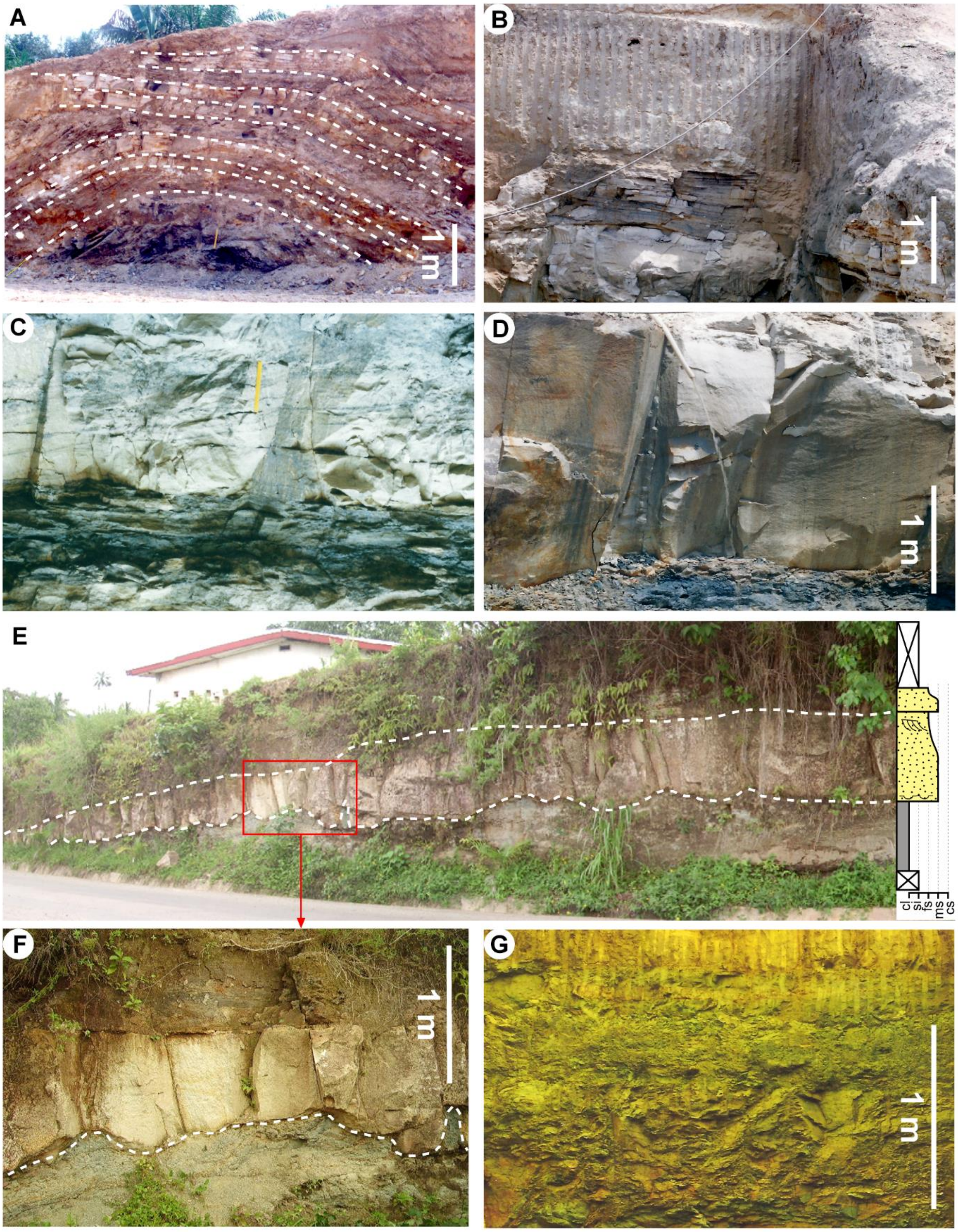

Figure 3.23. Field photos of FA7 at (**A**) Okoyong, (**B-G**) Mile 1 Mamfe.

3.3.8. FA 8: Medial alluvial fan

3.3.8.1 Description

FA 8 outcrops in Bachuo-Ntai and its environments (**Fig. 3.24**). It comprises predominantly of very coarse-grained sandstones (Sp and Sh) with intercalation of shale (Fmla) and conglomerate (Gcm). Siltstone (Fsl), paleosol (P) and coal (C) are locally present. Lithofacies substitution trend in outcrop is represented by the middle and upper part of **figure 3.5G**. Facies proportion within this FA is provided in **figure 3.13H**.

The sandstones are pinkish to grey in colour, and vary in thickness from 15 to 120 cm. They are mostly very coarse- to coarse-grained, angular to subrounded and poorly sorted. Horizontal bedding and fining upward within beds is common. Streaks of shale are scarce. The sandstones are mostly subarkose with subordinate arkose. The interbedded shale is dark grey, thickly laminated, non-fossiliferous and varies in thickness from 10 to 20 cm. The boundary between sandstones and shale is sharp.

The conglomerate (Gcm) show a thickening-upward and coarsening-upward trend. Bed thickness range from 5 cm to 30 cm, and clast size from 2 to 20 cm. They are rounded to well rounded, poor to fairly sorted and do not exhibit any preferred orientation. The smaller diameter clasts are better rounded than larger ones. They are polymictic and composed mainly of milky white quartzose and feldspathic rock fragments with a matrix of medium- to coarse-grained sandstone.

3.3.8.2 Interpretation

Field relationship (**Fig. 3.24**) and sedimentological attribute of this FA indicates that it is an alluvial fan deposit. Lack of boulder size particles reflects deposition in the middle part of a fan. Absence of defined channel and rhythmic alternation of beds of the same texture is typical of sheetflood (Blair and McPherson, 1994). FA8 is thus considered to be a medial alluvial fan sheetflood deposit on the hanging wall of the Mamfe half-graben (e.g. Kim et al., 2011).

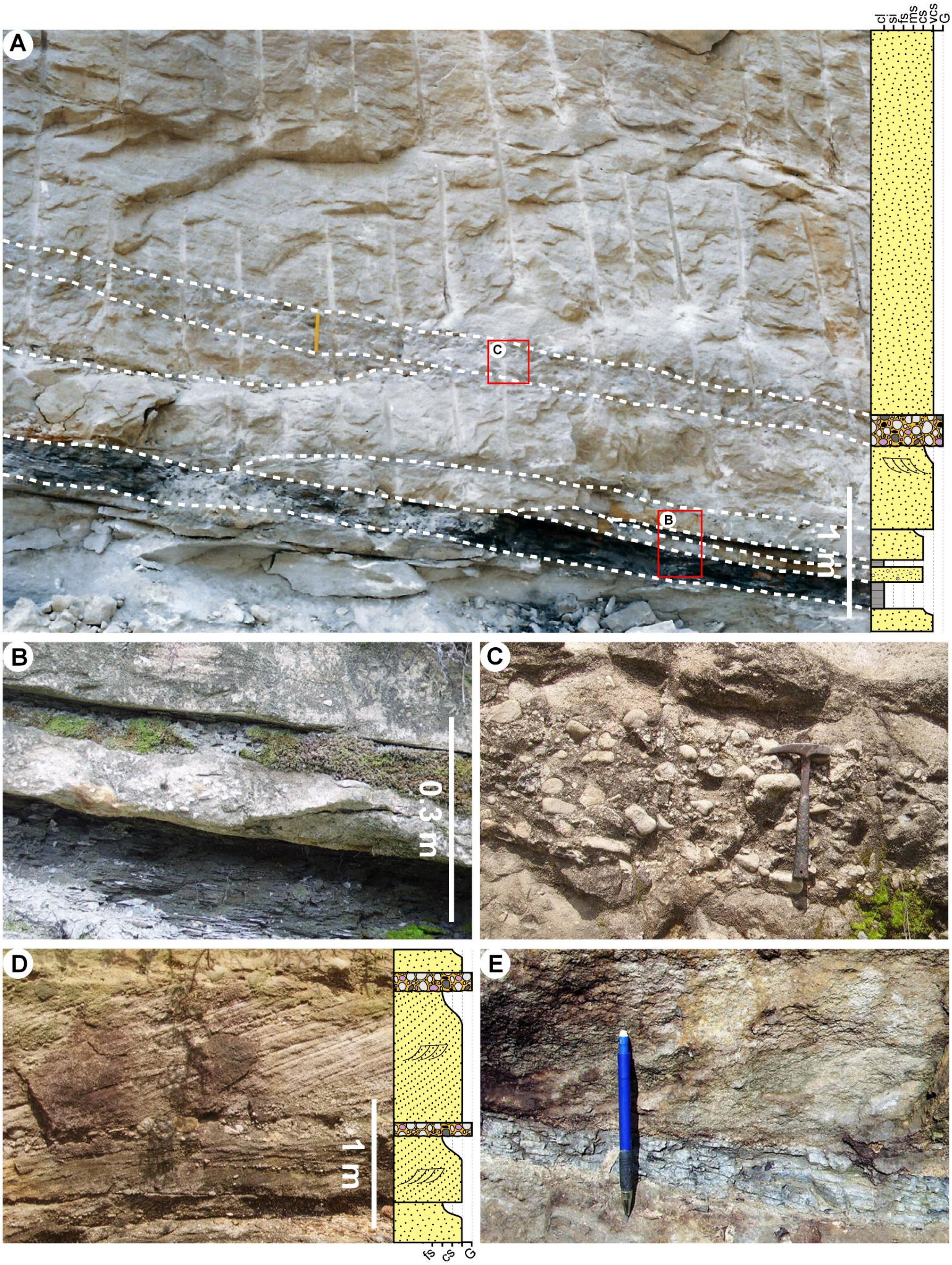

Figure 3.24. Outcrop of sheedflood alluvial deposits in and around Bachu-Ntai.

3.3.9 FA 9: Fluvial channel-overbank

3.3.9.1 Description

FA8 is 56 m thick and outcrops in the southwestern margin and central part of the Mamfe Basin and extends into SE Nigeria. It is comprised predominantly of sandstones (Sh, Sm, Sp) with interbeds of siltstone (Fsl), mudrocks (Fmla, Fm) and conglomerates (Ghg, Gcm). Lithofacies succession and substation trends in outcrop of FA9 are shown in **figure 3.5H-J**. The relative proportion of the lithofacies is shown in **figure 3.13I**.

The sandstones are 25-380 cm thick, very coarse- to coarse-grained and locally gravelly at their lower part where they are massive (Sm) and coarse- to medium grained at the top where they are graded. They are poor to moderately sorted and locally cross-bedded (Sp, St). The intercalated shales (Fmla) and mudstone (Fm) are non-fossiliferous and range in thickness from 20-150 cm. Boundaries between shale and sandstone are sharp. Siltstones (Fsl) range in thickness from 20-170 cm and commonly have erosive tops. The horizontally bedded clast-supported conglomerates (Ghg) are 50-80 cm thick and consists of subrounded to well-rounded clasts that are 2-35cm in diameter. Gcm is 30 cm thick, and clasts are 1-80 cm in diameter.

3.3.9.2 Interpretation

The textural and structural features, and the local relief indicate that FA9 are fluvial channel and overbank floodplain sediments. The Interbedding of fining upward cross-bedded sandstone with parallel laminated shale suggests that they are meandering stream deposits (e.g. Bassey and Ajonina, 2002; Bridge, 2003; Gouw, 2007; Bassey et al., 2013). The channels display erosive bases, sometimes with conglomeratic lag (Ghg, Gcm). Channel fill consists of very coarse- to medium-grained sandstones and occasionally conglomeratic with grain size decreasing from base to the top. At the top, the channel fill passes over to overbank fines, and both form a fining upward succession. The overbank deposits consist of siltstone, mudstone and shale. Many of the sandstone beds occur as isolated sandstone body bounded below and above by overbank fines and are interpreted as single storey of a meandering river. Amalgamated (multi-storey) channel fills are interpreted to be deposits of low sinuosity stream.

3.4 Discussion

3.4.1 Stratigraphy of the Mamfe Basin

Sediment thickness variation (depth to basement) in the Mamfe Basin is shown in **figure 3.22.** The sedimentary rocks exposed in the Cameroonian sector of the Mamfe Basin consist mostly of alternating succession of indurated sandstone, marlstone and shale that were collectively referred to as "Mamfe Schiefer" by Jaekel (1909). A Wealden age was inferred for these sediments on the basis of rare remains of the early Cretaceous fish *Proportheus kameruni* Jaekel (Jaekel, 1909). Reyment (1954) proposed the name Mamfe Formation as the English equivalent of Jaekel's (1909) "Mamfe Schiefer". The formation was not formerly defined, but considered to be the lateral equivalent of Albian-Turonian sediments in the Benue Trough. The bank of River Manyu in Mamfe town SW Cameroon was later proposed as its type locality, and the formation estimated to be about 700 m thick (Reyment, 1965).

Until now, no wells have been drilled in the Mamfe Basin and it is still a frontier basin. The few attempts that have been made at differentiating the lithic infill of the basin into stratigraphic units are based entirely on outcrop data. These attempts lack consistency in correlation, nomenclature, and rank of proposed lithostratigraphic units.

Lack of laterally persistent outcropping sections, rapid facies changes, rare fossils, thick vegetation and alluvial cover have impeded correlation and differentiation of the Cretaceous infill of the Mamfe Basin into stratigraphic units. The few attempts that have been made to differentiate the sediments in the Cameroonian sector of the basin include those of Le Fur (1965); Ajonina and Bassey (1997); Ajonina et al. (2001, 2006); Eyong (2003); Abolo (2008); and Bassey et al., (2013).

Le Fur (1965) referred to the sediments as basal Sandstone (Grès de base) and was divided it into 5 series (Cg^1-Cg^5). These series do not have formal stratigraphic status and were not delineated on the map of the basin (**Fig. 2.14**). These series from bottom to top were named: Lower conglomeratic sandstone series (Cg^1 & Cg^5), Manyu shale-sand series (Cg^2), Upper conglomeratic sandstone series (Cg^3), Cross River shale-sand series (Cg^4), and Cross River sandstone series (Cg^5).

Ajonina and Bassey (1997), and Ajonina et al., (2001) on the basis of field relationship and lithological features inferred a tripartite stratigraphic architecture for the Mamfe Formation and proposed its subdivision into a lower and upper member.

The lower member corresponds to Le Fur (1965) Cg^2 series, while the upper member estimated to be over 176 m thick corresponds to Cg^{3-5} series. The lower and upper members have recently been renamed as Manyu and Kesham members respectively (Bassey and Ajonina, 2002; Bassey et al., 2013).

Eyong (2003) assigned formation rank to Le Fur's (1965) series and renamed them as follows: Ngeme formation ($Cg^{1\&5}$), Nfaitok formation ($Cg^{2\&4}$), Baso formation (Cg^3), and Cross River formation (Cg^5). Abolo (2008) proposed a subdivision of the Mamfe Formation into three members: Etuko/Okoyong Member that corresponds to Cg^1 and Cg3, Nfaitok Member (Cg^2), and Manyu Member (Cg^{4-5}). Due to incomplete exposures and limited thickness of the outcrops, no type sections were proposed in the few attempts at differentiating the lithic infill of the basin.

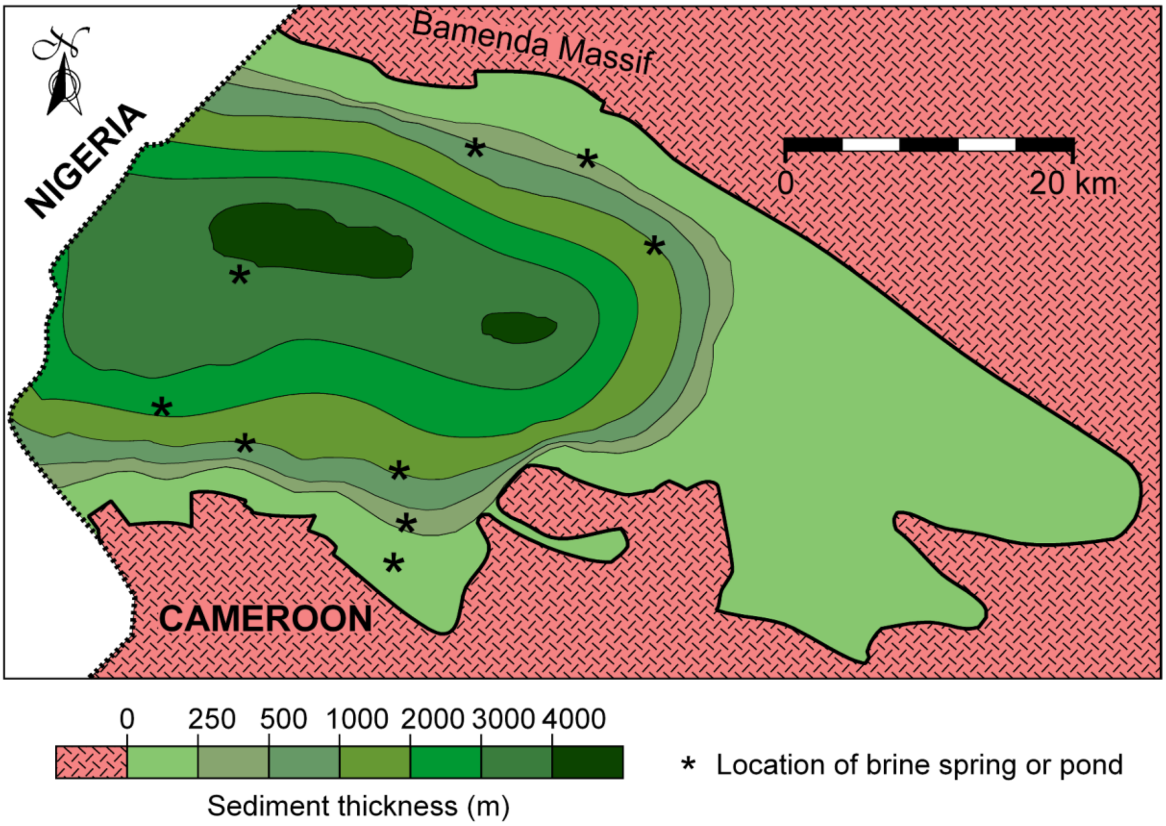

Figure 3.25. Sediment thickness map of the Mamfe Basin SW Cameroon.

Palynologic data together with data on sediment thickness variation within the studied area (**Fig. 3.25**) was used to group facies associations into lithostratigraphic units along an inferred depositional gradient (**Fig. 3.14** and **15**). The interpretation of depositional environments based on facies association has resulted in the characterization of three depositional sequences within the Mamfe Basin. These depositional sequences are referred to in this study as the basal, middle and upper depositional sequences and correspond to pre-rift, syn-rift and post-rift deposits respectively.

The delineation of the sediments in the basin into depositional sequences has necessitated the revision and redefinition of the existing informal lithostratigraphy of the Mamfe Basin. In order to avoid duplicity and confusion in the name and rank of stratigraphic units in the study area with formerly defined stratigraphic units in neighbouring basins in SE Nigeria, the names used by Eyong (2003) and Abolo (2008) have adopted with revision or redefinition. The proposed lithostratigraphy of the Mamfe Basin is summarized in **figure 3.26**, and the spatial distribution of the lithostratigraphic units within the basin is shown in **figure 3.27**. A conceptual schematic cross section showing the vertical and lateral distribution of the units is presented in **figure 3.28**

The basal (pre-rift) depositional sequence consists of debris flow alluvial fan deposits that unconformably overlie the Pan-African basement rocks. It is named the Etuko Formation. The middle (or syn-rift) depositional sequence is made up of fluvio-lacustrine and deltaic succession that is named the Mamfe Group. The group is underlain by an erosional unconformity and overlain by an angular unconformity, and is so named as to differentiate it from the Mamfe formation used in stratigraphic lexicon in Nigeria. The Mamfe Group is made up of the following formations from bottom to top: Nfaitok (fluvio-palustrine), Manyu (lacustrine), and Okoyong (fan-delta). The upper (post-rift) depositional sequence consists of fluvial deposits that are underlain by an angular unconformity. This fluvial succession is named Ikom-Munaya Formation.

3.4.1.1 Etuko Formation

History: Cg1 (Le Fur, 1965), Ngeme formation (Eyong, 2003), Etuko member (Abolo, 2008).

Type locality: The formation outcrops mainly in the northeastern border of the Mamfe Basin in Cameroon in the following localities: Etuko, Eyang-Ntui, and Ngeme waterfall.

Definition: The base is the Pan-African crystalline basement and its top is marked by a thick paleosol.

Description: It is comprised mainly of proximal alluvial fan deposits described in facies association FA1.

Thickness: It has a composite outcrop thickness of 20 m.

Age: It lacks fossils but is dated as pre-middle Barremian based on the palynologic age of the overlying Nfaitok formation.

3.4.1.2 Nfaitok Formation

History: Mamfe schiefer Jaekel (1909); Mamfe Formation (Reyment, 1954); Manyu shale-sand series (Le Fur, 1965); Lower member of Mamfe Formation (Ajonina et al., 2001; Bassey and Ajonina, 2002; Bassey et al., 2013); Nfaitok member of Nfaitok formation (Eyong 2003); Nfaitok member of Mamfe formation (Abolo, 2008).

Type localities: This formation outcrops in the following villages: Etuko, Nfaitok II; Obang, and Mbinjong.

Definition: The base of this unit is an erosional unconformity represented by the thick paleosol at the top of the underlying Etuko formation in Nfaitok II. The upper boundary is marked by thick black to dark grey shale and marlstone in the following villages Nchemba, Nfaitok and Mbinjong.

Description: Nfaitok formation comprises of lithofacies described in the floodplain (FA2) and palustrine (FA3) facies associations.

Thickness: The formation has composite thickness of 71 m.

Fossils: This formation lacks calcareous fossils but microflora is rare to common and often dominated by Classopollis pollen.

Age: A middle Barremian to early Aptian age range is inferred from its microflora assemblage.

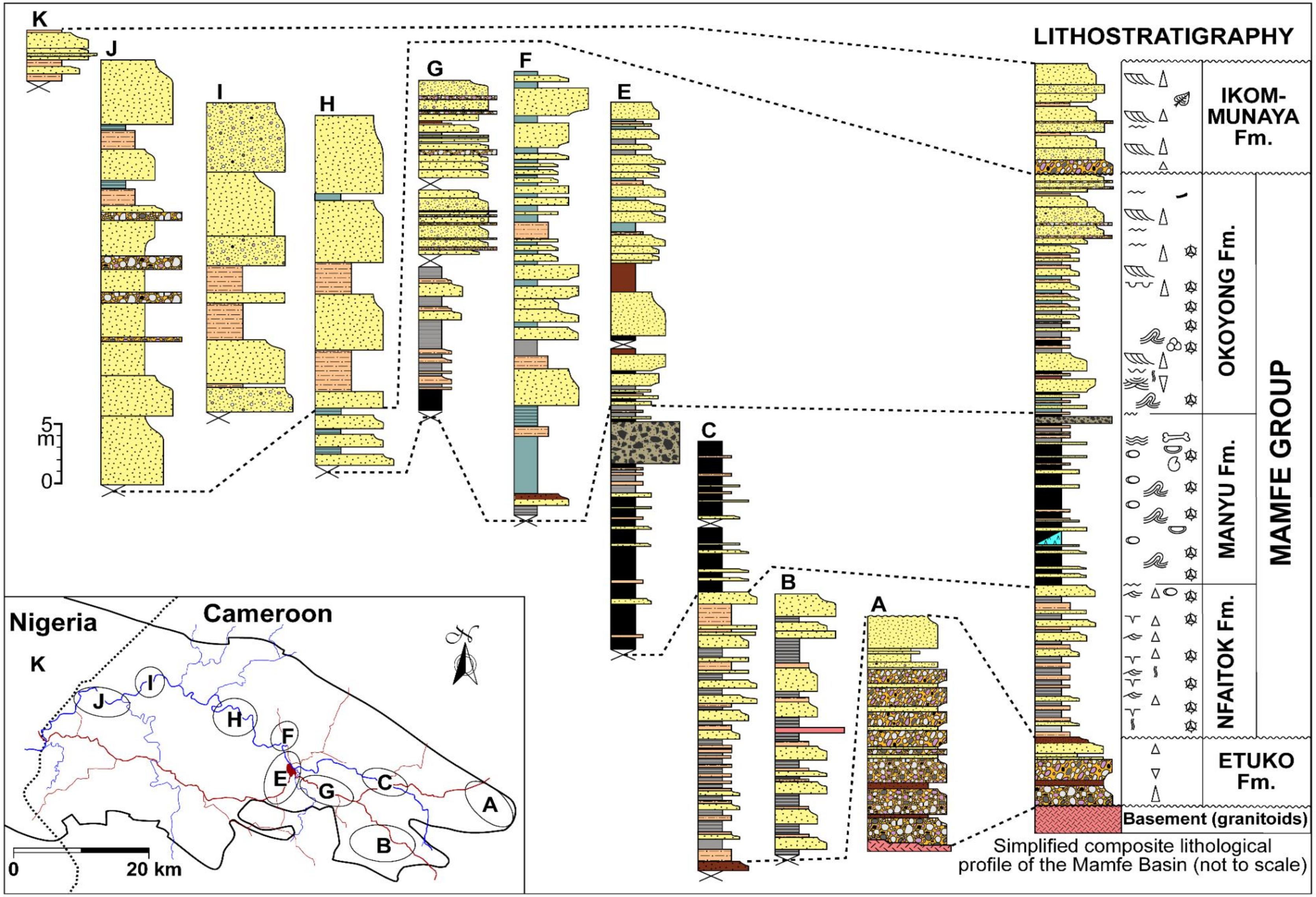

Figure 3.26. Composite lithogical logs from different locations in the Mamfe Basin showing the most typical facies of the basin and their correlation including the names of proposed lithostratigraphic units.

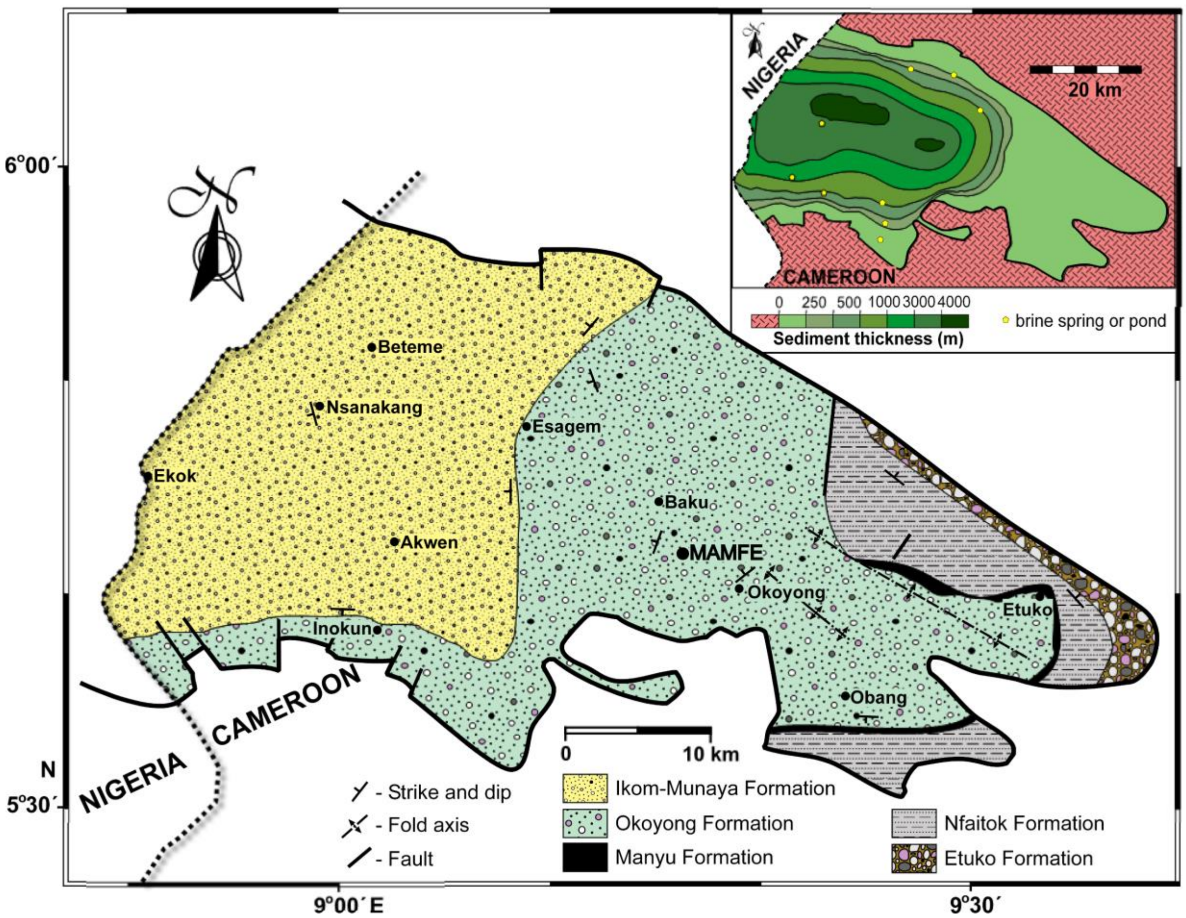

Figure 3.27. Simplified geological map of the Mamfe Basin in Cameroon showing the areal distribution of the proposed stratigraphic units.

3.4.1.3 Manyu Formation

History: Mamfe schiefer Jaekel (1909); Mamfe Formation (Reyment, 1954, 1965); Cross River shale-sand series (Le Fur, 1965); Lower member of Mamfe Formation (Ajonina et al., 2001; 2006; Bassey and Ajonina, 2002); Mamfe member of Nfaitok formation (Eyong 2003); Manyu member of Mamfe formation (Abolo, 2008). Manyu member of Mamfe Formation (Bassey et al., 2013).

Type localities: This formation outcrops in the following villages: Etuko, Nfaitok II; Besongabang and Mamfe Town.

Definition: The lower boundary of this formation is marked by the first appearance of thick black to dark grey calcareous shale and marlstone and the upper boundary is marked by volcaniclastics.

Description: Manyu Formation is composed of lithofacies that make up the sublittoral to profundal lake (FA5) and littoral-shoreline (FA6) facies association that have already been described in section 3.3.5 and 3.3.6.

Thickness: Manyu Formation has composite thickness of 95 m.

Fossils: Calcareous fossils are rare and undifferentiated, and include fish bones, ostracods, gastropods conchostracan (Eyong, 2003). Microflora is common but poorly preserved. The first angiosperms pollen recorded in this study is from this formation.

Age: Early Aptian to late Aptian.

3.4.1.4 Okoyong formation

History: Mamfe Formation (Reyment, 1954, 1965); Upper conglomeratic sandstones (Le Fur, 1965); Upper member of Mamfe Formation (Ajonina et al., 2001; 2006; Bassey and Ajonina, 2002); Bagba member of Nfaitok formation and Basso Formation (Eyong 2003); Okoyong member of Mamfe formation (Abolo, 2008). Kesham member of Mamfe Formation (Bassey et al., 2013).

Type localities: This formation outcrops in the following villages: Bachuo-Ntai, Okoyong; Mamfe Town; Besongabang, Baku; Kesham, and Akarem and Inokun.

Definition: The lower boundary of this formation is marked by the volcaniclastics in Mamfe and Baku. Its upper boundary is an angular unconformity that separate it from the overlying Ikom-Munaya Formation.

Description: The fluvio-deltaic (FA7) and medial alluvial fan (FA8) facies association already described make up this formation. These facies association together are referred to as a fan-delta. The proximal part of the alluvial fan is absent in Bachuo-Ntai and Okoyong localities in the southeastern margin of the basin but is recorded in Inokun and Akarem area on the south central margin of the Basin. This suggests that the width of the Mamfe Basin extended beyond its present limit.

Thickness: The composite thickness of 104 m was measured in this study although it has been estimated to be of over 200 m thick (Eyong, 2003; Abolo, 2008).

Fossils: Calcareous fossils are represented by rare foraminifera. Microflora is abundant and well preserved and diversified.

Age: late Aptian to early Albian.

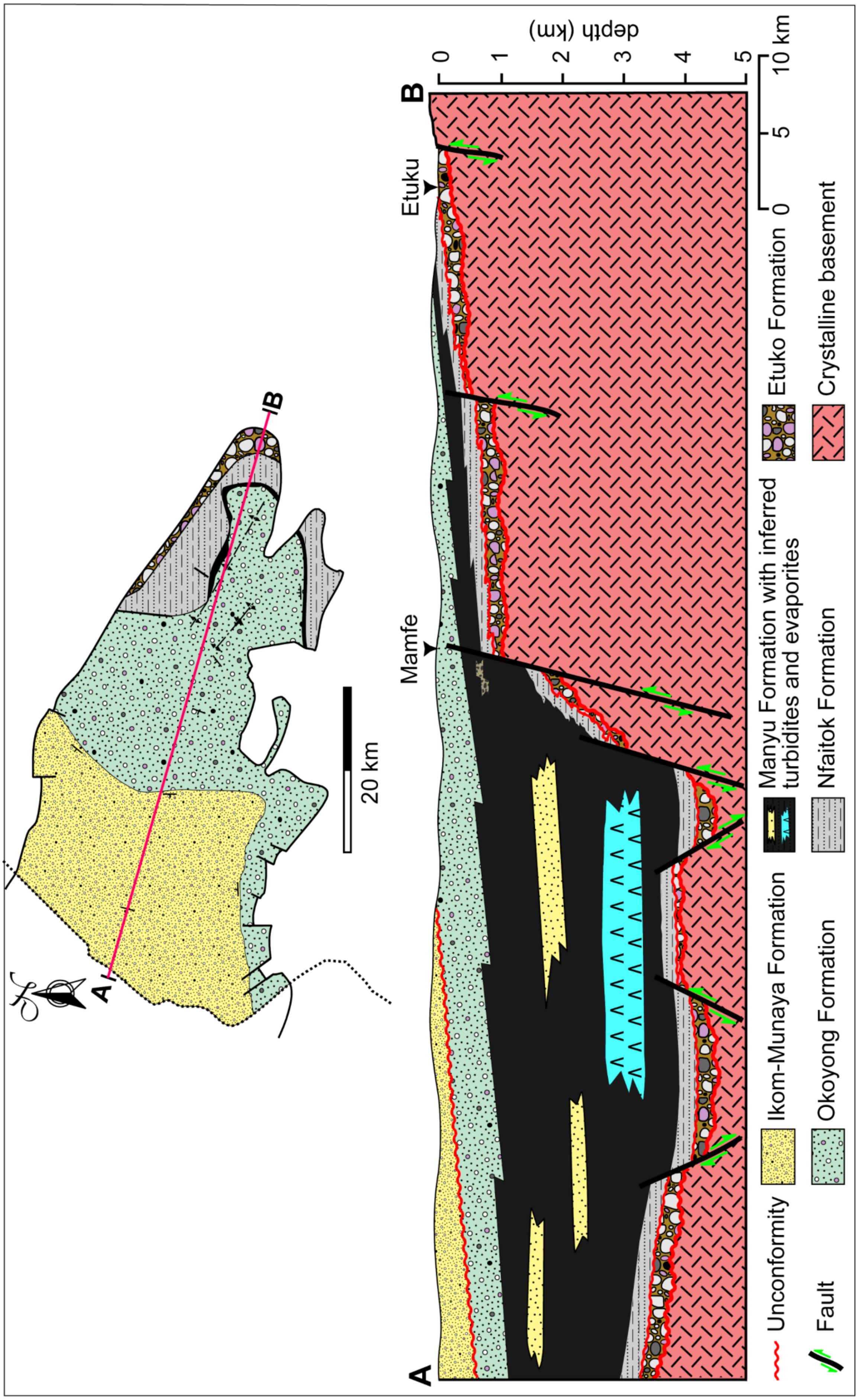

Figure 3.28. Hypothetical WNW-ESE cross section of the Mamfe Basin in Cameroon showing the vertical and lateral distribution of the stratigraphic units.

3.4.1.5 Ikom-Munaya

History: Mamfe Sandstone (Reyment, 1954); Upper conglomeratic sandstones Cross River Sandstone (Le Fur, 1965); Ogoja Sandstone (Uzuakpunwa, 1980); Ikom Sandstone (Ajibola, 1997; Ajonina et al., 2006); Upper member of Mamfe Formation (Ajonina et al., 2001; 2006; Bassey and Ajonina, 2002); Inokun member of Ngeme formation (Eyong, 2003), Cross River formation (Eyong, 2003); Manyu member of Mamfe Formation (Abolo, 2008), and Kesham member of Mamfe Formation (Bassey et al., 2013).

Type localities: This formation outcrops in the following localities: Ikom (Nigeria), Ekok, Akarem, Nsanakang, Akwen, Esagem

Definition: This formation is the topmost sedimentary succession in the Mamfe Basin. It is separated from the underlying syn-rift deposits of the Mamfe Group by an angular unconformity. The Ikom-Munaya Formation extends into the southern Benue Trough where it is mapped as the lateral equivalent of the Asu River Group. The Asu River Group is the basal sedimentary succession in the southern Benue Trough and is overlain unconformably by the Cross River Group.

Description: The lithofacies that make up this formation are the youngest sediments in the Mamfe Basin that have been mapped and described in this study as the fluvial channel-overbank facies association (FA9).

Thickness: A composite thickness of 77 m was measured for this formation in this study.

Fossils: Other than fossilized wood, no calcareous fossils and microflora was recorded or has been reported from this formation.

Age: Based on data from the Asu River Group, the age of this formation is inferred to range from middle Albian to early Cenomanian

3.5 Conclusions

The gravimetric data indicates that the sedimentary infill of the Mamfe Basin range in thickness from 0 to over 4500 m (Petters et al., 1987; Hell et al., 2000; and Heine, 2007). The spatial variation in sediment thickness in the basin suggests that the Mamfe Basin comprises two sub basins (**Fig. 3.28**). These sub basins probably acted as separate depocenters during the early part of the basin history but were less influential on sedimentation during the later stages of basin evolution.

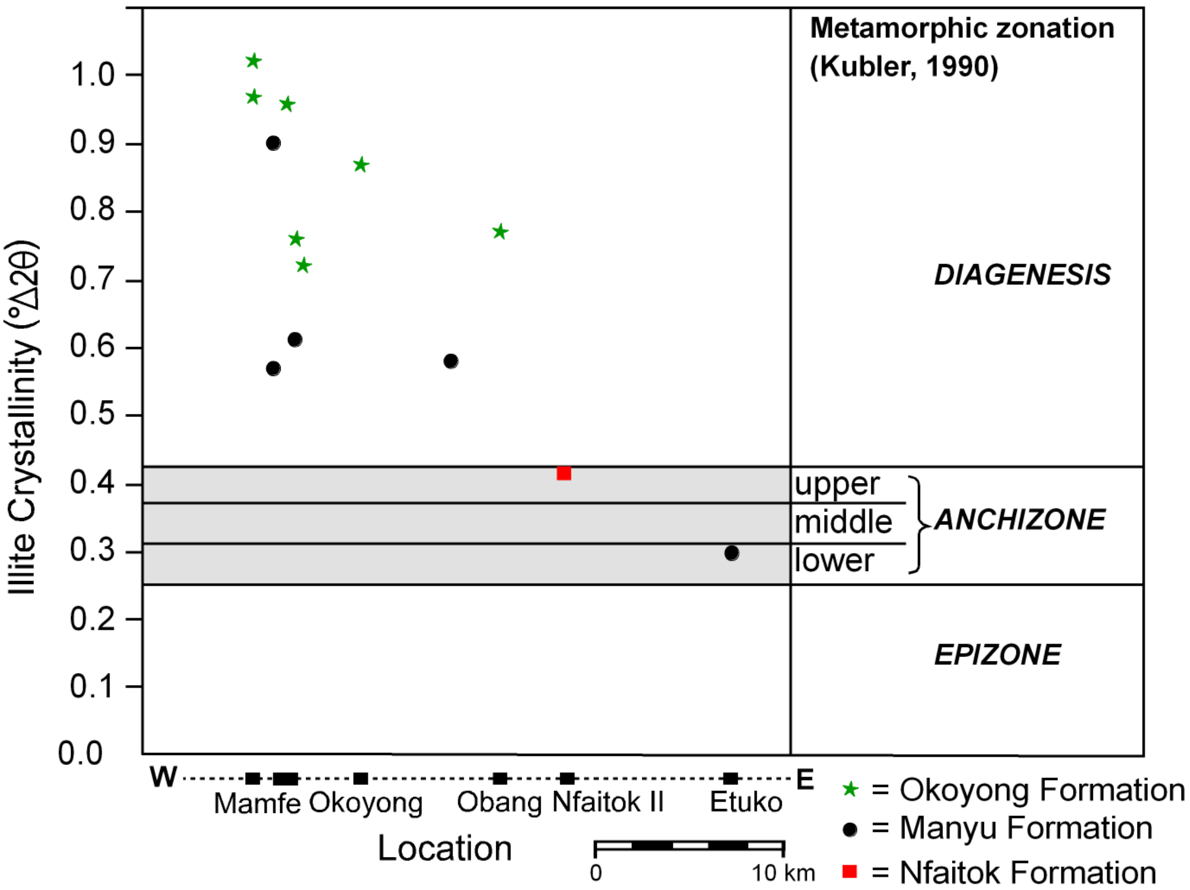

Figure 3.29. Spatial and temporal variation of illite crystallinity data in the Mamfe Basin in Cameroon.

Illite crystallinity (IC) as a measure of metamorphic transformation (Kübler, 1990) indicates that the Nfaitok Formation is within the upper anchizone (**Fig. 3.29**), and Manyu and Okoyong Formations are within the diagenetic stage metamorphism (except at contact with igneous intrusions). Illite crystallinity, thermal alteration index, and biomarkers yielded identical burial metamorphism data that suggest that the outcropping sediments in the eastern Mamfe Basin have been buried to depths of between 1200 and 4000 m. The westward younging of sediments in the basin (**Fig. 3.28**) correlates with illite crystallinity data (**Fig. 3.29**) and interpreted to have resulted from uplift and erosion of between 1.2 and 4 km thick sediments in the eastern part of the basin and not the previously reported westward migration of depocenter.

The thickness and volume of the sediments eroded from the southeastern flank of the basin suggests that the areal extend of the Mamfe Basin during the Early Cretaceous was much larger than its present limit.

4

PALYNOSTRATIGRAPHY OF THE MAMFE BASIN

ABSTRACT

Palynological analysis of outcrop samples from the Mamfe Basin in Cameroon yielded 128 palynomorphs, and lack dinoflagellates. Lack of dinoflagellate cysts suggests a predominantly continental depositional setting. The palynomorphs consists of poor to well preserved pollen and spores taxa with many previously undescribed new species. The palynoflora assemblage provide the first definitive paleontologic age for the sediments in the Mamfe Basin which until now are assumed to be Albian-Turonian in age. Angiosperm pollen grains are rare, and *Dicheiropollis etruscus* and elater-bearing pollen are absent from the palynoflora assemblage. This suggests that the Mamfe Group is younger than early Barremian and older than middle Albian. The palynoflora assemblage of the Mamfe Basin correspond to the West Africa regional palynostratigraphic reference section and zones CV to CIX of SNEA (P) in Gabon, and palynozones P-190 to P-280 in South America (Brazil) that have been assigned to Middle Barremian-Early Albian age. The Mamfe palynoflora is very similar to that reported from the Upper Cocobeach Group in Gabon, and the Antenor Navarro and Sousa Formations in Rio Do Pixe Basin of northeastern Brazil.

4.1 Introduction

The sedimentary succession in the Mamfe Basin is presumed to be the oldest Cretaceous sediments in the southern Benue Trough sub region, and have been mapped as the basal part of the Albian-Cenomanian Asu River Group. The age, environment of deposition and correlation of the lithic infill of the Mamfe half graben is still a subject of debate among researchers resulting to lack of consistency in correlation of the sediments in the basin. Correlations within the basin have been hampered by rapid facies change in the poorly exposed, often weathered and poorly- to non-fossiliferous outcrops, as well as lack of conventional stratigraphic markers, paleontological control, and subsurface samples. At present, the sediments in the Mamfe Basin lacks any direct and clearly defined age determinations in geologic and paleontologic literature.

Fossils that have been reported from the Mamfe Basin include fossil wood, fish remains, ostracods, gastropods, conchostracans, algae etc. (e.g. Jaekel, 1909; Reyment, 1954, 1965; Ajonina, 1997; Eyong, 2003). Most of these fossils are rare and have no biostratigraphic significance (Reyment, 1965; Eyong, 2003). Jaekel (1909) inferred a Wealden age for the sediments in the basin based on the presence of remains of the fish *Proportheus Kameruni Jaekel.* Fossil remains of a similar fish have been reported from the Cocobeach Formation of northern Gabon (Weiler, 1961). Reyment (1965) was of the opinion that Wealden age (Barremian-Aptian) assigned to the sedimentary infill of the Mamfe Basin was highly improbable. He proposed that the sediments in the Mamfe Basin were the lateral equivalent of the Albian-Turonian sediments in the southern and middle Benue Trough to the northwest of Mamfe Basin. The sedimentary infill of the Mamfe Basin has since then been mapped as the Mamfe Formation and correlated as the basal unit of the Asu River Group in the Benue Trough (Reyment, 1965; Murat, 1972; Dessauvagie, 1974; Adeleye, 1975; Hoque, 1977, 1984; Adeleye and Fayose, 1978; Petters and Ekweozor, 1982; Whiteman, 1982; Ojoh, 1990; Ajonina, 1997; Bassey and Ajonina, 2002; Bassey et al., 2013).

Differences in opinion regarding the time of deposition of the sediments in the Mamfe Basin is largely attributed to lack of age-diagnostic macrofossils in the sediments and no study on its microfossil content. Discrepancy and uncertainty in the supposed Albian-Turonian age assigned to the sediments in this basin has resulted in doubtful intra- and inter-basinal correlations. Lack of age-diagnostic macrofossils and the need to provide a better age control to use in correlating the sediments in the Mamfe Basin and the southern Benue Trough sub region has necessitated a micropaleontological analysis of the sediments for their microflora and microfauna content. The Lower Cretaceous biostratigraphy of Cameroon and Nigeria till date is imprecise because only the topmost part of the pre-Albian sediments have been drilled in wells. Foraminifera, ammonites, and microflora thus far are the only reliable evidence for dating important stratigraphic successions in the West African coastal and inland sedimentary basins (Reyment and Tait, 1972; Reyment, 1980; Petters, 1983; Kogbe and Me'hes, 1986; Ojoh, 1990; Lawal, 1991).

Palynology is a multifaceted subject that is primarily used in dating and correlation. It has been used as a biostratigraphic tool by petroleum exploration companies since the late 1930s (e.g. Jardiné and Magloire, 1965; Regali et al., 1974; Doyle et al., 1977, 1982). Its other applications include paleoenvironmental characterization, assessment of petroleum potential of source rocks, thermal maturity of organic matter in sediments, provenance analysis, and sequence stratigraphy (Rull, 2002; Batten and Stead, 2005; Jaramillo et al., 2005; Traverse, 2007; Zobaa et al., 2013).

Microflora have been used extensively in dating and correlation of Cretaceous sediments in the eastern Gulf of Guinea from Ghana to Angola and northeastern Brazil (e.g. Jardiné and Magloire, 1965; Jardiné, 1974; Jardiné et al., 1974; Regali et al., 1974; Jan du Chêne et al., 1978; Hughes et al., 1979; Allix et al., 1981; Doyle et al., 1977, 1982; Lawal and Moullade, 1986; Regali and Viana, 1989; Salard-Chedoldaeff, 1990; Lawal, 1991; Salard-Chedoldaeff and Dejax, 1991; Salard-Chedoldaeff and Boltenhagen, 1992; Doyle, 1992; Schrank, 1992, 1998; Dejax and Brunet, 1996; Wood et al., 1997; Jan du Chêne, 2000; Coimbra et al., 2002; Carvalho, 2004; Carvalho et al., 2006; Abubakar et al., 2006; Atta-Peters and Salami, 2006; Batten, 2007; Heimhofer and Hochuli, 2010; Abubakar et al., 2011).

For this study, samples from medium to pebbly sandstone, paleosol and conglomerate lithofacies were excluded from the palynological analysis. This is because microflora are generally rare or absent in coarse-grained clastic sediments, red or deeply weathered beds, limestones, dolomites, volcanic and metamorphosed rocks but are generally common in silt-sized sediments (e.g. Rowe and Jones, 1999; Traverse, 2007). The palynological study was limited to mudrocks and very fine-grained sandstone lithofacies of the Mamfe Group and Ikom-Munaya Formation.

4.2 Materials and Methods

4.2.1 Organic-walled microfossils

A total of 48 shale, mudstone, dark grey siltstone and very fine-grained sandstone samples were prepared for palynological analysis. Cleaned, crushed and weighed samples (10 to 20 g) were subjected to standard HCl and HF palynological maceration techniques (e.g. Wood et al., 1996; Traverse, 2007) at the Unidad de Paleopalinología, Instituto Argentino de Nivología, Glaciología y Ciencias Ambientales (IANIGLA), Mendoza Argentina, and the Center for Tropical Paleoecology and Archaeology (CTPA), Smithsonian Tropical Research Institute (STRI) Panama. The residue of the acid digestion was sieved through a 10µm mesh sieve to remove the fine fraction. Part of the residue was oxidized with 30% HNO_3 followed by dehumification with ammonium hydroxide (5%). Finally, the residues from each sample were strew mounted on glass slides using glycerine jelly. A minimum of 2 and maximum of 13 slides were prepared for each of the 48 samples and examined.

The slides were analyzed for their palynological content using transmitted light with the following microscopes and cameras: Leitz Dialux 20 microscope equipped with Wild Photoautomat MPS 55 camera and Kodak professional 100 ISO color film, Nikon Eclipse 80*i* microscope equipped with Nikon DMX 1200F digital camera, and Olympus BX61WI fluorescence confocal laser scanning microscope (CLSM). The resulting CLSM image stack were processed with Image-Pro Plus software (version 6.3). The depth of field resolution of some palynomorphs was improved by reconstructing the complete image of the palynomorph from a stack of images taken in different focusing conditions as described by Bercovici et al. (2009) using CombineZP software.

At most 450 palynomorphs were counted in the strewn slides of samples that were rich in palynomorphs, and as many as were available in samples that were not rich in palynomorphs. The following abundance categories were used to represent the total number of specimens of each taxon that was found in each sample. A = abundant (>20 specimens), C = common (11-20 specimens), F = few (5-10 specimens), S = scarce (2-4 specimens), and R = rare (1 specimen). The state of preservation of the palynomorph assemblage in a sample was classified as follows: Good = little or no evidence of alteration of main morphologic features and palynomorph is identifiable to the species level. Moderate = evidence of alteration of main morphologic features but palynomorph can be identified to the species level. Poor = palynomorph is fragmented, main morphological features have been destroyed (mostly by pyrite infestation), cannot be identified to either the species or genus level.

Non-metric Multidimensional Scaling statistical (NMDS) analysis using R software was carried out to determine the degree of similarity between the microflora assemblage of Mamfe Group with results of previous palynologic studies on age-equivalent Early Cretaceous successions in other regions within the West African-South American (WASA) Microflora Province of Herngreen and Chlonova (1981).

4.2.2 Preparation of figure illustrations

Photomicrographs that were taken with Wild Photoautomat MPS 55 camera were scanned on a flat-bed Epson GT-10000+ scanner at an optical resolution of 300 pixels per inch. Pictures requiring enlargement were scanned at a higher resolution of 600. A scale bar was created for each scanned photomicrograph using ImageJ software (v. 1.46j). Cropping, sharpening, tonal adjustments, and resizing were made in Adobe Photoshop (v. CS4). Each image was then imported to FreeHand (v. Mx) and placed in the proper location on the figure illustration (plate) page. Each figure illustration was saved as a TIFF file. The name of each numbered image on the illustration figure is followed by sample number (bold), slide number (brackets), and England Finder coordinates (for Nikon Eclipse 80*i* microscope) or Leitz Orthoplan stage coordinates (for Leitz Dialux 20 microscope).

4.3 Results

4.3.1 Palynomorph distribution and abundance

Of the 48 samples that were analyzed in this study for organic-walled microfossils, 30 contained pollen grains and spores, and 18 were barren. Majority of the samples from the Nfaitok, Manyu, and Okoyong Formations (Mamfe Group) contain microflora while all the 11 samples from the overlying Ikom-Munaya Formation were barren. Only the Mamfe Group is presented in the ensuing sections. The abundance of palynomorphs in the kerogen residue of palynomorphs-bearing samples was very low, hardly exceeding 5% of the residue, and their diversity per sample is low to high. A total of 128 taxa were recorded in this study with many previously undescribed species. The state of preservation of the palynomorphs is variable from poorly to well preserved.

The assemblage is composed of 36 genera and 76 species of spores, 16 genera and 34 species of pollen grains, 3 genera of algae, and numerous fungal remains. The taxa recorded in this study are listed in **table 4.1**. A semi-quantitative stratigraphic distribution of pollen and spores in the 30 samples from the formations that constitute the Mamfe Group is shown in **figure 4.1**. The palynomorph assemblage is made up entirely of terrestrial pollen and spores with a distinctive absence of dinoflagellate cyst. The stratigraphic abundance of each palynomorph group is shown in **figure 4.2.** Some of the taxa are illustrated in **figure 4.4** to **4.8**.

Many of the pollen and spores recorded in this study are well known within the low-latitude regions of Northern Gondwana Province of Brenner (1976), and have been extensively described in published literature. Their taxonomic descriptions are therefore not provided in this palynostratigraphically oriented study. A comprehensive taxonomic description of the new taxa recorded in this study will be provided in Mejia-Velasquez, Ajonina, and Jaramillo et al. (in preparation). The proposed name for new species are given in quotes in **table 4.1.**

Table 4.1. Taxonomic list of palynomorphs with author citations. The proposed name for new species is given in quotes

Pteridophyte and bryophyte spores
Acanthotriletes cf. *levidensis* Balme 1957
Acanthotriletes sp.
Aequitriradites sp.
Appendicisporites cf. *tricornitatus* Weyland & Krieger 1953
Appendicisporites sp.
Baculatisporites sp.
Biretisporites sp.
Cicatricosisporites cf. *potomacensis* Brenner 1963
Cicatricosisporites hallei Delcourt & Sprumont 1955
Cicatricosisporites neumanni Boltenhagen 1976
Cicatricosisporites sp. A (in Brenner 1992)
Cicatricosisporites sp. type 305 (in Brenner 1992)
Cicatricosisporites sp.
Cingutriletes "cingulumstriatum"
Concavisporites sinautus (Couper) Krutzsch 1959
Concavissimissporites cf. *verrucosus* Delcourt & Sprumont 1955
Contignisporites sp.
Cyathidites australis Couper 1953
Cyathidites minor Couper 1953
Cyathidites breviradiatus Helby 1966
Cyathidites "kyrtomatus"

Cyathidites sp.
Dictyophyllidites cf. harrisii Couper 1958
Ictyophyllidites sp.
Distaverrusporites "reticulatus"
Echitriletes "minutiechinus"
Echitriletes "perinatus"
Echitriletes "reticulatus"
Foveomonoletes sp.
Gleicheniidites sp.
Ischyosporites cf. *pseudoproblematicus*
Klukisporites sp.
Leptolepidites sp.
Leptolepidites verrucatus Couper 1953
Lycopodiumsporites "echimuratus"
Lycopodiumsporites "grandis"
Lycopodiumsporites cf. pseudoreticulatus Couper 1953
Lycopodiumsporites sp.
Microfoveolatosporis skottsbergii (Selling) Srivastava 1971
Pilosisporites "galeoides"
Pilosisporites sp. (in Regali et al. 1974)
Psilatriletes "kyrtomatus"
Psilatriletes sp.
Punctatisporites "bellus" aff. Foveotriletes labrus Mildenhall & Pocknall 1989
Retimonoletes sp.
Retipollenites sp.
Retriletes sp.
Rugumonoletes sp.
Rugutriletes sp.
Scabratriletes "cingulatus"
Scabratriletes sp.
Scabratriletes "undulaesuratus"
Scabratriletes sp.
Striatriletes "convergistriatus"
Striatriletes "nazcaensis"
Striatriletes "verrucosus"
Striatriletes sp.1
Striatriletes sp.2
Taurocusporites sp.
Todisporites sp.
Verrucosisporites cf. *asymmetricus* (Cookson & Dettmann) Pocock 1962
Verrumonoletes "minutus"
Verrumonoletes sp.
Verrutriletes "densoverrucatus"
Verrutriletes "distatuberatus"
Verrutriletes "leptoverrucatus"
Verrutriletes "magnoverrucatus"
Verrutriletes "minutiverrucatus"
Verrutriletes "minutus"
Verrutriletes "perinatus"
Verrutriletes "verruelongatus"

Verrutriletes sp.1
Verrutriletes sp.2
Verrutriletes sp.3

Gymnosperms pollen
Alisporites sp.
Araucariacites australis Cookson 1947
Araucariacites spp.
Balmeiopsis limbatus (Balme) Archangelsky 1977
Callialasporites dampieri (Balme) Dev 1961
Callialasporites microvelatus Schulz 1967
Callialasporites segmentatus (Balme) Srivastava 1963
Callialasporites trilobatus (Balme) Dev 1961
Callialasporites spp.
Classopollis classoides (Pflug) Pocock and Jansonius 1961
Classopollis simplex (Danzé, Corsin and Laveine) Reiser and Williams 1969
Classopollis spp.
Ephedripites multicostatus Brenner 1963
Ephedripites sp.
Equisetosporites cf. *ovatus* (Brenner 1968) De Lima 1980
Equisetosporites hughesii Pocock 1962
Equisetosporites leptomatus De Lima 1980
Equisetosporites minuticostatus De Lima 1980
Equisetosporites sp.
Gnetaceaepollenites aff. barghoornii
Gnetaceaepollenites barghoornii (Pocock) De Lima 1980
Gnetaceaepollenites sp.
Inaperturopollenites cf. *dubius* (Potonie and Venitz 1934) Pflug and Thomson 1953
Inaperturopollenites limbatus Balme 1957
Inaperturopollenites sp.
Steevesipollenites binodosus Stover 1964
Steevesipollenites sp.

Angiosperm pollen
Afropollis aff. *jardinus* Doyle, Jardiné and Doerenkamp 1982
Afropollis aff. *operculatus* Doyle, Jardiné and Doerenkamp 1982
Clavatipollenites sp.
Pennipollis reticulatus (Brenner) Friis, Pedersen and Crane 2000
Pennipollis cf. *reticulatus*
Retitricolpites "titanicus"
Stellatopollis cf. *barghoornii* Doyle 1975
cf. *Striatricolpites reticulatus* Regali, Uesugui and Santos 1974
Freshwater Algae
Chomotriletes sp.
Ovoidites sp.
Prasinophyceans algae
cf. Leiosphaeridia sp.
Fungal palynomorphs
incertae sedis

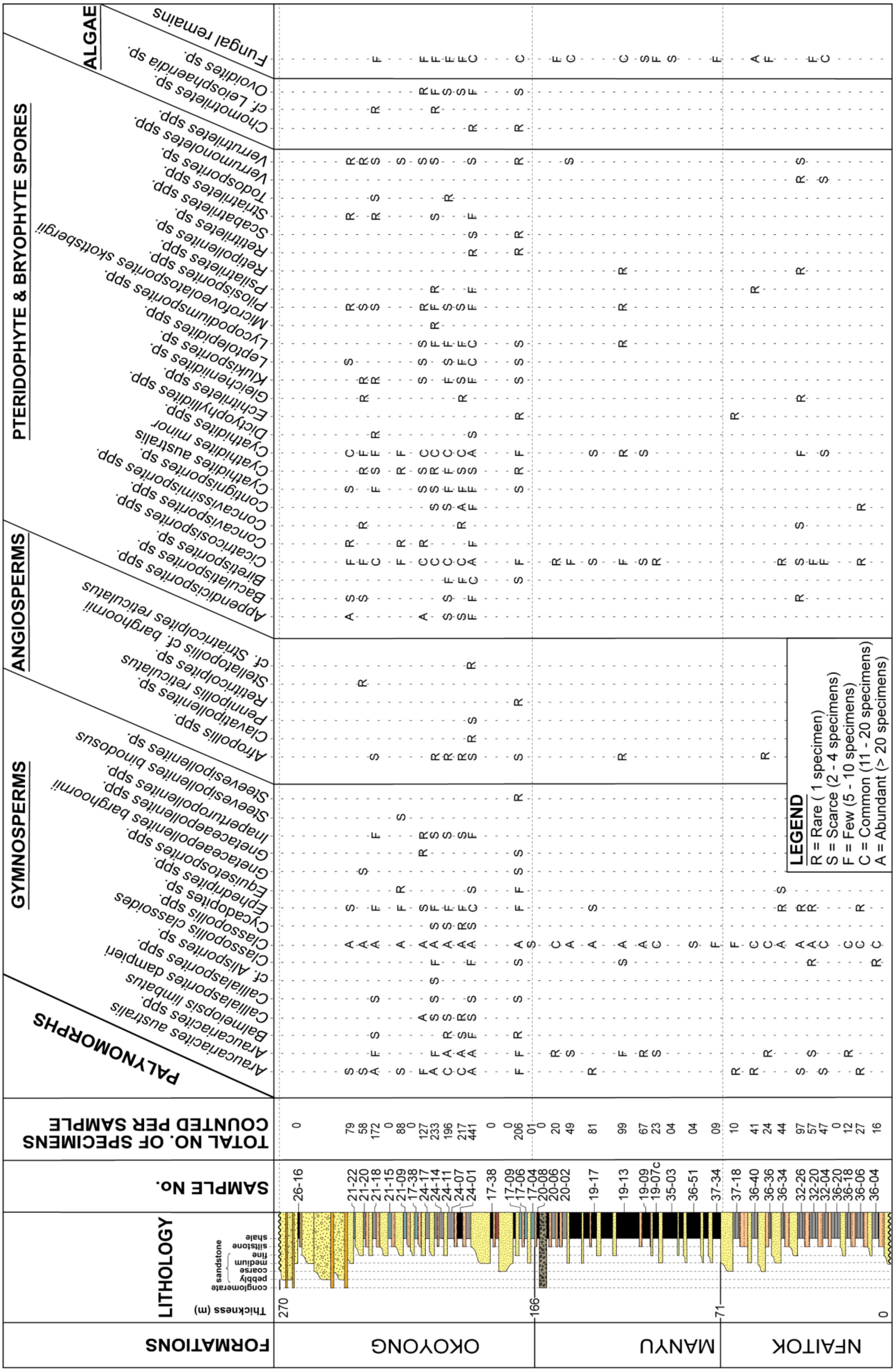

Figure 4.1. Semi-quantitative stratigraphic distribution of palynomorphs in the Mamfe Group.

4.3.1.1 Nfaitok Formation

Of the 11 samples from the Nfaitok Formation that were used in this study, only one was barren. Palynomorph abundance in kerogen residue range from 0 to 3.33%, diversity is low and preservation poor to moderate. A quantitative analysis of the pollen and spores content of the 10 palynomorph-bearing samples revealed that the palynoflora assemblage is dominated by gymnosperm pollen that account for between 75 and 100% (**figure 4.2a**).

Palynomorph abundance in samples from the Floodplain facies association varies from 1.7 to 3.3% and their diversity is very low. Gymnosperms are represented by *Classopollis classoides* and *Classopollis* sp. which together made up 95% of the palynoflora assemblage. *Araucariacites* spp., *Ephedripites* sp. are rare. Pteridophytes spores are represented by few *Cicatricosisporites* spp., *Cyathidites australis*, scarce *Concavissimissporites* sp., *Verrutriletes* spp. *Baculatisporites* sp., *Gleicheniidites* sp., *Retipollenites* sp., and *Verrumonoletes* sp. are rare. Fungal remains are few to common. Angiosperm pollen are rare and bryophytes spores are absent.

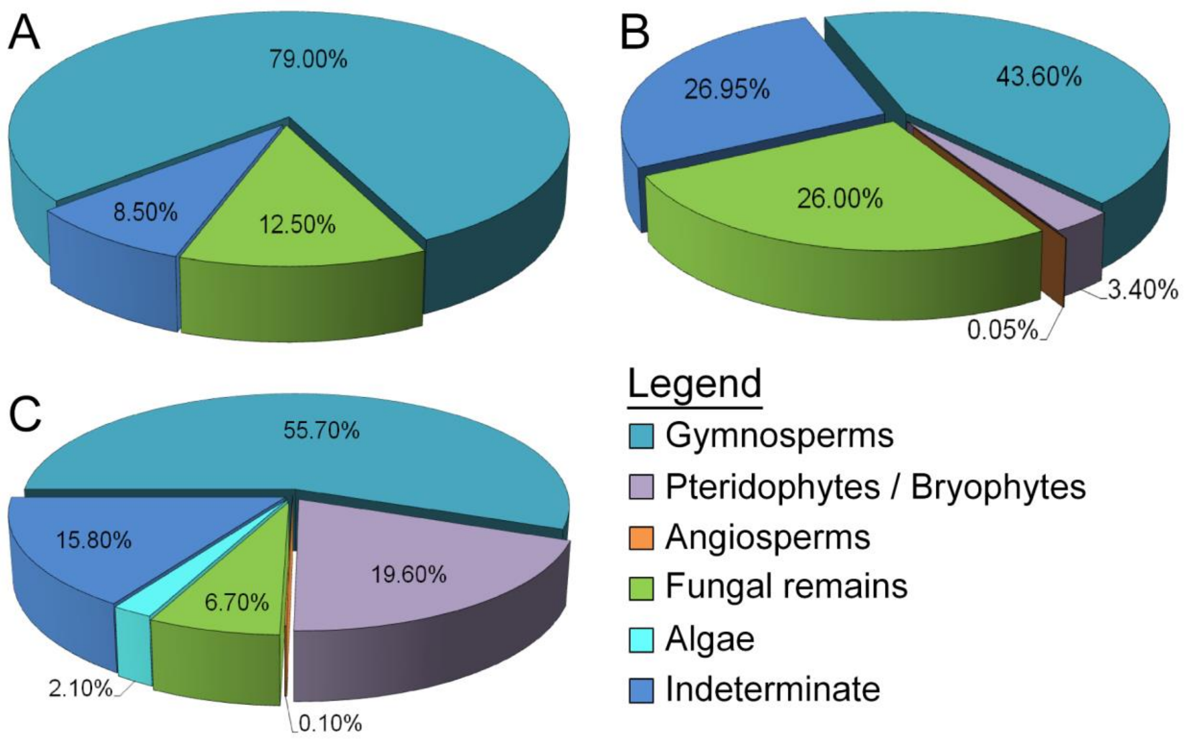

Figure 4.2. Relative abundance of the palynomorph groups in (A) Nfaitok Fm., (B) Manyu Fm., and (C) Okoyong Fm.

The palynoflora assemblage of samples from palustrine marshes facies association are made up predominantly of *Classopollis* sp. which account for over 98% of the palynomorphs. *Araucariacites* sp., *Ephedripites* sp., *Cicatricosisporites* sp., and *Contignisporites* sp. are rare. The samples lack angiosperm pollen and bryophyte spores.

In the fluvio-lacustrine samples, gymnosperms are represent by three taxa and made up mostly of *Classopollis* sp. (99%) and rare *Araucariacites australis*. The first appearance of angiosperm in this basin is recorded in this facies association and is represented by very rare *Afropollis* aff. *Jardinus*. Pteridophyte spores are rare and represented by *Cicatricosisporites* sp., *Echitriletes* sp., and *Psilatriletes* sp. Fungal remain are common and represent majority of the indeterminate fraction of the palynoflora assemblage.

4.3.1.2 Manyu Formation

Of the 10 samples from the Manyu Formation that were analysed in this study, only one was barren. Abundance and diversity of pollen and spores in palynomorph bearing sample is low (at most 13 taxa). The relatively low abundance and low diversity of palynomorphs in this formation may be attributed to hydrodynamic equivalence effect of the associated depositional environment (e.g. Catto, 1985; Tyson, 1995) rather than paleogeography and preservation. The palynomorphs are generally very poorly preserved. Many of the palynomorphs were only identifiable to genus level because of infestation by pyrite crystals and fungi. Most of the indeterminate palynomorphs recorded in this formation are due to “pyritization” which is prevalent in the profundal facies association.

The relative abundance of the various palynomorph groups within this formation as shown in **figure 4.2b** is dominated by gymnosperm pollen that account for 43.6% of the palynoflora assemblage.

The gymnosperm group is represented by *Classopollis* (>75%), a few to rare *Araucariacites* spp. and *Ephedripites* sp. Angiosperm is represented by a single specimen of poorly preserved *Afropollis* sp.

Pteridophyte spores make up on average, 3.4% of the total palynomorph assemblage of this formation. They are represented by scares to rare *Cicatricosisporites* sp., *Cyathidites* sp., *Lycopodiumsporites* sp., *Pilosisporites* sp., *Retipollenites* sp., and *Verrutriletes* sp.

4.3.1.3 Okoyong Formation

Nine out of the 16 deltaic swamp samples that were analysed for palynomorphs were barren of microflora. The palynomorphs are represented by gymnosperm and angiosperm pollen, pteridophyte and bryophyte spores, and fresh-water algae. Palynomorph abundance and diversity is relatively high (113 taxa), and the palynomorphs are moderately to well preserved. Gymnosperm, angiosperm, and pteridophyte palynomorphs are more common and diverse in samples from this formation than in the underlying formations of the Mamfe Group (**Fig.4.2c**).

The Gymnosperm group is the most abundant group in this formation, accounting on average for 55.7% of the total palynomorphs in the Okoyong Formation. Pollen grains of *Classopollis*, *Araucariacites*, and *Ephedripites* together make up more than 80% of the gymnosperm group. Also present in this group are a few to rare pollen of *Balmeiopsis limbatus*, *Inaperturopollenites* sp., *Alisporites* sp., *Callialasporites* dampieri, *Callialasporites* spp., *Steevesipollenites* spp., etc.

Angiosperm pollen grains were recorded in 7 samples and account for less than 0.10% of the total palynomorph in this formation. Abundance is low (1-4 specimen), and their diversity is relatively higher than in the underlying Nfaitok and Manyu Formations. They are represented by 6 genera. *Afropollis* is the most common genus. Others include monocolpate pollen *Clavatipollenites*, *Pennipollis*, and *Stellatopollis*. The first appearance of tricolpate angiosperm pollen in the Mamfe Basin is recorded in this formation and include *Retitricolpites*, and *Striatricolpites reticulatus*.

Pteridophyte spores are present in low to moderate amount, and account for 19.5% of the total palynomorph assemblage. They show a remarkably high diversity with the present of numerous previously undescribed echinate, striate and verrucate spores (see **table 4.1**). The most common trilete spores in this formation include *Cicatricosisporites* spp., *Cyathidites* spp., *Biretisporites*, *Appendicisporites*, *Klukisporites*, *Leptolepidites*, *Verrutriletes* spp., etc. Bryophyte spores recorded in this study occur within this formation and are represented by single specimen of *Aequitriradites* and *Taurocusporites*.

Fresh-water algae account for about 2.1% of the total palynomorph assemblage and is represented by rare to scares (1-2 specimens) of *Ovoidites* sp., and *Chomotriletes* sp. The stratigraphic ranges of representative palynomorph recorded in the Mamfe Group is shown in **figure 4.3**.

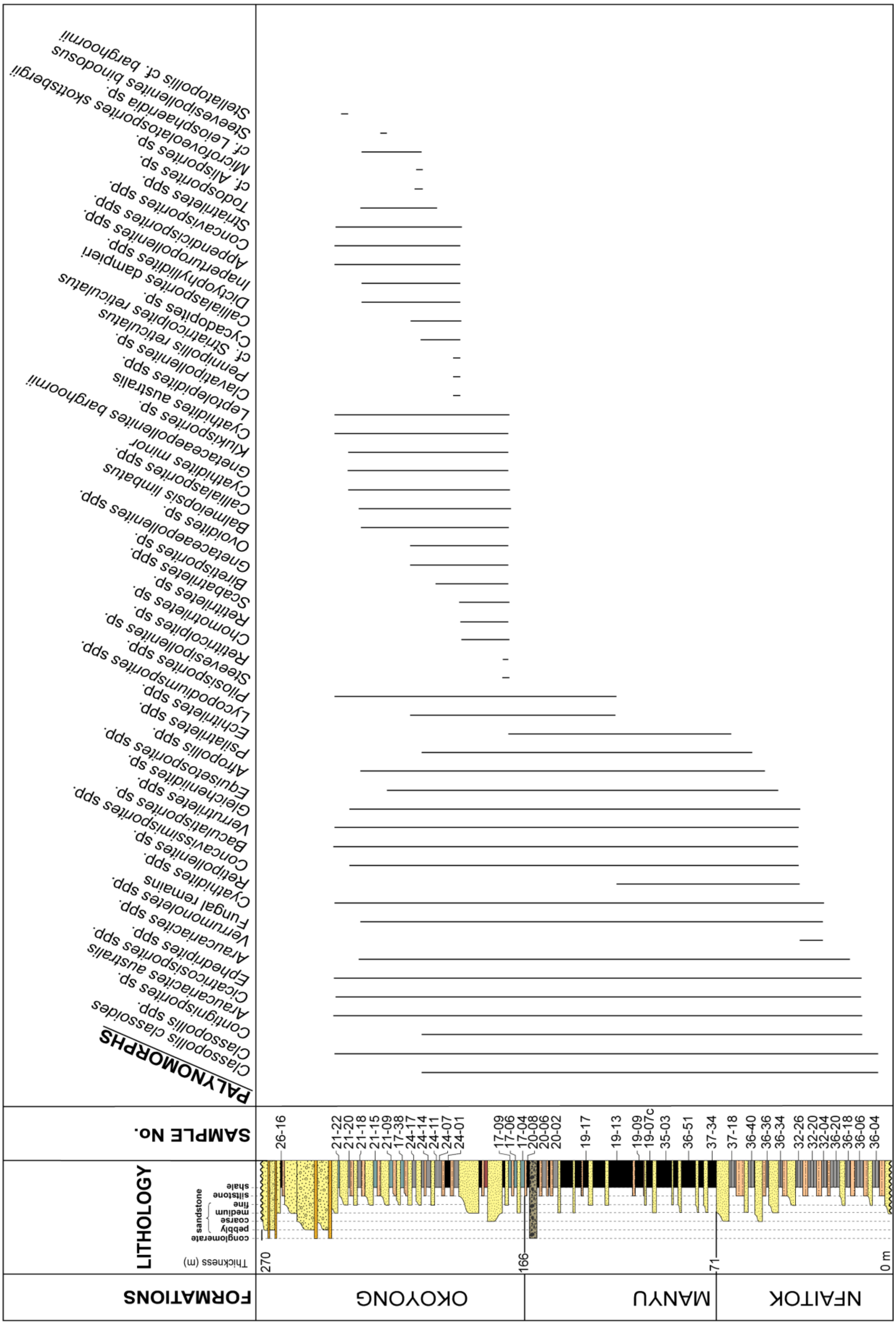

Figure 4.3. Stratigraphic ranges of representative palynomorphs in the Mamfe Group.

Figure 4.4. Taxon name is followed by sample number (bold), slide number (brackets), and England Finder coordinates (for Nikon Eclipse 80*i* microscope) or stage coordinates (for a Leitz Dialux 20 microscope). Unless stated, scale bar is 10 µm on all photomicrographs. Taxon names in "quotes" are new species.

A. *Cyathidites minor* Couper 1953, **21-09** (p4329), C46-4
B. *Cyathidites minor* Couper 1953, **24-01** (9601I), C44-0
C. *Cyathidites minor* Couper 1953, **21-18** (9305F), C24-0
D. *Cyathidites minor* Couper 1953, **21-18** (9305J), K25-0
E. *Cicatricosisporites* type 305 Brenner, **24-01** (9601L), H19-2
F. *Appendicisporites* cf*. tricornitatus* Weyland & Krieger 1953, **24-01** (9601M), G35-4
G. *Biretisporites* sp., 2**4-01** (9601G), X36-0
H. *Cicatricosisporites* sp., **24-01** (9601A), C44-4
I. *Cicatricosisporites* sp., **24-01**, (9601L), 107,9 /03.14
J. *Cingutriletes* "cingulumstriatum", **32-26** (p4325), N43-0
K. *Contignisporites* sp., **24-01** (9601M), T28-0
L. *Cyathidites australis* Couper 1953, **21-18** (9305J), O32-4
M. *Ischyosporites* cf. *'pseudoproblematicus*', **24-01** (9601E), H37-1
N. *Klukisporites* sp., **24-01** (9601K), P43-1
O. *Pilosisporites* sp1, **24-01** (9601B), M47-1
P. *Pilosisporites* sp., **21-18** (9305E), U35-0
Q. *Psilatriletes* sp., **24-14** (9304A), P33-0
R. *Retimonoletes* sp., **24-01** (9601E), E44-3
S. *Retipollenites* sp., **32-26** (p4325), R42-4
T. *Verrutriletes* sp., **21-18** (9305F), L33-3

Figure 4.5. Taxon name is followed by sample number (bold), slide number (brackets), and England Finder coordinates (for Nikon Eclipse 80*i* microscope). Unless stated, scale bar is 10 µm on all photomicrographs. Taxon names in "quotes" are new species.

A. *Cicatricosisporites neumanni* Boltenhagen 1976, **24-01** (9601I), K31-3
B. *Cicatricosisporites* cf. *potomacensis* Brenner 1963, **24-14** (9304G), Q45-0
C. *Cicatricosisporites* sp., **24-14** (9304B), G21-4-
D. *Concavisporites obtusangulus* (Potonié, 1934) Flug 1953, **21-20** (p4348), L32-1
E. *Cicatricosisporites neumanni* Boltenhagen 1976, **24-14** (9304B), G21-4
F. *Baculatisporites* sp., **24-01** (9601J), C30-0
G. *Dictyophyllidites cf. harrisii* Couper 1958, **24-01** (9601C), V33-1
H. *Gleicheniidites* sp. **32-26** (p4325), S42-3
I. *Punctatisporites "bellus"* aff. *Foveotriletes labrus* Mildenhall & Pocknall 1989, **24-18** (9305E), Q27-0
J. *Lycopodiumsporites* cf. *pseudoreticulatus* Couper 1953, **24-01** (9601C), N44-0
K. *Scabratriletes* sp., **32-26** (p4325), N43-2
L. *Verrucosisporites cf. asymmetricus* (Cookson & Dettmann) Pocock 1962, **24-01** (9601F), D32-0
M. *Verrutriletes* sp., **17-06** (9298H), C28-4
N. *Distaverrusporites "reticulatus*", **21-18** (9305E), T47-2
O. *Rugutriletes* sp., **24-01** (9601C), B29-2
P. *Taurocusporites* sp., **17-06** (9298H), H22-4
Q. *Lycodiumsporites* sp., **17-06** (9298H), L40-3
R. *Retriletes* sp. 2, **24-01** (9601E), Y39-2
S. *Verrutriletes* sp. **21-20** (p4348), U19-0
T. *Microfoveolatosporis skottsbergii* (Selling) Srivastava 1971, **24-14** (9304C), Y28-1

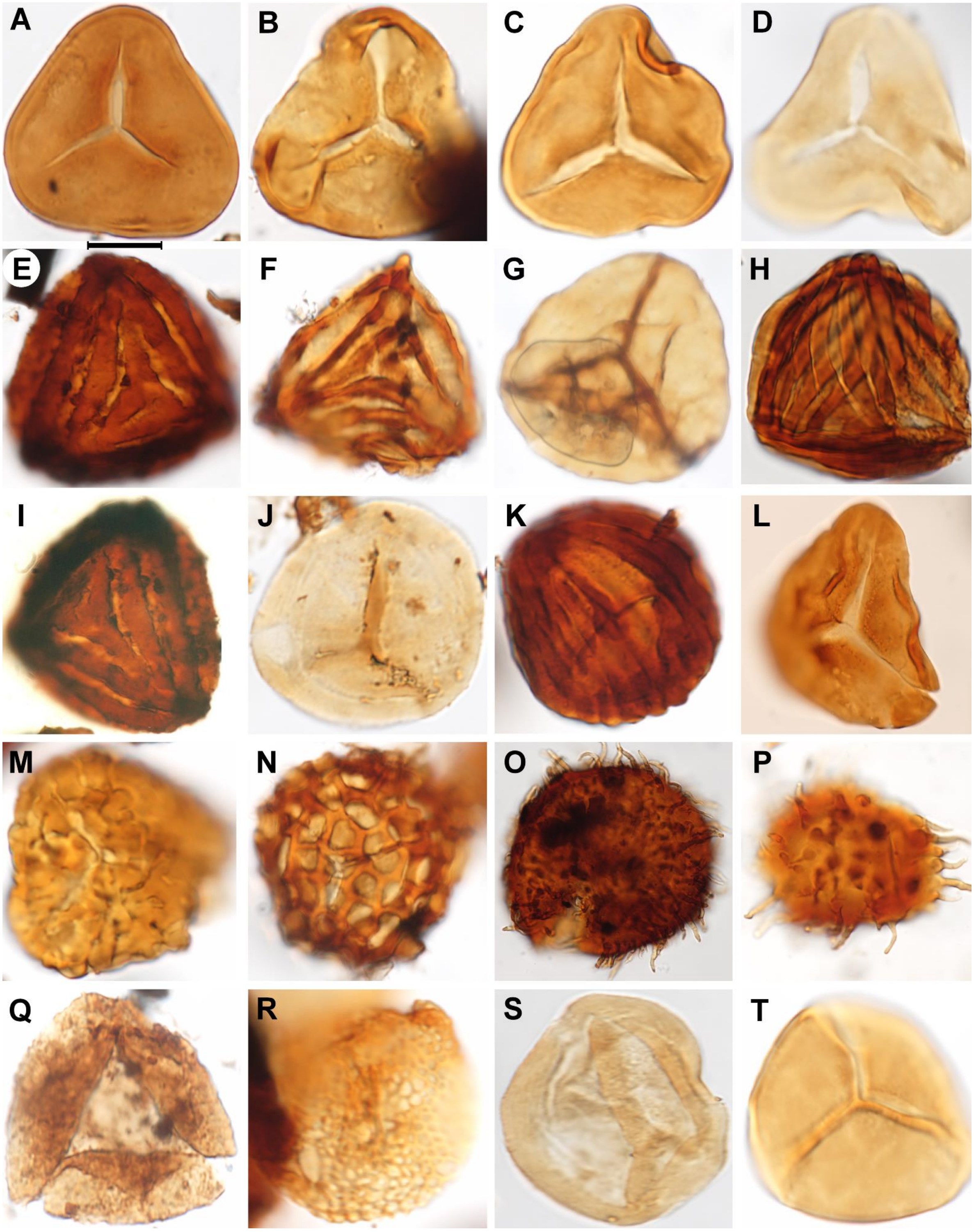

Figure 4.4.

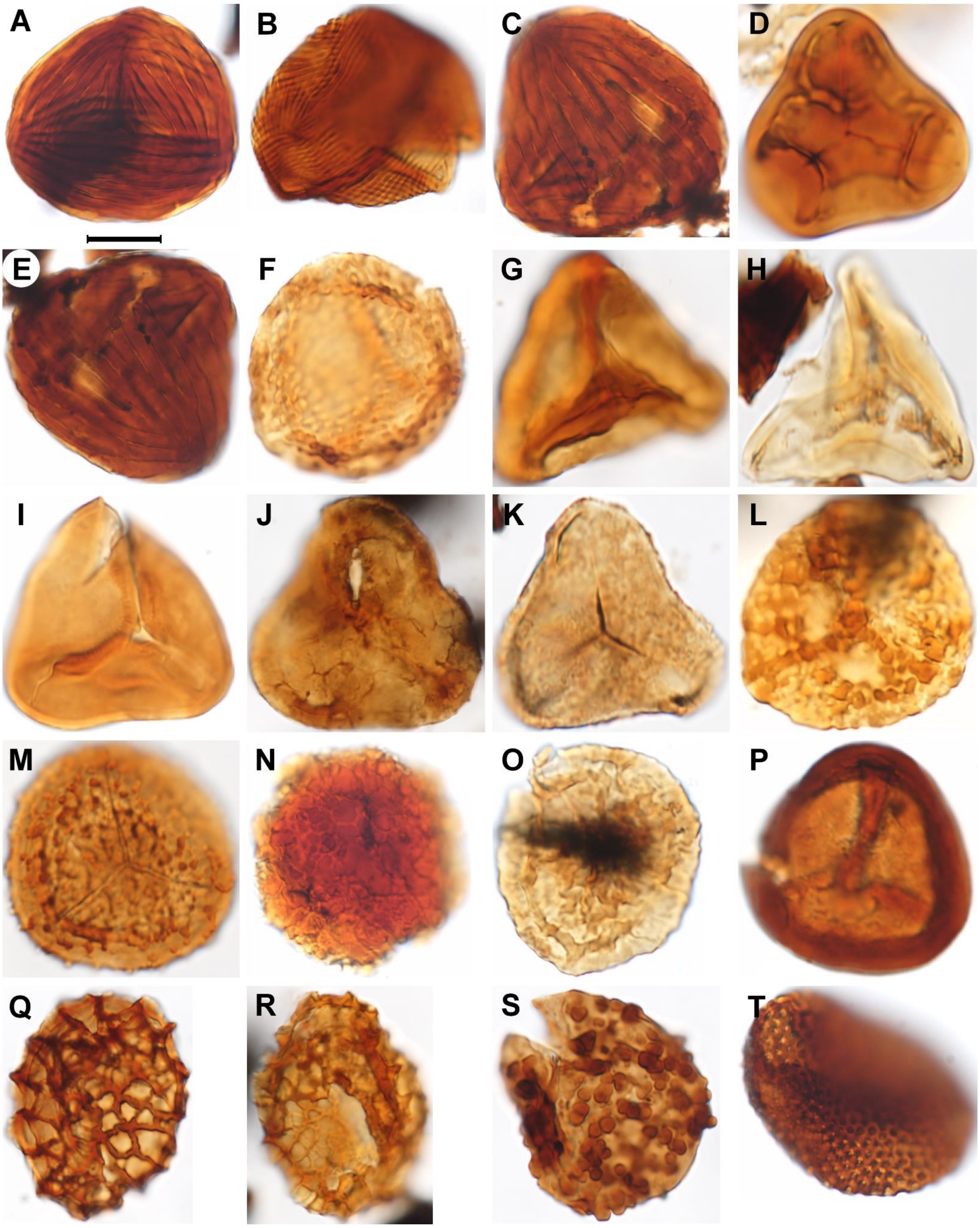

Figure 4.5.

Figure 4.6. Taxon name is followed by sample number (bold), slide number (brackets), and England Finder coordinates (for Nikon Eclipse 80*i* microscope). Unless stated, scale bar is 10 µm on all photomicrographs. Taxon names in “quotes” are new species.

A. *Lycopodiumsporites* “*echimuratus*”, **24-14** (9304F), J25-1
B. *Echitriletes 'minutiechinus'*-**17-06** (9298C), R40-1
C-D. *Striatriletes "convergistriatus"*, **24-01** (9601I), V23-3
E-F. *Striatriletes* "nazcaensis", **24-14** (9304C), H31-0
G. *Verrutriletes* “*distatuberatus*”, **24-14** (9304D), F40-4
H-I. *Verrutriletes* “*magnoverrucatus*”, **21-20** (p4348), M47-1
J-K. *Verrutriletes* “*margolaesuratus*”, **21-22** (p4344), Q39-2
L. *Psilatriletes* “*kyrtomatus*”, **36-20** (p4338), Q12-4, -1
M. *Echitriletes* “*perinatus*”, **24-01** (9601C), J32-0
N. *Echitriletes 'reticulatus'*- **24-11** (p4340), E11-3
O. *Scabratriletes* “*cingulatus*”, **21-20** (p4348), H31-1
P. *Scabratriletes* “*undulaesuratus*”, **24-14** (9304E), U39-0
Q-R. *Verrutriletes* “*minutiverrucatus*”, **20-02** (p4326), O16-4
S. *Verrutriletes “minutus”*, **21-09** (p4329), S32-0
T. *Verrutriletes* “*verruelongatus*”, **32-26** (p4325), S24-0

Figure 4.7. Taxon name is followed by sample number (bold), slide number (brackets), and England Finder coordinates (for Nikon Eclipse 80*i* microscope). Unless stated, scale bar is 10 µm on all photomicrographs. Taxon names in “quotes” are new species.

A. *Araucariacites* australis Cookson 1947, **24-14** (9304C), H45-1
B. *Araucariacites* australis Cookson 1947, **24-14** (9304G), C35-4
C. *Callialasporites dampieri* (Balme) Dev 1961, **24-01** (9601D), X23-3
D. *Callialasporites* cf. *segmentatus* (Balme) Srivastava 1963, **24-01** (9601J), L40-4
E. *Callialasporites* cf. *trilobatus* (Balme) Dev 1961, **21-18** (9305F), M35-1
F. *Callialasporites microvelatus* Schulz 1967, **21-18** (9305F), M34-0
G. *Classopollis* sp., **24-14** (9304D), O44-2
H. *Classopollis simplex* (Danzé, Corsin & Laveine) Reiser & Williams 1969, **17-06** (9298H), J39-2
I. *Classopollis* sp., **21-18** (9305E), L43-3
J. *Ephedripites multicostatus* Brenner 1963, **17-06** (9298H), C33-2
K. *Ephedripites* sp., **24-01** (9601G), R38-4
L. *Equisetosporites* sp., **17-06** (9298C), C32-1
M. *Equisetosporites* aff. *costaliferus*, **17-06** (p4332), W13-4
N. *Equisetosporites* cf. *leptomatus* De Lima 1980, **24-01** (9601C), D35-1
O. *Equisetosporites cf. ovatus* (Brenner 1968) De Lima 1980, **21-09** (p4329), L16-1
P. *Equisetosporites hughesii* Pocock 1962, **17-06** (9298C), L27-0
Q. *Gnetaceaepollenites barghoornii* (Pocock) De Lima 1980, **21-20** (p4374), J43-3
R. *Inaperturopollenites* sp., **24-14** (9304E), M42-2
S. *Inaperturopollenites limbatus* Balme 1957, **24-01** (9601G), M34-1
T. *Inaperturopollenites* cf. *dubius* (Potonie & Venitz 1934) Pflug & Thomson 1953, **32-26** (p4325), R38-0

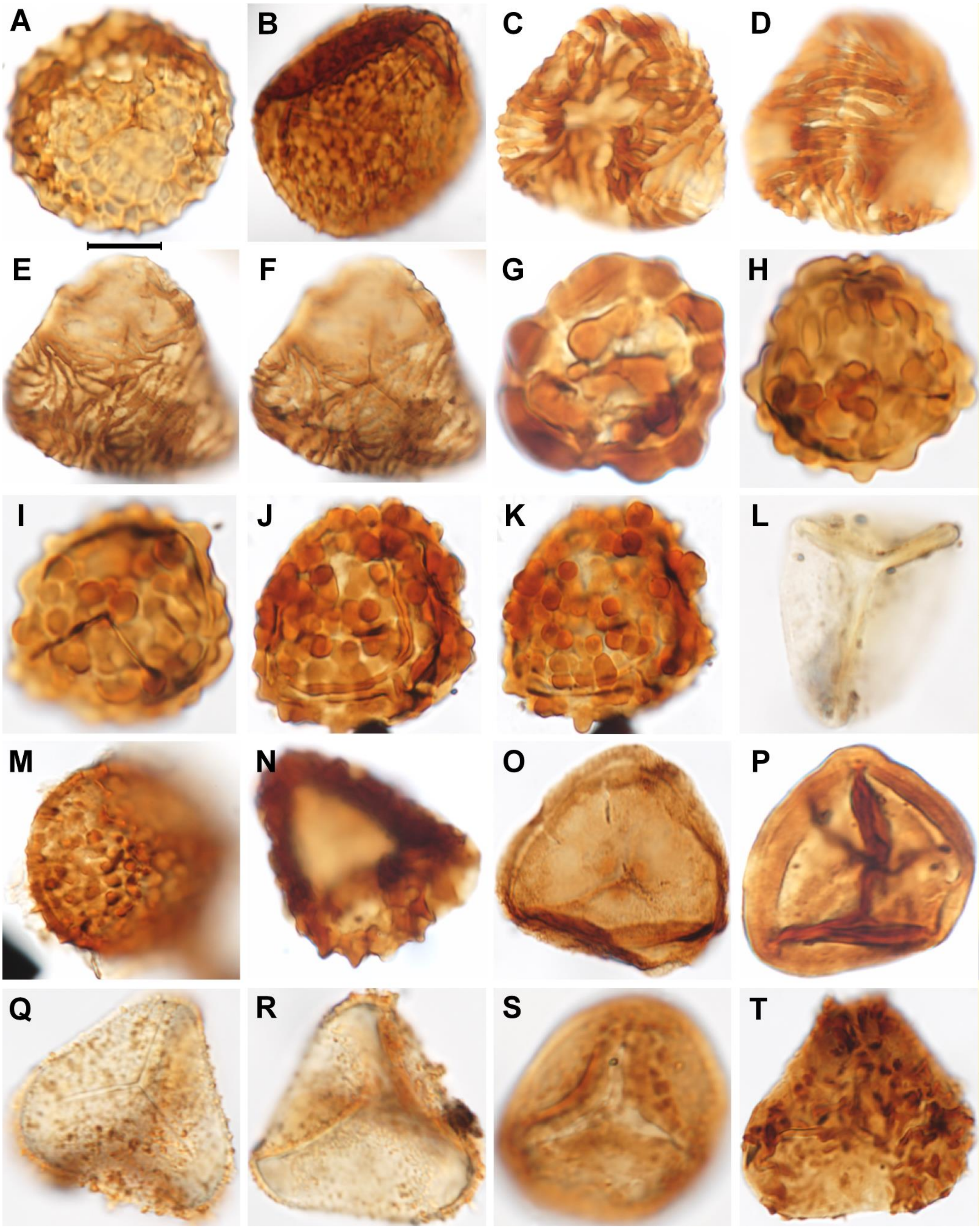

Figure 4.6.

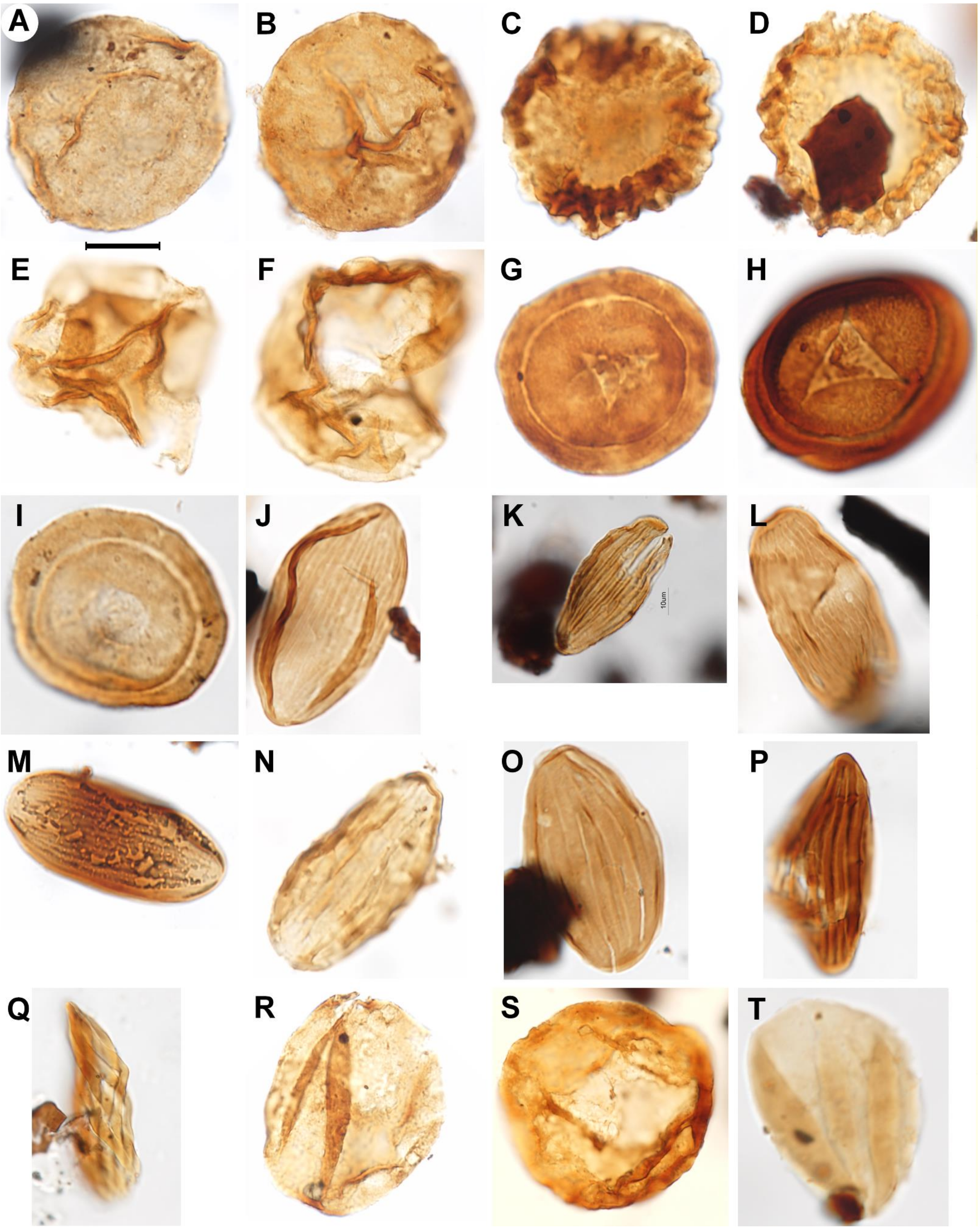

Figure 4.7.

Figure 4.8. Taxon name is followed by sample number (bold), slide number (brackets), and England Finder coordinates (for Nikon Eclipse 80*i* microscope). Unless stated, scale bar is 10 µm on all photomicrographs. Taxon names in “quotes” are new species. G-T are CLSM photomicrographs.

A. *Retitricolpites 'titanicus'*, **17-06** (9298C), C35-4
B-C. *Clavatipollenites* sp. **24-01** (9601G), Q37-0
D. *Chomotriletes* sp. **17-06** (9298H), D32-0
E. *Ovoidites* sp. **17-06** (9298I), Z21-1
F. *Araucariacites* australis Cookson 1947, **24-14** (9304B), Q21-4
G. *Alisporites* sp.**24-01** (9601G), X41-0b
H. *Cicatricosisporites neumanni* Boltenhagen 1976, **24-14** (93O4B), G21-4
I. *Cicatricosisporites neumanni* Boltenhagen 1976, **24-01** (9601I), k31-3
J. *Clavatipollenites* sp., **24-01** (9601G), Q37-0
K. *Microfoveolatosporis skottsbergii* (Selling) Srivastava 1971, **24-14** (9304C), Y28-1
L. *Pennipollis* cf. *reticulatus* (Brenner) Friis, Pedersen & Crane 2000, **24-01** (9601G), R33-1
M. *Pennipollis* sp., **24-01** (9601G), W31-4
N. *Striatriletes* ‘*nazcaensis’*, **24-14** (9304C), H31-1
O. *Afropollis* aff. *jardinus* Doyle, Jardiné & Doerenkamp 1977, **24-01** (9601G), J40-0
P. *Gnetaceaepollenites barghoornii (Pocock)* De Lima 1980, **17-06** (P4332), G10-4
Q. *Striatricolpites reticulatus* Regali, Uesugui and Santos 1974, **24-01** (9601G), W34-4
R. *Steevesipollenites binodosus* Stover 1964, **21-09** (P4329), L16-1
S. *Stellatopollis* cf. *barghoornii* Doyle 1975, **21-20** (4348), H31-1
T. *Equisetosporites* sp. **17-06** (9298C), U44-0

Figure 4.9. Taxon name is followed by sample number (bold), slide number (brackets), and England Finder coordinates (for Nikon Eclipse 80*i* microscope). Unless stated, scale bar is 10 µm on all photomicrographs. Taxon names in “quotes” are new species.

A. *Afropollis* aff. *jardinus* Doyle, Jardiné & Doerenkamp 1982, **24-01** (9601G), J40-0
B. *Alisporites* sp., **24-01**-(9601G), Y30-2
C. *Callialasporites dampieri* (Balme) Dev 1961, **24-14** (9304F), X40-2
D. *Cicatricosisporites hallei* Delcourt & Sprumont 1955, **24-01** (9601C), V30-4
E. *Cicatricosisporites hallei* Delcourt & Sprumont 1955, **24-01** (9601E), K39-0
F. *Classopollis* cf. *classoides* (Pflug) Pocock & Jansonius 1961 - **24-01 (**9601C), M33-0
G. *Pennipollis* sp. **24-01 (**9601G), W31-4
H. *Pennipollis* cf. *reticulatus* (Brenner) Friis, Pedersen & Crane 2000, **24-01** (9601G), R33-1
I-J. *Striatricolpites reticulatus* Regali, Uesugui and Santos 1974, **24-01** (9601G), W34-4
K. *Leptolepidites verrucatus* Couper 1953, **20-02** (9599B), Y33-4
L. *Leptolepidites* cf. *verrucatus* Couper 1953, **24-01**-(9601J), C39-0
M. *Balmeiopsis limbatus* (Balme) Archangelsky 1977, **17-06** (9298H), H21-0
N. *Equisetosporites minuticostatus* De Lima 1980, **17-06** (9298A), J36-0
O. *Gnetaceaepollenites barghoornii (Pocock)* De Lima 1980, **17-06** (p4332), H15-1
P. *Ephedripites* sp. **24-01** (9601G), R38-4
Q. *Striatriletes* sp**. 24-01**-(9601I), V23-3
R-T. *Stellatopollis* cf. *barghoornii* Doyle 1975, **21-20** (p4348), H31-1

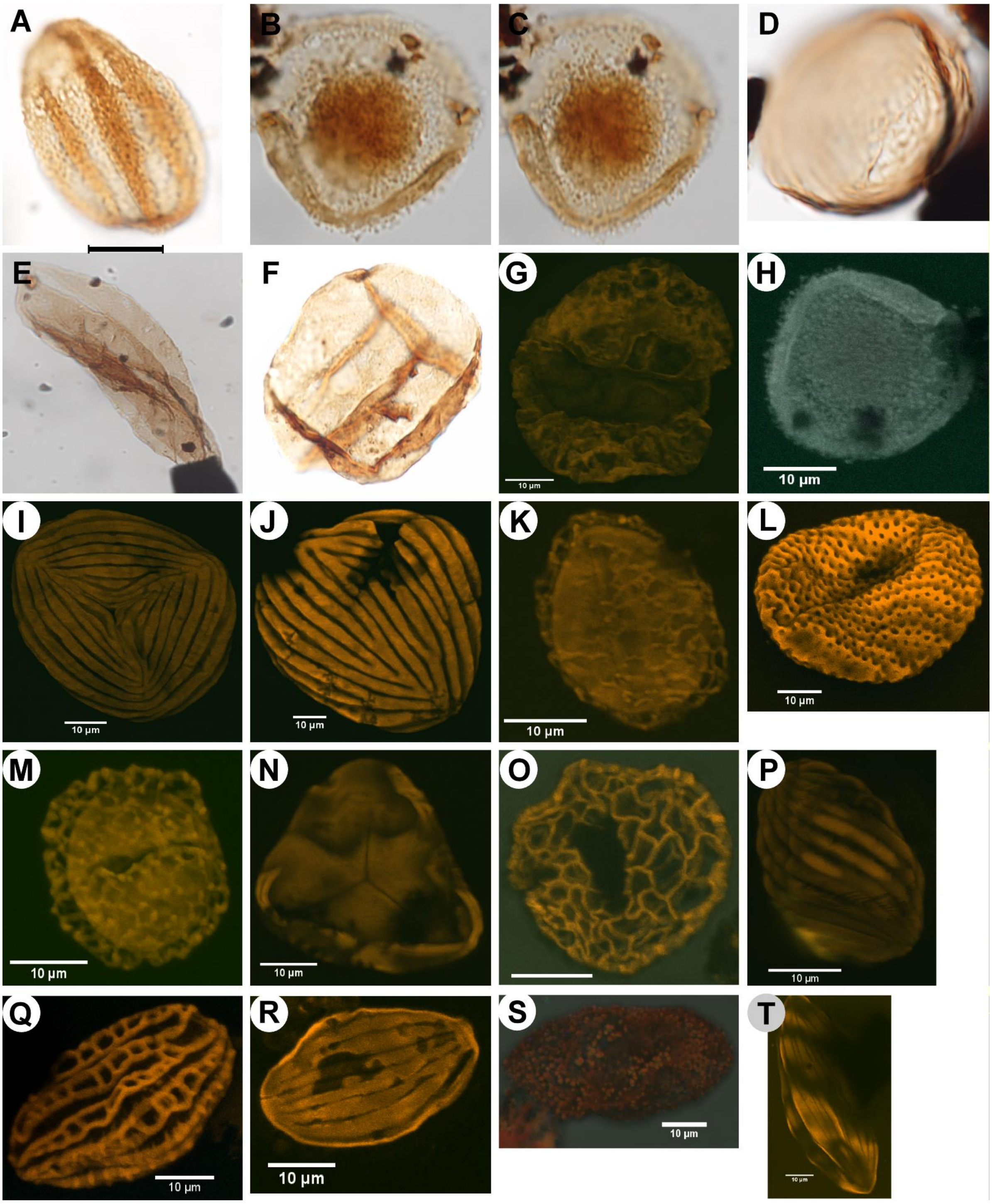
A
B
C
D
E
F
G
10 µm
H
10 µm
I
10 µm
J
10 µm
K
10 µm
L
10 µm
M
10 µm
N
10 µm
O
P
10 µm
Q
10 µm
R
10 µm
S
10 µm
T

Figure 4.8.

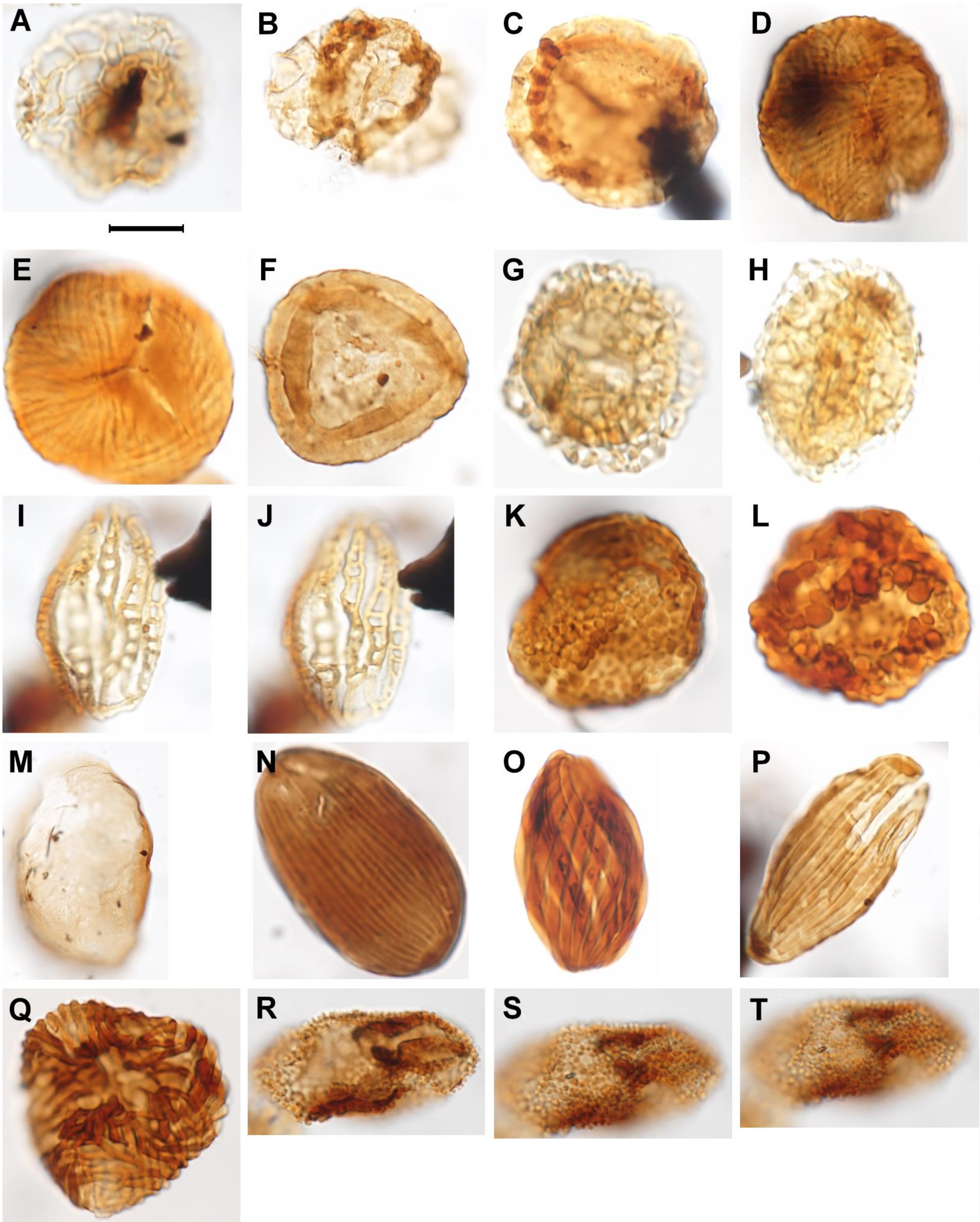

Figure 4.9.

4.4 Discussion

4.4.1 Age significance

Age assessment and correlation of Cretaceous palynomorphs is mindful of the remarkable influence of latitude on the composition and distribution of the flora. The effect of latitude on the distribution of flora in the Cretaceous led to pronounced provinicialization (Brenner, 1976; Herngreen and Chlonova, 1981, Srivastava, 1994; Herngreen et al., 1996). According to Herngreen et al. (1996), the West African-South American (WASA) Microfloral Province of Herngreen and Chlonova (1981) occupy the same geographic position as the Northern Gondwana Floral Province of Brenner (1976). This phytogeographic province (**Fig 4.10**) has been renamed Dicheiropollis etruscus/Afropollis province and assigned a pre-Albian early Cretaceous age (Herngreen et al., 1996; Herngreen, 1998).

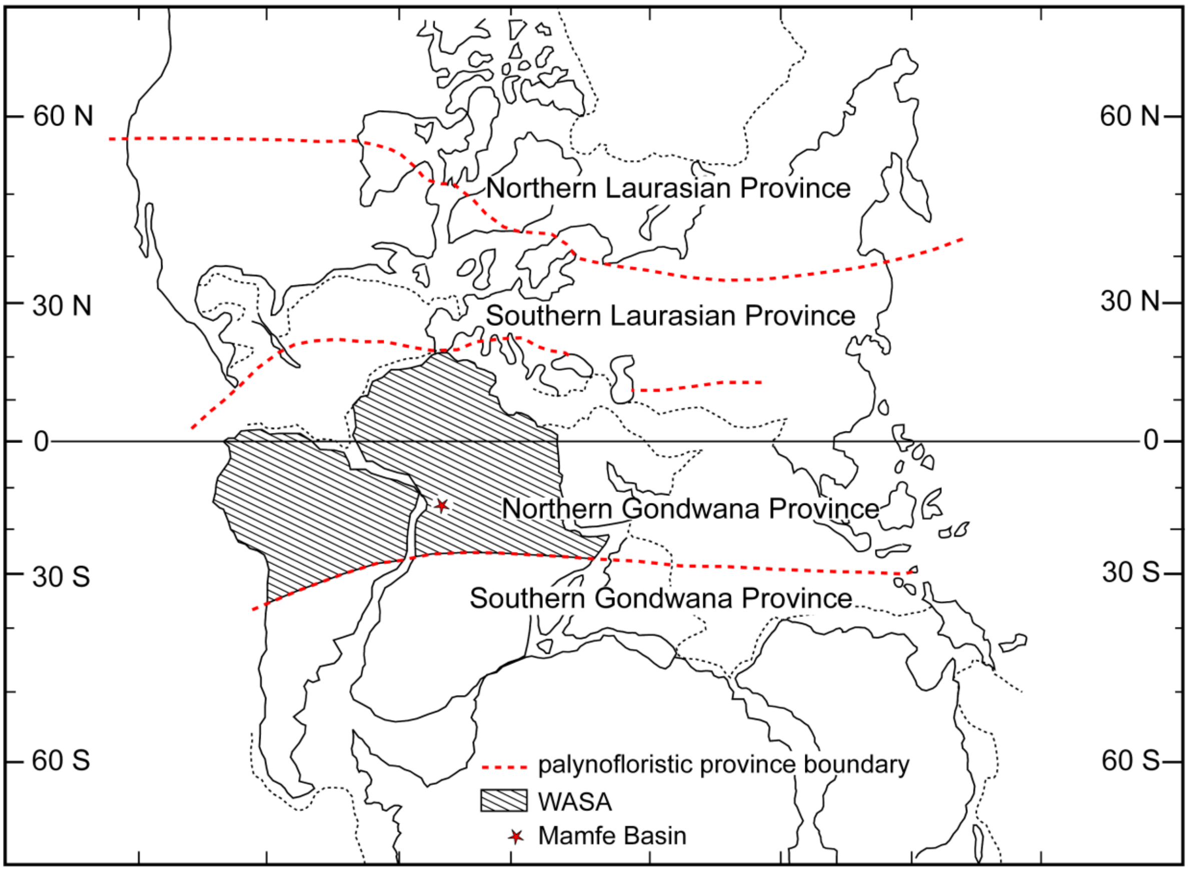

Figure 4.10. Early-Mid Cretaceous palynofloristic provinces (Brenner, 1976). Relative position of continents during the lower and middle Cretaceous after Smith et al., (1973), and WASA after Herngreen and Chlonova (1981).

Smith et al., (1973) Phanerozoic world map (**Fig 4.10**) indicates that the Mamfe Basin was located at paleolatitude 11^{o} S, and was within the geographical boundaries of the area assigned to Northern Gondwana palynofloral province. Age assessment and correlation of the microflora assemblage from Mamfe Basin rely on comparison with age-diagnostic palynomorphs recorded in other areas located within WASA/Northern Gondwana palynofloristic province.

Most of the pollen and spores recorded in this study have long age ranges and thus are not useful for dating. Age-diagnostic palynomorphs that have been recorded from equatorial Africa and northeastern Brazil are not many in the studied material. Age-diagnostic palynomorphs present in the microflora assemblage of the Mamfe Basin and their stratigraphic ranges within WASA are shown in **figure 4.11**.

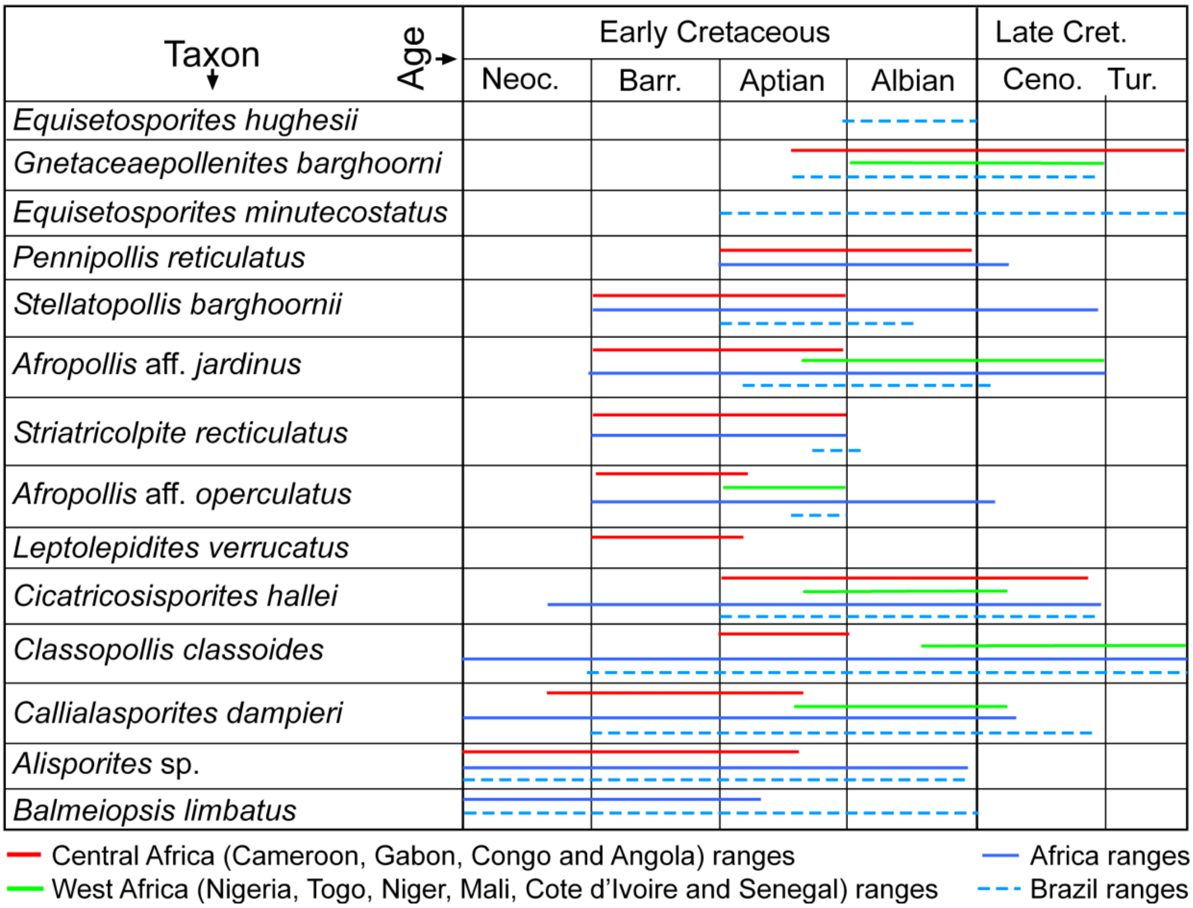

Figure 4.11. Stratigraphic ranges of some West African-South American (WASA) age-diagnostic palynomorphs present in the Mamfe Group (adapted from Salard-Cheboldaeff, 1990, Palynodata and White, 2008).

Analysis of stratigraphic distribution of age-diagnostic taxa within the Mamfe Basin (**Fig 4.3**, & **4.11**) shows that some of the palynomorphs can be used to effectively narrow down the geologic age of the studied succession of the Mamfe Group. The presence of *Afropollis* and lack elaterates in the Mamfe Group indicates that the group equates in part to the pre-Albian lower Cretaceous *Dicheiropollis etruscus*/*Afropollis* Province of Herngreen et al. (1996), Herngreen (1998).

Dicheiropollis etruscus is absent in the Mamfe Basin, and is a stratigraphic marker for Neocomian-early Barremian age in the *Dicheiropollis etruscus*/*Afropollis* palynoprovince (Herngreen, 1998). Absence of *D*. *etruscus* in the studied stratigraphic succession suggests that the Mamfe Group is younger than early Barremian.

Afropollis aff. *jardinus* is known from the Barremian to Aptian in Angola, Congo, Gabon and Cameroon; late Aptian in Nigeria; and late Aptian-early Albian in NE Brazil (Doyle et al., 1982; Regali, 1989; Salard-Cheboldaeff, 1990; Doyle, 1992; Palynodata and White, 2008). The first appearance datum (FAD) of the *Afropollis* aff. *jardinus* in the Mamfe Basin is in the upper part of the Nfaitok Formation.

Afropollis aff. *operculatus* was recorded as a single specimen in the deep-water facies of the Manyu Formation. It has been reported from early Aptian sediments succession in Angola, Congo and Cameroon. In Gabon and Egypt, this species range from late Barremian to early Aptian, and is recorded in late Aptian sediments in Nigeria and NE Brazil (Doyle et al., 1982; Regali and Viana, 1989; Salard-Cheboldaeff, 1990; Doyle, 1992). In the Mamfe Basin, 2 specimens of this pollen were recorded in the Manyu Formation.

The occurrence of *Classopollis classoides* in the Mamfe Basin is sporadic and ranges from lower Nfaitok to middle Okoyong Formation. Previous records of *C*. *classoides* range from the Neocomian to Aptian in Gabon and Egypt, and late Albian in the Benue Trough of Nigeria (Salard-Cheboldaeff, 1990; Lawal, 1991).

Leptolepidites verrucatus has been reported from the late Neocomian to early Barremian in Angola, Congo, and Cameroon; Aptian in Gabon, NE Brazil and Australia; and late Albian of Sudan (Jardiné, 1974; Salard-Cheboldaeff, 1990; Palynodata and White, 2008). In the Mamfe Basin, this trilete spore is recorded in the Okoyong Formation.

Balmeiopsis limbatus FAD in the Mamfe Basin is the lower Okoyong Formation. Its occurrence in this unit is sporadic and its last appearance datum (LAD) is the top of middle Okoyong Formation. This species has not been reported from Central Africa region. *B*. *limbatus* is a stratigraphic marker of Neocomian-Aptian deposits in Australia. It has been reported from the Jurassic-early Aptian of Egypt, Albian of Algeria; and Berriasian-Albian of NE Brazil (Salard-Cheboldaeff, 1990; Palynodata and White, 2008).

A single specimen of *Stellatopollis barghoornii* was recorded in the upper part of the Okoyong Formation. Records of this species range from the late Neocomian to Aptian in Libya; Barremian to Aptian in Angola, Congo, Gabon and Cameroon; late Barremian-early Aptian in Egypt; and Aptian-middle Albian in NE Brazil (Salard-Cheboldaeff, 1990; Palynodata and White, 2008).

Pennipollis reticulatus recorded in the Okoyong Formation has been reported in late Barremian-middle Aptian sediments in Egypt; and late Aptian-early Albian in NE Brazil (Palynodata and White, 2008; Heimhofer and Hochuli, 2010).

Equisetosporites minuticostatus occur in Aptian-Cenomanian deposits in NE Brazil (de Lima, 1980). In the Mamfe Basin, this species was recorded in deposits of the Nfaitok and Okoyong Formation.

Gnetaceaepollenites aff. *barghoornii* recorded in the Okoyong Formation has been reported from Albian-Turonian sediments in Angola, Congo, Gabon, and Cameroon; and late Aptian in NE Brazil.

Other stratigraphically significant palynomorphs in the Mamfe Basin include *Concavissimissporites verrucosus* and *Dictyophyllidites harrisii* that have been reported from the middle Barremian-early Albian of Angola, Congo, Gabon and Cameroon; and late Barremian-middle Albian of Cote d'Ivoire and Senegal (Salard-Cheboldaeff, 1990).

Striatricolpites reticulatus occur in the middle part of the Okoyong Formation. This species and has been reported in the early Aptian-early Albian sediments in in NE Brazil, Central African Republic, Chad and Morocco (De Lima, 1980; Regali and Viana, 1989; Salard-Cheboldaeff and Boltenhagen, 1992; Heimhofer and Hochuli, 2010).

Limited representation of flowering plants both numerically and morphologically in the studied succession of the Mamfe Basin is typical of Aptian and to a lesser extent, early Albian deposits in middle low latitudes (Batten, 2007). Using the concept of increasing diversity of angiosperm through time in the Cretaceous, the abundance and diversity of angiosperm pollen in the Okoyong Formation relative to the underlying

Nfaitok and Manyu Formations is interpreted as indicating a younger age for the Okoyong Formation.

From the ranges of biostratigraphically significant palynomorphs recorded in this study, it is reasonable to suggest a middle Barremian-early Aptian age range for deposits of the Nfaitok Formation, early to late Aptian age for the Manyu Formation, and late Aptian-early Albian age range for the Okoyong Formation.

The presence of abundant fern spores and absence of palynomorphs that are typical of the Albian-Cenomanian Elaterates Province of Herngreen et al., (1996) such as *Elaterocolpites*, *Elateroplicites*, *Elateropollenites*, *Elaterosporites*, *Galeacornea Cretacaeiporites* (e.g. Herngreen, 1974, 1998; Herngreen and Chlonova, 1981; Herngreen et al., 1996; Regali and Viana, 1989; Batten, 2007; Salard-Cheboldaeff, 1990), suggest that the maximum age range of the Okoyong Formation is probably late Aptian-early Albian. This age range is supported by the presence of single specimen of *Praebulimina* sp. and *Hedbergella* in this formation. Earliest record of *Praebulimina* sp. and *Hedbergella* sp. in the West African eastern Gulf of Guinea is from late Aptian-early Albian marine deposits in Gabon and the Kribi-Campo Basin in Cameroon (Kogbe and Me'hes, 1986; Nguene et al., 1992). These foraminifera have also been recorded in late Aptian-early Albian succession in the Oriental Basin of Ecuador (Villagomez et al., 1996).

From the combined stratigraphic ranges of the above-mentioned age-diagnostic palynomorphs in West African-South-American Microflora Province, it is reasonable to suggest an age range of middle Barremian to early Albian for the Mamfe Group.

4.4.2 Correlation

Results of comparison of the microflora of Mamfe Group with Cretaceous palynoflora assemblages in other regions within the West African-South American Microflora Province using Non-Metric Multidimensional Scaling technique is shown in **figure 4.12**. The microflora assemblage from Mamfe Basin shows the greatest similarity with the microflora assemblage reported from the Antenor Navarro and Sousa Formations in the Rio Do Pixe Basin of NE Brazil (Hessel et al., 1994; Mabesoone et al., 2000) and Upper Cocobeach Group of northern Gabon Basin (Jardine, 1974; Doyle et al., 1977, 1982; Doyle, 1992). It also correlates with the palynoflora from the Ise Formation in the Benin Embayment (Jan du Chêne, 2000); and the Hama Koussou Basin in Northern Cameroon (Dejax and Brunet, 1996).

Within the Northern Gondwana palynofloristic province, the Mamfe Basin assemblage is comparable to the microfloral assemblage reported from Egypt and northern Sudan (Schrank, 1992), Congo (Dejax, 1987), Senegal and Cote d'Ivoire (Jardiné and Magloire, 1965; Salard-Cheboldaeff and Dejax, 1991)

The palynoflora assemblage of the Mamfe Basin corresponds to the West Africa regional palynostratigraphic reference section and zones CV to CIX of SNEA (P) in Gabon, and palynozones P-190 to P-280 in South America (Brazil) that have been assigned to Middle Barremian-Early Albian age (**Fig. 4.13**).

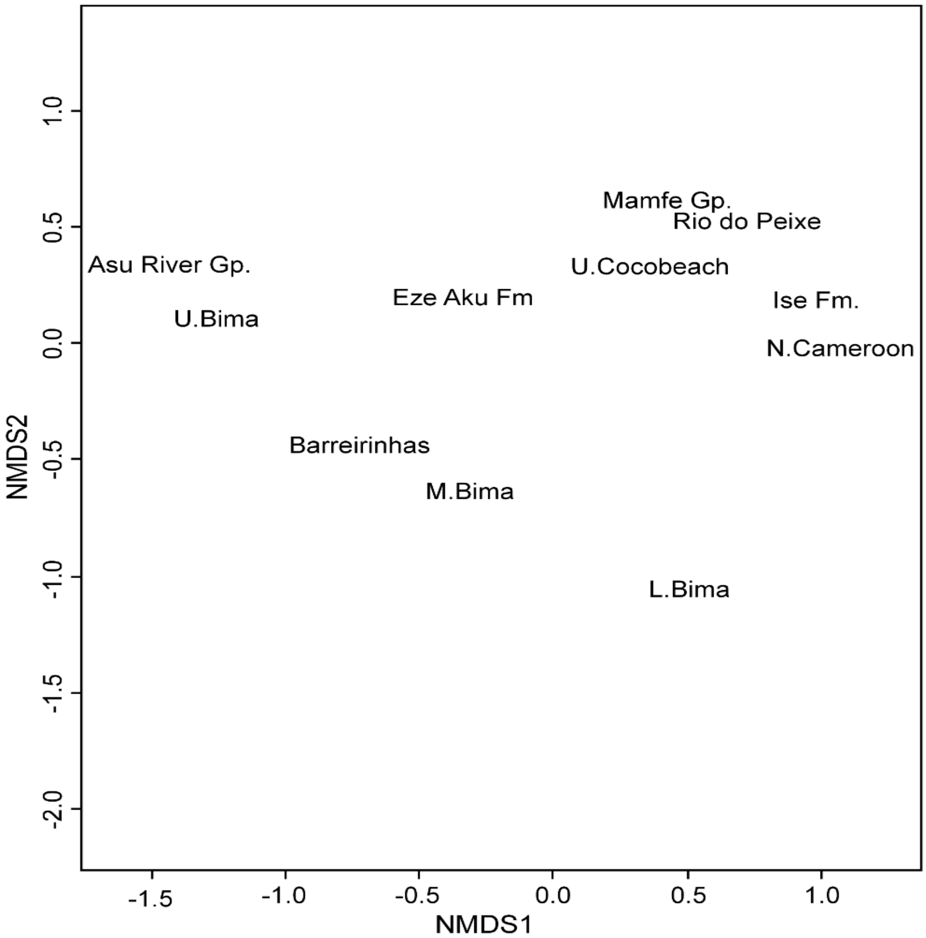

Figure 4.12. Non-metric multidimensional scaling comparison of the microflora assemblage of the Mamfe Basin with microflora assemblages of age-equivalent stratigraphic units from some basins within WASA.

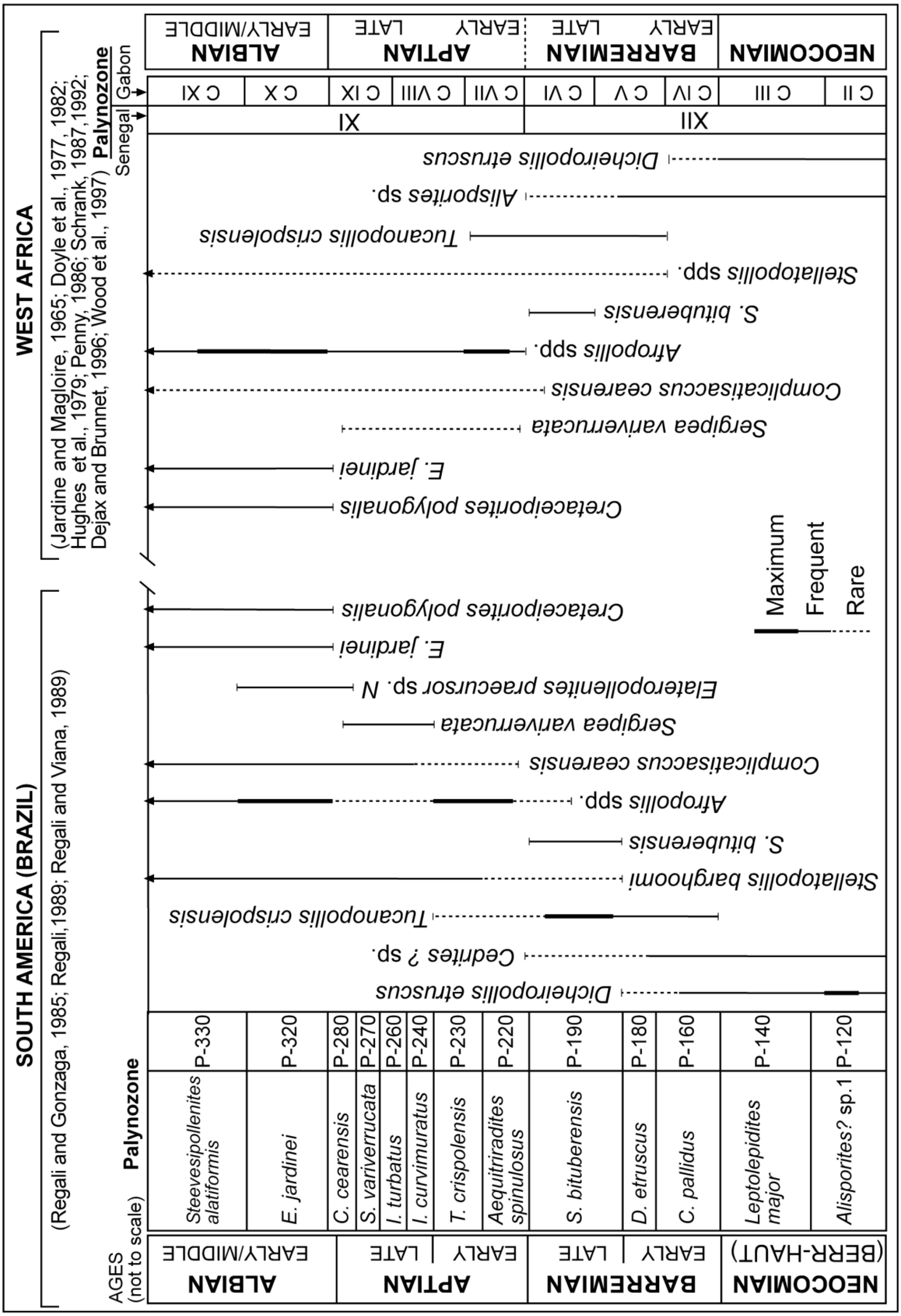

Figure 4.13. Correlation of Early Cretaceous palynostratigraphic age- markers in the West African-South American (WASA) Microflora Province (modified from Regali and Viana, 1989).

The Mamfe microflora is different from that of the Benue Trough because it is relatively older than the elater-bearing Asu River Group that belongs to the Albian-Cenomanian Elaterate Province of Herngreen et al. (1996). The Mamfe Group is older than the basal sediments in the adjoining Abakaliki Basin. Based on the palynological age of the sediments in the Mamfe Basin, a new lithostratigraphic correlation for the southern Benue is proposed in **figure 4.14** & **4.15**.

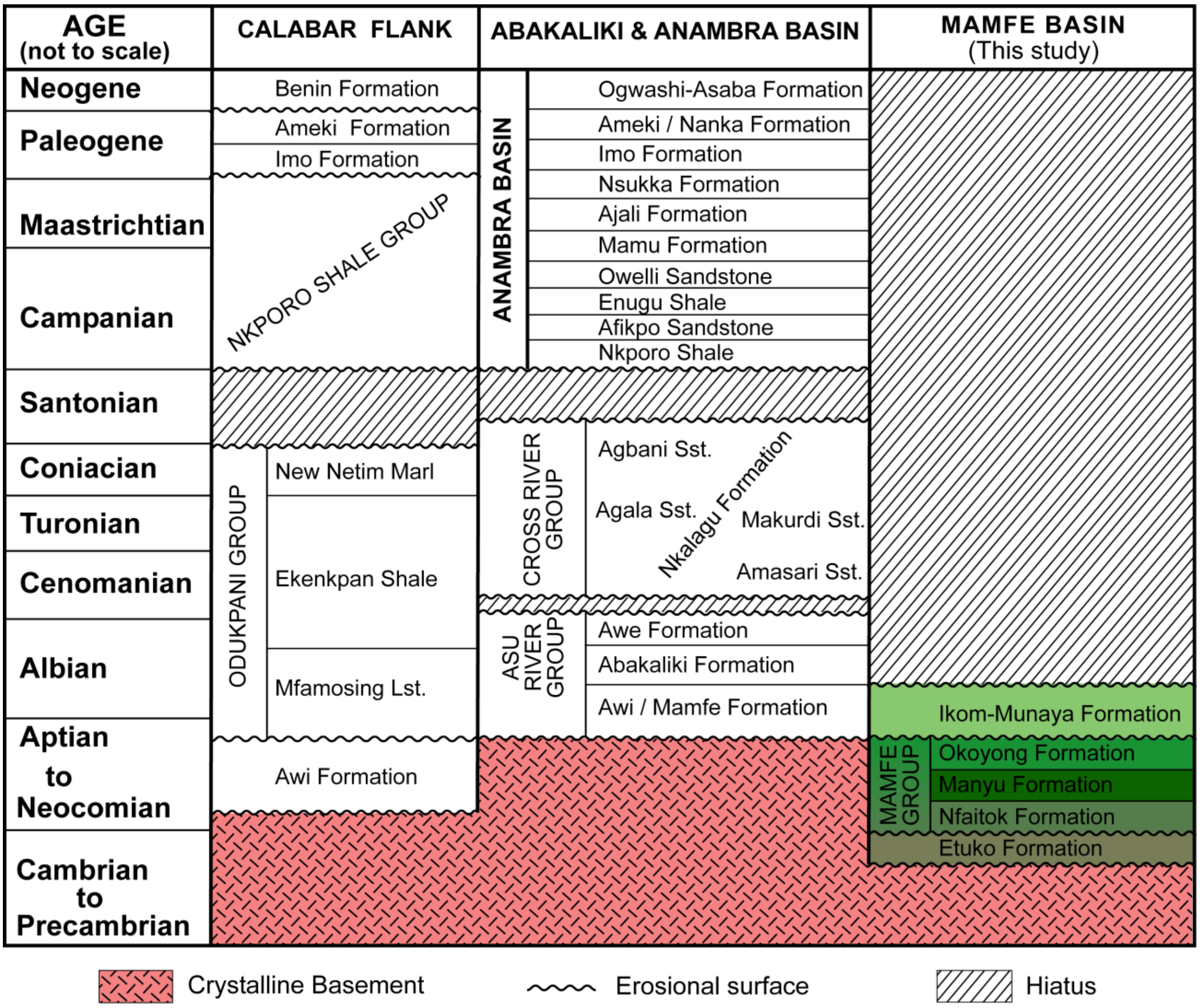

Figure 4.14. Revised lithostratigraphic correlation of the Calabar Flank, southern Benue Trough, and Mamfe Basin.

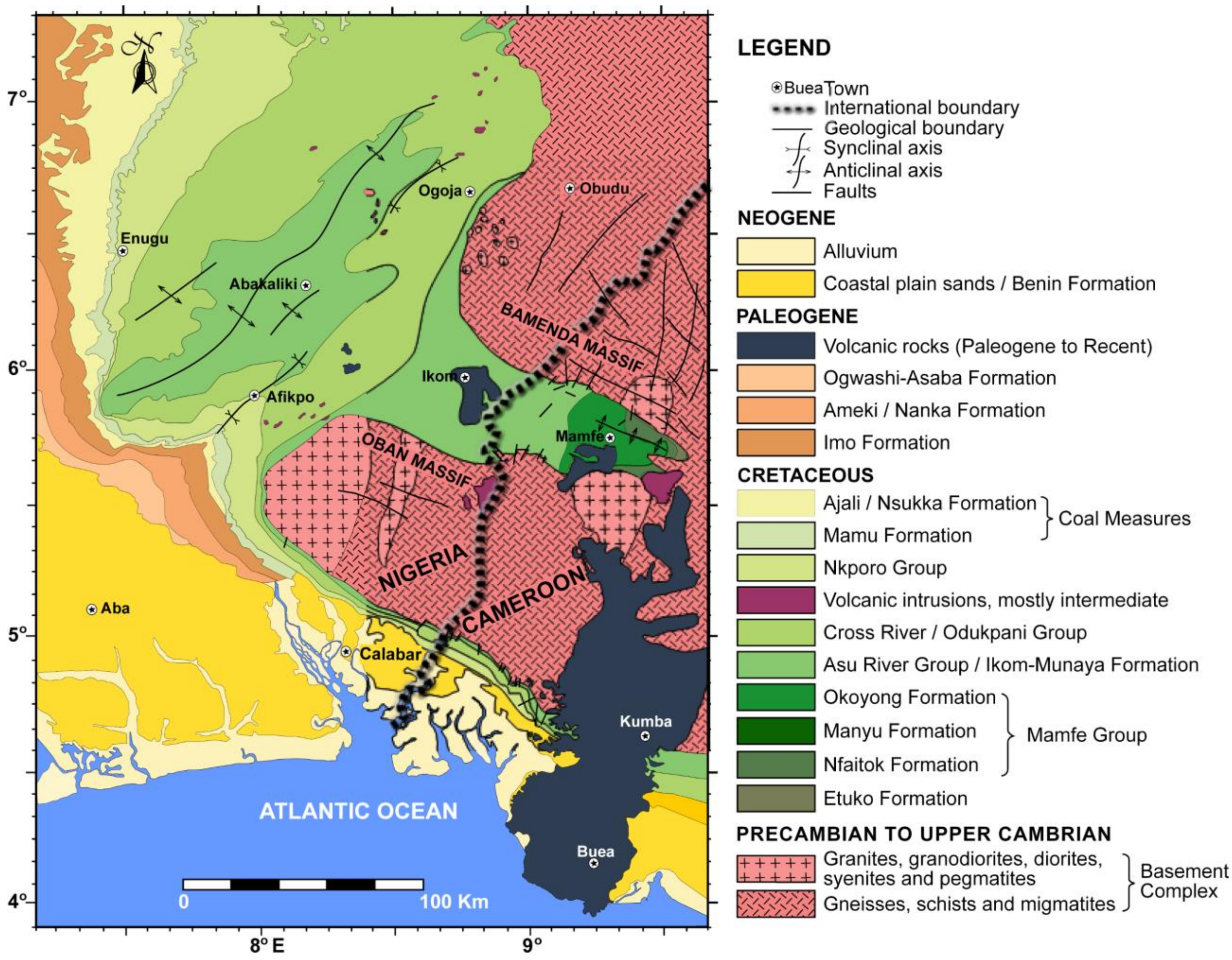

Figure 4.15. Revised geological map of part of southeastern Nigeria and southwestern Cameroon.

4.5 Conclusions

The microflora assemblage of the Mamfe Basin indicates that the sedimentary infill of the basin is older than the Albian-Turonian age that has until now been assigned to it. The microflora indicates a predominantly continental depositional setting for the sediments in the basin with a marine ingression that is poorly represented by rare foraminifera and evaporites.

The presence of *Afropollis* and absence of elater-bearing taxa in the microflora assemblage of the Mamfe Group indicates that the group belongs to the pre-Albian Lower Cretaceous *Dicheiropollis etruscus*/*Afropollis* Province while the elater-bearing Asu River Group belongs to the Albian-Cenomanian Elaterates Province of Herngreen et al. (1996). The Mamfe group is thus older than the basal sedimentary succession in the southern Benue Trough sub region.

The palynological age of the sedimentary succession of the Mamfe Basin together with its separation from the Benue Trough by the Ikom Ridge (Ajonina, 1997) supports suggestion by Benkhelil (1989) that the pre-Albian Benue Trough consisted of isolated sub basins. The Mamfe Basin is therefore not a rift-splay segment of the Benue Trough as previously envisaged (Ajonina, 1997; Bassey et al., 2013) but a forerunner of the Benue Trough.

5

PALEOGEOGRAPHY OF THE MAMFE BASIN

ABSTRACT

The outcropping sedimentary succession in the Cameroonian portion of the Mamfe Basin has been differentiated into pre-rift, syn-rift, and post-rift depositional sequences. Sedimentation was mostly continental in fluvio-deltaic and lacustrine environments.

The pre-rift (basal) depositional sequence unconformably overlies the Pan-African basement and consist of pre-middle Barremian debris flow alluvial fan deposits (Etuko Formation) that outcrop in the northeastern margin of the basin. This formation represents the oldest outcrop of Cretaceous sediments in the southern Benue Trough region. It was deposited in a narrow shallow lowland that was part of the Afro-Brazilian Depression.

The syn-rift (middle) depositional sequence is a middle Barremian-early Albian succession that is mapped as the Mamfe Group. Syn-rift deposition in the Mamfe basin occurred during the period of the Medio-African and NE-Brazil Great Lakes. Sedimentological, palynological, and geochemical data indicates an arid to semi-arid climate during the evolution of the syn-rift depositional sequence. A late Aptian-early Albian marine ingression into the basin is represented by vast halite dominated evaporites. The marine ingression into the Mamfe Basin was from the Douala Basin rather than the Benue Trough as previously reported. The evaporites deposits in the Mamfe Group implies that the South Atlantic salt province extended further north than the Douala Basin.

The post-rift (upper) depositional sequence (Ikom-Munaya Formation) is underlain by an angular rift-propagation unconformity that coincides with the opening of the Equatorial Atlantic and Benue Trough in the early-middle Albian. This sedimentary succession is the topmost and youngest Cretaceous strata in the Mamfe Basin and is coeval with pre-rift/basal syn-rift Asu River Group sediments in the southern Benue Trough.

Microflora, lithofacies, palynofacies, and clay mineral composition of sediments of the middle and upper depositional sequences indicate a progressive shift from a dry arid to semi-arid climate in the Nfaitok and Manyu Formations towards a more humid and wet climate in the Okoyong and Ikom-Munaya Formations. The age of the sediments in the Mamfe Basin suggests that the basin is not a rift-splay segment of the Benue Trough as earlier reported. The westward younging of sediments in the basin is due to uplift and erosion of between 1.2 and 4 km thick sediments from the eastern part and not the westward migration of depocenter previously reported. The basin was much larger in the Early Cretaceous than its present limits. The Mamfe Basin is a forerunner of the Benue Trough and its sedimentary evolution is closely related to the opening of the South Atlantic Ocean.

5.1 Introduction

The Mamfe Basin is located at the northeastern-most part of the Gulf of Guinea, 200 km from the continental margin of the Atlantic coast of eastern Gulf of Guinea, and about 150 km from the centre of the early Cretaceous triple-junction that met at the present-day Niger Delta.

How and when this basin was formed is still largely speculative due to inadequate geophysical data and lack of subsurface samples. Dumort (1968) was of the opinion that the Mamfe Basin was formed in the Albian as a result of basement rifting associated with the reactivation of an east-west mylonite zone. Whiteman (1982) envisaged the tectonic evolution of the Mamfe Basin to be intimately related to that of the Benue Trough with which it is physically linked. The similarity in the mode of tectonic evolution between the Mamfe Basin and Benue Trough was inferred from the presence in both basins of fold axis that are parallel to their respective basin axis.

Ajonina (1997) was of the view that the steady eastward decrease in the width of the Mamfe Basin implied that rifting tension and the degree of rifting attained in the basin decreased from west to east, suggesting that rifting originated from the western end of the basin. He thus inferred that the basin is a rift-splay segment of the Benue Trough.

It is believed that rifting was accompanied by rapid tectonic subsidence in response to the thermal recovery of the lithosphere following the thermal disturbance that led to the stretching and thinning of the crust beneath both basins. Petters et al. (1987) reported a stretching of about 19 km perpendicular to the axis of the Mamfe Basin. The total amount of subsidence attained in the Mamfe Basin is calculated to be 7.4 km, with an average total tectonic subsidence of 4.6 km (Heine, 2007, pers comm). Rifting in the Mamfe Basin was envisaged to have been aborted in the Upper Albian-Lower Cenomanian due to the subcrustal contraction and compression that led to the westward displacement of its depositional axis (e.g. Olade, 1975; Ajonina, 1997; Ajonina et al., 2001).

Although very little is known about the nature of tectonic processes and geological structures that controlled rifting and sedimentation in this basin, field and preliminary gravimetric and magnetometric surveys indicate that the basin is a half graben with a segmented NW-SE trending border fault on its northern margin (e.g. Petters et al. 1987; Ajonina, 1997; Hell et al., 2000; Ndougsa-Mbarga et al., 2007; Oden et al., 2012, 2015). The sedimentary infill of the Mamfe Basin has a maximum thickness of over 4500 m (Petters et al. 1987; Fairhead et al. 1991; Hell et al., 2000; Heine, 2007), and suggests that this basin was a major depocenter in the eastern Gulf of Guinea during the Early Cretaceous. The nearness of this basin to the meeting point of the three arms of the South Atlantic triple-junction make its tectono-sedimentary evolution susceptible to effects of tectonic and sea-level changes in either or all the arms of the triple-junction as well as the sub-regional climate.

Microflora assemblage reflects the ecology and climate of the area at the time of deposition (Brenner, 1976; Herngreen and Chlonova, 1981, Srivastava, 1994; Herngreen et al., 1996; Abbink et al., 2004). Trends in the distribution of palynomorphs are interpreted to reflect environmental-driven changes of the predominant vegetation (Abbink et al., 2004; Heimhofer and Hochuli, 2010). Data on stratigraphic distribution and relative abundance of palynomorphs makes it possible to recognise changes in climate and paleoenvironments (e.g. Batten, 2007; Heimhofer et al., 2012).

The climate of an area is determined by its latitude. The composition and distribution of flora in the Cretaceous was highly influenced by latitude leading to provinicialization. The effect of latitude on the distribution of flora in the Cretaceous led to pronounced provinicialization (Brenner, 1976; Herngreen and Chlonova, 1981, Srivastava, 1994; Herngreen et al., 1996). It is inferred from microflora assemblage that the Mamfe Basin was located on paleolatitude 11^{o} S which was within the geographical boundaries of the area assigned to Northern Gondwana palynofloral province (**Fig. 4.10**). Use of microflora assemblage for paleoclimatic interpretation of equatorial regions is made with reservation because of effects of provinicialization and also because the botanical affinities of the main microflora elements are not known. The Sporomorph EcoGroup (SEG) model of Abbink et al., (2001, 2004) is used in this study to infer paleoclimate and paleogeographic conditions from quantitatively important palynomorphs in the microflora assemblage. Supplementary evidence of paleoclimate is also inferred from sedimentological and mineralogical proxies.

The results from sedimentological, geochemical and palynological analyses are integrated into a paleogeographic model that relate the effects of climate on sedimentation pattern in the Mamfe Basin. The resulting conceptual model is compared to Early Cretaceous paleoclimatic and paleogeographic models for the of the eastern Gulf of Guinea region (e.g. Popoff, 1988; Benkhelil, 1989; Ojoh, 1990;

Petters; 1991; Matos; 1992; Da Rosa and Garcia, 2000; Garcia et al., 2005; Guiraud et al., 2005, Séranne and Anka, 2005).

The data presented in this study justify the revision of existing models on tectono-sedimentary evolution of the Mamfe Basin (e.g. Ajonina, 1997; Ajonina et al., 2001; Bassey et al., 2013). These models relied on the correlation of the lithic infill of the Mamfe Basin with the Asu River Group and subsidence data from the adjoining Abakaliki Basin. This study has shown that these paleogeographic reconstructions linking the Mamfe Basin and southern Benue might only be reliable for the middle Albian-Cenomanian post-rift succession (Ikom-Munaya Formation) in the central and western part of the Mamfe Basin.

5.2 Paleoecology and paleoclimate

The palynological assemblage from the Mamfe Basin indicates deposition in a continental setting. The composition of the palynoflora place the basin within the Northern Gondwana Province of Brenner (1976) which occupy the same geographic area as the West African-South American (WASA) Microflora Province of Herngreen and Chlonova (1981).

The microflora is a mixture of pollen and spores taxa that suggest derivation from plants that colonized both dry and wet habitats. The assemblage is characterized by predominance of *Classopollis* pollen together with low to moderate numbers of *Araucariacites* and fern spores, low ephedroid pollen, and rare angiosperm pollen (**Fig. 5.1**). The assemblage has typical features of the late Early Cretaceous low-latitude assemblages (Brenner, 1976; Doyle et al., 1982; Herngreen et al., 1996; Herngreen, 1998; Heimhofer and Hochuli, 2010).

This study reveals an increase in palynomorph abundance and diversity from the Nfaitok Formation to the Okoyong Formation. The assemblage in the Nfaitok, Manyu and Okoyong formations are dominated by conifers (*Classopollis, Araucariacites*, *Callialasporites*) with subordinate pteridophytes, bryophytes, angiosperms, algae, and lycopods. This suggests that conifers were the most prevalent vegetation in the area bordering the Mamfe Basin.

From the abundance trend it seems reasonable to infer that the paleoecology of the Mamfe Basin during the middle Barremian-early Albian comprised of a coastal community that was dominated by a cheirolepidacean woodland of conifers (*Classopollis*) with a shrub-type plant cover of gnetalean association (*Ephedripites* and *Equisetosporites,* Gnetaceaepollenites, and Steevesipollenites) thriving under a relatively warm and dry climate (e.g. Schrank & Mahmoud, 1998; Abbink et al., 2001, 2004; Heimhofer and Hochuli, 2010).

Conifers of the family Cheirolepidaceae are considered thermophilous and drought-resistant and have thrived in a wide range of habitats, ranging from well-drained upland to coastal lowlands to even saline habitats (Doyle et al., 1982).

In the woodland and forested areas, pteridophytes (ferns) such as *Cicatricosisporites*, *Cyathidites*, *Verrumonoletes*, *Retipollenites*, *Biretisporites, Gleicheniidites,* and angiosperm (e.g. *Afropollis*) probably thrived as undergrowth around riversides on lowland (e.g. Doyle et al., 1982; Abbink et al., 2004; Heimhofer and Hochuli, 2010). The Zygnematacean algae represented by *Ovoidites* and *Chomotriletes* formed a hydrophile community in freshwater marshes. Araucarian forests sometimes with different types of Pteridosperm (e.g. *Alisporites*) dominated at higher elevation in the upland bordering the basin (**Fig. 5.2**).

The observed trend in the distribution of gymnosperm pollen and pteridophyte spores are best explained as a response of vegetation to changes in regional climatic conditions, especially to moisture availability (e.g. Abbink et al., 2004).

Classopollis was produced by the extinct conifer family Cheirolepidaceae (Doyle *et al*., 1982) and dominated in regions with arid climates. *Classopollis* is most commonly recorded in nearshore marine-lagoonal environments and often associated with evaporites. *Classopollis* is known to be a good indicator of warm dry to semi-arid paleoclimate (Abbink et al., 2004). Batten (1975) correlated maximal abundance of *Classopollis* with increase in aridity. Within the Mamfe Group, the relative abundance of *Classopollis* decreases upward, whereas fern spores increase. These trends reflect the progressive increase of humid conditions. However, *Classopollis* is conspicuously more abundant than the spores, making up 50%. This indicates that despite the increase in humidity, the climate was semi-arid to arid.

The ephedroid group pollen grains are related to the modern gymnosperms *Ephedra* and *Welwitschia* (Gnetales), which are found in arid to semi-arid environments. Members of this group are less tolerant to saline conditions than *Classopollis* (Doyle et al., 1982), and were used to support the interpretation of a probable arid to semiarid climate in the rift valleys of the Early Cretaceous of Gabon

(Salard-Cheboldaeff and Boltenhagen, 1992).

Araucariacites according to Doyle *et al*. (1982) is related to a tropically-centred group that are found in lowland deposits of the Early Cretaceous age. These authors mentioned that an increase in aridity resulted in a decline of *Araucariacites* abundance. *Araucariacites* is characteristic of humid and subtropical to tropical climates, and in association with *Callialasporites* reflect a warm climate without large seasonal variations.

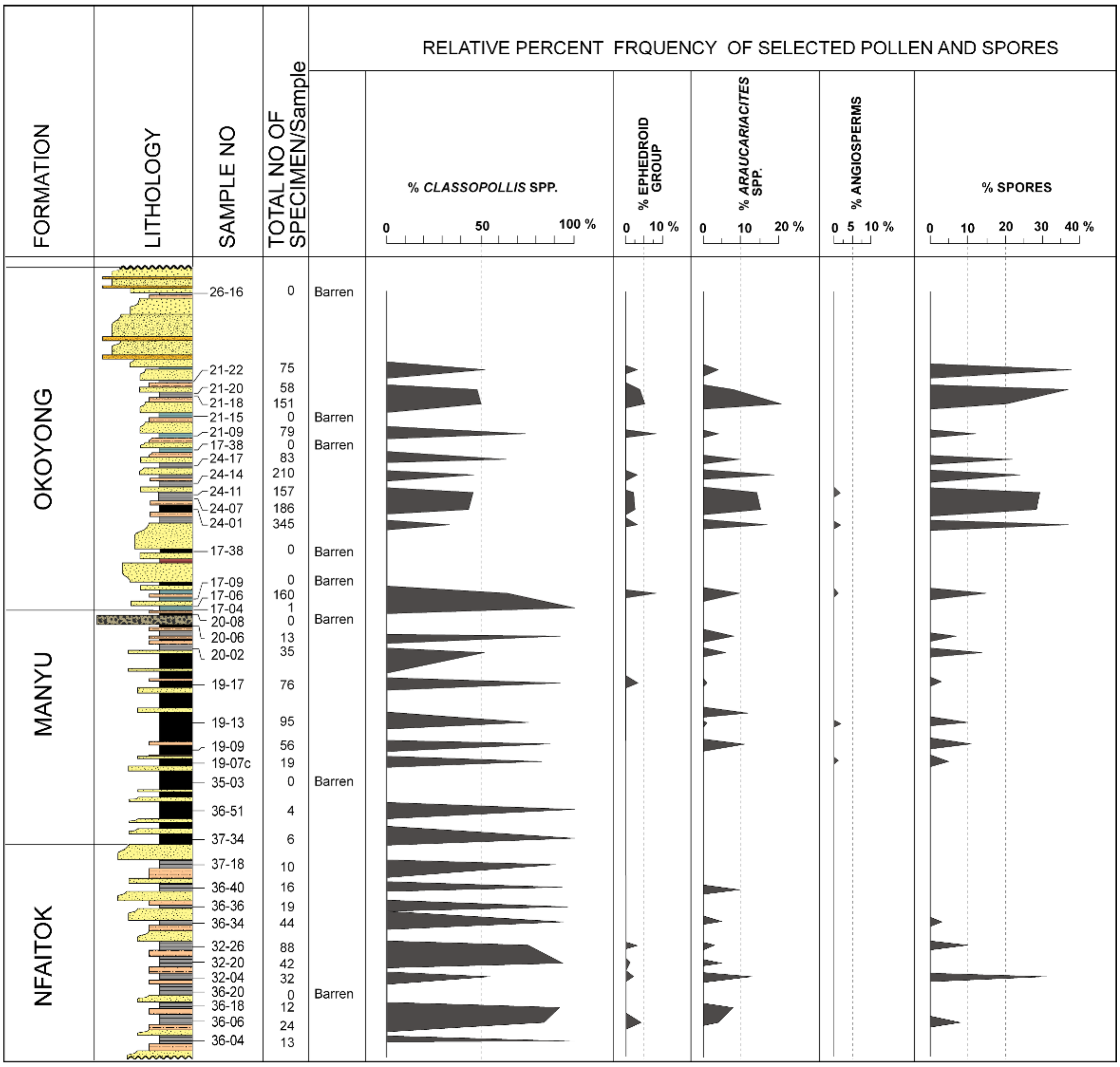

Figure 5.1. Quantitative distribution of major palynomorph groups across the Mamfe Group

Afropollis is the most abundant angiosperm pollen genus in the Mamfe Group succession although it is recorded only in small amounts. This genus has been interpreted as typical of arid environments (e.g. Doyle et al. 1982).

Spores that are indicative of warmer and drier lowland habitat in the microflora assemblage include *Clavatipollenites*, *Concavisporites*, *Concavissimissporites*, *Contignisporites*, *Cycadopites*, *Cyathidites*, *Gleicheniidites*, *Punctatisporites*, *Todisporites*. Wetter and warmer lowland habitat is represented by *Cicatricosisporites*, and *Baculatisporites*. The predominance of conifers over pteridophytes and bryophytes in the microfloral assemblage suggests a warm dry but locally humid climate.

The abundance and diversity trend observed in the palynologic data suggests that the sediments of the Nfaitok and Manyu Formations were deposited in at least a seasonally dry or semi-arid climate (e.g. Batten, 1975). Sedimentological evidence for this interpretation include frequent desiccation marks seen in the shale and siltstone units, predominance of fine grained siliciclastics, the presence of evaporites, dolomitic marlstones and the thick paleosol at the lower part of the Okoyong Formation in Baku. The mudstone unit overlying this paleosol contains abundant and diversified drought-resistant ephedroid group pollen.

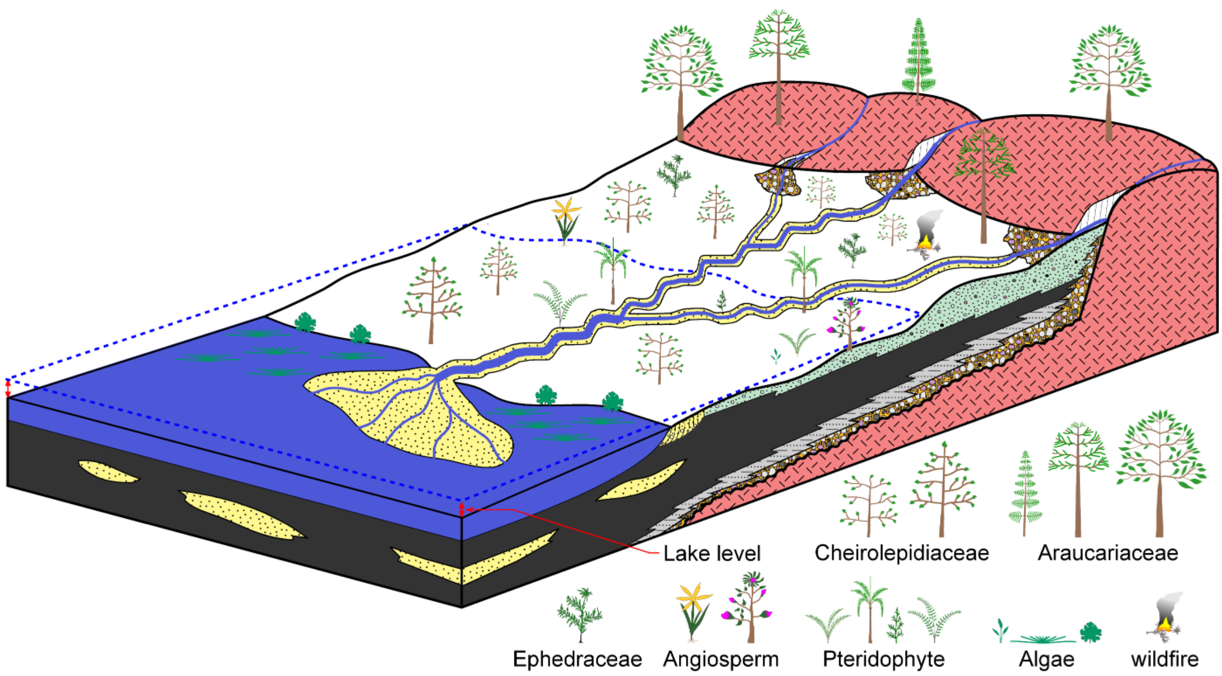

Figure 5.2. Hypothetical reconstruction of the paleoflora assemblage based on palynomorphs recorded in the Mamfe Group.

The upwards increase in species diversity and decrease in the abundance of *Classopollis* (**Fig. 5.1**) represents a shift from a warm and dry climate towards a regionally warm and humid climate. This shift towards a humid climate that was favourable to terrestrial vegetation is reflected by the increase in the abundance of *Araucariacites* and increase in the diversity of pteridophyte genera at the expense of *Classopollis.* High abundance and diversity of ferns, which require moisture for reproduction is considered as a good indicator of humid conditions (Herngreen et al., 1996; Abbink et al., 2004).

The increase in abundance and diversity in the palynomorph assemblage of the Okoyong Formation suggests the prevalence of favourable climatic conditions for terrestrial vegetation. A mark decrease in the abundance of Classopollis in the Okoyong Formation is accompanied by an increase in the abundance and diversity in pteridophyte spores, angiosperm pollen and Araucariacites. This points to a shift in the climate to more humid conditions. The presence of charcoal fragments and increase in the diversity of the palynoflora within the Okoyong Formation support regionally warm and humid conditions rather than local environmental conditions (e.g. Salard-Cheboldaeff and Dejax, 1991; Dejax and Brunet, 1996). High abundances of pteridophytes are characteristic of relatively moist and lush vegetation occurring, for example, along riversides and/or in costal lowlands (Heimhofer et al., 2012).

The climatic trend towards a humid climate in the Okoyong Formation is also supported by a marked increase in coarse grain clastic sediments that signify substantial and energetic water transport and hence high precipitation rates. Kaolinite is abundant in the clay mineral assemblage. Formation of kaolinite is believed to be associated with intense chemical weathering under humid tropical to subtropical conditions (Chamley, 1989; Dinis and Soares, 2007).

Abundant charcoal (fusian) fragment with diameter > 10 µm in the Okoyong formation suggests nearby wildfire (e.g. Scott, 2010). Wildfire fusain are generated in seasonally drier regimes. The wildfires are usually triggered by lightning, but may also result from volcanic eruptions, boulder slides. Wildfires triggered by lightning strikes are favoured in strongly seasonal climates where vigorous plant growth is promoted by a distinct wet season, followed by a dry season creating a tinder that becomes fire-prone during thunder storms at the onset of the net wet season (Sellwood and Valdes, 2005). These thunder storms produce lightning but not always rain. It is inferred from this palynofloral assemblage and presence of charcoal fragments that the climate was locally humid and regionally warm to semi-arid.

The composition of the microflora assemblage recorded in this study is in agreement with Early Cretaceous palynoflora records from the eastern Gulf of Guinea and NE Brazil and other parts of the West African-South American Microflora Province (e.g. Jardiné and Magloire, 1965; Jardiné et al., 1974; Regali et al., 1974; Regali and Viana, 1989; Doyle et al. 1977, 1982; De Lima, 1983; Salard-Cheboldaeff 1990; Salard-Cheboldaeff and Dejax, 1991; Salard-Cheboldaeff and Boltenhagen, 1992; Dejax and Brunet, 1996; Jan du Chêne, 2000; Atta-Peters and Salami, 2006; Carvalho et al., 2006; Heimhofer and Hochuli, 2010).

5.3. Sedimentary evolution

The sedimentary evolution of the Mamfe Basin like most other rift basins of its type was influenced principally by the interplay between tectonics and climatic on depositional trends (sedimentation, e.g. Lambiase, 1990; Schlische, 1991; Meléndez et al., 2009). Tectonics affects accommodation (space available for sediments to fill) and source area relief, while climate influences source area vegetation cover, weathering, erosion, and discharge (e.g. Shanley and McCabe, 1994; Cross and Lessenger, 1998; Catuneanu et al., 2009; Martins-Neto and Catuneanu, 2010). Sediment supply is a by-product of both tectonism and climate (Catuneanu, 2006). Tectonic subsidence increases accommodation while tectonic uplift decreases accommodation, and rejuvenation of weathering and erosion processes in source areas. A wetter climate increases the efficiency of weathering and erosion, and enhances the competence and capacity of transport agent. Accommodation in rift basins is generated mainly by tectonic subsidence (Martins-Neto and Catuneanu, 2010).

The basal pre-rift sediments in the basin (Etuko Formation) are the oldest outcrop of Cretaceous sediments in the southern Benue Trough region. It is inferred to have been deposited in a narrow shallow lowland that was part of the Afro-Brazilian Depression (Garcia et al., 2005). Deposition of this alluvial succession was under humid climatic conditions. The formation is inferred to be coeval with the lower Mundeck Formation in the Douala-Kribi/Campo Basin (Ntamak-Nida et al., 2008), Antenor Navarro Formation in the Rio do Peixe Basin in SE Brazil (Da Rosa and Garcia, 2000).

The syn-rift succession (Mamfe Group) evolved during the period of the Medio-African-NE Brazil Great lakes (Popoff, 1988). The depositional trend of this syn-rift succession was influenced by lake level that was susceptible to tectonic subsidence during a predominantly semi-arid to arid climatic conditions.

The fluvio-lacustrine Nfaitok Formation represents deposition in a shallow lake that evolved from overfilled through balanced filled to underfilled lake (Bohacs et al., 2000, Meléndez et al., 2009; Bohacs et al., 2013). Deposition was mostly by an axial trunk river with extensive floodplain on the hanging-wall of the half graben (**Fig. 5.3**). The predominance of fine-grained siliciclastics suggests low competence and low capacity river and is consistent with the semi-arid to arid climate that prevailed in the region at the time. Strata onlap in this initial syn-rift deposits resulted from the growth of the basin with time.

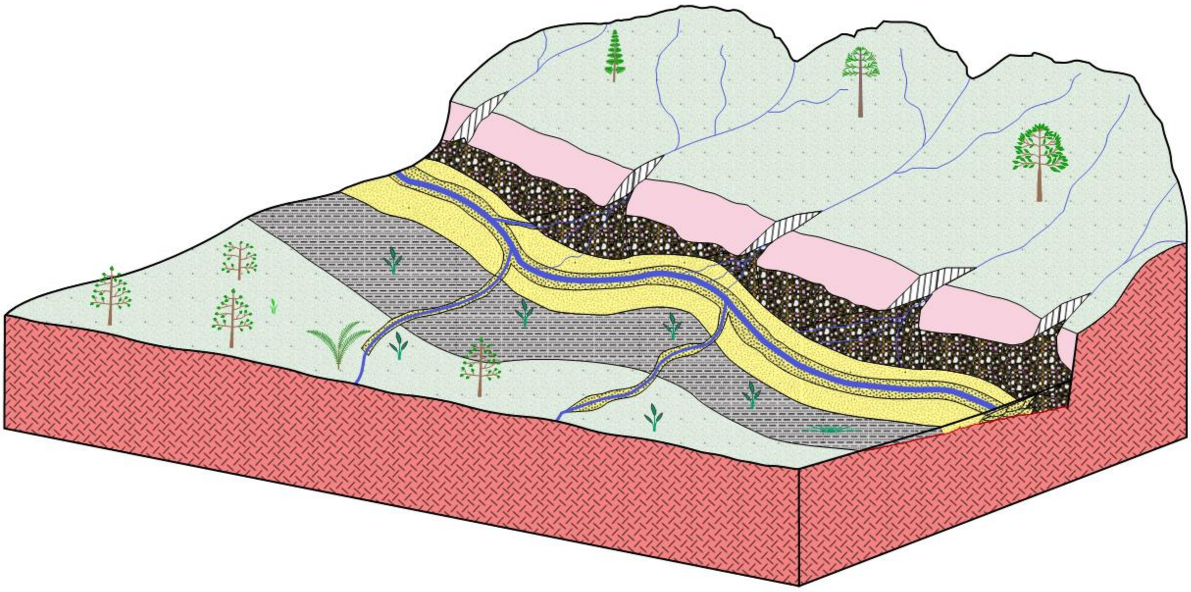

Figure 5.3. Paleogeography the Mamfe Basin during the deposition of the Etuko and Nfaitok Formation.

The Manyu Formation is a predominantly retrogradational fining-upward succession that represents deposits of a lacustrine system that evolved from deep-water balanced filled to mostly underfilled lake in the lower part of the formation, passing upward to shallow-water balanced filled lake in the upper part. Sedimentation was principally influenced by tectonic subsidence along the basin margin boundary fault and the formation of a basement horst (Ikom Ridge) at the western part of the basin (**Fig. 5.4**).

Rapid increase in subsidence rate during rifting resulted in the deepening of the lake (increase in accommodation) and decrease in sedimentation rates due to a progressively larger depositional surface area over which the sediments were spread (**Fig. 5.4**). Base level change during this time of the basin evolution was controlled principally by tectonic subsidence. Cyclic sedimentation shown by the facies association of this formation resulted from alternating periods of active subsidence separated by periods of relative quiescent. During periods of active subsidence, the base level rose steadily and led to a landward shift in facies. During the quiescent periods, base level initially became stable, then fell progressively leading to initial aggradation of facies at river mouth, before a basin ward shift (progradation) occurred. This led to the deposition of siltstone and sandstone as turbidites within distal deep-water facies (darky-grey to back shale and marlstone).

The occurrence of TOC-rich black shale containing abundant pyrite and siderite in the basin is indicative of the prevalence of anoxic conditions in the bottom water of the basin. It is inferred from the barren nature of the shale and brine seepages from within the Aptian sediments that salinity stratification was the most probable cause of bottom water anoxia. Basement topography might also have played a rule in restricting bottom water circulation (e.g. Evaporite beds are also inferred from numerous brine seepages to occur in the basin (e.g. Eseme et al., 2002; 2006b).

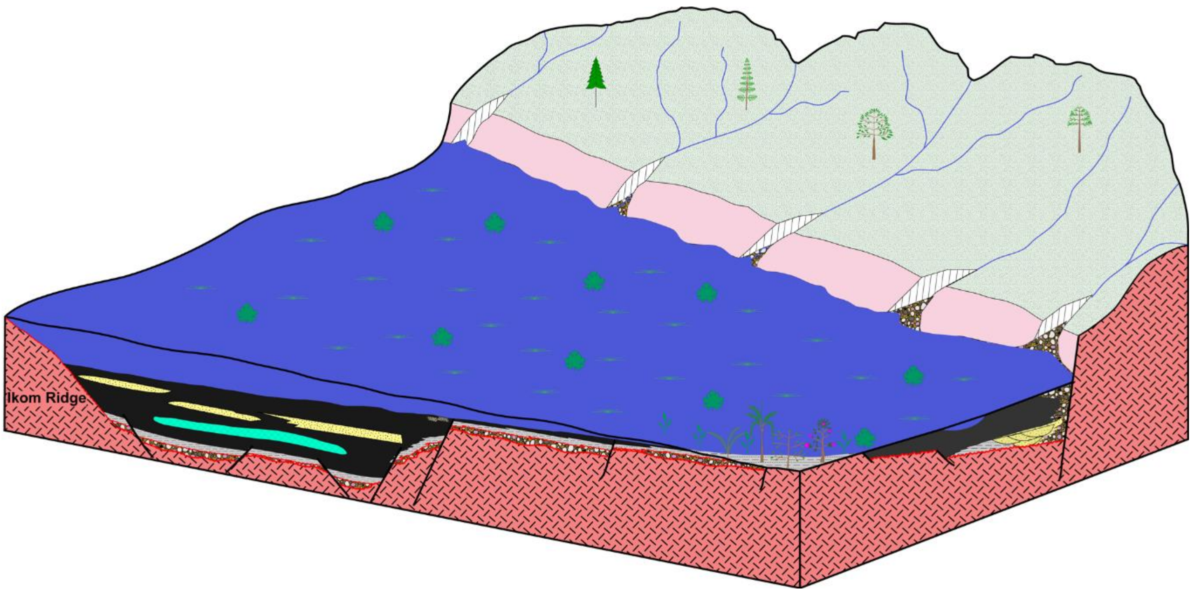

Figure 5.4. Paleogeography the Mamfe Basin during the deposition of the Manyu Formation.

Also, the facies association of dark grey to black shale/marlstone, siltstone and fine grained sandstone suggest deposition in deep water setting far away from river mouths, or clastic input starvation associated with periods of low annual precipitation. Gradation from dark grey to black shale/marlstone to siltstone is suggestive of gradual fall in base level in the upper part of the formation. The thickness of individual beds within the dark grey to black shale/marlstone siltstone and sandstone succession suggests that base level fluctuations were frequent and probably seasonally induced. Climate is thus believed to have been the main cause of cyclic sedimentation in the Manyu Formation.

A steady increase in the rate of sediment supply led to a gradual fall in the rate of deepening. Maximum depth was attained when sediment supply equalled the rate of subsidence. Thereafter, the basin began to gradually fill up as the rate of sediment supply exceeded the rate of accommodation towards the top of the Manyu Formation.

A turn-around from increasing to decreasing subsidence (accommodation) coupled with an increase in sedimentation rates led to the gradual infilling of the basin and change in environment of deposition from balanced filled lacustrine setting in the upper part of the Manyu Formation to overfilled fluvio-deltaic deposition of Okoyong Formation in late Aptian-early Albian (**Fig. 5.5**).

The increase in the rate of sediment supply during the deposition of the coarsening-upward fan-delta deposits of the Okoyong Formation is attributed to a better developed drainage system that resulted from more humid and wetter climatic conditions at the sediment source upstream. It is inferred from sedimentological and palynological data that tectonic processes were the major factor that controlled the sedimentary evolution of the basin from inception to probably late Aptian.

The upward decrease in the frequency of cyclicity and increase in the sizes of clasts exhibit in the Mamfe and Okoyong sections suggests a progressively shallower water conditions resulting from fall in base level due to gradual infilling (e.g. Shanley and McCabe, 1994; Martins-Neto and Catuneanu, 2010). These sediments are inferred to be the prograding complex associated with the gradual infilling of the basin as a result of waning subsidence and increase in sediment supply leading to an overall fall in base level (e.g. Cross and Lessenger, 1998). Sandstones were deposited as a prograding complex during periods of high annual precipitation and high clastic input while the shale intercalation were deposited during periods of low annual precipitation and low clastic input. The predominance of sandstone over shale suggests that the rate of sediment supply far exceeded that for accommodation space creation resulting to progradation (e.g. Catuneanu, 2006; Catuneanu et al., 2009), or that climatic changes had an overriding control over base level change.

Syn-rift sedimentation in the Mamfe Basin was terminated by folding in the late Aptian-Albian that is probably related to the opening of the Equatorial Atlantic Ocean.

This tectonic event has been reported in other WCARS basins and is regarded as a regional unconformity (Guiraud and Maurin, 1992; Genik, 1993; Guiraud et al., 2005).

Post-rift sedimentation is represented by fluviatile Ikom-Munaya Formation. This stratigraphic unit is the topmost sediments in the Mamfe Basin and are the basal sediments in the adjoining southern Benue Trough. They are separated from the underlying syn-rift deposits by an angular unconformity.

Vitrinite reflectance, thermal alteration index, biomarkers, and illite crystallinity yielded similar burial metamorphism (thermal maturity) data that suggest that the outcropping sediments in the eastern Mamfe Basin have been buried to depths of between 1.2 and 4 km. The westward younging of sediments in the basin is due to uplift and erosion of between 1.2 and 4 km thick sediments in the eastern part and not the previously reported westward migration of depocenter (Ajonina et al., 2001, 2007).

Lack of proximal facies that are supposed to be associated with the medial alluvial fan deposits of the Okoyong Formation suggests that the areal extend of this Mamfe Basin was much larger in the Early Cretaceous than its present limits. The eastward decrease in the width of the basin to less than 10 km at the eastern end is attributed to this uplift and erosion and erosion at the southeastern part of the hanging-wall block and not due to differential rifting as earlier reported (Ajonina, 1997; Ajonina et al., 2001). The timing of uplift is not certain, but might be attributed to either the Albian-Cenomanian or Santonian tectonic events that has been reported from the Benue Trough (Olade, 1975; Benkhelil, 1989; Guiraud et al., 1992).

It is doubtful if sediments younger than Albian were deposited in the Mamfe Basin as reported (e.g. Reyment, 1965; Ajonina, 1997; Ajonina et al., 2001; Abolo, 2008).

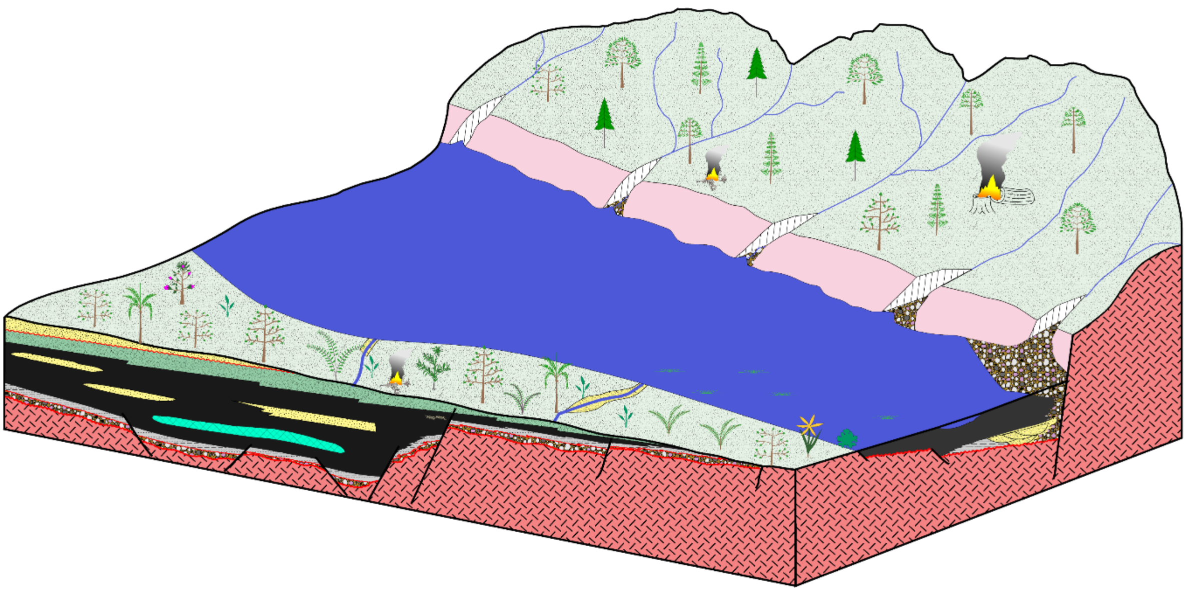

Figure 5.5. Paleogeography the Mamfe Basin during the deposition of the Okoyong Formation on the hangingwall of the basin.

5.4. Discussion

Of the 20 samples that were that were analysed for calcareous microfossils in this study, 19 lacked calcareous microfossils and one sample (24-01) contained single specimens of the foraminifera *Praebulimina* sp. and *Hedbergella* sp. (**Fig. 5.6**).

The presences of *Praebulimina* sp., *Hedbergella* sp. dolomitized marlstone, and halite dominated evaporites (e.g. Eseme et al., 2006) support a marine ingression into the Mamfe Basin. Reyment (1954; 1965) and Petters (1991) proposed that the marine incursion into this basin occurred during the Cenomanian-Turonian transgression and highstand in the southern Benue Trough. Le Fur (1965) however, was of the view that the Cenomanian-Turonian marine incursion into the Mamfe Basin was from Douala Basin to the southeast of Mamfe Basin.

The oldest record of planktonic foraminifera in West Africa is in the Albian and represented by *Hedbergella* sp. (Petters, 1978a, b; Kogbe and Me'hes, 1986; Nguene et al., 1992). *Praebulimina* sp. and *Hedbergella* sp. were reported by Petters (1978a, b) to be the first foraminifers to colonize new seaways. Earliest record of *Praebulimina* sp. and *Hedbergella* sp. in the West African eastern Gulf of Guinea is from late Aptian-Albian marine deposits in Gabon and the Kribi- Campo Basin in Cameroon (Kogbe and Me'hes, 1986; Nguene et al., 1992).

This foraminifera assemblage has also been recorded in late Aptian-early Albian succession in the Oriental Basin of Ecuador (Villagomez et al., 1996). Within the

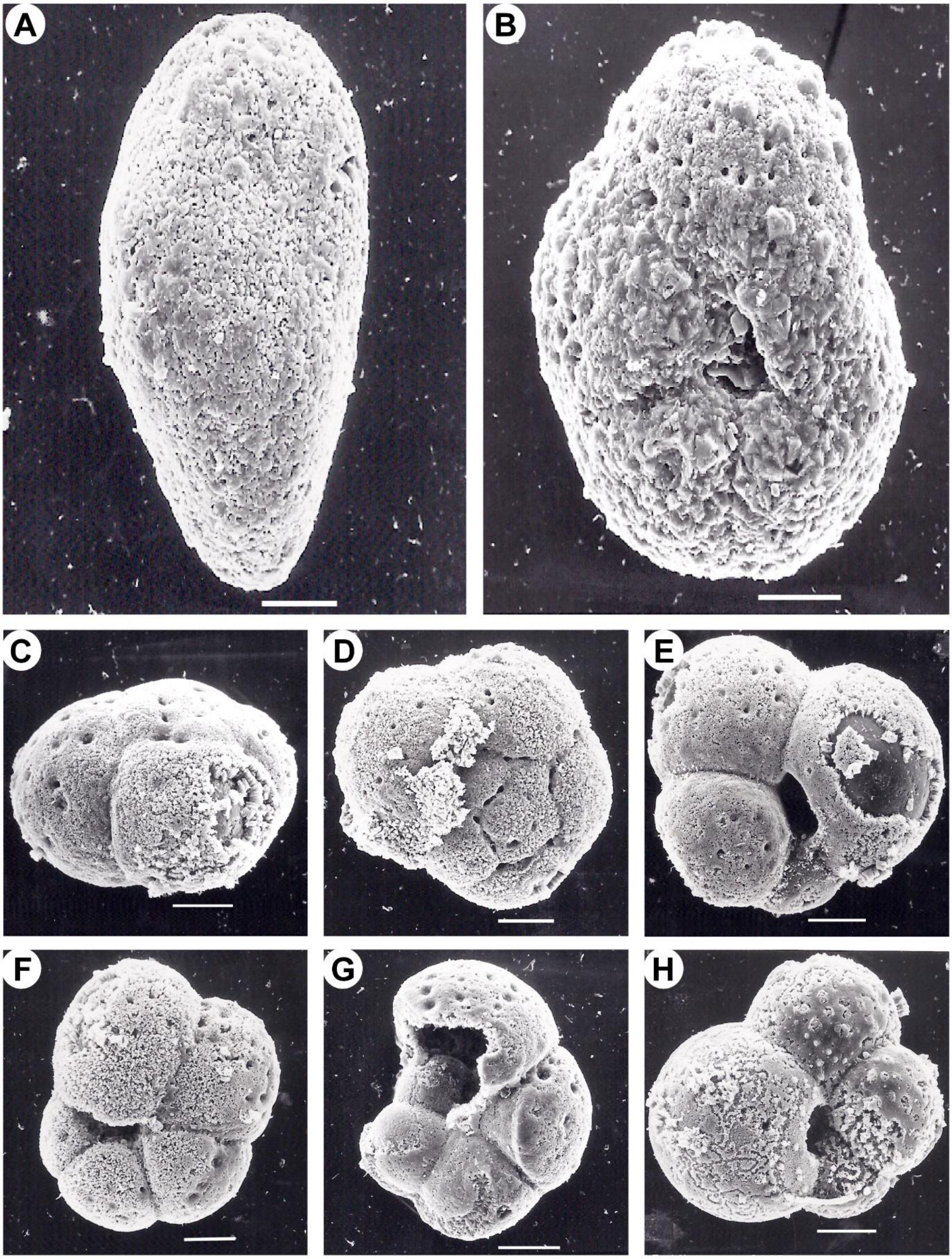

Figure 5.6. Foraminifera from Okoyong Formation (sample 24-01). Scale bar is 20 µm. (**A & B**) Praebulimina sp.; (**C-H**). Hedbergella sp. **C** = side view, **D** = spiral view, **E** = umbilica view.

Kribi/Campo Basin, these primitive planktonic foraminifera characterize paleo-water depths not exceeding 200 m (Nguene et al., 1992).

Palynological analysis of the sample that yielded foraminifera did not record any dinoflagellates. Rather, the sample contained *ovoidites* sp. that is characteristic freshwater marshes. The foraminifera could thus be reworked material, although there is no physical evidence of reworking. Kuhnt (2002, pers. Comm.) was of the opinion that these foraminifera are primitive juvenile forms that were probably washed into the Mamfe Basin during a marine transgression. The prasinophycean algae *Leiosphaeridia* sp. observed in three samples from Mamfe mile 1, Baku, and Okoyong are also indicative of a marine ingression into the Mamfe Basin (e.g. Quattrocchio and Volkheimer, 1990; Volkheimer et al., 2007; Volkheimer, 2008, pers. comm.).

The fish *Proportheus Kameruni Jaekel* that was reported from the Mamfe Basin (Jaekel, 1909) is synonymous with ichthyodectiform fish *Cladocyclus Agassiz*, 1841 (Taverne, 1986). *C. Agassiz* has been reported from shallow marine sediments of Aptian-Albian age in Brazil (Bardack, 1965), Aptian in Gabon (Weiler, 1961; Taverne, 2010), and Cenomanian in Morocco (Forey and Cavin, 2007).

The palynological age and stratigraphy of the Mamfe Group precludes a middle Albian-Turonian transgression into the basin from either the Benue Trough (Reyment, 1965; Petters, 1991; Ajonina et al., 2007) or Kumba through Baru-Ayundip ria (Le Fur, 1965). The foraminifer-bearing sample and the overlying deltaic swamp facies in the Mamfe Basin lack elaterates that characterize the Albian-Cenomanian sedimentary successions in the West African-South American microfloral province (Herngreen and Chlonova, 1981; Herngreen et al., 1996; Herngreen, 1998). Elaterates however, are common in the shales of the Asu River Group (Doyle et al., 1982; Ojoh, 1990; Lawal, 1991). The shales of the Asu River Group (Abakaliki Formation) were deposited during the first marine transgression in the southern Benue Trough in the middle Albian (Petters, 1978; Petters and Ekweozor, 1982; Benkhelil, 1989; Ojoh, 1990). The Mamfe Group on the account of lack of elaterates and rare angiosperms is older than the Asu River Group. The marine deposits in the Mamfe Group thus predates the middle Albian marine transgression in the Benue Trough.

The marine ingression into the Mamfe Basin probably occurred during the middle Aptian-Albian global sea level rise (from KAp4 to KAp7 of Haq, 2014). Valença et al. (2003) reported that Aptian-Albian sea level rise created temporal seaway in the interior of Brazil between the Potiguar and Araripe Basins (**Fig. 5.7**). This eustatic sea level rise resulted to fauna exchange between the Equatorial and South Atlantic Ocean (e.g. Arai, 2000). The late Aptian-early Albian is represented in Cameroon by Aptian evaporites that are thus far not been recognised in Nigeria (Reyment, 1980; Reijers and Petters, 1987; Ojoh, 1990).

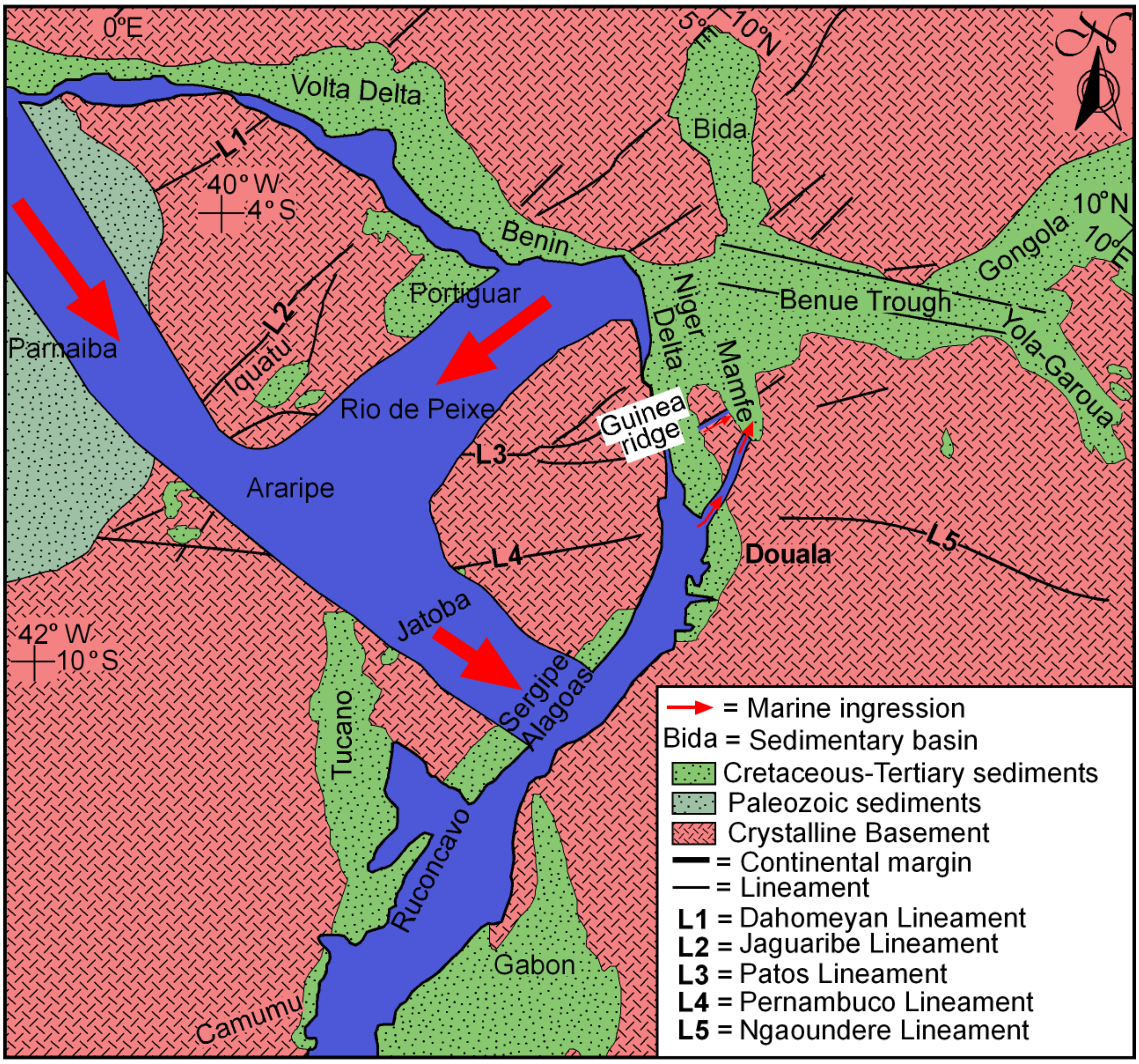

Figure 5.7. Late Aptian interior seas in NE Brazil (modified from Valença et al., 2003).

Vast halite dominated evaporites of marine origin are inferred to occur in the Mamfe Basin (Eseme et al., 2006b). The evaporites are inferred to be hosted in the Mamfe Group. There are over 25 brine springs and ponds in the Cameroonian sector of the Mamfe Basin.

Thirty-two to thirty-six thousand tons of artisinally mined salt was exported annually from this basin between 1942 and 1945 (Kah, 2006). Over 1200 tons of salt consisting dominantly of grade 1 halite are lost annually as brines seepages across the basin (Eseme et al., 2006b).

Absence of Lower Cretaceous evaporites in supposedly coeval sediments of the Asu River Group in the Calabar Flank and southern Benue Trough (Reijers and Petters 1987, 1997; Reijers, 1998; Akande et al., 1998; Uma, 1999) support Le Fur (1965) suggestion that a marine ingression into the Mamfe Basin was from Douala and not from the Benue Trough. The absence of Aptian evaporite deposits in the Calabar Flank and southern Benue Trough has been attributed to the Guinea Ridge that prevented the incursion of the South Atlantic Ocean from Douala (Reijers and Petters, 1987). The ingression into the Mamfe Basin according to palynological dating of the succession in this study is older than suggested by Le Fur (1965), and is inferred to have occurred in the late Aptian-early Albian. The Mamfe Basin evaporites are therefore inferred to be coeval with late Aptian halite dominated evaporites in both sides of the South and Equatorial Atlantic margin (Sergipe-Alagoas and Ceará Basins in NE Brazil, and North Gabon and Douala Basins in Africa). The Mamfe evaporites are thus considered in this study to be the northernmost part of the "Aptian salt basin series" of the South Atlantic salt province (**Fig. 5.8**).

This salt province extends from Walvis ridge in Angola to the edge of the Douala Basin in Cameroon (e.g. Reijers and Petters, 1987; Benkhelil et al., 2002; Davison et al., 2004; Davison, 2007; Karner and Gamboa, 2007; Ntamack et al., 2010; Chaboureau et al. 2012; Kissaaka et al., 2012). The Aptian evaporites were deposited in basins that were separated by basement highs. The evaporites are thought to be diachronous within and between basins and evolved from south to north (Davison et al., 2004; Davison, 2007).

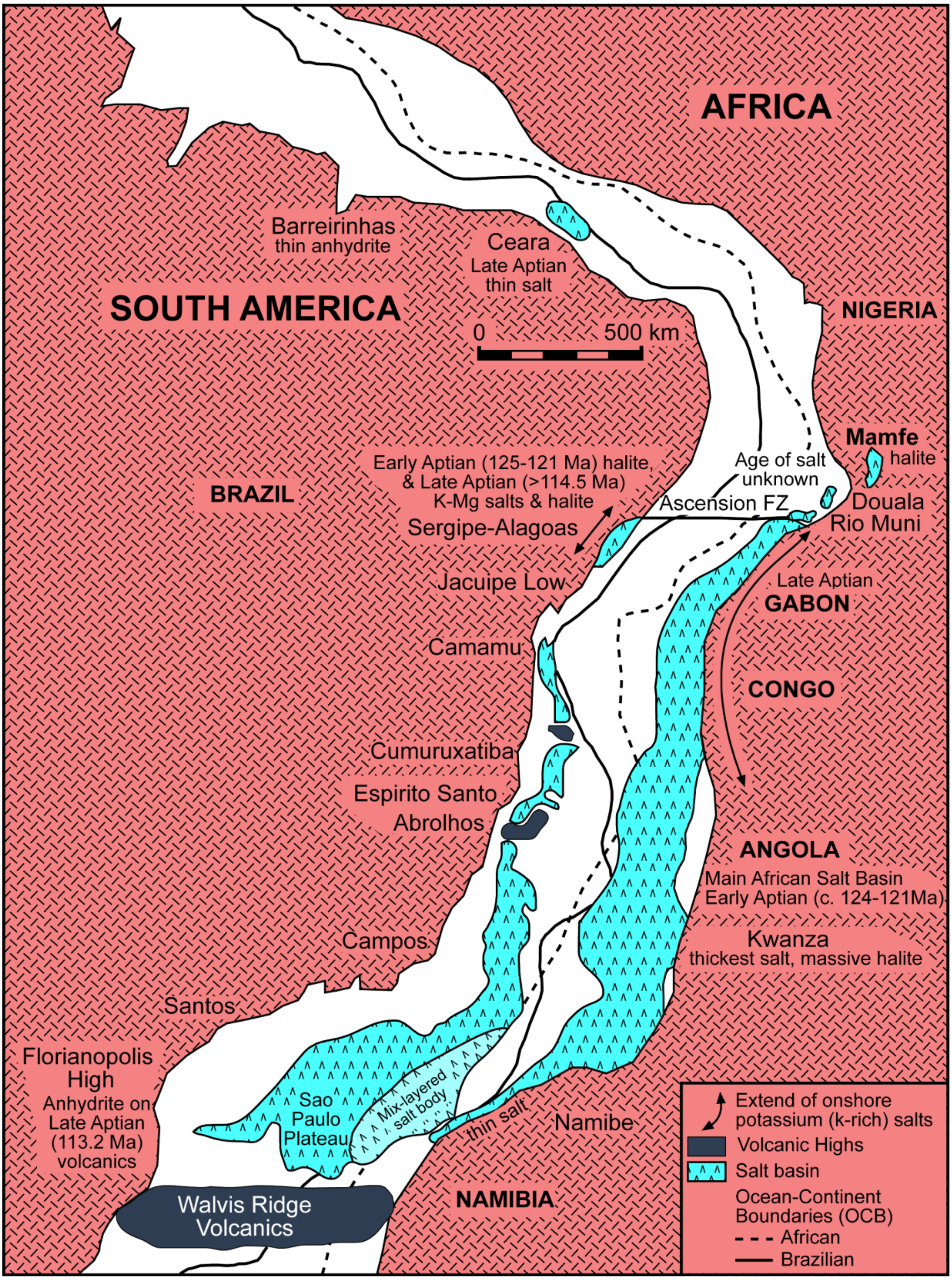

Figure 5.8. South Atlantic salt province (modified from Davison, 2007).

5.5 Conclusions

The new data presented in this study indicates that the outcropping sediment in the eastern part of the Mamfe Basin in Cameroon are considerably older than those at the central and western part. Their ages range from pre-middle Barremian to early Albian in the pre-rift and syn-rift succession in eastern part of the basin, and middle to late Albian in the post-rift succession in the central and western part of the Basin. It is doubtful if post Albian sediments were deposited in the eastern Mamfe Basin and later eroded. The westward younging of sediments in the basin is attributed to uplift and erosion of between 1.2 and 4 km thick sediments from the eastern part of the basin. The eastward decrease in the width of the basin is also attributed to this uplift and erosion and not due to differential rifting as earlier reported (Ajonina, 1997; Ajonina et al., 2001).

In view of the results presented in this study, the existing paleogeographic reconstructions linking the Mamfe Basin and southern Benue are only valid for the Albian-Cenomanian post-rift sediments (Ikom-Munaya Formation) in the central and western part of the Mamfe Basin.

Because the post-rift sediments are not folded, folding in the Mamfe Basin was pre-middle Albian and not related to the Cenomanian and Santonian Folding events in the Benue Trough (e.g. Olade, 1975; Benkhelil, 1989; Ojoh, 1990). The tectonic activity (uplift and folding) in the Mamfe Basin may be related to the opening of the Equatorial Atlantic and Benue Trough in the early Albian but not to either the Cenomanian, or Santonian epeirogeny, or activity of the Cameroon Volcanic line. It is inferred that the pre-rift and syn-rift tectonics in the basin are related to the opening of the South Atlantic while the post rift tectonic and sedimentation are related to the opening of the Equatorial Atlantic and the Benue Trough.

The late Aptian volcaniclastics towards the top of the lacustrine sediments in the Mamfe Basin may be coeval or related to the pyroclasts underneath the Asu River Group in the Abakaliki Basin (e.g. Nwachukwu, 1972; Olade, 1979; Hoque, 1984; Ojoh, 1990). The Abakaliki pyroclasts are believed to represent the earliest phase of Cretaceous magmatism in the Benue Trough and are associated with continental rifting that preceded the separation of Africa from South America.

The result of this study support the suggestions of Benkhelil (1989), and Dejax and Brunet (1996) that the pre-Albian Benue Trough region consisted of discrete and isolated depocenters that were merged in the late Aptian-Albian to form the Benue Trough.

Although the Mamfe Basin is physically linked to the Benue Trough, it was a discrete depocenter and its evolution preceded the initiation of the Benue Trough. The Mamfe Basin is therefore a forerunner of the Benue Trough and not a rift-splay segment of the trough as earlier suggested (Ajonina, 1997; Ajonina et al., 2001).

The evaporites in the Mamfe Basin are older than the first marine transgression in the Benue Trough. The marine incursion into the Mamfe Basin was from the Douala Basin in the Aptian and not from the Benue Trough in the Albian-Cenomanian.

The palynoflora, maceral and clay mineral composition of the Mamfe Group indicates a progressively shift from a drier arid to semi-arid climate in the basal fluvio-lacustrine units towards a more humid and wet climate in the fan-delta and fluviatile succession at the top. The fill up of the Mamfe Basin to base-level in the Aptian-Albian is thus attributed to a better developed sediment delivery drainage system that resulted from a wetter climate rather than tectonics.

6

GENERAL CONCLUSIONS AND OUTLOOK

6.1 Conclusions

This research was undertaken to characterize the depositional environments and age of the sedimentary infill of the Mamfe Basin within the context of the early Cretaceous paleogeography of the eastern Gulf of Guinea region from southern Benue Trough to northern Gabon. Outcrop to micro scale facies analysis using multidisciplinary techniques resulted in the characterization of alluvial, fluvial, palustrine, lacustrine, and deltaic depositional environments within the Mamfe Basin.

The observed vertical and lateral transition in depositional settings in the basin necessitated a revision and redefinition of the basin-fill lithostratigraphy into five formations which from bottom to top are: Etuko, Nfaitok, Manyu, Okoyong and Ikom-Munaya. This study supports the tripartite stratigraphic framework that was proposed for the Mamfe Basin (Ajonina, 1997; Ajonina and Bassey, 1997). This stratigraphic framework correspond to three depositional sequences that represent pre-rift (Etuko), syn-rift (Nfaitok, Manyu, Okoyong), and post-rift (Ikom-Munaya) deposits. The palynoflora assemblage recorded in this study provides the first definitive paleontologic age for the sediments in the Mamfe Basin.

The pre-rift depositional sequence (Etuko Formation) consist of proximal debris flow alluvial fan deposits at the northeastern margin (footwall) of the Basin. These alluvial deposits are about 20 m thick, non-fossiliferous and are older than middle Barremian. They are separated from the overlying syn-rift sediments by a thick paleosol.

The syn-rift depositional sequence is about 270 m thick in outcrop and dated palynologically as middle Barremian-early Albian. It consists of fluvial, palustrine, lacustrine, deltaic, and medial alluvial fan succession that have been mapped in this study as the Mamfe Group. The group outcrops mainly in the eastern part of the Mamfe Basin in Cameroon and consists of Nfaitok, Manyu, and Okoyong Formations respectively. The palynoflora assemblage of the Mamfe Group corresponds to the West African regional palynostratigraphic reference section zones CV to CIX of SNEA (P) in Gabon, and palynozones P-190 to P-280 in South America (Brazil). These zones have been assigned a middle Barremian-early Albian age. The Mamfe Group is thus coeval with early Cretaceous syn-rift phase I sediments in other basin of the West and Central African rift system.

Nfaitok Formation is the basal unit of the Mamfe Group and consists of about 71 m fluvio-palustrine deposits of an axial river with an extensive fllodplain on the hanging-wall of the Mamfe half-graben. The axial river on the basin floor separated alluvial fan sedimentation on the footwall of the half-graben from floodplain deposition on the hanging-wall (see **Fig. 5.3**). Lithofacies and microflora support deposition during a dry semi-arid to arid climate. This formation is dated as middle Barremian-early Aptian.

Manyu Formation is a littoral to profundal lacustrine deposits that is made up of a cyclic succession of poorly-fossiliferous dark grey to black shales, marlstones, poorly sorted feldspathic sandstones, siltstones, evaporites, and volcaniclastics at the top. The volcaniclastics deposit in this formation marks a turn-around from deepening upward to shallowing upward facies association. Lithofacies, playnofacies, palynoflora, and clay mineral composition suggests that climate was the major cause of the basel-level turn-around from rising to falling at the top of the of this formation. The Manyu Formation has a composite outcrop thickness of about 95 m. Its palynologic Aptian age suggests that the Mamfe Basin was a part of the Barremian-middle Albian Medio-African and NE-Brazilian Great Lakes.

The Okoyong Formation is a low gradient shallow water lacustrine fan-delta succession on the hanging-wall of the Mamfe half-graben. It is over 100 m thick in outcrops in the eastern Mamfe Basin. It consists of a coarsening and thickening upward alternating succession of lithic arkoses, siltstones and greenish to dark grey mudrocks. The formation is late Aptian-early Albian in age. Lithofacies, palynoflora, and clay mineralogy of this formation suggests that it was deposited during a comparatively more humid and wetter climate than the underlying fomations (Nfaitok and Manyu Fms).

A marine incursion into the Mamfe Basin during sy-rift deposition is represented by halite dominated evaporites, rare *Praebulimina* sp., *Hedbergella* sp. and

Leiosphaeridia sp. Aptian evaporites are absent in the Benue Trough and suggest that the marine ingression into the Mamfe Basin was from the south (Douala Basin) and not the west (Benue Trough) as earlier reported (Reyment, 1965; Ajonina et al., 2007). The evaporites deposit in the Mamfe Group implies that the South Atlantic salt province extended further north than the Douala Basin (e.g. Reijers and Petters, 1987; Davison, 2007). Syn-rift sedimentation was termination by a tectonic event that resulted in folding.

The post-rift depositional sequence (Ikom-Munaya Formation) is underlain by an angular unconformity that is considered in this study to coincide with the opening of the Equatorial Atlantic and Benue Trough. It consists of non-fossiliferous fluvial deposits in the central part of the basin that extend to the western part in SE Nigeria. Their absence from the eastern part of the basin is attributed to an uplift that resulted to their erosion from this part of the basin.

The eastward decrease in the width of the basin is also attributed to this uplift and erosion and not due to differential rifting as earlier reported (Ajonina, 1997; Ajonina et al., 2001). The uplift and erosion of between 1.2 and 4 km thick sediments from the eastern part of the Mamfe Basin suggests that the areal extend of this basin was much larger in the Early Cretaceous than its present limits.

The petroleum source rock potential of the syn-rift succession in the Mamfe Basin is summarized in **figure 6.1** and **6.2**. Their kerogen content is similar to that other rift basins (e.g. Katz, 1995; Harris et al., 2004; Bohacs, 2012). Samples from Nfaitok Formation (fluvio-palustrine) contain mostly woody and coaly and rarely herbaceous kerogen (vitrinite dominated terestrial kerogen, Caroll and Bohacs, 2001), and have TOC ranging from 0.31 to 2.52 wt.%. They have fair to good hydrocarbon source rock potential and are peak mature to overmature. Lacustrine samples from the Manyu Formation contain mostly amorphous and algal/herbaceous kerogen (mixed type II/III), and have TOC ranging from 0.65 to 7.46 wt.%. They are good to excellent hydrocarbon source rocks and are thermally early to peak mature. The organic matter of fluvio-deltaic samples from Okoyong Formation is dominated by woody and coaly kerogen and have TOC ranging from 0.28 to 3.16 wt.%. They are mostly poor source rocks and thermally immature to early mature. The petroleum source rock of the Mam

The petroleum source rock data indicates that the Mamfe Basin is oil and gas-prone. Deltaic and fluvial sandstones are potential reservoirs, and mudrocks and evaporites are potential seals. There are high potential for structural and stratigraphic traps in the basin because the sediments are faulted, folded, and exhibit rapid facies change. There are chances of oil and gas targets in the down dip regions in the central part of the basin where the sediments are very thick (e.g. Abolo, 2008; Ajonina et al., 2012).

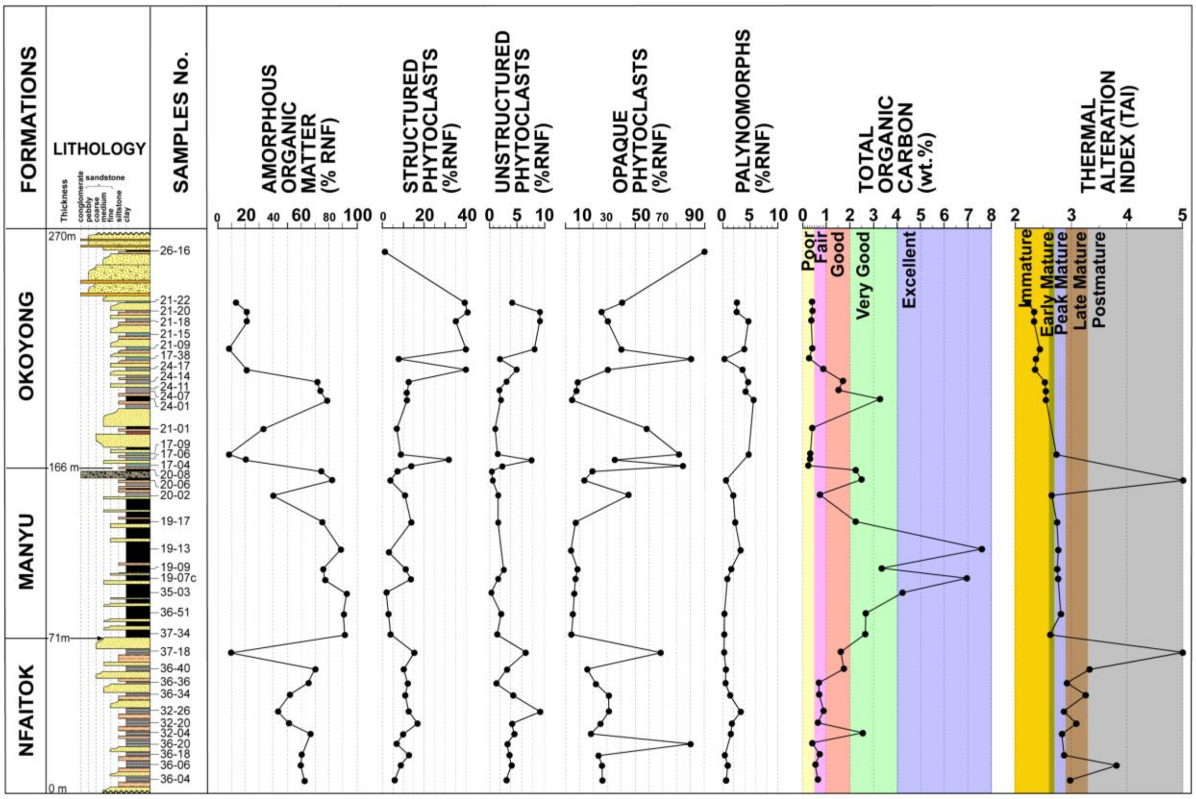

Figure 6.1. Stratigraphic variation of organic matter components, TOC, and TAI in the Mamfe Group with interpretation (Peters and Cassa, 1994) for petroleum source rock potential.

Lithofacies, palynofacies, microflora, and clay mineral composition of the studied sedimentary succession of the Mamfe Basin show a progressively shift from a warm and dry arid to semi-arid climate in the Nfaitok (fluvio-palustrine) and Manyu (lacustrine) Formations towards a more humid and wet climate in the Okoyong (fan-delta) and Ikom-Munaya Formations at the top of the basin. Frequent occurrence of charcoal in the medial alluvial succession of the Okoyong Formation suggest deposition during a seasonally drier climate regime that supported wildfire-prone environments. The base-level fall that let to the fill up of the Mamfe Basin in the Albian resulted from increase sedimentary supply associated with wetter climate and a better developed sediment delivery drainage system.

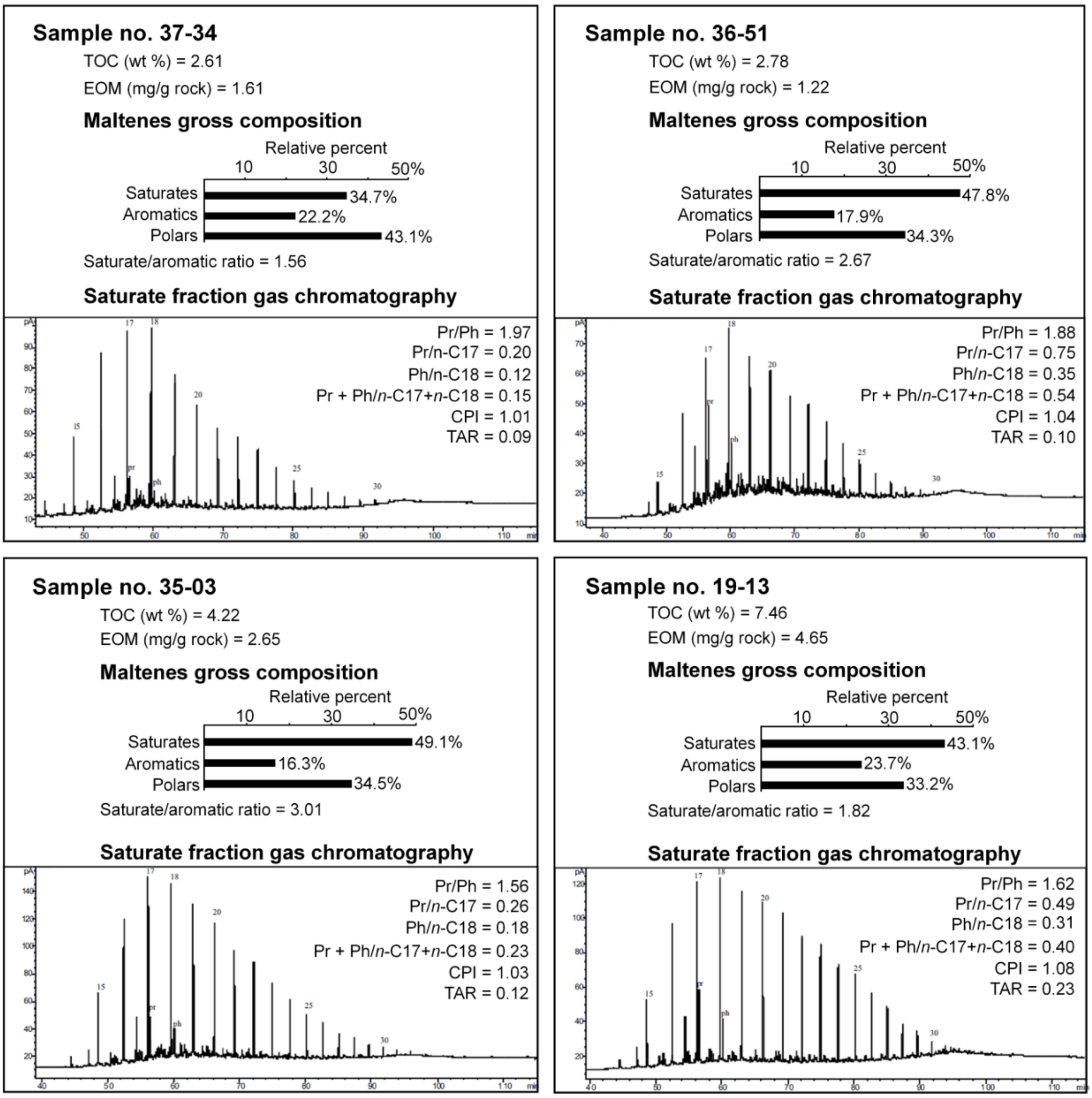

Figure 6.2. Bulk geochemical parameters for selected samples from the Manyu Formation.

Vitrinite reflectance, thermal alteration index, biomarkers, and illite crystallinity yielded similar burial metamorphism (thermal maturity) data that suggest that the outcropping sediments in the eastern Mamfe Basin have been buried to depths of between 1200 and 4000 m. The westward younging of sediments in the basin is due to uplift and erosion of between 1200 and 4000 m thick sediments in the eastern part and not the previously reported westward migration of depocenter. Lack of proximal facies associated with the medial alluvial fan deposits of the Okoyong Formation in the southeastern part of the basin suggests that the Mamfe Basin extended beyond its present limits. The marked decrease in the width of the basin at its eastern end to less than 10 km is attributed to uplift and erosion at the southeastern part of the hangingwall block.

Early Cretaceous paleocurrent trends in the Mamfe Basin are similar to present day drainage pattern. This suggests that Cenozoic uplift in the region due to activity of the Cameroon Volcanic Line has no significant effect on the sediment routing direction in the basin.

The palynological age of the sediments in the eastern part of the Mamfe Basin indicates that deposition in this part of the basin predates the basal sediments in the southern Benue Trough. The age suggest that the Mamfe Basin is one of the several satellite basins that served as forerunner to the opening of the Benue Trough (e.g. Dejax and Bunnet, 1996). The Mamfe Basin is therefore not a rift-splay segment of the Benue Trough as previously proposed (Ajonina, 1997).

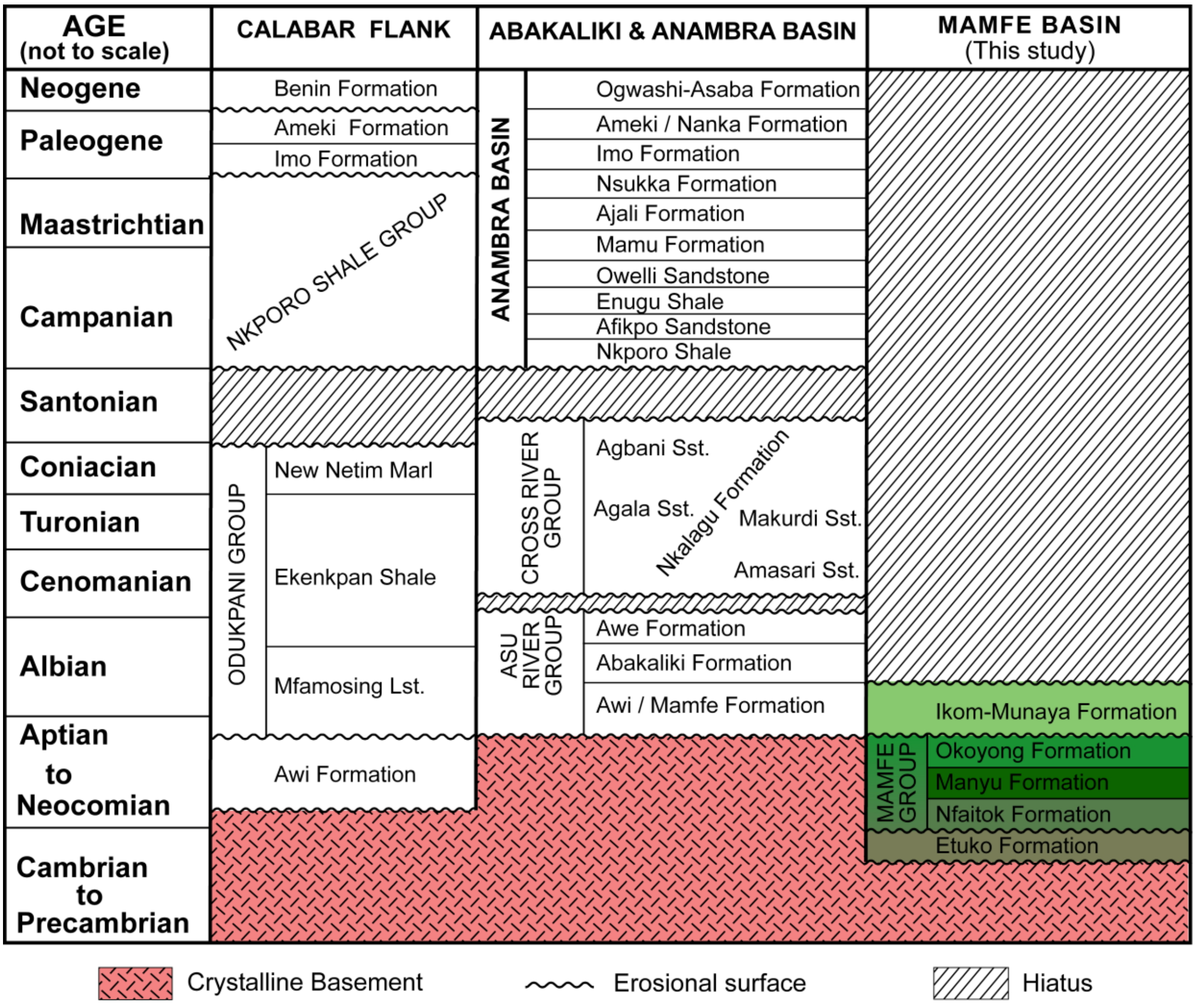

Figure 6.3. Revised lithostratigraphic correlation of the Mamfe Basin and southern Benue Trough.

A revised lithostratigraphic correlation (**fig. 6.3)** and and geologic map (**fig. 6.4**) is proposed for the Lower Cretaceous succession in the Mamfe Basin and southern Benue Trough (Abakaliki and Anambra Basins) and consists of Etuko Formation, Mamfe Group (Nfaitok, Manyu, Okoyong), and Asu River Group (Ikom-Munaya/Awi, Abakaliki, Awe).

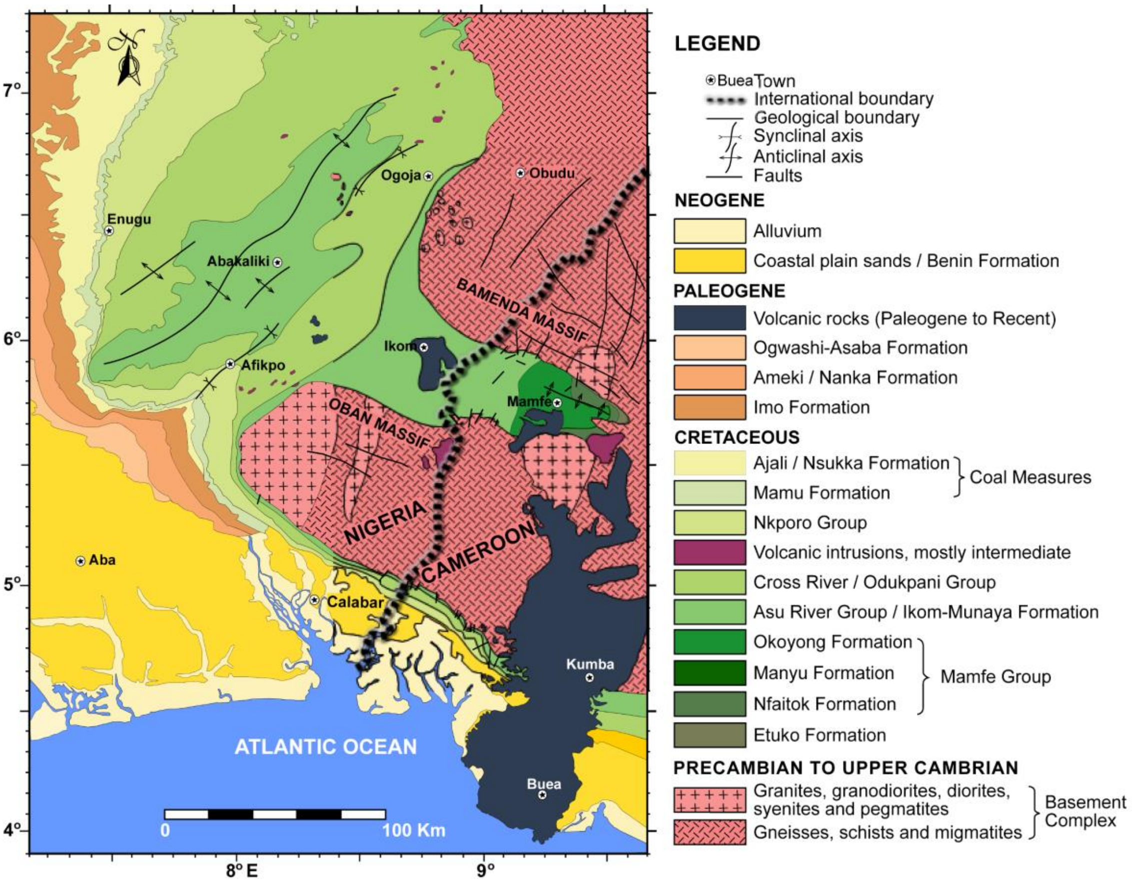

Figure 6.4. Revised geological map of the Mamfe Basin and southern Benue Trough (modified from Dumort, 1968; Gerbeth et al., 1976; and Toteu et al., 2001).

6.2 Outlook

Although this research has provided new insights on the sedimentary geology of the Mamfe Basin in Cameroon, a detailed structural mapping is needed to understand the origin and tectonic history of the basin. Structural mapping will help in differentiating local and regional influences on sedimentation pattern in the basin.

Interaction of axial and transverse drainage deposits in a half-graben setting reflects both climatic influences and tectonics associated with fault growth. Detailed field mapping, accurate dating, and paleoclimatic studies are needed to determine the relative importance of these variables on sedimentation in the basin.

Further research is needed to delineate the variable transitions between the lake-basin types (Bohacs et al., 2000; Caroll and Bohacs, 2001) that are represented by the formations in the Mamfe Group.

The interplay between tectonics and climate on base-level turn-around towards the top of the Manyu Formation also merits further investigation.

Radiometric dating of the pillow basalts in the volcaniclastic facies at the top of the Manyu Formation is needed to ascertain whether this volcaniclastic deposit is a syn-depositional or post depositional tectonic intrusive (e.g. Oden et al., 2016). The radiometric age will also help to ascertain whether this volcaniclastic sediments are coeval or related to the Aptian pyroclasts in the in Abakaliki Basin that mark the onset of rifting in the Benue Trough.

The relationship between lead-zinc mineralization and evaporites in the Mamfe Basin is not clear and needs to be investigated.

Detailed geochemical analysis of subsurface samples is needed to accurately delineate the petroleum system of the Mamfe Basin.

The Isopach map of the Mamfe Basin indicates that it is made up of two subbasins which probably acted as separate depocenters during the early part of the basin history. Their influence on sedimentation during the later stages of basin evolution needs to be investigated.

The timing of folding and faulting and uplift in the Mamfe Basin is not certain. Whether these events are related to the opening of the equatorial Atlantic in the late Aptian-early Albian, Santonian epeirogeny in the Benue Trough, or the initiation of the Cameroon Volcanic Line (CVL) in the Paleogene need to be investigated.

REFERENCES CITED

Abbink, O. A., Van Konijnenburg - Van Cittert, J. H. A., and Visscher, H., 2004. Sporomorph ecogroup model for the Northwest European Jurassic-Lower Cretaceous I: concepts and framework. *Netherlands Journal of Geosciences/Geologie en Mijnbouw*, v. **83**, p. 17-38.

Abbink, O. A., Targarona, J., Brinkhuis, H., and Visscher, H., 2001. Late Jurassic to earliest Cretaceous palaeoclimatic evolution of the southern North Sea *Global and Planetary Change*, v. **30**, p. 231-256.

Abolo, G. M., 2008. Geology and Petroleum potential of the Mamfe Basin, Cameroon, Central Africa. *Africa Geoscience Review, Special Publication*, v. **1 & 2**, p. 65-77.

Abubakar, M. B., Obaje, N. G., Luterbacher, H. P., Dike, E. F. C., and Ashraf, A. R., 2006. A report on the occurrence of Albian-Cenomanian elater-bearing pollen in Nasara-1 well, Upper Benue Trough, Nigeria: Biostratigraphic and palaeoclimatological implications. *Journal of African Earth Sciences*, v. **45**, p. 347-354.

Abubakar, M. B., Luterbacher, H. P., Ashraf, A. R., Ziedner, R., and Maigari, A. S., 2011. Late Cretaceous palynostratigraphy in the Gongola Basin (Upper Benue Trough, Nigeria). *Journal of African Earth Sciences*, v. **60**, p. 19-27.

Adediran, S. A., and Adegoke, O. S., 1987. Evolution of sedimentary basins of the Gulf of Guinea. In: G. Matheis, and H. Schandlemeier, eds., *Current Research in African Earth Sciences*, Balkema, Rotterdam, p. 283-286.

Adediran, S. A., Adegoke, O. S., and Oshin, I. O., 1991. The continental sediments of the Nigerian Coastal Basins. *Journal of African Earth Sciences (and the Middle East)*, v. **12**, p. 79-84.

Adeleye, D. R., 1975. Nigerian Late Cretaceous stratigraphy and paleogeography. *AAPG Bulletin*, v. **59**, p. 2302-2313.

Adeleye, D. R., and Fayose, E. A., 1978. Stratigraphy of the type section of Awi Formation, Odukpani area, southeastern Nigeria. *Journal of Mining and Geology*, v. **15**, p. 33-37.

Agumanu, A. E., 1989. The Abakaliki and the Ebonyi Formations: sub-divisions of the Albian Asu River Group in the southern Benue trough, Nigeria. *Journal of African Earth Sciences*, v. **9**, p. 195-207.

Ajibola, O. A., 1997. Aspects of Sedimentology and Depositional Environments of the Ogoja Sandstones in Ikom area of Southeastern Nigeria. M.Sc. thesis, University of Ibadan, 87 pp.

Ajonina, H. N., 1997. Sedimentology and Petroleum Potentials of the Middle Cretaceous sediments of the Mamfe Formation, Mamfe Embayment, southwestern Cameroon. MSc. thesis, University of Ibadan, Ibadan, 152 pp.

Ajonina, H. N., and Bassey, C. E., 1997. Stratigraphy and depositional environments of the Mamfe Formation and its implication on the tectono-sedimentary evolution of the Ikom-

Mamfe Embayment. *Nigerian Association of Petroleum Explorationist (NAPE) 15th Annual international Conference and Exhibition*, Lagos, Nigeria, p. 39.

Ajonina, H. N., Ajibola, O. A., and Bassey, C. E., 1998. A review of the Sedimentology and reservoir quality of sandstones of the Mamfe Formation exposed in parts of southeastern Nigeria and southwesthern Cameroon. *16th Annual International Conference and Exhibition of the Nigerian Association of Petroleum Explorationist (NAPE)*, Lagos, Nigeria, p. 52.

Ajonina, H. N., Ajibola, O. A., and Bassey, C. E., 2001. The Mamfe Basin, S.E. Nigeria and S.W. Cameroon: A review of basin filling model and tectonic evolution. *Journal of the Geosciences Society of Cameroon*, v. **1**, p. 24-25.

Ajonina, H. N., Betzler, C., and Jaramillo, C., 2010. Paleoclimatic significance of an Early Cretaceous fan-delta sedimentary succession in the eastern Mamfe Basin, SW Cameroon. *2010 Afrikagruppe deutscher Geowissenschaftler (AdG)*, Frankfurt, Germany, p. 30.

Ajonina, H. N., Betzler, C., Volkheimer, W., and Eyong, J. T., 2008. Palynology and depositional environments of Early Cretaceous sediments in the Mamfe Basin, west Africa and their relationship to other Gondwanic regions in South America. *12th International Palynological Congress (IPC-XII) 8th International Organisation of Paleobotany Conference (IOPC)*, Bonn, Germany, p. 8.

Ajonina, H. N., Betzler, C., Eyong, J. T., Eseme, E., and Hell, J. V., 2007. Stratigraphy and sedimentary evolution of the Mamfe Basin, southwest Cameroon, West Africa. *4th International Limnogeology Congress*, Barcelona, Spain, p. 57.

Ajonina, H. N., Njilah, I. K., Ndjeng, E., Hell, J. V., Bassey, C. E., and Ajibola, O. A., 2006. Sedimentology and reservoir potential of sandstones of the Mamfe Formation, Mamfe Basin, southeast Nigeria and southwest Cameroon. *Annales de la Faculté des Sciences Université de Yaoundé I, série Science de la Nature et de la vie*, v. **36**, p. 117-132.

Ajonina, H. N., Jaramillo, C., Volkheimer, W., Mejía, P., Betzler, C., Hell, J. V., and Njilah, I. K., 2010. Palynostratigraphy and age of the Lower Cretaceous Mamfe Group, Mamfe Basin, SW Cameroon, eastern West Africa. *8th European Palaeobotany-Palynology Conference (EPPC)*, Budapest, Hungary, p. 51-52.

Ajonina, H. N., Betzler, C., Hell, J. V., Eseme, E., Volkheimer, W., Jaramillo, C., and Eghombi, G. N., 2012. Hydrocarbon potential of the Mamfe Basin, SW Cameroon. *GV & Sediment Meeting 2012*, Hamburg, Germany, p. 31.

Akande, S. O., and Mucke, A., 1989. Mineralogical, textural and paragenetic studies of the Lead-Zinc-Copper mineralization in the lower Benue Trough (Nigeria) and their genetic implications. *Journal of African Earth Sciences*, v. **9**, p. 23-29.

Akande, S. O., and Viczian, I., 1995. Clay mineralogy, diagenesis, paleothermometry and hydrocarbon potential of Cretaceous shales in the southern Benue trough, Nigeria. *Geology Carpathica, Series Clays*, v. **4**, p. 55-65.

Akande, S. O., and Erdtmann, B. D., 1998. Burial metamorphism (thermal maturation) in Cretaceous sediments of the southern Benue Trough and Anambra Basin, Nigeria. *AAPG Bulletin*, v. **82**, p. 1191-1206.

Akande, S. O., Ojo, O. J., Erdtmann, B. D., and Hetenyi, M., 2005. Paleoenvironments, organic petrology and Rock-Eval studies on source rock facies of the Lower

Maastrichtian Patti Formation, southern Bida Basin, Nigeria. *Journal of African Earth Sciences*, v. **41**, p. 394-406.

Akande, S. O., Egenhoff, S. O., Obaje, N. G., Ojo, O. J., Adekeye, O. A., and Erdtmann, B. D., 2012. Hydrocarbon potential of Cretaceous sediments in the Lower and Middle Benue Trough, Nigeria: Insights from new source rock facies evaluation. *Journal of African Earth Sciences*, v. **64**, p. 34-47.

Ala, M. A., and Selley, R. C., 1997. The West African coastal basins. In: R. C. Selley, ed., *Sedimentary Basins of the World, 3*, Elsevier Science B.V., Amsterdam, p. 173-186.

Alexander, J., and Fielding, C. R., 2006. Coarse-grained floodplain deposits in the seasonal tropics: towards a better facies model. *Journal of Sedimentary Research*, v. **76**, p. 539-556.

Allix, P., Grossdidier, E., Jardine, S., Legoux, O., and Popoff, M., 1981. Découverte d' Aptien supérieur à Albien inférieur daté par microfossiles dans la série détritique crétaceé du fossé de la Bénoué. *Comptes Rendu de l'Académie des Sciences de Paris*, v. **292**, p. 1292-1294.

Arai, M., 2000. Relict of Mid-Cretáceous interior seas in Brazil (1). *Revista Brasileira de Geociências*, v. **30**, p. 436-438.

Arthaud, M. H., Caby, R., Fuck, R. A., Dantas, E. L., and Parente, C. V., 2008. Geology of the northern Borborema Province, NE Brazil and its correlation with Nigeria, NW Africa. *Geological Society, London, Special Publications*, v. **294**, p. 49-67.

Aslan, A., 2003. Floodplain sediments. In: G. V. Middleton, ed., *Encyclopadia of Sediments and Sedimentary Rocks*, Kluwer Academic Press Publishers, Dordrecht, p. 285-287.

Aslanian, D., and Moulin, M., 2010. Comment on 'A new scheme for the opening of the South Atlantic Ocean and the dissection of an Aptian salt basin' by Trond H. Torsvik, Sonia Rousse, Cinthia Labails and Mark A. Smethurst. *Geophysical Journal International*, v. **183**, p. 20-28.

Atta-Peters, D., and Salami, M. B., 2006. Aptian–Maastrichtian palynomorphs from the offshore Tano Basin, western Ghana. *Journal of African Earth Sciences*, v. **46**, p. 379-394.

Avbovbo, A. A., 1980. Basement geology in the sedimentary basins of Nigeria. *Geology*, v. **8**, p. 323-327.

Avbovbo, A. A., Ayoola, E. O., and Osahon, G. A., 1986. Depositional and structural styles in the Chad Basin of northeastern Nigeria. *AAPG Bulletin*, v. **70**, p. 1787-1798.

Bardack, D., 1965. Anatomy and evolution of chirocentrid fishes. *The University of Kansas Paleontological Contributions, Vertebrata*, v. **10**, p. 1-88.

Basent, G. G., Rajendra, S. B., Ashok, K. B., Dinesh, K., Kusum, L. P., Adarsh, K. M., Jagdish, P. G., Gaur, C. D., and Nizhat, J. T., 2005. Geochemical characterization and source investigation of oils discovered in Khoraghat-Nambar structures of the Assam-Arakan Basin, India. *Organic Geochemistry*, v. **36**, p. 161-181.

Basile, C., Mascle, J., and Guiraud, R., 2005. Phanerozoic geological evolution of the Equatorial Atlantic domain. *Journal of African Earth Sciences*, v. **43**, p. 275-282.

Bassey, C. E., and Ajonina, H. N., 2002. Petrology of the Cenomanian Upper Member of the Mamfe Formation, Mamfe Embayment, southwestern Cameroon. *Journal of Mining and Geology*, v. **38**, p. 27-34.

Bassey, C. E., Eminue, O. O., and Ajonina, H. N., 2013. Stratigraphy and depositional environments of the Mamfe Formation and its implication on the tectonosedimentary evolution of the Ikom-Mamfe Embayment, West Africa. *Central European Journal of Geosciences*, v. **5**, p. 394-406.

Batten, D. J., 1975. Wealden paleoecology from the distribution of plant fossils. *Proceedings of Geologist's Association 85 (for 1974)*, p. 433-458.

Batten, D. J., 1996. Palynofacies and paleoenvironmental interpretation. In: J. Jasonius, and D. C. McGregor, eds., *Palynology: Principles and Applications*, American Association of Stratigraphic Palynologists Foundation, Dallas, p. 1011-1064.

Batten, D. J., 2007. Spores and pollen from the Crato Formation: biostratigraphic and paleoenvironmental implications. In: D. M. Martill, G. Bechly, and R. F. Loveridge, eds., *The Crato Fossil Beds - Window into an Ancient World*, Cambridge University Press, New York, p. 566-573.

Batten, D. J., and Stead, D. T., 2005. Palynofacies analysis and its stratigraphic applications. In: E. A. M. Koutsoukos, ed., *Applied Stratigraphy*, Springer, The Netherlands, p. 203-226.

Beauvais, A., and Colin, F., 1993. Formation and transformation processes of iron duricrust systems in tropical humid environment. *Chemical Geology*, v. **106**, p. 77-101.

Bellanca, A., Claps, M., Erba, E., Masetti, D., Neri, R., Premoli Silva, I., and Venezia, F., 1996. Orbitally induced limestone/marlstone rhythms in the Albian—Cenomanian Cismon section (Venetian region, northern Italy): Sedimentology, calcareous and siliceous plankton distribution, elemental and isotope geochemistry. *Palaeogeography, Palaeoclimatology, Palaeoecology*, v. **126**, p. 227-260.

Bellieni, G., Macedo, M. H. F., Petrini, R., Piccirillo, E. M., Cavazzini, G., Comin-Chiaramonti, P., Ernesto, M., Macedo, J. W. P., Martins, G., Melfi, A. J., Pacca, I. G., and De Min, A., 1992. Evidence of magmatic activity related to Middle Jurassic and Lower Cretaceous rifting from northeastern Brazil(Ceara-Mirim): K/Ar age, palaeomagnetism, petrology and Sr-Nd isotope characteristics. *Chemical Geology*, v. **97**, p. 9-32.

Belmonte, Y. C., 1966. Stratigraphie du bassin sedimentaire du Cameroun. In: J. E. van Hinte, ed., *Proceedings of the second West African Micropaleontological Colloquium*, E.J.Brill, Leiden, Netherlands, p. 7-24.

Benkhelil, J., 1989. The origin and evolution of the Cretaceous Benue Trough (Nigeria). *Journal of African Earth Sciences*, v. **8**, p. 251-282.

Benkhelil, J., Mascle, J., and Guiraud, M., 1998. Sedimentary and structural characteristics of the cretaceous along the Côte d'Ivoire-Ghana transform margin and in the Benue Trough: a comparison. In: J. Mascle, G. P. Lohmann, and M. Moullade, eds., *Proceedings of the Ocean Drilling Program, Scientific Results*, v. **159**, p. 93-99.

Benkhelil, J., Giresse, P., Poumot, C., and Ngueutchoua, G., 2002. Lithostratigraphic, geophysical, and morpho-tectonic studies of the South Cameroun shelf. *Marine and Petroleum Geology*, v. **19**, p. 499-517.

Benvenuti, M., 2003. Facies analysis and tectonic significance of lacustrine fan-deltaic successions in the Pliocene-Pleistocene Mugello Basin, Central Italy. *Sedimentary Geology*, v. **157**, p. 197-234.

Bercovici, A., Hadley, A., and Villanueva-Amadoz, U., 2009. Improving depth of field resolution for palynological photomicrography. *Palaeontologia Electronica*, v. **12**, p. 1-12.

Bhattacharya, J. P., and MacEachern, J. A., 2009. Hyperpycnal Rivers and Prodeltaic Shelves in the Cretaceous Seaway of North America. *Journal of Sedimentary Research*, v. **79**, p. 184-209.

Bheemalingeswara, K., Solomon, G., and Ebrahim, N. H., 2013. Petrography and geochemistry of ferricrete near Shire, northern Ethiopia. *Momona Ethiopian Journal of Science*, v. **5**, p. 32-50.

Binks, R. M., and Fairhead, J. D., 1992. A plate tectonic setting for Mesozoic rifts of West and Central Africa. *Tectonophysics*, v. **213**, p. 141-151.

Blair, T. C., 1999a. Sedimentary processes and facies of the waterlaid Anvil Spring Canyon alluvial fan, Death Valley, California. *Sedimentology*, v. **46**, p. 913-940.

Blair, T. C., 1999b. Sedimentology of the debris-flow-dominated Warm Spring Canyon alluvial fan, Death Valley, California. *Sedimentology*, v. **46**, p. 941-965.

Blair, T. C., and McPherson, J. G., 1994. Alluvial fans and their natural distinction from rivers based on morphology, hydraulic proccesses, sedimentary proccesses, and facies assemblages. *Journal of Sedimentary Research*, v. **A64**, p. 450-489.

Blair, T. C., and McPherson, J. G., 1999. Grain-size and textural classification of coarse sedimentary particles. *Journal of Sedimentary Research*, v. **69**, p. 6-19.

Blair, T. C., and McPherson, J. G., 2008. Quaternary sedimentology of the Rose Creek fan delta, Walker Lake, Nevada, USA, and implications to fan-delta facies models. *Sedimentology*, v. **55**, p. 579-615.

Blair, T. C., and McPherson, J. G., 2009. Processes and forms of alluvial fans. In: A. J. Parsons, and A. D. Abrahams, eds., *Geomorphology of Desert Environments*, 2nd edn, Springer Netherlands, p. 413-467.

Boggs, S., Jr., 2009. *Petrology of Sedimentary Rocks*. 2nd edn. Cambridge University Press, UK, 600 pp.

Bohacs, K. M., 2012. Relation of Hydrocarbon Reservoir Potential to Lake-Basin Type: An Integrated Approach to Unraveling Complex Genetic Relations Among Fluvial, Lake-Plain, Lake Margin, and Lake Center Strata. In: O. W. Baganz, Y. Bartov, K. M. Bohacs, and D. Nummedal, eds., *Lacustrine Sandstone Reservoirs and Hydrocarbon Systems*, AAPG Memoir, 95, Tulsa, Okla, v. **AAPG memoir, 95**, p. 13-56.

Bohacs, K. M., Carroll, A. R., Neal, J. E., and Mankiewicz, P. J., 2000. Lake-basin type, source potential, and hydrocarbon character: an integrated sequence-stratigraphic-geochemical framework. In: E. H. Gierlowski-Kordesch, and K. R. Kelts, eds., *Lake Basins through Space and Time*: AAPG Studies in Geology, American Association of petroleum Geologists, Tulsa, p. 3-33.

Bohacs, K. M., Lamb-Wozniak, K., Demko, T. M., Eleson, J., McLaughlin, O., Lash, C., Cleveland, D. M., and Kaczmarek, S., 2013. Vertical and lateral distribution of lacustrine carbonate lithofacies at the parasequence scale in the Miocene Hot Spring limestone, Idaho: An analog addressing reservoir presence and quality. *AAPG Bulletin*, v. **97**, p. 1967-1995.

Bond, D. P. G., and Wignall, P. B., 2010. Pyrite framboid study of marine Permian-Triassic boundary sections: A complex anoxic event and its relationship to contemporaneous mass extinction. *Geological Society of America Bulletin*, v. **122**, p. 1265-1279.

Bordenave, M. L., 1993. Geochemical methods and tools in petroleum exploration. In: M. L. Bordenave, ed., *Applied Petroleum Geochemistry*, Éditions Technip, Paris, p. 207-216.

Bordenave, M. L., Espitalié, J., Leplat, P., Oudin, J. L., and Vandenbroucke, M., 1993. Screening techniques for source rock evaluation. In: M. L. Bordenave, ed., *Applied Petroleum Geochemistry*, Éditions Technip, Paris, p. 217-278.

BouDagher-Fadel, M. K., 1996. Re-evaluation of the phylogeny of Early Cretaceous planktonic foraminifera (Praehedbergellidae). *Cretaceous Research*, v. **17**, p. 767-771.

Brenner, G. J., 1976. Middle Cretaceous floral provinces and early migrations of angiosperms. In: C. B. Beck, ed., *Origin and early evolution of angiosperms*, Columbia University Press, New York, p. 23-47.

Brenner, G. J., 1992. Palynological Analyses of Selected Core Samples From KEN-Bf 180, *Maryland Geological Survey Open-File Report 9-02-7*, p. 27-30.

Bridge, J. S., 2003. *Rivers and Floodplains: Forms, Processes, and Sedimentary Record*. Blackwell Science Ltd, Oxford, 491 pp.

Brown, K. E., and Cohen, A. D., 1995. Stratigraphic and micropetrographic occurrences of pyrite in sediments at the confluence of carbonate and peat-forming depositional systems, southern Florida, USA. *Organic Geochemistry*, v. **22**, p. 105-126.

Browne, S. E., and Fairhead, J. D., 1983. Gravity study of the Central African Rift system: A model of continental disruption 1. The Ngaoundere and Abu Gabra Rifts. *Tectonophysics*, v. **94**, p. 187-203.

Brownfield, M. E., and Charpentier, R. R., 2006. *2006, Geology and total petroleum systems of the West-Central Coastal Province (7203), West Africa*, 52 pp.

Brunet, M., Dejax, J., Brillanceau, A., Congleton, J., Downs, W., Dupéron-Laudoueneix, M., Eisenmann, V., Flanagan, K., Flynn, L., Helntz, E., Hell, J., Jacobs, L., Jéhenne, Y., Ndjeng, E., Mouchelin, G., and Pilbeam, D., 1988. Mise en évidence d'une sédimentation précoce d'âge Barrémien dans le fossé de la Bénoué en Afrique occidentale (Bassin du Mayo Oulo Léré, Cameroun), en relation avec l´ouverture de l'Aflantique sud. *Comptes Rendue de l'Académie des Science*, v. **306**, p. 1125-1130.

Buckley, L., and Tyson, R. V., 2003. Organic Facies Analysis of the Cretaceous Lower and Basal Upper Colorado Group (Cretaceous), Western Canada Sedimentary Basin - A preliminary Report. *Saskatchewan Geological Survey Summary of Investigations*, v. **1**, p. 1-13.

Bumby, A. J., and Guiraud, R., 2005. The geodynamic setting of the Phanerozoic basins of Africa. *Journal of African Earth Sciences*, v. **43**, p. 1-12.

Burke, K. C., Dessauvagie, T. F. J., and Whiteman, A. J., 1972. Geological history of the Benue valley and adjacent areas. In: T. F. J. Dessauvagie, and A. J. Whiteman, eds., *Proceedings on the conference on African Geology*, Ibadan University press, Ibadan, p. 187-205

Cainelli, C., and Mohriak, W. U., 1999. Some remarks on the evolution of sedimentary basins along the eastern Brazilian. *Episodes*, v. **22**, p. 206-216.

Carroll, A. R., and Bohacs, K. M., 2001. Lake-type controls on petroleum source rock potential in nonmarine basins. *AAPG Bulletin*, v. **85**, p. 1033-1053.

Carvalho, M. A., 2004. Palynological assemblage from Aptian/Albian of the Sergipe Basin: Paleoenvironmental reconstruction. *Revista Brasileira de Paleontologia*, v. **7**, p. 159-168.

Carvalho, M. A., Filho, J. G. M., and Menezes, T. R., 2006. Paleoenvironmental reconstruction based on palynofacies analysis of the Aptian–Albian succession of the Sergipe Basin, Northeastern Brazil. *Marine Micropaleontology*, v. **59**, p. 56-81.

Catto, N. R., 1985. Hydrodynamic distribution of palynomorphs in a fluvial succession, Yukon. *Canadian Journal of Earth Sciences*, v. **22**, p. 1552-1556.

Catuneanu, O., 2006. *Principles of Sequence Stratigraphy*. Elsevier, Amsterdam, 375 pp.

Catuneanu, O., Guiraud, R., Eriksson, P., Thomas, B., Shone, R., and Key, R., 2005. Phanerozoic evolution of Africa. *Journal of African Earth Sciences*, v. **43**, p. vii-ix.

Catuneanu, O., Abreu, V., Bhattacharya, J. P., Blum, M. D., Dalrymple, R. W., Eriksson, P. G., Fielding, C. R., Fisher, W. L., Galloway, W. E., Gibling, M. R., Giles, K. A., Holbrook, J. M., Jordan, R., Kendall, C. G. S. C., Macurda, B., Martinsen, O. J., Miall, A. D., Neal, J. E., Nummedal, D., Pomar, L., Posamentier, H. W., Pratt, B. R., Sarg, J. F., Shanley, K. W., Steel, R. J., Strasser, A., Tucker, M. E., and Winker, C., 2009. Towards the standardization of sequence stratigraphy. *Earth-Science Reviews*, v. **92**, p. 1-33.

Chaboureau, A.-C., Donnadieu, Y., Sepulchre, P., Robin, C., Guillocheau, F., and Rohais, S., 2012. The Aptian evaporites of the South Atlantic: a climatic paradox? *Climate of the Past*, v. **8**, p. 1047-1058.

Chaboureau, A.-C., Guillocheau, F., Robin, C., Rohais, S., Moulin, M., and Aslanian, D., 2013. Paleogeographic evolution of the central segment of the South Atlantic during Early Cretaceous times: Paleotopographic and geodynamic implications. *Tectonophysics*, v. **604**, p. 191-223.

Chamley, H., 1989. *Clay Mineralogy*. Springer, Berlin, 623 pp.

Chorowicz, J., 2005. The East African rift system. *Journal of African Earth Sciences*, v. **43**, p. 379-410.

Chumakov, N. M., Zharkov, M. A., Herman, A. B., Doludenko, M. P., Kalandadze, N. M., Lebedev, E. L., Ponomarenko, A. G., and Rautian, A. S., 1995. Climatic belts of the mid-Cretaceous time. *Stratigraphy and Geological Correlation*, v. **3**, p. 241-260.

Coimbra, J. C., Arai, M., and Carreño, A. L., 2002. Biostratigraphy of Lower Cretaceous microfossils from the Araripe basin, northeastern Brazil. *Geobios*, v. **35**, p. 687-698.

Combaz, A., 1964. Les palynofacies. *Revue de Micropaléontologie*, v. **7**, p. 205-218.

Combaz, A., 1980. Les kérogènes vus au microscope. In: B. Durand, ed., *Kerogen: Insoluble Organic Matter from Sedimentary Rocks*, Éditions Technip, Paris, p. 55-110.

Cross, T. A., and Lessenger, M. A., 1998. Sediment volume partitioning: rationale for stratigraphic model evaluation and high-resolution stratigraphic correlation. In: F. M. Gradstein, K. O. Sandvik, and N. J. Milton, eds., *Sequence Stratigraphy–Concepts and Applications*, Norwegian Petroleum Society, Special Publication v. **8**, p. 171 - 195.

Da Rosa, Á. A. S., and Garcia, A. J. V., 2000. Palaeobiogeographic aspects of northeast Brazilian basins during the Berriasian before the break up of Gondwana. *Cretaceous Research*, v. **21**, p. 221-239.

Dada, S. S., 2008. Proterzoic evolution of the Nigeria-Boborema province. *Geological Society, London, Special publication*, v. **294**, p. 121-136.

Dalrymple, R. W., 2010a. Interpreting sedimentary successions: facies, facies analysis and facies models. In: N. P. James, and R. W. Dalrymple, eds., *Facies Models 4.*, Geological Association of Canada, Canada, p. 3-18.

Dalrymple, R. W., 2010b. Introduction to siliciclastic facies models. In: N. P. James, and R. W. Dalrymple, eds., *Facies Models 4*, Geological Association of Canada, Canada, p. 59-72.

Dalrymple, R. W., Kendall, A. C., and Pufahl, P. K., 2010. Introduction to biological and chemical sedimentary facies models. In: N. P. James, and R. W. Dalrymple, eds., *Facies Models 4*, Geological Association of Canada, Canada, p. 323-339.

Davies-Vollum, K. S., and Smith, N. D., 2008. Factors affecting the accumulation of of organic-rich deposits in a modern avulsive floodplain: examples from the Cumberland marshes, Saskatchewan, Canada. *Journal of Sedimentary Research*, v. **78**, p. 683-692.

Davison, I., 2005. Central Atlantic margin basins of North West Africa: Geology and hydrocarbon potential (Morocco to Guinea). *Journal of African Earth Sciences*, v. **43**, p. 254-274.

Davison, I., 2007. Geology and tectonics of the South Atlantic Brazilian salt basins. *Geological Society, London, Special Publications*, v. **272**, p. 345-359.

Davison, I., Bate, R., and Reeves, C., 2004. Early opening of the South Atlantic: Berriasian rifting to Aptian salt deposition. *PESGB/HGS 3rd International Joint Meeting - Africa: the continent of challenge and opportunity*, London, 7-8th September 2004.

De Lima, M. R., 1980. Formação Santana (Cretáceo do Nordeste do Brasil). III. Descrição sistemática dos polens da turma plicates (subturma costates). *Revista de la Asociación Paleontológica Argentina*, v. **1**, p. 15-47.

De Lima, M. R., 1983. Paleoclimatic reconstruction of the Brazilian Cretaceous based on palynological data. *Revista Brasileira de Geociências*, v. **13**, p. 223-228.

Dejax, J., 1987. Une étude palynologique dans le Crétacé inférieur du Congo, Thèse Université Paris VI, 186 pp.

Dejax, J., and Brunet, M., 1996. Les flores fossils du Basinn d’Hama-Koussou, Crétacé inférieur du Nord-Cameroun: corrélations biochronologiques avec le fossé de la Bénoué, implications paléogeographiques. In: S. Jardine, I. De Klasz, and J.-P. Debenay, eds., *Géologie de l'Afrique et de l'Atlantique Sud: Actes Colloques d'Angers, 1994*, Elf Aquitaine, Mémoire 16, p. 145-173.

Dessauvagie, T. F. J., 1974. Explanatory notes to the geological map of Nigeria. *Journal of Mining and Geology*, v. **1&2**, p. 1-28.

Dinis, P., and Soares, A. F., 2007. Controlling factors on clay mineral assemblages: insghts from facies analysis of Pliocene to Pleistocene coastal margin deposits, Western Portugal. *Geologica Acta*, v. **5**, p. 177-192.

Doyle, J. A., 1992. Revised palynological correlations of the lower Potomac Group (USA) and the Cocobeach sequence of Gabon (Barremian-Aptian). *Cretaceous Research*, v. **13**, p. 337-349

Doyle, J. A., Jardine, S., and Dorenkamp, A., 1982. Afropollis, a new genus of early angiosperm pollen, with notes on the Cretaceous palynostratigraphy and paleoenvironments of northern Gondwana. *Bulletin des Centres de Recherches Exploration-Production Elf-Aquitaine*, v. **6**, p. 39-117.

Doyle, J. A., Biens, P., Doerenkamp, A., and Jardiné, S., 1977. Angiosperm pollen from the Pre-Albian Lower Cretaceous of equatorial Africa. *Bulletin des Centres de Recherches Exploration-Production Elf-Aquitaine*, v. **1**, p. 451-473.

Dumort, J. C., 1968. *Notice explicative sur la feuille Douala-Ouest*. Direction des Mines et de Geologie, Cameroun, 69 pp.

Eberth, D. A., and Miall, A. D., 1991. Stratigraphy, sedimentology and evolution of a vertebrate-bearing, braided to anastomosed fluvial system, Cutler Formation (Permian-Pennsylvanian), north-central New Mexico. *Sedimentary Geology*, v. **72**, p. 225-252.

Edet, A., and Okereke, C. S., 2014. Hydrogeologic framework of the shallow aquifers in the Ikom–Mamfe Embayment, Nigeria using an integrated approach. *Journal of African Earth Sciences*, v. **92**, p. 25-44.

Edet, E. A., Teme, S. C., and Esu, E. O., 1994. Lineament analysis for groundwater exploration in Precambrian Oban Massif and Obudu plateau, S.E. Nigeria. *Journal of Mining and Geology*, v. **30**, p. 87-96.

Ehinola, O. A., Sonibare, O. O., Javie, D. M., and Oluwole, E. A., 2008. Geochemical apraisal of organic matter in the Mid-Cretaceous sediments of the Calaba Flank, southeastern Nigeria. *European Journal of Scientific Research*, v. **23**, p. 567-577.

Ekwere, S. J., and Ukpong, E. E., 1994. Geochemistry of saline groundwater in Ogoja, Cross, River State of Nigeria. *Journal of Mining and Geology,* v. **30**, p. 11-15.

Ekwueme, B. N., and Kröner, A., 2006. Single zircon ages of migmatitic gneisses and granulites in theObudu Plateau: Timing of granulite-facies metamorphism in southeastern Nigeria. *Journal of African Earth Sciences*, v. **44**, p. 459-469.

Ekwueme, B. N., Caen-Vachette, M., and Onyeagocha, A. C., 1991. Isotopic ages from the Oban Massif and southeast Lokoja: implications for the evolution of the Basement Complex of Nigeria. *Jouraal of African Earth Scieaces*, v. **12**, p. 489-503.

Elsheikh, A. A., Gao, S. S., and Liu, K. H., 2014. Formation of the Cameroon Volcanic Line by lithospheric basal erosion: Insight from mantle seismic anisotropy. *Journal of African Earth Sciences*, v. **100**, p. 96-108.

Ercegovac, M., and Kostiæ, A., 2006. Organic facies and palynofacies: Nomenclature, classification and applicability for petroleum source rock evaluation. *International Journal of Coal Geology*, v. **68**, p. 70-78.

Eseme, E., Agyingi, C. M., and Foba-Tendo, J., 2002. Geochemistry and genesis of brine emanations from Cretaceous strata of the Mamfe Basin, Cameroon. *Journal of African Earth Sciences*, v. **35**, p. 467-476.

Eseme, E., Littke, R., and Agyingi, C. M., 2006a. Geochemical characterization of a Cretaceous black shale from the Mamfe Basin, Cameroon. *Petroleum Geoscience*, v. **12**, p. 69-74.

Eseme, E., Abanda, P. A., Agyingi, C. M., Foba-Tendo, J., and Hannigan, R. E., 2006b. Composition and applied sedimentology of salt from brines of the Mamfe Basin, Cameroon. *Journal of Geochemical Exploration*, v. **91**, p. 41-55.

Eyong, J. T., 2003. Litho - Biostratigraphy of the Mamfe Cretaceous Basin, S.W. Province of Cameroon – West Africa. Ph.D thesis, University of Leeds, 265 pp.

Eyong, J. T., Wignall, P., Fantong, W. Y., Best, J., and Hell, J. V., 2013. Paragenetic sequences of carbonate and sulphide minerals of the Mamfe Basin (Cameroon):

Indicators of palaeo-fluids, palaeo-oxygen levels and diagenetic zones. *Journal of African Earth Sciences*, v. **86**, p. 25-44.

Fairhead, J. D., 1988. Mesozoic plate tectonic reconstructions of the central South Atlantic Ocean: The role of the West and Central African rift system. *Tectonophysics*, v. **155**, p. 181-191.

Fairhead, J. D., and Binks, R. M., 1991. Differential opening of the Central and South Atlantic Oceans and the opening of the West African rift system. *Tectonophysics*, v. **187**, p. 191-203.

Fairhead, J. D., Okereke, C. S., and Nnange, J. M., 1991. Crustal structure of the Mamfe basin, West Africa, based on gravity data. *Tectonophysics*, v. **186**, p. 351-358.

Ferber, C. T., and Wells, N. A., 1995. Paleolimnology and taphonomy of some fish deposits in “Fossil” and “Uinta” Lakes of the Eocene Green River Formation, Utah and Wyoming. *Palaeogeography, Palaeoclimatology, Palaeoecology*, v. **117**, p. 185-210.

Fielding, C. R., Allen, J. P., Alexander, J., and Gibling, M. R., 2009. Facies model for fluvial systems in the seasonal tropics and subtropics. *Geology*, v. **37**, p. 623-626.

Firth, J. V., 1993. Palynofacies and thermal maturation analysis of sediments from the Nankai Trough. *Proceedings of the Ocean Drilling Program, Scientific Results*, v. **131**, p. 57-69.

Fitton, J. G., 1980. The Benue trough and cameroon line -- A migrating rift system in West Africa. *Earth and Planetary Science Letters*, v. **51**, p. 132-138.

Fitton, J. D., and Dunlop, H. M., 1985. The Cameroon Line, West Africa and its bearing on the origin of oceanic and continental alkali basalts. *Earth and Planetary Science Letters*, v. **72**, p. 23-38.

Flemming, B. W., 2003. Flaser. In: G. V. Middleton, ed., *Encyclopadia of Sediments and Sedimentary Rocks*, Kluwer Academic Press Publishers, Dordrecht, p. 282-283.

Forey, P. L., and Cavin, L., 2007. A New Species of Cladocyclus (Teleostei: Ichthyodectiformes) from the Cenomanian of Morocco. *Palaeontologia Electronica*, v. **3**, p. 1-12.

Garcia, A. J. V., da Rosa, A. A. S., and Goldberg, K., 2005. Paleoenvironmental and paleoclimatic control on early diagenetic processes and fossil record in Cretaceous continental sandstones of Brazil. *Journal of South American Earth Sciences*, v. **19**, p. 243-258.

García-Del-Cura, M. Á., Sanz-Montero, M. E., De-los-Ríos, M. A., and Ascaso, C., 2014. Microbial dolomite in fresh water carbonate deposits. *Sedimentology*, v. **61**, p. 41-55.

Genik, G. J., 1992. Regional framework, structural and petroleum aspects of rift basins in Niger, Chad and the Central African Republic (C.A.R.). *Tectonophysics*, v. **213**, p. 169-185.

Genik, G. J., 1993. Petroleum geology of Cretaceous-Tertiary Rift Basins in Niger, Chad and Central African Republic. *AAPG Bulletin*, v. **77**, p. 1405-1434.

Gerbeth, A., Wahmhoff, A., Wieß, K. H., and Wojoiechowski, A., 1976, Geological map of Nigeria (1: 1,000,000): Deutsche Forschungsgemeinschaft.

Gierlowski-Kordesch, E. H., 2010. Lacustrine carbonates. In: A. M. Alonso-Zarza, and L. H. Tanner, eds., *Carbonates in Continental Settings: Facies, environments and Processes*: Developments in Sedimentology Elsevier, Amsterdam, p. 1-101.

Gill, R., 2010. *Igneous Rocks and Processes: A Practical Guide*. 1st edn. John Wileys & Sons Ltd, Oxford, 428 pp.

Gindre-Chanu, L., Warren, J. K., Puigdefabregas, C., Sharp, I. R., Peacock, D. C. P., Swart, R., Poulsen, R., Ferreira, H., and Henrique, L., 2015. Diagenetic evolution of Aptian evaporites in the Namibe Basin (south-west Angola). *Sedimentology*, v. **62**, p. 204-233.

Gomes, N. S., and Fernandes, S. M., 1995. Contribution to the petrology and diagenesis of the hyaloclastites of Macau Formation, Potiguar Basin, RN, Brazil. *Boletim de Geociências da PETROBRAS*, v. **9**, p. 223-236.

Gouw, M. J. P., 2007. Alluvial architecture of fluvio-deltaic successions: a review with special reference to Holocene settings. *Netherlands Journal of Geosciences / Geologie en Mijnbouw*, v. **86**, p. 211-227.

Grant, N. K., 1971. South Atlantic, Benue Trough, and Gulf of Guinea Cretaceous Triple Junction. *Geological Society of America Bulletin*, v. **82**, p. 2295-2298.

Guggenheim, S., Bain, D. C., Bergaya, F., Brigatti, M. F., Drits, V. A., Eberl, D. D., Formoso, M. L. L., Galán, E., Merriman, R. J., Peacor, D. R., Stanjek, H., and Watanabe, T., 2002. Report of the Association Internationale pour l'Etude des Argiles (AIPEA) Nomenclature Committee for 2001: Order, disorder and crystallinity in phyllosilicates and the use of the 'Crystallinity Index'. *Clay Minerals*, v. **37**, p. 389-393.

Guillemain, C., 1908. Ergebnisse geologischer Forschung im deuschen Schutzgebit Kamerun. *Mitt.aus den Deutschen Schutzgebieten*, v. **21**, p. 15-33.

Guillemain, C., and Harbort, E., 1909. Profil der Kreideschichten am Mungo. Beiträge zur Geologie von Kamerun, No. 17. *Abhandlungen der Königlichen Preußischen Geologischen Landesanstalt, Neue Folge*, v. **62**, p. 405-432.

Guiraud, M., 1990. Tectono-sedimentary framework of the early Cretaceous Continental Bima Formation (Upper Benue Trough, NE Nigeria). *Journal of African Earth Sciences*, v. **10**, p. 341-353.

Guiraud, R., and Maurin, J.-C., 1992. Early Cretaceous rifts of Western and Central Africa: an overview. *Tectonophysics*, v. **213**, p. 153-168.

Guiraud, R., Binks, R. M., Fairhead, J. D., and Wilson, M., 1992. Chronology and geodynamic setting of Cretaceous-Cenozoic rifting in West and Central Africa. *Tectonophysics*, v. **213**, p. 227-234.

Guiraud, R., Bosworth, W., Thierry, J., and Delplanque, A., 2005. Phanerozoic geological evolution of Northern and Central Africa: An overview. *Journal of African Earth Sciences*, v. **43**, p. 83-143.

Hallam, A., 1967. The depth significance of shales with bitumenous laminae. *Marine Geology*, v. **5**, p. 494.

Halliday, A. N., Dickin, A. P., Fallick, A. E., and Fitton, J. G., 1988. Mantle dynamics: a Nd, Sr, Pb, and O isotopic study of the Cameroon Line Volcanic Chain. *Journal of Petrology*, v. **29**, p. 181-211.

Haq, B. U., 2014. Cretaceous eustasy revisited. *Global and Planetary Change*, v. **113**, p. 44-58.

Haq, B. U., Hardenbol, J., and Vail, P. R., 1987. Chronology of fluctuating sea levels since the Triassic (250 million years ago to present). *Science*, v. **235**, p. 1156-1167.

Harris, N. B., Freeman, K. H., Pancost, R. D., White, T. S., and Mitchell, G. D., 2004. The character and origin of lacustrine source rocks in the Lower Cretaceous synrift section, Congo Basin, west Africa. *AAPG Bulletin*, v. **88**, p. 1163-1184.

Hart, G. F., 1996. Maceral palynofacies of Louisiana deltaic plain in terms of organic constituents and hydrocarbon potentials. In: A. Traverse, ed., *Sedimentation of Organic Particles*, Cambridge, New York, p. 141-176.

Heimhofer, U., and Hochuli, P.-A., 2010. Early Cretaceous angiosperm pollen from a low-latitude succession (Araripe Basin, NE Brazil). *Review of Palaeobotany and Palynology*, v. **161**, p. 105-126.

Heimhofer, U., Hochuli, P.-A., Burla, S., Oberli, F., Adatte, T., Dinis, J. L., and Weissert, H., 2012. Climate and vegetation history of western Portugal inferred from Albian near-shore deposits (Galé Formation, Lusitanian Basin). *Geological Magazine*, v. **149**, p. 1046-1064.

Heine, C., 2007. Formation and evolution of intracontinental sedimentary basins. Ph.D. thesis, School of Geosciences, The University of Sydney, Australia.

Hell, J. V., Ngako, V., Béa, V., Olinga, J. B., and Eyong, J. T., 2000. Rapport final des travaux sur l'étude de reconnaissance géologique et géophysique du bassin sedimentaire de Mamfe. IRGM-SNH, unpublished report, 50 pp.

Herngreen, G. F. W., 1974. Middle Cretaceous palynomorphs from northeastern Brazil. *Sciences Géologiques, Bulletin*, v. **27**, p. 101-116.

Herngreen, G. F. W., 1998. Cretaceous sporomorph provinces and events in the equatorial region. *Zentralblatt für Geologie und Paläontologie II*, v. **11/12**, p. 1313-1323.

Herngreen, G. F. W., and Chlonova, A. F., 1981. Cretaceous microfloral provinces. *Pollen et Spores*, v. **23**, p. 441-555.

Herngreen, G. F. W., Kedves, M., Rovnina, L. V., and Smirnova, S. B., 1996. Cretaceous palynofloral provinces: a review. In: J. Jansonius, and D. C. McGregor, eds., *Palynology: principles and applications*, American Association of Stratigraphic Palynologists Foundation, Dallas, p. 1157-1188.

Hessel, M. H. R., de Lima, M. R., Carvalho, I. S., and Fernandes, A. C. S., 1994. The Rio do Peixe Basin. In: G. Beurlen, D. d. A. Campos, and M. C. Vivers, eds., *Stratigraphic range of Cretaceous mega- and microfossils of Brazil*, Universidade Federal do Rio de Janeiro, Rio de Janeiro, p. 353-370.

Hillier, R. D., Waters, R. A., and Marriott, S. B., 2011. Alluvial fan and wetland interactions: evidence of seasonal slope wetlands from the Silurian of south central Wales, UK. *Sedimentology*, v. **58**, p. 831-853.

Hofmann, P., Duckensell, M., Chpitsglous, A., and Schwark, L., 2005. Geochemical and organic petrological characterization of the organic matter of lacustrine Eocene oil shales (Prinz von Hessen, Germany): reconstruction of the depositional environment. *Journal of Paleolimnology*, v. **33**, p. 155-168.

Hoque, M., 1977. Petrographic differentiation of tectonically controlled Cretaceous sedimentary cycles, southeastern Nigeria. *Sedimentary Geology*, v. **17**, p. 235-245.

Hoque, M., 1984. Pyroclastics from the lower Benue trough of Nigeria and their tectonic implications. *Journal of African Earth Sciences*, v. **2**, p. 351-358.

Hoque, M., and Nwajide, C. S., 1984. Tectono-sedimentary evolution of an elongated intracratonic basin (aulacogen): the case study of the Benue Trough of Nigeria. *Journal of Mining and Geology*, v. **21**, p. 19-26.

Hourcq, V., 1956. Bassins sedimentaires du Cameroun. In: E. J. Guzman, ed., *Symposium sobre Yacimientos de petroleo y Gas, xx Congreso Geologico international, Mexico*, p. 45-68.

Hughes, N. F., Drewry, G. E., and Laing, J. F., 1979. Barremian earliest angiosperm pollen. *Palaeontology*, v. **22**, p. 513-535.

Hunt, J. M., 1995. *Petroleum Geochemistry and Geology*. Freeman and Company, New York, 743 pp.

Ibrahim, M. I. A., 2002. New angiosperm pollen from the upper Barremian-Aptian of the Western Desert, Egypt. *Palynology*, v. **26**, p. 107-133.

Iliya, A. G., and Bassey, N. E., 1993. A regional study of Oban and Obudu Precambian Massifs, southeastern Nigeria. *Journal of Mining and Geology*, v. **29**, p. 101-110.

Ingram, R. L., 1954. Terminology for the thickness of stratification and parting units in sedimentary rocks. *Bulletin of the Geological Society of America*, v. **65**, p. 937-938.

Iverson, R. M., 1997. The physics of debris flows. *Reviews of Geophysics*, v. **35**, p. 245-296.

Iverson, R. M., 2003. Gravity-driven mass flows. In: G. V. Middleton, ed., *Encyclopedia of Sediments and Sedimentary Rocks*, Kluwer Academic Publishers, Dordrecht, p. 347-353.

Iverson, R. M., 2014. Debris flows: behaviour and hazard assessment. *Geology Today*, v. **30**, p. 15-20.

Jaekel, O., 1909. Fischreste aus der Mamfe-Schiefern. Beiträge zur Geologie von Kamerun, No. 10. *Abhandlungen der Königlichen Preußischen Geologischen Landesanstalt, Neue Folge*, v. **62**, p. 392-398.

Jan du Chêne, R., 2000. Palynologyical study of the Lower Cretaceous section from the well ISE-2, Nigeria. Geological implications for the deep offshore interpretation of the Benin Embayment. *Africa Geoscience Review*, v. **7**, p. 1-17.

Jan du Chêne, R., De Klasz, I., and Archibong, E. E., 1978. Biostratigraphic study of the borehole Ojo-1, SW Nigeria, with special emphasis on the Cretaceous microflora. *Revue de Micropaléontologie*, v. **21**, p. 123-139.

Jardiné, S., 1974. Microflores des formations du Gabon attribuées au Karoo. *Review of Palaeobotany and Palynology*, v. **17**, p. 75-112.

Jardiné, S., and Magloire, L., 1965. Palynologie et stratigraphie du Crétacé des bassins du Sénégal et de Cote d'Ivoire. *Mem. Bur. Rech. Géol. Minières*, v. **32**, p. 187-245.

Jardiné, S., Biens, P., and Doerenkamp, A., 1974. Dicheiropollis etruscus, un pollen caractéristique du Crétacé Inférieur Afro-Sudaméricain. Conséquences pour l'évaluation des unités climatiques et implications dans la dérive des continents. *Sci. Géol., Bull.*, v. **27**, p. 87-100.

Javor, B. J., and Mountjoy, E. W., 1976. Late Proterozoic microbiota of the Miette Group, southern British Columbia. *Geology*, v. **4**, p. 111-119.

Kah, H. K., 2006. A priceless commodity: the politics of salt production and commercialisation in the Cross River Basin of Cameroon 1916-1961. *African Study Monographs*, v. **27**, p. 1-13.

Kamguia, J., Nouayou, R., Tabod, C. T., Tadjou, J. M., Manguelle-Dicoum, E., and Kande, H. L., 2008. Geophysical signature of geological units inferred from the analysis of geoid maps in Cameroon and its surroundings. *Journal of African Earth Sciences*, v. **52**, p. 1-8.

Kampunzu, A. B., and Popoff, M., 1991. Distribution of the main Phanerozoic African rifts and associated magmatism: introductory notes. In: A. B. Kampunzu, and R. T. Lubala, eds., *Magmatism in Extensional Structural Settings*, Springer-Verlag, Berlin, p. 2–10.

Karner, G. D., and Gambôa, L. A. P., 2007. Timing and origin of the South Atlantic pre-salt sag basins and their capping evaporites. *Geological Society, London, Special Publications*, v. **285**, p. 15-35.

Katz, B. J., 1995. Facotrs controlling the development of lacustrine petroleum source rocks - an update. In: A. Y. Huc, ed., *Paleogeography, Paleoclimate and Source Rocks*: AAPG Studies in Geology, The American Association of Petroleum Geologists, Tulsa, p. 61-79.

Keighley, D., 2008. A lacustrine shoreface succession in the Albert Formation, Moncton Basin, New Brunswick. *Bulletin of Canadian Petroleum Geology*, v. **56**, p. 235-258.

Kelts, K., 1988. Environments of deposition of lacustrine petroleum source rocks: an introduction. In: A. Fleet, K. Kelts, and M. R. Talbot, eds., *Lacustrine Petroleum Source Rocks*: Geological Society Special Publication, p. 3-26.

Kim, W., Connell, S. D., Steel, E., Smith, G. A., and Paola, C., 2011. Mass-balance control on the interaction of axial and transverse channel systems. *Geology*, v. **39**, p. 611-614.

Kissaaka, J. B. I., Ntamak-Nida, M. J., Ngueutchoua, G., Owono, F. M., Nitcheu, A. L. D., Kuetche, P. G. F., and Bourquin, S., 2012. Syn-rift tectonic markers from outcrops and offshore seismic data of the southern part of Kribi-Campo sub-basin (Cameroon, West African margin). *Comunicações Geológicas*, v. **99**, p. 35-42.

Klappa, C. F., 1980. Rhizoliths in terrestrial carbonates: classification, recognition,genesis and significance. *Sedimentology*, v. **27**, p. 613-629.

Kogbe, C. A., and Me'hes, K., 1986. Micropaleontology and biostratigraphy of the coastal basins of West Africa. *Journal of African Earth Sciences (1983)*, v. **5**, p. 1-100.

Kraus, M. J., 1999. Paleosols in clastic sedimentary rocks: their geologic applications. *Earth-Science Reviews*, v. **47**, p. 41-70.

Kraus, M. J., 2002. Basin-scale changes in floodplain paleosols:implications for interpreting alluvial architecture. *Journal of Sedimentary Research*, v. **72**, p. 500-509.

Kraus, M. J., and Riggins, S., 2007. Transient drying during the Paleocene–Eocene Thermal Maximum (PETM): Analysis of paleosols in the bighorn basin, Wyoming. *Palaeogeography, Palaeoclimatology, Palaeoecology*, v. **245**, p. 444-461.

Kübler, B., 1990. "Cristallinité" de l'illite et mixed-layers: breve révision. *Schweizer Mineralogische und Petrographische Mitteilungen*, v. **70**, p. 89-93.

Kübler, B., and Jaboyedoff, M., 2000. Illite crystallinity. *Comptes Rendue de l'Académie des Science*, v. **331**, p. 75-89.

Lajoie, J., 1984. Volcaniclastic rocks. In: R. G. Walker, ed., *Facies Models*, Geoscience Canada, v. **2**, p. 39-52.

Lamb, M. P., and Mohrig, D., 2009. Do hyperpycnal-flow deposits record river-flood dynamics? *Geology*, v. **37**, p. 1067-1070.

Lambiase, J. J., 1990. A model for tectonic control of lacustrine stratigraphic sequences in a continental rift basin. In: B. K. Katz ed., *Lacustrine basin exploration - case studies and modern analogs*, AAPG Memoir v. **50**, p. 265-273.

Lana, C. C., and Carvalho, I. S., 2002. Cretaceous conchostracans from Potiguar Basin (northeast Brazil): relationships with West African conchostracan faunas and palaeoecological inferences. *Cretaceous Research*, v. **23**, p. 351-362.

Lawal, O., 1991. Palynological age and correlation of a black shale section in the Eze-Aku formation, lower benue trough, Nigeria. *Journal of African Earth Sciences (and the Middle East)*, v. **12**, p. 473-482.

Lawal, O., and Moullade, M., 1986. Palynological biostratigraphy of Cretaceous sediments in the Upper Benue Basin, N. E. Nigeria. *Revue de Micropaléontologie*, v. **29**, p. 61-83.

Le Fur, Y., 1965. Mission Socle Crétacé: Rapport de fin de campagne 1964-1965 sur les indices de plomb & zinc du Golfe de Mamfé. B. R. G. M. Cameroon, 30 pp.

Le Maitre, R. W., and IUGS, 2002. *Igneous Rocks: A Classification and Glossary of Terms*. 2 edn. Cambridge University Press, New York, 236 pp.

Lee, J. I., and Lee, Y. I., 2001. Kübler illite "crystallinity" index of the Cretaceous Gyeongsang basin, Korea: implications for basin evolution. *Clays and Clay Minerals*, v. **49**, p. 36-43.

Leeder, M. R., 1982. *Sedimentology – Process and Product*. George Allen & Unwin, London, 344 pp.

Leeder, M., 2011. *Sedimentology and Sedimentary Basins: From Turbulence to Tectonics*. 2nd edn. Wiley-Blackwell, Oxford, 768 pp.

Leeder, M. R., Mack, G. H., and Salyards, S. L., 1996. Axial–transverse fluvial interactions in half-graben: Plio-Pleistocene Palomas Basin, southern Rio Grande Rift, New Mexico, USA. *Basin Research*, v. **8**, p. 225-241.

Lefranc, J. P., and Guiraud, R., 1990. The continental intercalaire of northwestern Sahara and its equivalents in the neighbouring regions. *Journal of African Earth Sciences (and the Middle East)*, v. **10**, p. 27-77.

Lijmbach, G. W., 1975. On the origin of petroleum. *Proceeings of the 9th World Petroleum Congress*. London, Applied Science Publishers, p. 357-369.

Mabesoone, J. M., Viana, M. S. S., and Neumann, V. H., 2000. Late Jurassic to Mid-Cretaceous lacustrine sequences in the Araripe-Potiguar Depression of Northeastern Brazil. In: E. H. Gierlowski-Kordesch, and K. R. Kelts, eds., *Lake Basins through Space and Time*: AAPG Studies in Geology, The American Association of petroleum Geologists, Tulsa, p. 197-208.

Mack, G. H., and James, W. C., 1994. Paleoclimate and global distribution of paleosols. *Journal of Geology*, v. **102**, p. 360-366.

Mack, G. H., James, W. C., and Monger, H. C., 1993. Classification of paleosols. *Geological Society of America Bulletin*, v. **105**, p. 129-136.

Mack, G. H., Hook, S., Giles, K. A., and Cobban, W. A., 2015. Sequence stratigraphy of the Mancos Shale, lower Tres Hermanos Formation, and coeval middle Cenomanian to middle Turonian strata, southern New Mexico, USA. *Sedimentology*, p. n/a-n/a.

Maisey, J. G., 2000. Continental break up and the distribution of fishes of Western Gondwana during the Early Cretaceous *Cretaceous Research*, v. **21**, p. 281-314.

Maluski, H., Coulon, C., Popoff, M., and Baudin, P., 1995. $^{40}Ar/^{39}Ar$ chronology, petrology and geodynamic setting of Mesozoic to early Cenozoic magmatism from the Benue Trough, Nigeria. *Journal of the Geological Society, London*, v. **152**, p. 311-326.

Martínez, M. A., Prámparo, M. B., Quattrocchio, M. E., and Zavala, C. A., 2008. Depositional environments and hydrocarbon potential of the Middle Jurassic Los Molles Formation, Neuquén Basin, Argentina: palynofacies and organic geochemical data. *Revista Geológica de Chile*, v. **35**, p. 279-305.

Martins-Neto, M. A., and Catuneanu, O., 2010. Rift sequence stratigraphy. *Marine and Petroleum Geology*, v. **27**, p. 247-253.

Marzoli, A., Piccirillo, E. M., Renne, P. R., Bellieni, G., Lacumin, M., Nyobe, J. B., and Tongwa, A. T., 2000. The Cameroon Volcanic Linine revisited: petrogenesis of the continental basaltic magmas from lithospheric and asthenospheric mantle sources. *Journal of Petrology*, v. **41**, p. 87-109.

Mateer, N. J., Wycisk, P., Jacobs, L. L., Brunet, M., Luger, P., Arush, M. A., Hendriks, F., Weissbrod, T., Gvirtzman, G., Mbede, E., Dina, A., Moody, R. T. J., Weigelt, G., El-Nakhal, U. A., Hell, J., and Stets, J., 1992. Correlation of nonmarine Cretaceous strata of Africa and the Middle East. *Cretaceous Research*, v. **13**, p. 273-318.

Matos, R. M. D., 1992. The Northeast Brazilian rift system. *Tectonics*, v. **11**, p. 766-791.

Matsumoto, T., 1980. Inter-regional correlation of transgressions and regressions in the Cretaceous period. *Cretaceous Research*, v. **1**, p. 359-373.

Maurin, J. C., and Guiraud, R., 1990. Relationships between tectonics and sedimentation in the Barremo-Aptian intracontinental basins of Northern Cameroon. *Journal of African Earth Sciences*, v. **10**, p. 331-340.

McFarlane, M. J., 1991. Some sedimentary aspects of lateritic weathering profile development in the major bioclimatic zones of tropical Africa. *Journal of African Earth Sciences (and the Middle East)*, v. **12**, p. 267-282.

Meléndez, N., Liesa, C. L., Soria, A. R., and Meléndez, A., 2009. Lacustrine system evolution during early rifting: El Castellar Formation (Galve sub-basin, Central Iberian Chain). *Sedimentary Geology*, v. **222**, p. 64-77.

Miall, A. D., 1985. Architectural-element analysis: a new method of facies analysis applied to fluvial deposits. *Earth-Science Reviews*, v. **22**, p. 261-308.

Miall, A. D., 1996. *The Geology of Fluvial Deposits - Sedimentary Facies, Basin Analysis, and Petroleum Geology*. Springer, Berlin, 582 pp.

Miall, A. D., 2010. Alluvial Deposits. In: N. P. James, and R. W. Dalrymple, eds., *Facies Models 4*, Geological Association of Canada, Canada, p. 105-137.

Mohriak, W. U., Szatmari, P., and Anjos, S., 2012. Salt: geology and tectonics of selected Brazilian basins in their global context. In: G. I. Alsop, S. G. Archer, A. J. Hartley, N. T. Grant, and R. Hodgkinson, eds., *Salt Tectonics, Sediments and Prospectivity*, Geological Society, London, Special Publications, v. **361**, p. 131-158.

Moulin, M., Aslanian, D., and Unternehr, P., 2010. A new starting point for the South and Equatorial Atlantic Ocean. *Earth-Science Reviews*, v. **98**, p. 1-37.

Murat, R. C., 1972. Stratigraphy and paleogeography of the Cretaceous and lower Tertiary in southern Nigeria. In: T. F. J. Dessauvagie, and A. J. Whiteman, eds., *African Geology*, Ibadan University Press, Ibadan, p. 251-266.

Nanson, G. C., and Croke, J. C., 1992. A genetic classification of floodplains. *Geomorphology*, v. **4**, p. 459-486.

Nanson, G. C., and Gibling, M. R., 2003. Rivers and alluvial fans. In: G. V. Middleton, ed., *Encyclopedia of Sediments and Sedimentary Rocks*, Kluwer Academic Publishers, Dordrecht, p. 568-583.

Ndougsa-Mbarga, T., Manguelle-Dicoum, E., Campos-Enriquez, J.-O., and Atangana, Q. Y., 2007. Gravity anomalies, sub-surface structure and oil and gas migration in the Mamfe, Cameroon-Nigeria, sedimentary basin. *Geofísica Internacional*, v. **46**, p. 129-139.

Neba, A. S., 1987. *Modern Geography of the Republic of Cameroon*. 2 edn. Neba Publishers, New Jersey, 204 pp.

Ngako, V., Njonfang, E., Aka, F. T., Affaton, P., and Nnange, J. M., 2006. The North-South Paleozoic to Quaternary trend of alkaline magmatism from Niger-Nigeria to Cameroon: Complex interaction between hotspots and Precambrian faults. *Journal of African Earth Sciences*, v. **45**, p. 241-256.

Nguene, F. R., Tamfu, S. F., Loule, J. P., and Ngassa, C., 1992. Palaeoenvironnements of the Douala and Kribi-Campo sub-basins, in Cameroon, West Africa. In: R. Curnelle, ed., *Géologie Africaine: 1er Colloque de Stratigraphie et de paléogéographie des bassins sédimentaires Ouest-Africains; 2ème Colloque Africain de Micropaléontologie, Libreville - Gabon, 6 - 8 mai 1991; recueil des communications*, Elf Aquitaine, Boussens, p. 129-139.

Ngwa, J. A., ed., 1985. Atlas of Cameroon. Collin <> Longman, 33 pp.

Njanko, T., Nédélec, A., and Affaton, P., 2006. Synkinematic high-K calc-alkaline plutons associated with the Pan-African Central Cameroon shear zone (W-Tibati area): Petrology and geodynamic significance. *Journal of African Earth Sciences*, v. **44**, p. 496-510.

Njilah, I. K., 1991. Geochemistry and Petrogenesis of Tertiary-Quaternary Volcanic Rocks from Oku-Ndu area, N.W. Cameroon. Ph.D thesis, University of Leeds, 345 pp.

Njilah, I. K., Ajonina, H. N., Kamgang, K. V., Tchindjang, M., and Tessi, V., 2004. K-Ar ages, mineralogy, major and trace element geochemistry of the Tertiary-Quaternary lavas from the Ndu Volcanic Ridge N.W. Cameroon. *African Journal of Science and Technology*, v. **5**, p. 47-56.

Nkono, C., Féménias, O., and Demaiffe, D., 2014. Geodynamic model for the development of the Cameroon Hot Line (Equatorial Africa). *Journal of African Earth Sciences*, v. **100**, p. 626-633.

Ntamak-Nida, M. J., Baudin, F., Schnyder, J., Makong, J. C., Komguem, P. B., and Abolo, G. M., 2008. Depositional environments and characterisation of the organic matter of the Lower Mundeck Formation (Barremian?-Aptian) of the Kribi-Campo sub-basin (South Cameroon): Implications for petroleum exploration. *Journal of African Earth Sciences*, v. **51**, p. 207-219.

Ntamak-Nida, M. J., Bourquin, S., Makong, J. C., Baudin, F., Mpesse, J. E., Ngouem, C. I., Komguem, P. B., and Abolo, G. M., 2010. Sedimentology and sequence stratigraphy from outcrops of the Kribi-Campo sub-basin: Lower Mundeck Formation (Lower Cretaceous, southern Cameroon). *Journal of African Earth Sciences*, v. **58**, p. 1-18.

Nton, M. E., 1990. Sedimentology and depositional environments of Awi Formation, Calabar

Flank, S. E. Nigeria. M.Sc. thesis, University of Ibadan, Ibadan, 82 pp.

Nwachukwu, S. O., 1972. The tectonic evolution of the southern portion of the Benue Trough, Nigeria. *Geological Magazine*, v. **109**, p. 411-419.

Nwajide, C. S., and Reijers, T. J. A., 1996. Sequence archtecture in outcrops. Examples from the Anambra Basin, Nigeria. *NAPE Bulletin*, v. **11**, p. 23-32.

Nyong, E. E., and Ramanathan, R. M., 1985. A record of oxygen-deficient paleoenvironments in the Cretaceous of the Calabar Flank, SE Nigeria. *Journal of African Earth Sciences*, v. **3**, p. 455-460.

O'Brien, N. R., 1996. Shale lamination and sedimentary processes. *Geological Society, London, Special Publications*, v. **116**, p. 23-36.

Obaje, N. G., 2009. *Geology and Mineral Resources of Nigeria*. Springer Heidelberg, 221 pp.

Obaje, N. G., Ligouis, B., and Abaa, S. I., 1994. Petrographic composition and depositional environments of Cretaceous coals and coal measures in the Middle Benue Trough of Nigeria. *International Journal of Coal Geology*, v. **26**, p. 233-260.

Obaje, N. G., Wehner, H., Scheeder, G., Abubakar, M. B., and Jauro, A., 2004. Hydrocarbon prospectivity of Nigeria's inland basins: From the viewpoint of organic geochemistry and organic petrology. *AAPG Bulletin*, v. **88**, p. 325-353.

Oboh-Ikuenobe, F. A., Obi, C. G., and Jaramillo, C. A., 2005. Lithofacies, palynofacies, and sequence stratigraphy of Palaeogene strata in Southeastern Nigeria. *Journal of African Earth Sciences*, v. **41**, p. 79-100.

O'Brien, N. R., 1996. Shale lamination and sedimentary processes. In: A. E. S. Kemp, ed., *Palaeoclimatology and Palaeoceanography from Laminated Sediments*: Geological Society Special Publication, The Geological Society, Bath, U.K., p. 23-36.

O'Brien, N. R., and Slatt, R. M., 1990. *Argillaceous Rocks Atlas*. Springer-Verlag, New York, 141 pp.

Oden, M. A., Okpamu, T. A., and Amah, E. A., 2012. Comparative analysis of fracture lineaments in Oban and Obudu areas, SE Nigeria. *Journal of Geography and Geology*, v. **4**, p. 36-47.

Oden, M. I., Egeh, E. U., and Amah, E. A., 2015. The Ikom-Mamfe basin, Nigeria: A study of fracture and mineral vein lineament trends and Cretaceous deformations. *Journal of African Earth Sciences*, v. **101**, p. 35-41.

Oden, M. I., Umagu, C. I., and Udinmwen, E., 2016. The use of jointing to infer deformation episodes and relative ages of minor Cretaceous intrusives in the western part of Ikom – Mamfe basin, southeastern Nigeria. *Journal of African Earth Sciences*, v. **121**, p. 316-329.

Odigi, M. I., and Amajor, L. C., 2008. Origin of carbonate cements in Cretaceous sandstones from Lower Benue Trough, Nigeria: evidence from petrography and stable isotope composition. *Scientia Africana*, v. **7**, p. 123-139.

Offodile, M. E., 1976. The geology of the Middle Benue, Nigeria. *Palaentological Institute, University Uppsala, Special Publication*, v. **4**, p. 1-166.

Ofoegbu, C. O., 1985. A review of the geology of the Benue Trough Nigeria. *Journal of African Earth Sciences*, v. **3**, p. 283-291.

Ofoegbu, C. O., and Onuoha, K. M., 1991. Analysis of magnetic data over the Abakaliki

Anticlinorium of the Lower Benue Trough, Nigeria. *Marine and Petroleum Geology*, v. **8**, p. 174-183.

Ojoh, K. A., 1990. Cretaceous geodynamic evolution of the southern part of the Benue Trough (Nigeria) in the equatorial domain of the south Atlantic. Stratigraphy, basin analysis and paleo-oceanography. *Bulletin des Centres de Recherches Exploration-Production Elf Aquitaine*, v. **14**, p. 419-442.

Okeke, P. O., Sowa, A. O., and Icheagwu, M. C., 1987. The thickness of the Cretaceous sediments in the southern Benue Trough, Nigeria, and its tectonic implications. In: G. Matheis, and H. Schandelmeier, eds., *Current Research in African Earth Sciences*, Balkema, Rotterdam, p. 295-298.

Olade, M. A., 1975. Evolution of Nigeria's Benue Trough (Aulacogen): a tectonic model. *Geological Magazine*, v. **112**, p. 575-583.

Olade, M. A., 1979. The Abakaliki pyroclastics of southern Benue trough Nigeria: their petrology and tectonic significance. *Journal of Mining and Geology*, v. **16**, p. 17-25.

Oti, M. N., and Koch, R., 1990. Mid Cretaceous shelf carbonates: The Mfamosing Limestone, Lower Benue Trough (Nigeria). *Facies*, v. **22**, p. 87-102.

Palynodata Inc., and White, J. M., 2008. Palynodata Datafile: 2006 version, with Introduction by J. M. White, Geological Survey of Canada Open File 5793, 1 CD-ROM.

Pedreira, A. J., and Bahia, R. B. C., 2000. Sedimentary basins of Rondônia State, Brazil: response to the geotectonic evolution of the Amazonic Craton. *Revista Brasileira de Geociências*, v. **30**, p. 477-480.

Penaye, J., Toteu, S. F., Van Schmus, W. R., and Nzenti, J. P., 1993. U–Pb and Sm–Nd preliminary geochronologic data on the Yaoundé series, Cameroon: re-interpretation of the granulitic rocks as the suture of a collision in the “Centrafrican belt”. *Comptes Rendu de l’Académie des Sciences de Paris*, v. **317**, p. 789-794.

Peters, K. E., and Cassa, M. R., 1994. Applied source rock geochemistry. In: L. B. Magoon, and W. G. Dow, eds., *The petroleum system—From source to trap*, AAPG Memoir 60, Tulsa, Oklahoma, p. 93-117.

Peters, K. E., Walters, C. C., and Moldowan, J. M., 2005a. *The Biomarker Guide: Volume 1, Biomarkers and Isotopes in the Environment and Human History*. Cambridge University Press, 474 pp.

Peters, K. E., Walters, C. C., and Moldowan, J. M., 2005b. *The Biomarker Guide: Volume 2, Biomarkers and Isotopes in Petroleum Systems and Earth History*, v. 2. Cambridge University Press, 475-1155 pp.

Petersen, H. I., Nytoft, H. P., and Nielsen, L. H., 2004. Characterisation of oil and potential source rocks in the northeastern Song Hong Basin, Vietnam: indications of a lacustrine-coal sourced petroleum system. *Organic Geochemistry*, v. **35**, p. 493-515.

Petters, S. W., 1978a. Stratigraphic evolution of the Benue Trough and its implications for the Upper Cretaceous paleogeography of West Africa. *Journal of Geology*, v. **86**, p. 311-322.

Petters, S. W., 1978b. Mid-Cretaceous paleoenvironments and biostratigraphy of the Benue Trough, Nigeria. *Geological Society of America Bulletin*, v. **89**, p. 151-154.

Petters, S. W., 1982. Central West African Cretaceous-Tertiary benthic foraminifera and stratigraphy. *Palaeontographica*, v. **Abt. A 179**, p. 1-104.

Petters, S. W., 1983. Gulf of Guinea planktonic foraminiferal biochronology and Geological history of the South Atlantic. *Journal of Foraminiferal Research*, v. **13**, p. 32-59.

Petters, S. W., 1991. *Regional Geology of Africa*. Springer Verlag, Berlin, 722 pp.

Petters, S. W., 1995. Southeastern Benue Trough and Ikom-Mamfe embayment. In: B. N. Ekwueme, E. E. Nyong, and S. W. Petters, eds., *Geological excursion guidebook to Oban Massif, Calabar Flank, Mamfe embayment, southeastern Nigeria*, Nigerian Mining and Geoscience Society, Calabar, p. 26-36.

Petters, S. W., and Ekweozor, C. M., 1982a. Petroleum geology of Benue Trough and southeastern Chad basin, Nigeria. *AAPG Bulletin*, v. **66**, p. 1141-1149.

Petters, S. W., and Ekweozor, C. M., 1982b. Origin of mid-Cretaceous black shales in the Benue Trough, Nigeria. *Palaeogeography, Palaeoclimatology, Palaeoecology*, v. **40**, p. 311-319.

Petters, S. W., Okereke, C. S., and Nwajide, C. S., 1987. Geology of Mamfe rift, S.E. Nigeria. In: G. Matheis, and H. Schandlemeier, eds., *Current Research in African Earth Sciences*, Balkema, Rotterdam, p. 299-302.

Philpotts, A. N., and Ague, J. J., 2009. *Principles of Igneous and Metamporphic Petrology*. 2nd edn. Cambridge University Press, New York, 667 pp.

Pizzuto, J. E., Moody, J. A., and Meade, R. H., 2008. Anatomy and dynamics of a floodplain, Powder River, Montana, U.S.A. *Journal of Sedimentary Research*, v. **78**, p. 16-28.

Plint, A. G., 2010. Wave- and storm-dominated shoreline and shallow-marine systems. In: N. P. James, and R. W. Dalrymple, eds., *Facies Models 4*, Geological Association of Canada, p. 167-199.

Popoff, M., 1988. Du Gondwana à l'atlantique sud: les connexions du fossé de la bénoué avec les bassins du Nord-Est brésilien jusqu'à l'ouverture du golfe de Guinée au crétacé inférieur. *Journal of African Earth Sciences (and the Middle East)*, v. **7**, p. 409-431.

Potter, P. E., 2003. Mudrocks. In: G. V. Middleton, ed., *Encyclopadia of Sediments and Sedimentary Rocks*, Kluwer Academic Press Publishers, Dordrecht, p. 451-459.

Potter, P. E., Maynard, J. B., and Depetris, P. J., 2005. *Mud and Mudstones: Introduction and Overview*. Springer-Verlag, Heidelberg, 297 pp.

Quattrocchio, M. E., and Volkheimer, W., 1990. Jurassic and Lower Cretaceous dinocysts from Argentina: Their biostratigraphic significance. *Review of Palaeobotany and Palynology*, v. **65**, p. 319-330.

Rakovan, J., 2005. A word to the wise: Pillow basalt. *Rocks & Minerals*, v. **80**, p. 287.

Rand, H. M., and Mabesoone, J. M., 1982. Northeastern Brazil and the final separation of South America and Africa. *Palaeogeography, Palaeoclimatology, Palaeoecology*, v. **38**, p. 163-183.

Rankenburg, K., Lassiter, J. C., and Brey, G., 2005. The role of continental crust and lithospheric mantle in the genesis of Cameroon Volcanic Line lavas: constraints from isotopic variations in lavas and megacrysts from the Biu and Jos Plateaux. *Journal of Petrology*, v. **46**, p. 160-190.

Reading, H. G., 2003. Facies models. In: G. V. Middleton, ed., *Encyclopadia of Sediments and Sedimentary Rocks*, Kluwer Academic Press Publishers, Dordrecht, p. 268-272.

Regali, M. S. P., 1989. Evoluçao da paleoflora no Cretaceo das margens equatorial de nordeste do Brasil. *Revista Escola de Minas*, v. **42**, p. 17-33.

Regali, M. S. P., and Viana, C. F., 1989. Late Jurassic–Early Cretaceous in Brazilian sedimentary basins: correlation with the international standard scale. Rio de Janeiro, Petróleo Brasileiro S.A. Serviço de Desenvolvimento de Recursos Humanos, p. 47-95.

Regali, M. S. P., Uesugui, N., and Santos, A. S., 1974. Palinologia dos sedimentos meso-cenozoicos do brasil (1). *Boletim technico da PETROBRAS*, v. **17**, p. 177-191.

Reijers, T. J. A., 1996. *Selected chapters on geology: sedimentary geology and sequence stratigraphy in Nigeria and three case studies and a field guide*. Shell Petroleum Development Company (SPDC), Warri, Nigeria, 197 pp.

Reijers, T. J. A., 1998. The Mfamosing Limestone in SE Nigeria: outcrop-subsurface correlation and reservoir development. *Journal of Petroleum Geology*, v. **21**, p. 467-482.

Reijers, T. J. A., and Petters, S. W., 1987. Depositional environments and diagenesis of Albian carbonates on the Calabar Flank, SE Nigeria. *Journal of Petroleum Geology*, v. **10**, p. 283-294.

Reijers, T. J. A., and Petters, S. W., 1997. Sequence stratigraphy based on microfacies analysis: Mfamosing Limestone, Calabar Flank, Nigeria. *Geologie en Mijnbouw*, v. **76**, p. 197-215.

Reineck, H. E., and Singh, I. B., 1980. *Depositional Sedimentary Environments: With Reference to Terrigenous Clastics*. 2nd edn. Springer-Verlag, Berlin, 549 pp.

Renaut, R. W., and Gierlowski-Kordesch, E. H., 2010. Lakes. In: N. P. James, and R. W. Dalrymple, eds., *Facies Models 4*, Geological Association of Canada, Canada, p. 541-575.

Retallack, G. J., 1988. Field recognition of paleosols. In: J. Reinhardt, and W. R. Sigleo, eds., *Paleosols and weathering through geologic time: Principles and applications*: Geological Society of America Special Paper p. 1-20.

Retallack, G. J., 2001. *Soils of the Past: An Introduction to Paleopedology*. 2nd edn. Blackwell Science Ltd, Oxford, 404 pp.

Reyment, R. A., 1954. The stratigraphy of the Southern Cameroons. *Geologiska Föreningens I Stockholm Förhandlingar*, v. **76**, p. 661-683.

Reyment, R. A., 1965. *Aspects of the geology of Nigeria*. Ibadan University press, Ibadan, 145 pp.

Reyment, R. A., 1980. Paleo-oceanology and paleobiogeography of the Cretaceous South Atlantic Ocean. *Oceanologica Acta*, v. **3**, p. 127-133.

Reyment, R. A., and Tait, E. A., 1972. Biostratigraphical dating of the early history of the South Atlantic Ocean. *Philosophical Transactions of the Royal Society of London. Series B, Biological Sciences*, v. **264**, p. 55-95.

Reyment, R. A., and Dingle, R. V., 1987. Palaeogeography of Africa during the Cretaceous Period. *Palaeogeography, Palaeoclimatology, Palaeoecology*, v. **59**, p. 93-116.

Ricci-Lucchi, F., and Amorosi, A., 2003. Bedding and internal structures. In: G. V. Middleton, ed., *Encyclopedia of Sediments and Sedimentary Rocks*, Kluwer Academic Publishers, Dordrecht, p. 53-59.

Roberts, S. B., Stanton, R. W., and Flores, R. M., 1994. A debris flow deposit in alluvial, coal-bearing facies, Bighorn Basin, Wyoming, USA: Evidence for catastrophic termination of a mire. *International Journal of Coal Geology*, v. **25**, p. 213-241.

Rodriguez, N. D., and Philip, R. P., 2015. Source rock facies distribution predicted from oil geochemistry in the Central Sumatra Basin, Indonesia. *AAPG Bulletin*, v. **99**, p. 2005-2022.

Romero, A. M., and Philp, R. P., 2012. Organic geochemistry of the Woodford Shale, southeastern Oklahoma: How variable can shales be? *AAPG Bulletin*, v. **96**, p. 493-517.

Rowe, N. P., and Jones, T. P., 1999. Locating and collecting. In: T. P. Jones, and N. P. Rowe, eds., *Fossil Plants and Spores: modern techniques*, Geological Society, London, p. 5-8.

Rull, V., 2002. High-impact palynology in petroleum geology: applications from Venezuela (northern South America). *AAPG Bulletin*, v. **86**, p. 279-300.

Sáez, A., Anadón, P., Herrero, M. J., and Moscariello, A., 2007. Variable style of transition between Palaeogene fluvial fan and lacustrine systems, southern Pyrenean foreland, NE Spain. *Sedimentology*, v. **54**, p. 367-390.

Salard-Cheboldaeff, M., 1990. Intertropical African palynostratigraphy from Cretaceous to Late Quaternary times. *Journal of African Earth Sciences (and the Middle East)*, v. **11**, p. 1-24.

Salard-Cheboldaeff, M., and Dejax, J., 1991. Evidence of Cretaceous to Recent West African intertropical vegetation from continental sediment spore-pollen analysis. *Journal of African Earth Sciences*, v. **12**, p. 353-361.

Salard-Cheboldaeff, M., and Boltenhagen, E., 1992. La palynologie des évaporites d'Afrique équatoriale et ses rapports avec le paléoenvironment. *Journal of African Earth Sciences*, v. **14**, p. 1991-195.

Sarmiento, L. F., and Rangel, A., 2004. Petroleum systems of the upper Magdalena Valley, Colombia. *Marine and Petroleum Geology*, v. **21**, p. 373-391.

Schieber, J., 1998. Possible indicators of microbial mat deposits in shales and sandstones: examples from the Mid-Proterozoic Belt Supergroup, Montana, U.S.A. *Sedimentary Geology*, v. **120**, p. 105-124.

Schieber, J., 2003a. Black shales. In: G. V. Middleton, ed., *Encyclopedia of Sediments and Sedimentary Rocks*, Kluwer Academic Press Publishers, Dordrecht, p. 83-85.

Schieber, J., 2003b. Depositional fabric of mudstones. In: G. V. Middleton, ed., *Encyclopadia of Sediments and Sedimentary Rocks*, Kluwer Academic Press Publishers, Dordrecht, p. 203-206.

Schieber, J., 2007. Microbial Mats on Muddy Substrates – Examples of Possible Sedimentary Features and Underlying Processes. In: J. Schieber, P. K. Bose, P. G. Eriksson, S. Banerjee, S. Sarkar, W. Altermann, and O. Catuneanu, eds., *Atlas of microbial mat features preserved within the clastic rock record*, Elsevier, p. 117-134.

Schlische, R. W., 1991. Half-graben filling models: Implications for the evolution of continental extensional basins. *Basin Research*, v. **3**, p. 123-141.

Schrank, E., 1991. Mesozoic palynology and continental sediments in NE Africa (Egypt and Sudan) - a review. *Journal of African Earth Sciences (and the Middle East)*, v. **12**, p. 363-373.

Schrank, E., 1992. Nonmarine Cretaceous correlations in Egypt and northern Sudan: palynological and palaeobotanical evidence. *Cretaceous Research*, v. **13**, p. 351-368.

Schrank, E., and Mahmoud, M. S., 1998. Palynology (pollen, spores and dinoflagellates) and Cretaceous stratigraphy of the Dakhla Oasis, central Egypt. *Journal of African Earth Sciences*, v. **26**, p. 167-193.

Scotese, C. R., Boucot, A. J., and Mckerrow, W. S., 1999. Gondwanan palaeogeography and palaeoclimatology. *Journal of African Earth Sciences*, v. **28**, p. 99-114.

Scott, A. C., 2010. Charcoal recognition, taphonomy and uses in palaeoenvironmental analysis. *Palaeogeography, Palaeoclimatology, Palaeoecology*, v. **291**, p. 11-39.

Séranne, M., and Anka, Z., 2005. South Atlantic continental margins of Africa: A comparison of the tectonic vs climate interplay on the evolution of equatorial west Africa and SW Africa margins. *Journal of African Earth Sciences*, v. **43**, p. 283-300.

Shalaby, M. R., Hakimi, M. H., and Abdullah, W. H., 2012. Organic geochemical characteristics and interpreted depositional environment of the Khatatba Formation, northern Western Desert, Egypt. *AAPG Bulletin*, v. **96**, p. 2019-2036.

Shanley, K. W., and McCabe, P. J., 1994. Perspectives on the sequence stratigraphy of continental strata. *AAPG Bulletin*, v. **78**, p. 544-568.

Perspectives on the sequence stratigraphy of continental strata. *AAPG Bulletin*, v. **78**, p. 544-568.

Sheldon, N. D., 2005. Do red beds indicate paleoclimatic conditions?: A Permian case study. *Palaeogeography, Palaeoclimatology, Palaeoecology*, v. **228** p. 305-319.

Sheldon, N. D., and Tabor, N. J., 2009. Quantitative paleoenvironmental and paleoclimatic reconstruction using paleosols. *Earth-Science Reviews*, v. **95**, p. 1-52.

Sibuet, J.-C., Hay, W. W., Prunier, A., Montadert, L., Hinz, K., and Fritsch, J., 1984. Early evolution of the South Atlantic Ocean: role of the rifting episode. *Deep Sea Drilling Project Initial Reports*, v. **75**, p. 469-481.

Smith, G. A., 2000. Recognition and significance of streamflow-dominated piedmont facies in extensional basins. *Basin Research*, v. **12**, p. 399-411.

Smith, N. D., 2003. Avulsion. In: G. V. Middleton, ed., *Encyclopedia of Sediments and Sedimentary Rocks*, Kluwer Academic Publishers, Dordrecht, p. 34-36.

Smith, G. A., Briden, J. C., and Drewry, G. E., 1973. Phanerozoic world maps. In: N. F. Hughes, ed., *Organisms and Continents through Time: Methods of assessing relationships between past and present biological distributions and the position of continents*, The Palaeontology Association, London, v. **12**, p. 1-42.

Srivastava, S. K., 1994. Evolution of Cretaceous phytogeoprovinces, continents and climates. *Review of Palaeobotany and Palynology*, v. **82**, p. 197-224.

Stow, D. A. V., 2005. *Sedimentary Rocks in the Field a Colour Guide*. Mason Publishing Ltd, London, 320 pp.

Stow, D. A. V., and Piper, D. J. W., 1984. Deep-water fine-grained sediments: history, methodology and terminology. In: D. A. V. Stow, and D. J. W. Piper, eds., *Fine-Grained Sediments*, Geological Society Special Publication p. 3-14.

Suggate, R. P., 1998. Relations between depth of burial, vitrinite reflectance and geothermal gradient. *Journal of Petroleum Geology*, v. **21**, p. 5-32.

Talbot, M. R., and Allen, P. A., 1996. Lakes. In: H. G. Reading, ed., *Sedimentary Environments: Processes, Facies and Stratigraphy*, Blackwell Publishing, Oxford, p. 83-

124.

Talling, P. J., Masson, D. G., Sumner, E. J., and Malgesini, G., 2012. Subaqueous sediment density flows: Depositional processes and deposit types. *Sedimentology*, v. **59**, p. 1937-2003.

Tanyileke, G. Z., Kusakabe, M., and Evans, W. C., 1996. Chemical and isotopic characteristics of fluids along the Cameroon Volcanic Line, Cameroon. *Journal of African Earth Sciences*, v. **22**, p. 433-441.

Tardy, Y., Kobilsek, B., and Paquet, H., 1991. Mineralogical composition and geographical distribution of African and Brazilian periatlantic laterites. The influence of continental drift and tropical paleoclimates during the past 150 million years and implications for India and Australia. *Journal of African Earth Sciences (and the Middle East)*, v. **12**, p. 283-295.

Taverne, L., 1986. Ostéologie et affinités systématiques de Chirocentrites vexillifer du Crétacé supérieur de la Mésogée eurafricaine. Considérations sur la phylogénie des Ichthyodectiformes, poissons téléostéens du Jurassique et du Crétacé. *Annales de la Société Royale Zoologique de Belgique*, v. **116**, p. 33-54.

Taverne, L., 2010. Les Ichthyodectidae (Teleostei, Ichthyodectiformes) des schistes bitumineux de l'Aptien (Crétacé inférieur) de Guinée Equatoriale et du Gabon. *Bulletin de l'Institut royal des Sciences Naturelles de Belgique, Sciences de la Terre*, v. **80**, p. 115-143.

Thomas, J. V., Parkash, B., and Mohindra, R., 2002. Lithofacies and palaeosol analysis of the Middle and Upper Siwalik Groups (Plio-Pleistocene), Haripur-Kolar section, Himachal Pradesh, India. *Sedimentary Geology*, v. **150**, p. 343-366.

Tijani, M. N., 2004. Evolution of saline waters and brines in the Benue-Trough, Nigeria. *Applied Geochemistry*, v. **19**, p. 1355-1365.

Tijani, M. N., Loehnert, E. P., and Uma, K. O., 1996. Origin of saline groundwaters in the Ogoja area, Lower Benue Trough, Nigeria. *Journal of African Earth Sciences*, v. **23**, p. 237-252.

Torsvik, T. H., Rousse, S., Labails, C., and Smethurst, M. A., 2009. A new scheme for the opening of the South Atlantic Ocean and the dissection of an Aptian salt basin. *Geophysical Journal International*, v. **177**, p. 1315-1333.

Toteu, S. F., Penaye, J., and Djomani, Y. P., 2004. Geodynamic evolution of the Pan-African belt in central Africa with special reference to Cameroon. *Canadian Journal of Earth Sciences*, v. **41**, p. 73-85.

Toteu, S. F., Van Schmus, W. R., Penaye, J., and Michard, A., 2001. New U–Pb and Sm–Nd data from north-central Cameroon and its bearing on the pre-Pan African history of central Africa. *Precambrian Research*, v. **108**, p. 45-73.

Traverse, A., 2007. *Paleopalynology: Second Edition*. Springer, 817 pp.

Tucker, M. E., and Wright, V. P., 1990. *Carbonate Sedimentology*. Blackwell Science Ltd, Oxford, 482 pp.

Tyson, R. V., 1995. *Sedimentary Organic Matter*. Chapman & Hall, London, 615 pp.

Tyson, R. V., and Pearson, T. H., 1991. Modern and ancient continental shelf anoxia: an overview. In: R. V. Tyson, and T. H. Pearson, eds., *Modern and Ancient Continental Shelf Anoxia*: Geological Society Special Publication, The Geological Society London, Bath, p. 1-24.

Tyson, R. V., and Follows, B., 2000. Palynofacies prediction of distance from sediment source: a case study from the Upper Cretaceous of the Pyrenees. *Geology*, v. **28**, p. 569-571.

Uzuakpunwa, A. B., 1974. The Abakaliki pyroclastics - Eastern Nigeria: new age and tectonic implications. *Geological Magazine*, v. **111**, p. 65-70.

Uzuakpunwa, A. B., 1980. A pre-Albian succession in parts of southeastern Nigeria. *Cahier Geologiques*, v. **96**, p. 358-362.

Valença, L. M. M., Neumann, V. H., and Mabesoone, J. M., 2003. An overview on Callovian-Cenomanian intracratonic basins of Northeast Brazil: Onshore stratigraphic record of the opening of the southern Atlantic. *Geologica Acta*, v. **1**, p. 261-275.

Velde, B., and Meunier, A., 2008. *The Origin of Clay Minerals in Soils and Weathered Rocks*. Springer-Verlag Berlin, 406 pp.

Villagómez, R., Jaillard, E., Bulot, L., Rivadeneira, M., and Vera, R., 1996. The Aptian-Late Albian marine transgression in the Oriente Basin of Ecuador. *Proceedings of Third International Symposium on Andean Geodynamics (ISAG)*. St Malo, France, ORSTOM, ORSTOM, p. 521-524.

Volker, H. X., Wasklewicz, T. A., and Ellis, M. A., 2007. A topographic fingerprint to distinguish alluvial fan formative processes. *Geomorphology*, v. **88** p. 34–45.

Volkheimer, W., Scafati, L., and Melendi, D. L., 2007. Palynology of Danian warm climatic wetland in Central Northen Patagonia, Argentina. *Revista Española de Micropaleontología*, v. **38**, p. 117-134.

Waples, D. W., 1980. Time and temperature in petroleum formation: application of Lopatin's method to petroleum exploration. *AAPG Bulletin*, v. **64**, p. 916-926.

Warr, L. N., and Rice, A. H. N., 1994. Interlaboratory standardization and calibration of clay mineral crystallinity and crystallite size data. *Journal of Metamorphic Geology*, v. **12**, p. 141-152.

Weiler, W., 1961. Fischreste aus der Cocobeach Formation (Untere Kreide) in Nord-Gabun, Äquatorial-Afrika. *Paläontologische Zeitschrift*, v. **35**, p. 191-199.

White, T., and Arthur, M. A., 2006. Organic carbon production and preservation in response to sea-level changes in the Turonian Carlile Formation, U.S. Western Interior Basin. *Palaeogeography, Palaeoclimatology, Palaeoecology*, v. **235** p. 223-244.

Whiteman, A. J., 1982. *Nigeria: Its Petroleum Resources and Potentials*, v. 1 & 2. Graham and Trotman, 394 pp.

Wignall, P. B., Newton, R., and Brookfield, M. E., 2005. Pyrite framboid evidence for oxygen-poor deposition during the Permian-Triassic crisis in Kashmir. *Palaeogeography, Palaeoclimatology, Palaeoecology*, v. **216**, p. 183-188.

Wilson, R. C., 1928. *Notes on the Geology of the Mamfe Division, Cameroons Province*. Geological Survey of Nigeria Occasional Paper # **6**, 23 pp.

Wilson, M., and Guiraud, R., 1992. Magmatism and rifting in Western and Central Africa, from Late Jurassic to Recent times. *Tectonophysics*, v. **213**, p. 203-225.

Wood, G. D., Gabriel, A. M., and Lawson, J. C., 1996. Palynological techniques - processing and microscopy. In: J. Jansonius, and D. C. McGregor, eds., *Palynology: principles and* *applications*, American Association of Stratigraphic Palynologist Foundation, v. **1**, p. 29-50.

Wood, G. D., Miller, M. A., Krebs, W. N., Sofer, Z., and Hedlund, R. W., 1997. Palynology, palynofacies and geochemistry of the Early Cretaceous (Pre-Salt) Cocobeach Group, North Gabon Subbasin Gabon. *Africa Geoscience Review*, v. **4**, p. 481-498.

Wright, J. B., 1968. South Atlantic continental drift and the Benue Trough. *Tectonophysics*, v. **6** p. 301-310.

Wright, J. B., Hastings, D. A., Jones, W. B., and Williams, H. R., 1985. *Geology and Mineral Resources of West Africa*. George Allen and Union, 188 pp.

Zobaa, M. K., El Beialy, S. Y., El-Sheikh, H. A., and El Beshtawy, M. K., 2013. Jurassic–Cretaceous palynomorphs, palynofacies, and petroleum potential of the Sharib-1X and Ghoroud-1X wells, north Western Desert, Egypt. *Journal of African Earth Sciences*, v. **78** p. 51-65.